Fakultät für Medizin

Institut für Medizinische Mikrobiologie, Immunologie und Hygiene

The Wnt/β-catenin pathway in gastrointestinal development, homeostasis, and carcino-genesis

Michael Allgäuer

Vollständiger Abdruck der von der Fakultät für Medizin der Technischen Universität München zur Erlangung des akademischen Grades eines

Doctor of Philosophy (Ph.D.)

genehmigten Dissertation.

Vorsitzender: Prof. Dr. med. Jürgen Ruland

Betreuer: Prof. Dr. med. Markus Gerhard

Prüfer der Dissertation:

1. Prof. Dr. rer. nat. Klaus-Peter Janssen

2. Prof. Dr. rer. nat. Andreas Jung

Die Dissertation wurde am 28.02.2018 bei der Fakultät für Medizin der Technischen Universität München eingereicht und durch die Fakultät für Medizin am 12.03.2018 angenommen.

For my wife, Wiebke.

1 Introduction

1.1 Anatomy and physiology of the gastrointestinal tract

The digestive tract can be thought of as a hollow tube made up of distinct sections that include the mouth, esophagus, stomach, duodenum, small intestine, colon, rectum, and anus. The basic architecture is the same in all segments. Innermost is an endoderm-derived epithelial lining, supported by mesoderm-derived connective tissue, the lamina propria and a thin muscular layer, the muscularis mucosae (Thompson, DeLaForest, and Battle 2018). This is followed by the connective tissue of the submucosa that contains lymphatics and lymphoid tissue, ectoderm-derived nerves and ganglia, and vessels. Peristalsis is achieved by an outer muscular layer that itself is covered by adventitia or serosa.

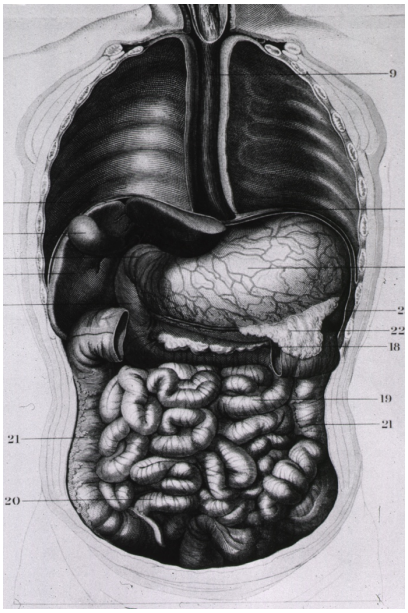

Figure 1: The digestive tract. Reprinted from the "Atlas of human anatomy and physiology", Edinburgh, 1857. (http://resource.nlm.nih.gov/101434495)

Specific physiological tasks are largely addressed by specialized epithelial linings. The esophagus has squamous mucosa to withstand mechanical forces while propelling food into the stomach. Gastric mucosa contains acid and protease producing cells to aid digestion of proteins whereas intestinal mucosa is characterized by maximizing available surface by growing in villi and crypts with cells to absorb nutrients. Lastly, colonic mucosa recovers water and electrolytes.

1.2 The Wnt/β-catenin pathway — history and overview

In 1982, Roel Nusse and Harold Varmus published their report on a novel proto-oncogene int-1. They had identified it as the tumor initiating gene in murine mammary carcinogenesis that was induced by insertional activation by the mouse mammary tumor virus (MMTV) (Nusse and Varmus 1982). It was found that int-1 had a close homologue in the fruit fly *Drosophila melanogaster* which was called wingless since its deletion

caused absence of wing tissue in flies (Sharma and Chopra 1976). As research evolved and a plethora of related genes was discovered, int-1 was named Wnt1 from combining wingless and Int1 (Nusse et al. 1991). In vertebrates, there are 19 secreted Wnt proteins, some of which are more closely related to each other (Gavin, McMahon, and McMahon 1990). Subsequent studies revealed that the protein sequence of int1 was highly conserved across species including mice with 99% homology to the human sequence (van Ooyen, Kwee, and Nusse 1985). This underscored the evolutionary importance of this pathway down to sea anemones (Kusserow et al. 2005) and also turned out to be instrumental because it allowed to study Wnt signaling across many species (Nusse and Varmus 2012). The effect of gene deletions or ectopic expression could be investigated in *Xenopus laevis* embryos, since it was found that injection of int1 caused duplication of the dorsal axis (McMahon and Moon 1989).

Wnts are small proteins of 40 kDa that act as growth factors influencing cell proliferation, polarization, and orchestrate directional expansion of tissues to form organs (Goldstein et al. 2006, Niehrs and Acebron 2012, Loh, van Amerongen, and Nusse 2016). Up until 2003, Wnts could not be produced or isolated in significant quantities to study their functions and it was found that these secreted glycoproteins had covalently attached lipids (Willert et al. 2003). It is not yet solved how Wnt proteins reach their target cells and diffusion is less likely given their lipid modifications (Boutros and Niehrs 2016). Several mechanisms have been proposed including exovesicles, cytonemes, and filopodia. In the intestine, a different mechanism was recently proposed by which Wnt proteins are transferred to $Lgr5^{+}$ positive cells in the vicinity where they remain bound to Frizzled receptors and get distributed and diluted along the crypt villus axis by subsequent cell divisions (Farin et al. 2016).

Wnt ligands bind in mouse and human to one of 10 frizzled transmembrane receptors (Fz) on the cell surface that in turn recruit Dishevelled to the plasma membrane (MacDonald, Tamai, and He 2009). LDL receptor related proteins 5 and 6 (LRP5/6) act as co-receptors for Wnt ligands (Wehrli et al. 2000) and are phosphorylated by GSK3 and casein kinase 1 leading to interaction with Axin (Mao, Wang, et al. 2001, Davidson et al. 2005, Zeng et al. 2005).

Finally, there are two additional protein families Norrins (Xu et al. 2004) and R-spondins that activate Wnt signaling by interacting with Frizzled/LRP receptor complexes. R-spondins were also found to interact with Lgr5 and potentiate low levels of Wnt signaling (de Lau et al. 2011).

Studies in *Drosophila* showed that levels of β-catenin's homologue armadillo were increased in the presence of Wnt proteins (Riggleman, Schedl, and Wieschaus 1990, Peifer, Pai, and Casey 1994). β-catenin was known to interact with cell adhesion protein E-cadherin (Ozawa, Baribault, and Kemler 1989). Interestingly, β-catenin bound to the cell membrane and β-catenin as a mediator of Wnt signaling are differentially regulated. While the first is stable over extended periods of time, the latter is tightly regulated and has a much shorter half-life. Studies in *Caenorhabditis elegans* showed that these two functions are even carried out by different forms of β-catenin (Korswagen, Herman, and Clevers 2000).

Further studies revealed that β-catenin/armadillo could be found not only at the cell membrane but also in the cytoplasm and nucleus of cells (Funayama et al. 1995). Furthermore, experimental manipulation of β-catenin/Armadillo levels cause dorsal axis duplication (McCrea, Brieher, and Gumbiner 1993) or elimination (Heasman et al. 1994) in *Xenopus laevis* embryos, resembling the effects of modified Wnt-1 levels and indicating a central role of β-catenin.

When investigating colorectal cancer patients, it was discovered that APC and β-catenin interacted with each other (Rubinfeld et al. 1993, Su, Vogelstein, and Kinzler 1993). Studies in *Drosophila* showed that GSK-3beta, that was known for its role in glucose metabolism, was a negative regulator of the Wnt pathway (Siegfried, Chou, and Perrimon 1992) and formed a complex with β-catenin/Armadillo and APC (Rubinfeld et al. 1996). Axin was revealed as an additional member acting as a scaffold (Behrens et al. 1998, Ikeda et al. 1998) and this complex was subsequently named destruction complex since it was discovered that β-catenin is phosphorylated (Yost et al. 1996) and after ubiquitination by E3 ubiquitin ligase β-TrCP degraded in the proteasome (Aberle et al. 1997, Orford et al. 1997).

The classical view is that the destruction complex is disassembled by recruiting Axin and Dishevelled (Dvl) to the cell membrane binding LRP and frizzled receptors, respectively. This was recently challenged and new mechanisms were proposed. One is that the destruction complex stays intact regardless of the current status of Wnt signaling and β-catenin is continuously phosphorylated. In the state of active Wnt signaling ubiquitination of β-catenin would be suppressed, which would lead to a saturation of the destruction complex with bound, phosphorylated β-catenin, which in turn would allow newly synthesized β-catenin to accumulate and translocate to the nucleus (Li et al. 2012). Yet

other findings point to different mechanisms of dynamic phosphorylation of β-catenin (Hernandez, Klein, and Kirschner 2012) or Axin (Kim et al. 2013).

Since the Wnt pathway promotes growth and cell division it needs to be tightly regulated to achieve spatiotemporal control. LRP5/6 are inhibited by extracellular Wnt inhibitor dickkopf1 (Mao, Wu, et al. 2001). Secreted frizzled-related proteins (sFRPs) that possess binding motifs similar to frizzled receptors (Finch et al. 1997) and Wnt-inhibitory factor-1 (WIF-1) (Hsieh et al. 1999) bind to extracellular Wnt proteins, thereby controlling their availability to bind to LRP and frizzled receptors. Recently, another regulator was identified — Notum, an extracellular carboxylesterase that cleaves essential lipid modifications off Wnt proteins, thereby hampering their interactions with Fz receptors (Kakugawa et al. 2015).

β-catenin accumulates in the cytoplasm and translocates to the nucleus where it interacts with TCF/Lef1 (Behrens et al. 1996, Huber et al. 1996, Molenaar et al. 1996). In the Wnt-off state, TCF/Lef1 is associated with Groucho and causes repression of Wnt target genes. Upon β-catenin interaction, Groucho dissociates and β-catenin binds TCF/Lef1 inducing transcription of Wnt target genes (Cavallo et al. 1998, Daniels and Weis 2005). One of these target genes is *Axin2* which was shown to be a reliable and general marker for Wnt signaling pathway activation (Yan et al. 2001, Lustig et al. 2002, Jho et al. 2002). Interestingly, it was found that not absolute β-catenin levels matter but fold-changes of β-catenin levels. Therefore, even small amounts of nuclear β-catenin that might go unnoticed by immunohistochemistry can induce a change in Wnt target gene transcription (Goentoro and Kirschner 2009).

The Wnt pathway employing β-catenin as effector molecule inducing TCF/Lef1 mediated transcription of target genes is named the ‘canonical Wnt pathway’. Wnt proteins have been grouped into canonical Wnts (Wnt1, Wnt3A, Wnt8) that were found to induce double axis formation in *Xenopus* embryos (McMahon and Moon 1989) and transformation of mouse C57MG epithelial mammary cells (Wong, Gavin, and McMahon 1994).

Other Wnt proteins (Wnt4, Wnt5A and Wnt11) were found to activate two other pathways that will not be the focus of this work: the planar cell polarity pathway (PCP), which acts via GTPases of the rho/cdc42 family to activate jun kinase which regulates cell shape, polarization, and division (Veeman, Axelrod, and Moon 2003, Qian et al. 2007) and the Wnt/Ca^{2+} cascade, that influences Ca^{2+} ions within cells causing activation of Ca^{2+}-dependent enzymes, like protein kinase C (Niehrs 2004).

However, recent evidence suggests that this distinction might be oversimplified not representing the complex reality of biological systems with diverse simultaneous inputs (van Amerongen and Nusse 2009) as there is overlap between these pathways (van Amerongen et al. 2012, Thrasivoulou, Millar, and Ahmed 2013).

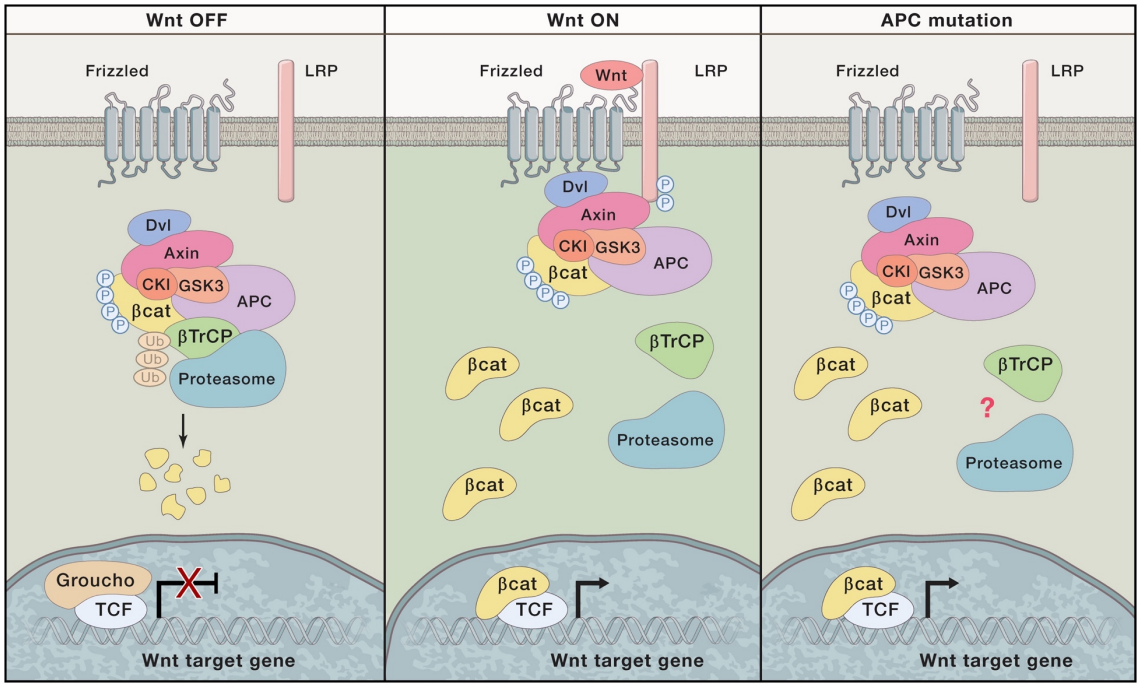

Figure 2: The Wnt/β-catenin pathway.
The left image illustrates the state of inactive Wnt signaling when levels of free β-catenin are tightly regulated. APC, Axin, Dvl, CK1, GSK-3, and β-TrCP form the so-called destruction complex. β-catenin is phosphorylated by CK1 and GSK-3 which allows ubiquitination by β-TrCP. This marks β-catenin for proteasomal degradation. Transcription factors of the T-cell factor (TCF) family are repressed by Groucho. The center image illustrates the state of active Wnt signaling when free β-catenin accumulates and translocates into the nucleus to bind to TCF and initiate transcription of Wnt target genes. Wnt proteins bind to frizzled and LRP receptors which leads to the recruitment of Axin to the cell membrane causing the destruction complex to fall apart. The right image illustrates the state of aberrant constitutively active Wnt signaling by mutations in Wnt pathway components, e.g. APC. These impair formation of the destruction complex with consecutive accumulation of β-catenin, its translocation to the nucleus, and transcription of Wnt target genes. Reprinted with permission from Nusse R and Clevers H. Wnt/β-Catenin Signaling, Disease, and Emerging Therapeutic Modalities. Cell. 2017 Jun 1;169(6):985-999. Copyright 2017 Elsevier.

1.3 The Wnt/β-catenin pathway in gastrointestinal development

During gastrulation three germ layers develop from the epiblast: ectoderm, mesoderm, and endoderm (Wells and Melton 1999). The endoderm gives rise to definitive (embryonic) endoderm and visceral endoderm (extraembryonic endoderm) of which the

yolk sack forms. Definitive (embryonic) endoderm is the origin of the epithelia of lungs, thyroid, thymus, esophagus, stomach, intestines, liver, and pancreas.

The following experimental findings illustrate the important role of Wnt/β-catenin signaling in embryonic development and intestinal morphogenesis. Knockouts of Wnt3 and β-catenin demonstrated defects in vertebral anterior-posterior body axis formation (Liu et al. 1999, Huelsken et al. 2000) while mutations in APC and Axin led to axis duplications (Zeng et al. 1997, Ishikawa et al. 2003). Mice deficient for Wnt transcription factors Tcf4 and Tcf1 exhibited an absence of caudal structures due to early defects in hindgut development (Gregorieff, Grosschedl, and Clevers 2004), while a knockout of Tcf4 alone revealed regular development of endoderm into intestinal epithelium but lack of a proliferative stem cell compartment in crypts (Korinek et al. 1998).

Expression patterns of several Wnt proteins were studied in murine gut development revealing distinct patterns: Wnt5a was confined to the mesenchyme. Wnt4 was found in intestinal epithelium and mesenteric progenitors, while Wnt5b, Wnt6, and Wnt11 were expressed in esophageal epithelium. Wnt11 could also be detected in colonic epithelium but also in the gastric mesenchyme underscoring the influence of Wnt signaling in gastrointestinal morphogenesis (Lickert et al. 2001).

1.4 The Wnt target gene *Sox17* in gastrointestinal development

Definitive (embryonic) endoderm was found to be induced in *Xenopus* by relatives of murine Sox17 (Hudson et al. 1997). The pivotal role of Sox17 was confirmed in a knockout mouse model when its deletion led to defective mid- and hindgut development at E8.5-9.5 (Kanai-Azuma et al. 2002). Subsequently, Sox17 was shown to interact with β-catenin and induce transcription of endodermal genes Foxa1 and Foxa2 (Sinner et al. 2004).

Sox17 is part of a family of more than 20 Sox transcription factors that are highly conserved through different species and characterized by a DNA-binding HMG domain (Bowles, Schepers, and Koopman 2000). Sox proteins were found to act as modifiers of Wnt signaling in either enhancing or suppressing target gene transcription in association with β-catenin and TCF transcription factors (Kormish, Sinner, and Zorn 2010).

It was further shown that the formation of extra-hepatobiliary system is Sox17 dependent and that downregulation of Sox17 was necessary in Pdx1-expressing cells to lead to pancreatic development (Spence et al. 2009). Sox17 was further discovered to be involved

in cardiovascular development (Sakamoto et al. 2007) and hematopoietic stem cell development (Kim, Saunders, and Morrison 2007). However, little is known about whether Sox17 plays a functional role in intestinal epithelium.

1.5 The Wnt/β-catenin pathway in gastrointestinal stemness and homeostasis

The epithelial lining of the intestine renews itself every 4-5 days (Stevens and Leblond 1947), which makes it one of the most proliferative tissue in adult mammals. The driving and essential force behind maintaining intestinal homeostasis is Wnt/β-catenin signaling as was illustrated in elegant experiments knocking out various components of the Wnt pathway. A knockout of Tcf4 led to a lack of a proliferative stem cell compartment in crypts (Korinek et al. 1998) and Tcf4 was subsequently confirmed to be of continued importance in homeostasis of the adult murine intestine (van Es, Haegebarth, et al. 2012). Conditional deletion of β-catenin caused crypt ablation, increased apoptosis, reduced goblet cells, and led to detachment of absorptive cells (Ireland et al. 2004). Codeletion of R-spondin receptors Lgr4 and Lgr5 resulted in loss of intestinal crypts (de Lau et al. 2011). Overexpression of extracellular Wnt repressor Dkk1 led to reduced proliferation and loss of crypts and secretory cell lines (Pinto et al. 2003, Kuhnert et al. 2004). A mouse model with conditional deletion of Wnt target gene c-Myc (He et al. 1998, van de Wetering et al. 2002) was shown to negatively affect size and proliferative capacity of crypt progenitor cells with deleted c-Myc. Due to incomplete recombination some cells retained intact copies of c-Myc thereby outcompeting and substituting the c-Myc deleted crypts.

A screen of Wnt proteins, receptors, and transcription factors by in situ hybridization revealed a surprising plethora of differentially expressed genes implicating an even more extensive role of Wnt signaling in intestinal homeostasis than what was previously appreciated (Gregorieff et al. 2005).

This highly proliferative activity takes its origin from adult stem cells. In the 40ties of the last century, it was discovered that intestinal crypts are the source of intestinal self-renewal (Friedman 1945). However, the nature of the intestinal stem cell remained elusive.

More recently, crypt base columnar (CBC) cells, that are situated between Paneth cells at the crypt bottoms, were found to express Lgr5 and give rise to all intestinal cell types *in*

vivo and *in vitro* (Barker et al. 2007, Sato et al. 2009). Paneth cells constitute a niche for intestinal stem cells by synthesizing Wnt, notch, and EGF signals (Sato et al. 2011) and in turn depend on Wnt signaling for their own maturation (van Es et al. 2005). Interestingly, it was shown that quiescent precursors of Paneth and enteroendocrine cells can upon tissue injury regain stem cell properties and reconstitute all epithelial lineages (van Es, Sato, et al. 2012, Buczacki et al. 2013). $Lgr5^+$ intestinal stem cells divide daily and engage in "neutral competition", meaning that either of resulting daughter cells remains as stem cell while the other differentiates (Lopez-Garcia et al. 2010, Snippert et al. 2010).

However, a second population of intestinal stem cells residing at the "+4 position" was also described. Those are marked by Bmi1 and were also found to possess self-renewal capacity plus give rise to all intestinal cell types (Sangiorgi and Capecchi 2008). $Bmi1^+$ intestinal stem cells are quiescent but can repopulate the pool of $Lgr5^+$ stem cells after tissue injury (Tian et al. 2011, Yan et al. 2012) so these two populations appear to cooperate with each other (Takeda et al. 2011).

1.6 The Wnt/β-catenin pathway in gastrointestinal carcinogenesis

1.6.1 Colorectal cancer

Since Wnt/β-catenin signaling potently controls proliferation and stemness in the intestine, it is not surprising that it was found to be deregulated in intestinal tumorigenesis. Discoveries in cancer biology have led to better understanding of Wnt/β-catenin signaling in homeostasis and development and vice versa (Nusse and Varmus 2012).

The causative gene of familial adenomatous polyposis (FAP) — a genetic syndrome predisposing affected individuals to develop hundreds to thousands of polyps and ultimately colorectal cancer — was identified and named Adenomatous polyposis coli (*APC*) (Groden et al. 1991, Kinzler et al. 1991). This condition is also replicated, albeit with small intestinal and not colonic polyposis, in the $APC^{min/+}$ mouse (Moser, Pitot, and Dove 1990). *APC* was found to be mostly affected by truncating mutations and to undergo loss of heterozygosity in malignant progression (Miyaki et al. 1994).

Subsequently, *APC* was noticed to not only be mutated in hereditary colorectal cancer but also the majority of sporadic colorectal carcinomas (Wood et al. 2007). Conditional

deletion of *APC* led to immediate Wnt signaling activation with nuclear accumulation of β-catenin and caused intestinal epithelial cells to retain a "crypt progenitor-like" phenotype (Sansom et al. 2004). A mouse model of transient APC suppression developed polyposis and carcinomas in concert with additional mutations and showed regression of tumors upon restoration of APC, underscoring the instrumental role of Wnt signaling in colorectal tumorigenesis (Dow et al. 2015).

However, not all cases showed mutations in *APC* and research focused on β-catenin. In fact, 5-10% of sporadic colorectal cancers exhibit mutations of *CTNNB1* (the gene encoding β-catenin) affecting critical phosphorylation sites important in its regulation (Morin et al. 1997).

Since then, additional components and target genes of the Wnt pathway were noted to be altered in colorectal cancer to include *AXIN1* (Jin et al. 2003), *AXIN2* (Liu et al. 2000, Lammi et al. 2004), R-spondins (Seshagiri et al. 2012), *SOX9*, *TCF3* (Cancer Genome Atlas 2012), and *TCF4* (Bass et al. 2011). Mice injected with R-spondin1 showed increased crypt proliferation and β-catenin accumulation (Kim et al. 2005). Sequencing efforts recently confirmed that Wnt signaling is altered in 92% and 97% of non-hypermutated and hypermutated colorectal cancers, respectively (Cancer Genome Atlas 2012).

Colorectal cancer and its precursors are well studied. In 1990, Fearon and Vogelstein proposed a model of step-wise colorectal tumorigenesis from aberrant crypt focus, to adenoma, and finally carcinoma (Fearon and Vogelstein 1990). The cascade starts with deregulated Wnt/β-catenin signaling due to mutations of *APC* or less frequently *CTNNB1*. This is followed by mutations in *KRAS* or, in case of microsatellite instable tumors, *BRAF*. The combination of mutant APC and KRAS was shown to lead to a marked increase in tumor formation in a mouse model (Janssen et al. 2006). Subsequently, additional alterations in e.g. *BAX*, *PIK3CA*, *PTEN*, *SMAD4*, *TGFBR2*, and *TP53* ensue in the course to invasive cancer (Markowitz and Bertagnolli 2009).

1.6.2 Gastric cancer

Gastric cancer ranks as the fifth most common cancer worldwide making up 7% of all new cancer cases and causing 9% of worldwide cancer mortality (Stewart and Wild 2015). Around 70% of cases occurred in developing countries and 2/3 of those alone in China. Notably there are less-developed countries such as India and most of Africa with

a lower incidence, whereas more developed parts of the world including Japan, Korea, and Eastern Europe have higher rates of gastric cancer (Forman and Burley 2006, Ferlay et al. 2015). 5‑year survival rates on a worldwide scale are still low with 25-30% (Torre et al. 2016), while Japan and South Korea, countries with a high incidence of gastric cancer, have shown a marked improvement (> 50%) due to early detection (Hartgrink et al. 2009).

Risk factors for the development of gastric cancer include male sex, a diet high in salt intake (e.g. salt-preserved foods in Japan) (Chen et al. 1996, Ward and Lopez-Carrillo 1999, Tsugane 2005), processed red meat (Gonzalez et al. 2006), smoking (Ladeiras-Lopes et al. 2008), but overall the most important risk factor is infection with the gram negative, spiral-shaped bacterium *Helicobacter pylori,* which shows higher prevalence in older age cohorts, lower socioeconomic groups, and developing countries (TheEUROGAST-StudyGroup 1993). 89% of non-cardia gastric cancers or globally around 780,000 cases are linked to *H. pylori* infection (Plummer et al. 2015). While a large fraction of the world's population is infected by *H. pylori* only a minority of individuals develop gastric cancer. Bacterial factors like *CagA* (cytotoxin-associated gene A) positivity (Blaser et al. 1995, Plummer et al. 2007) or host factors like interleukin-1 polymorphisms (El-Omar et al. 2000) are associated with an increased risk of gastric cancer. $CagA^+$ strains of *H. pylori* inject Cytotoxin-associated gene A (*CagA*) into gastric epithelial cells (Odenbreit et al. 2000) where it is phosphorylated and in turn activates SHP-2 tyrosine phosphatase that acts via the MAPK/ERK pathway influencing growth, migration, and adhesion (Higashi et al. 2002). It was further found to interact with E-cadherin liberating cell-membrane bound β-catenin that in turn leads to increased Wnt signaling (Murata-Kamiya et al. 2007). A mouse model of systemic expression of CagA developed gastric hyperplasia, polyps, and gastric and intestinal adenocarcinomas demonstrating the oncogenic capacity of CagA (Ohnishi et al. 2008).

Prophylactic eradication of *H. pylori* was shown to decrease the risk of gastric cancer (Ma et al. 2012). Another study with shorter follow-up showed a decrease in gastric atrophy, a predisposing condition for gastric carcinoma, but also an increase in esophagitis (Lee et al. 2013). Due to eradication of *H. pylori*, better food preservation and hygiene, gastric carcinomas arising in the gastric antrum have decreased. In contrast, cancers of the gastroesophageal junction have increased due to obesity and chronic reflux (Rugge et al. 2016).

While most cases of gastric cancer are sporadic, about 10% of patients have a family history of gastric cancer (La Vecchia et al. 1992). 1-3% of gastric cancer patients are afflicted by one of several currently defined genetic syndromes. The most prominent is hereditary diffuse gastric cancer (HDGC) which in 30-40% of patients is due to a truncating germline mutation of *CDH1*, the gene encoding E-cadherin (Guilford et al. 1998), while some patients harbor mutations in *CTNNA1*, encoding α-E-catenin which is involved in cell adhesion together with E-cadherin (Majewski et al. 2013). These patients carry a cumulative life-time risk of 70% for men and 56% for females for developing gastric cancer and females have a 42% incidence of (lobular) breast carcinoma (Hansford et al. 2015). Another recently established autosomal-dominant cancer syndrome is gastric adenocarcinoma and proximal polyposis of the stomach (GAPPS). Affected individuals develop polyposis of the proximal stomach with sparing of gastric antrum, duodenum, small intestine, and colon. Polyps are mainly of fundic gland-type, that when sporadic are usually benign, but can develop high-grade dysplasia in this syndrome and progress to invasive carcinoma. Criteria for identification of patients have been proposed to include >100 predominantly fundic gland polyps, some with dysplasia (or >30 if there is already an affected family member), restricted to the gastric body and fundus without duodenal or intestinal polyps in the setting of an autosomal dominant inheritance pattern and absence of other heritable polyposis syndromes (Worthley et al. 2012). Point mutations in promoter 1B of *APC* (Li et al. 2016) were found as the underlying genetic alteration. Other cancer predisposition syndromes, which can manifest with gastric cancer, include familial adenomatous polyposis (FAP) (Wood et al. 2014, Mankaney et al. 2017), Lynch syndrome (Capelle et al. 2010), Li-Fraumeni syndrome (Masciari et al. 2011), and germline mutations in *BRCA2* (Jakubowska et al. 2002).

Most sporadic gastric cancers evolve through the so-called Correa cascade of multistep gastric carcinogenesis. It starts with chronic inflammation (chronic gastritis) causing atrophy (atrophic gastritis) and adaptive reactions of the gastric mucosa (intestinal metaplasia) that progress to dysplasia (neoplastic changes restricted to the epithelium), and ultimately carcinoma (Correa 1988). But there are also some cancers that do not follow an “intestinal path” but develop from gastric dysplasia without intestinal metaplasia into gastric adenocarcinoma, e.g. in the cancer predisposition syndrome GAPPS, gastric cancer arises from foveolar hyperplasia and not intestinal metaplasia (Worthley et al. 2012).

Most tumors arising in the stomach are adenocarcinomas that can be grouped by various classification systems. The WHO describes tubular and papillary carcinomas (both falling into Lauren intestinal type (Lauren 1965)), poorly cohesive (with or without signet ring cells) corresponding to Lauren diffuse type, plus mucinous and mixed tumors. In addition, there are some other rare histological variants.

Four distinct molecular subtypes of gastric adenocarcinoma were delineated (Cancer Genome Atlas Research 2014): Epstein-Barr virus (EBV)-associated tumors, microsatellite instability (MSI)-high tumors, genomically stable tumors, and tumors with chromosomal instability (CIN). A more recent molecular classification incorporated clinical outcomes and also identified four subtypes that are slightly different but overall confirmed such a subtyping: MSS (microsatellite stable)/TP53- (TP53 mutations), MSS/TP53+, microsatellite instability (MSI)-high, and MSS/EMT (epithelial to mesenchymal transition) (Cristescu et al. 2015).

Overall, *TP53* was found to be mutated in about half of gastric cancers making it the most frequently mutated gene. About one third of cases showed amplifications in receptor tyrosine kinases of the MAPK/ERK pathway to include EGFR, FGFR2, HER2, KRAS, and MET (Deng et al. 2012). Additional mutations were found in proteins involved in cell cycle regulation (e.g. CCND1, CCNE1, CDK6) and transcription factors (e.g. GATA4, GATA6, MYC) (Dulak et al. 2012) as well as chromatin remodeling (ARID1A) (Wang et al. 2011). Hepatocyte nuclear factor-4α (HNF4α), a substrate of AMPK, was found to be upregulated in gastric cancers and activate WNT5A, linking tumor metabolism to Wnt signaling (Chang et al. 2016).

Gastric cancer is not a Wnt driven process compared to colorectal cancer. Nevertheless, earlier studies showed Wnt activation in around 30% of gastric carcinomas (Park et al. 1999, Clements et al. 2002) and mutations or loss of heterozygosity of *APC* were detected in 18% and 21% of cases, respectively (Tahara 2004). The TCGA study of gastric adenocarcinoma revealed that in non-hypermutated gastric cancers, frameshift and non-sense mutations of *APC* occurred in 7% of cases and missense mutations of *CTNNB1* in 4% of cases whereas hypermutated cancers showed no significant number of *APC* or *CTNNB1* mutations (Cancer Genome Atlas Research 2014). Mutations in *CTNNB1* were more commonly found in intestinal type gastric carcinoma (Ogasawara et al. 2006, Park et al. 1999). Familial cancer predisposition syndromes involving Wnt activation like FAP (*APC* germline mutations) or GAPPS (mutations of the *APC* promoter) lead to Wnt driven gastric carcinogenesis (Abraham et al. 2000, Worthley et al. 2012). Along the same line,

the *Apc* ^{1648} mouse model not only develops colonic polyps but can also exhibit antral polyposis and dysplasia (Fox et al. 1997). The *K19*-Wnt1 transgenic mouse expresses Wnt1 in the gastric epithelium and was shown to develop small preneoplastic lesions that progressed to tumors when bred with mice with increased prostaglandin synthesis (Oshima et al. 2006).

Symptoms of gastric cancer can be quite unspecific and therefore patients might not present until the disease is more advanced. Ultimately, most patients experience weight loss, anemia, fatigue, early satiety or pain. Tumor stage is determined clinically based on results of endoscopy, endoscopic ultrasound, CT-scanning, and optionally biopsy of local lymph nodes.

Endoscopic mucosal resection (EMR) and endoscopic submucosal dissection (ESD) are minimally invasive surgical procedures to resect early gastric cancers that are still limited to the mucosa and have not extended into the submucosa (Gotoda 2007). Larger, non-metastasized tumors are usually treated by total gastrectomy if located in the cardia or fundus and by distal gastrectomy if situated in the antrum.

However, a substantial number of patients presents with distant metastases most commonly to the liver or in the case of diffuse type gastric cancer, peritoneal dissemination. Then conventional chemotherapy remains the mainstay of therapy and it is also applied in the perioperative and adjuvant setting (Smyth et al. 2016). In recent years, targeted therapy against HER2 has reached clinical practice (Bang et al. 2010) and HER2 testing by IHC is routinely performed for patients with advanced gastric cancer (Bartley et al. 2016).

Nevertheless, patients with advanced or recurrent gastric cancer have a median survival of less than one year (Group et al. 2013) so new treatment options are desperately needed. As discussed, a subset of gastric cancers displays alterations in the Wnt pathway. Due to the ubiquitous nature of Wnt signaling in maintaining homeostasis and stemness it is challenging to avoid undesirable side effects (Kahn 2014). But some compounds are already in clinical trials including antagonists that inhibit Porcupine which is essential for production of Wnt proteins (Chen et al. 2009, Proffitt et al. 2013) or agents that inhibit tankyrase which ubiquitinates Axin proteins marking them for degradation (Kulak et al. 2015).

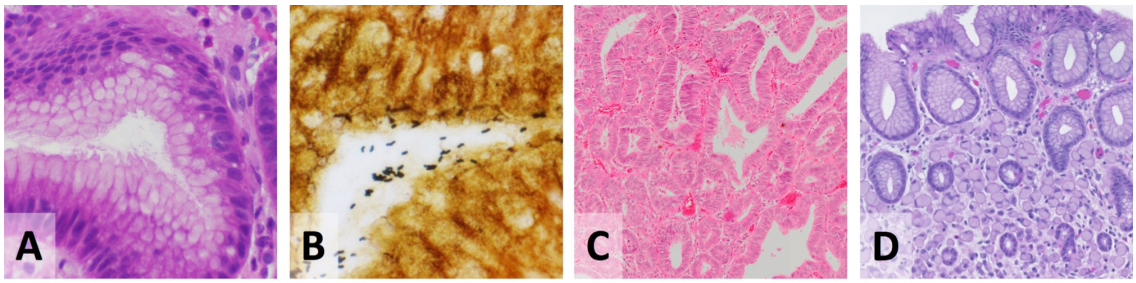

Figure 3: *H. pylori* and the two types of gastric adenocarcinoma according to Lauren.
H. pylori can be difficult to recognize on routine H&E stained sections (A) but can be highlighted by e.g. Warthin-Starry stain (B). Moderately differentiated, intestinal-type gastric adenocarcinoma (C) in a patient with *H. pylori* infection. Diffuse-type gastric cancer in a patient with *CDH1* germline mutation (D). Photomicrographs taken at 400x (A), 1000x (B), 100x (C), and 200x (D) original magnification.

1.6.3 RNF43

E3 ubiquitin-protein ligase RNF43 (RNF43) is made of 783 amino acids yielding a molecular weight of 85.7 kDa. In addition to this 'canonical' sequence three other isoforms exist with molecular weights of 81.2 kDa, 72.1 kDa, and 95.0 kDa (UniProtKB 2017).
The gene *RNF43* is encoded on the reverse strand on chromosomal band 17q22 (Ensembl 2017). RNF43 has a N-terminal signal peptide, a helical transmembrane domain (UniProtKB 2017), a RING-type Zinc finger motif, and two C-terminal nuclear localization signals (OMIM 2017).
Germline mutations of *RNF43* have been linked to the autosomal dominant sessile serrated polyposis cancer syndrome (and sporadic sessile and traditional serrated adenomas) in which affected individuals develop multiple sessile serrated polyps of the colon and have an up to 54% lifetime risk of colorectal cancer plus may also develop tumors of other organs (Gala et al. 2014, Taupin et al. 2015, Tsai et al. 2016, Yan et al. 2017, OMIM 2017) but so far results are conflicting and two studies of larger cohorts could only confirm *RNF43* germline mutations in a small number of affected patients (Buchanan et al. 2017, Quintana et al. 2018).
Somatic mutations of *RNF43* were found in colon cancer (Giannakis et al. 2014, Jo et al. 2015), gastric cancer (Wang et al. 2014, Jo et al. 2015), pancreatic neoplasms (Furukawa et al. 2011, Wu et al. 2011), liver fluke-associated cholangiocarcinoma (Ong et al. 2012), endometrial cancer (Giannakis et al. 2014), and ovarian tumors (Ryland et al. 2013). Recently, mutations of *RNF43* were found to occur when gastric adenomas progress to carcinomas (Min et al. 2016). Mutations of *RNF43* were frequently frameshift mutations

leading to the production of a truncated protein indicating that RNF43 acts as a tumor suppressor gene.

Despite early reports suggesting that RNF43 acts as an oncogene in colorectal cancer (Yagyu et al. 2004, Sugiura, Yamaguchi, and Miyamoto 2008), it was indeed found to act as a tumor suppressor due to its capacity of inhibiting the Wnt signaling pathway in a negative feedback loop being a Wnt target gene itself (Koo et al. 2012, Takahashi et al. 2014, Loregger et al. 2015). It was shown that this inhibition is achieved by two different mechanisms depending on the subcellular localization of the protein.

When localized at the cell membrane, RNF43 and its homologue ZNRF3 inhibit Wnt signaling by ubiquitinating cytoplasmic loops of frizzled receptors resulting in their endocytosis and lysosomal degradation (Hao et al. 2012, Koo et al. 2012). In turn, RNF43 and ZNRF3 are proposed to be downregulated by interaction with LGR5 after binding of R-spondin (de Lau et al. 2014, Zebisch and Jones 2015). A mouse model of concurrent deletion of Rnf43 and Znrf3 exhibited adenomatous transformation of the intestinal epithelium (Koo et al. 2012).

When expressed in the nucleus, our group showed that RNF43 suppresses Wnt signaling by tethering TCF4 to the nuclear membrane (Loregger et al. 2015). A nuclear localization of RNF43 was described in other studies before (Sugiura, Yamaguchi, and Miyamoto 2008, Miyamoto, Sakurai, and Sugiura 2008, Shinada et al. 2011, Nailwal et al. 2015, Xie et al. 2015), which would also fit to a recent association of RNF43 and DNA damage response (Gala et al. 2014).

1.7 Objectives

1. Assess the function of Wnt target gene *Sox17* in development and homeostasis of definite intestinal epithelium in a conditional mouse model with intestine-specific knockout of *Sox17*.

2. Determine tissue distribution of mRNA transcripts and proteins of the Wnt/β-catenin signaling pathway to characterize the contribution of Wnt signaling to reestablishing homeostasis and stemness in mouse models of acute intestinal perturbation by conditional deletion of essential genes and Wnt target genes in gastrointestinal tumorigenesis. To achieve this the following specific objectives were determined:
    - Establish in situ hybridization for *Axin2* and *Olfm4*.
    - Establish in situ hybridization for *Sox17*, *Rnf43*, *RNF43,* and *OLFM4*.

3. Study the role of RNF43 in gastric carcinogenesis.
    - Establish an immunohistochemical stain for the detection of endogenous RNF43 protein in gastric tissue samples and cell culture pellets.
    - Assess the expression of RNF43 in gastric cancer cell lines.
    - Determine the subcellular distribution of RNF43 in gastric cancer cell lines under conditions of overexpression and endogenously by different experimental approaches.
    - Investigate RNF43's influence on Wnt signaling in gastric cancer cell lines.

2 Material and Methods

2.1 Materials

2.1.1 Consumables

BD Falcon™ Cell Culture Flasks, 25 cm^2 / 75 cm^2	BD Bioscience, Heidelberg, Germany
BD Falcon™ Conical Tubes, 15 ml / 50 ml	BD Bioscience, Heidelberg, Germany
BD Falcon™ Multiwell Cell Culture Plate, 6 / 12 / 24 well	BD Bioscience, Heidelberg, Germany
BD Falcon™ Round-Bottom Polypropylene Tubes	BD Bioscience, Heidelberg, Germany
BD Falcon™ Standard Tissue Culture Dish, 10 cm^2	BD Bioscience, Heidelberg, Germany
Blotting Paper	Whatman, Dassel, Germany
Cell scrapers, 30 cm	Corning, Kaiserslautern, Germany
Combitips advanced®, 0.5 / 2.5 / 5 ml	Eppendorf, Hamburg, Germany
DNA Pick-up Tips	Süd-Laborbedarf Gauting, Gauting, Germany
Eppendorf Safe-Lock Tubes, 1.5 / 2 ml	Eppendorf, Hamburg, Germany
Greiner CELLSTAR® serological pipette, 2 / 5 / 10 / 25 ml	Greiner Bio-One, Solingen, Germany
Menzel™ Microscope Coverslips	Menzel-Gläser, Braunschweig, Germany
MµltiGuard™ Barrier Pipet Tips, 10 / 20 / 200 / 1000 µl	Sorenson BioScience, Salt Lake City, USA
Nalgene™ Cryotubes	Thermo Scientific, Karlsruhe, Germany
Novex® Gel Cassettes	Invitrogen, Karlsruhe, Germany
Novex® Gel Combs	Invitrogen, Karlsruhe, Germany
Parafilm® M All-Purpose Laboratory Film	Bemis Company, Neenah, USA
Protran® Nitrocellulose Membrane	Whatman, Dassel, Germany

Quali- PCR Tubes	Kisker Biotech, Steinfurt, Germany
SafeSeal-Tips Professional Line, 10 / 100 / 1000 µl	Biozym Scientific, Hessisch Oldendorf, Germany
SuperFrost™ Plus Microscope Slides	Menzel-Gläser, Braunschweig, Germany
TipOne® Bevelled Filter Tips, 20 µl	STARLAB, Hamburg, Germany
TipOne® Graduated Filter Tips, 10 / 20 / 200 / 1000 µl	STARLAB, Hamburg, Germany
X-ray film for western blot detection	Kodak, Stuttgart, Germany

2.1.2 Equipment

ASP 300 S	Leica Microsystems, Wetzlar, Germany
Axiovert 40 microscope	Carl Zeiss, Oberkochen, Germany
C1000 Touch™ Thermal Cycler	BioRad Laboratories, Munich, Germany
CFX384 Touch™ Real-Time PCR Detection System	BioRad Laboratories, Munich, Germany
CHEMOCAM Imager 3.2	INTAS Science Imaging Instruments, Göttingen, Germany
Corning® Lambda® plus single channel pipettor, 0.5-10 / 2-20 / 20-200 / 200-1000 µl	Sigma-Aldrich, Munich, Germany
Curix 60 automatic film processor	AGFA, Düsseldorf, Germany
Electrophoresis Chambers	BioRad Laboratories, Munich, Germany
Electrophoresis PowerPac™ Power Supply	BioRad Laboratories, Munich, Germany
Eppendorf® Easypet® pipetting aid	Eppendorf, Hamburg, Germany
Eppendorf® Multipette® Plus	Eppendorf, Hamburg, Germany
Eppendorf™ 5424 Microcentrifuge	Eppendorf, Hamburg, Germany
Gel Doc™ XR+ Gel Documentation System	BioRad Laboratories, Munich, Germany
Heatable magnetic stirrer	IKA-Werke, Staufen, Germany
HeraCell 240 CO_2 Incubator	Heraeus, Hanau, Germany
Herasafe™, Biological Safety Cabinet	Heraeus, Hanau, Germany

Hettich MIKRO 200 tabletop microliter centrifuge	Hettich, Tuttlingen, Germany
Ice machine	Scotsman, Vernon Hills, USA
Laboratory balance	Kern & Sohn, Balingen-Frommern, Germany
Laboratory freezer -20 °C	Liebherr-International, Biberach an der Riß, Germany
Laboratory freezer -80 °C	Gesellschaft für Labortechnik, Burgwedel, Germany
Laboratory precision balance	Sartorius Lab Instruments, Göttingen, Germany
Laboratory refrigerator 4-8 °C	Liebherr-International, Biberach an der Riß, Germany
Leica SP5 Confocal microscope	Leica Biosystems, Nußloch, Germany
Megafuge 2.0RS	Heraeus, Hanau, Germany
Multipette® (X)stream	Eppendorf, Hamburg, Germany
Multitron II incubation shaker	INFORS AG, Bottmingen, Switzerland
NanoDrop™ 1000 Spectrophotometer	Thermo Scientific, Karlsruhe, Germany
Neubauer cell counting chamber/hemocytometer	Paul Marienfeld GmbH & Co. KG, Lauda-Königshofen, Germany
Olympus Virtual Slide System VS120	Olympus, Hamburg, Germany
Orion Microplate Luminometer	Berthold Detection Systems, Pforzheim, Germany
pH Electrode	WTW, Xylem Analytics Germany, Weilheim, Germany
pH Meter	WTW, Xylem Analytics Germany, Weilheim, Germany
Provit 2200 Autoclave	Holzner, Nußloch, Germany
Sequenza™ Slide Rack and Coverplate™ system	Thermo Scientific, Karlsruhe, Germany
Sonoplus UW 2070	BANDELIN electronic, Berlin, Germany
Sorvall™ Primo™ Benchtop Centrifuge	Thermo Scientific, Karlsruhe, Germany
Sunrise™ Microplate Reader	Tecan Deutschland, Crailsheim, Germany

Thermomixer compact	Eppendorf, Hamburg, Germany
Titramax 100 microplate shaker	Heidolph Instruments, Schwabach, Germany
Trans-Blot® SD Semi-Dry Transfer Cell	BioRad Laboratories, Munich, Germany
Transsonic T460	Elma Schmidbauer, Singen, Germany
Vortex-Genie 2	Scientific Industries, Bohemia, USA
Waterbaths	Gesellschaft für Labortechnik, Burgwedel, Germany
XCell II™ Blot Module	Invitrogen, Karlsruhe, Germany
XCell SureLock™ Mini-Cell	Invitrogen, Karlsruhe, Germany

2.1.3 Chemicals and Reagents

5% goat serum	Cell Signaling Technology, Leiden, Netherlands
Acetic acid	Merck, Darmstadt, Germany
Acetic anhydride	Carl Roth, Karlsruhe, Germany
Acetone	Merck, Darmstadt, Germany
Acrylamide	AppliChem, Darmstadt, Germany
Acrylamide 4K solution, 40%	AppliChem, Darmstadt, Germany
Agar-Agar	Carl Roth, Karlsruhe, Germany
Albumin	AppliChem, Darmstadt, Germany
Ammonium persulfate (APS)	AppliChem, Darmstadt, Germany
Ampicillin	AppliChem, Darmstadt, Germany
Blocking Reagent	Roche, Penzberg, Germany
Blotting Grade Non-Fat Dry Milk	BioRad Laboratories, Munich, Germany
CHAPS	Sigma-Aldrich, Munich, Germany
Chloramphenicol	AppliChem, Darmstadt, Germany
cOmplete™, EDTA-free Protease Inhibitor Cocktail	Roche, Penzberg, Germany
Di-sodium hydrogen phosphate ($Na_2HPO_4x2H_2O$)	Merck Chemicals, Schwalbach, Germany
DIG RNA Labeling Mix	Roche, Penzberg, Germany
Dithiothreitol (DTT)	AppliChem, Darmstadt, Germany

DNA Gel Loading Dye (6X)	Thermo Scientific, Karlsruhe, Germany
DPX Mountant for histology	Sigma-Aldrich, Munich, Germany
Eosin 1%, ethanol based	Morphisto, Frankfurt a. M., Germany
Ethanol absolute for molecular biology	AppliChem, Darmstadt, Germany
Ethylenediaminetetraacetic acid (EDTA)	AppliChem, Darmstadt, Germany
Formamide	Sigma-Aldrich, Munich, Germany
Glycerin	AppliChem, Darmstadt, Germany
Glycine	Merck, Schwalbach, Germany
Hematoxylin Solution, 5%	Morphisto, Frankfurt a. M., Germany
Heparin	Sigma-Aldrich, Munich, Germany
Hydrochloric acid (HCl)	Merck, Schwalbach, Germany
Hydrogen peroxide, 30%	Merck, Schwalbach, Germany
Isopropyl alcohol	AppliChem, Darmstadt, Germany
Kaiser's glycerol gelatine	Merck, Schwalbach, Germany
Kanamycin	AppliChem, Darmstadt, Germany
Levamisole	Sigma-Aldrich, Munich, Germany
Lipofectamine® 2000 Transfection Reagent	Invitrogen, Karlsruhe, Germany
Methanol, absolute	Carl Roth, Karlsruhe, Germany
NBT/BCIP Ready-to-Use Tablets	Roche, Penzberg, Germany
NP-40	Sigma-Aldrich, Munich, Germany
Orange DNA Loading Dye (6X)	Thermo Scientific, Karlsruhe, Germany
Pefabloc® SC	Roche, Penzberg, Germany
peqGOLD Universal-Agarose	PEQLAB Biotechnologie, Erlangen, Germany
Pierce™ ECL Western Blotting Substrate	Thermo Scientific, Karlsruhe, Germany
Potassium chloride (KCl)	Merck Chemicals, Schwalbach, Germany
Protein A Agarose	Roche, Penzberg, Germany
Restore™ Western Blot Stripping Buffer	Thermo Scientific, Karlsruhe, Germany
RNase AWAY™ Surface Decontaminant	Thermo Scientific, Karlsruhe, Germany
RNasin® Ribonuclease Inhibitor	Promega, Mannheim, Germany
Roti®-GelStain	Carl Roth, Karlsruhe, Germany
Roticlear®	Carl Roth, Karlsruhe, Germany
Saponin	Carl Roth, Karlsruhe, Germany

SignalStain® Antibody Diluent	Cell Signaling Technology, Leiden, Netherlands
SignalStain® DAB Substrate	Cell Signaling Technology, Leiden, Netherlands
Sodium chloride (NaCl)	Merck, Schwalbach, Germany
Sodium citrate	Carl Roth, Karlsruhe, Germany
Sodium Dodecyl Sulfate (SDS), Lauryl	ICN Labsolutions, Northeim, Germany
Sodium hydroxide (NaOH)	AppliChem, Darmstadt, Germany
SuperSignal™ West Pico PLUS Chemiluminescent Substrate	Thermo Scientific, Karlsruhe, Germany
Tetramethylethylenediamine (TEMED)	AppliChem, Darmstadt, Germany
Triethanolamine	Carl Roth, Karlsruhe, Germany
Tris	Carl Roth, Karlsruhe, Germany
Tris Base	AppliChem, Darmstadt, Germany
Triton X-100	AppliChem, Darmstadt, Germany
Tryptone	AppliChem, Darmstadt, Germany
Tween 20	AppliChem, Darmstadt, Germany
VECTASHIELD Mounting Medium with DAPI	Vector Laboratories, Burlingame, USA
XT Sample Buffer	BioRad Laboratories, Munich, Germany
Xylene	AppliChem, Darmstadt, Germany
Yeast extract	Sigma-Aldrich, Munich, Germany
Yeast t-RNA	Roche, Penzberg, Germany

2.1.4 Buffers and solutions

10x PBS	137 mM NaCl 2.7 mM KCl 100 mM Na_2HPO_4 * $2H_2O$ 2 mM KH_2PO_4 pH 7.4

TAE	40 mM Tris 20 mM Acetic acid 1 mM EDTA
10x TBS	500 mM Tris 1.5 M NaCl pH 7.6
1x TBS-T	10x TBS diluted 1:10 in ddH_2O 0.1% Tween 20
6x Loading dye	10 mM Tris-HCl, pH 7.6 60 mM EDTA 60% (v/v) glycerol 0.03% (w/v) Bromphenol blue filled up to 50 ml with ddH_2O
Citrate buffer	10 mM Sodium Citrate pH 6.0

Protein complex immunoprecipitation (Co-IP)

NP-40 lysis buffer	50 mM Tris-HCl 150 mM NaCl 1% NP-40 1 tablet of cOmplete™ Protease Inhibitor Cocktail to 50ml pH 8.0

Subcellular fractionation

RIPA buffer	50 mM Tris-HCl, pH 7.4 150 mM NaCl 1% Triton X-100 1% Sodium deoxycholate 0.1% SDS

	1 tablet of cOmplete™ Protease Inhibitor Cocktail to 50ml
CLB buffer	10 mM HEPES 10 mM NaCl 5 mM $NaHCO_3$ 1 mM $CaCl_2$ 0.5 mM $MgCl_2$ 5 mM EDTA pH 7.4
TSE buffer	10 mM Tris, pH 7.5 300 mM Sucrose 1 mM EDTA 0.1% NP-40
Western Blot	
Running buffer	25 mM Tris 0.2 M Glycine 0.1% (w/v) SDS
Transfer buffer	39 mM Glycine 48 mM Tris Ultra 0.04% SDS 20% Methanol
SDS lysis buffer	62.4 mM Tris, pH 6.8 2% SDS 10% Glycerol 50 mM DTT 0.01% Bromophenol blue
Cell lysis buffer	20 mM Tris Ultra 150 mM NaCl

	1 mM EDTA 1 mM EGTA 2.5 mM $Na_4P_2O_7$ 1% Triton X-100
Separating gel	7.5 ml Tris 2.5 M, pH 8.8 2.0 ml polyacrylamide, 40% 5.44 ml ddH_2O 0.05 ml APS, 10% (w/v) 10 µl TEMED
Stacking gel	0.5 ml Tris 0.5 M, pH 6.5 0.2 ml polyacrylamide, 40% 1.30 ml ddH_2O 0.01 ml APS, 10% (w/v) 2 µl TEMED

TOP/FOP luciferase reporter assay

Lysis buffer	1% (v/v) Triton X-100 25 mM Glycylglycine, pH 7.8 15 mM $MgSO_4$ 4 mM EGTA 1 mM DTT, added fresh store at 4 °C

Immunofluorescence

Fixation solution	Methanol/Acetone, 1:1, stored at -20 °C
IF blocking buffer	3% (w/v) BSA 1% (v/v) Triton X-100 1% (w/v) Saponin in PBS

Wash solution 1	3% (w/v) BSA 1% (w/v) Saponin in PBS
Wash solution 2	1% (w/v) Saponin in PBS

Murine genotyping

Laird's Buffer (Laird et al. 1991)	200 mM NaCl 100 mM Tris-Cl, pH 8.0 5 mM EDTA 0.2% SDS

In situ hybridization (Gregorieff and Clevers 2015)

DEPC-ddH_2O	0.1% diethyl pyrocarbonate in ddH_2O incubate overnight (fume hood), autoclave
DEPC-PBS (PBSo)	10x PBS 1:10 in 1l DEPC-ddH_2O
20x SSC	3 M NaCl 300 mM $C_6H_5Na_3O_7$ pH 7.0
Acetic anhydride solution	670 µl Triethanolamine 300 µl Acetic Anhydride ad 50 ml DEPC water pH 8.0 (~5 drops of 37% HCl)
Hybridization buffer	50% Formamide 5x SSC 2% Blocking Reagent

	5 mM EDTA 0.05% CHAPS 50 µg/ml Heparin 50 µg/ml Yeast t-RNA
Blocking buffer	0.5% Blocking Reagent
NTM buffer	0.1 M Tris, pH 9.5 0.05 M $MgCl_2$ 0.1 M NaCl
NBT/BCIP solution	10 ml NTM buffer 0.8 M Levamisole 1 NBT/BCIP Ready-to-Use Tablet

2.1.5 Media

Bacterial media

Luria-Bertani (LB)-Agar Plates	0.5% (w/v) NaCl 0.5% (w/v) Yeast extract 1.0% (w/v) Tryptone 1.5% (w/v) Agar-Agar pH 7.4 (with NaOH) autoclave, cool down to 50-60 °C, add antibiotics (e.g. 100 µg/ml ampicillin), pour culture plates, and store at 4 °C
Luria-Bertani (LB)-Medium	1.0% (w/v) NaCl 0.5% (w/v) Yeast extract 1.0% Tryptone pH 7.4 (with NaOH) autoclave, cool down to 50-60 °C, add

	antibiotics (e.g. 100 µg/ml ampicillin), and store at 4 °C
Cell culture media	
Complete growth medium	500 ml DMEM 50 ml FBS/FCS 5 ml penicillin (10,000 µg/ml) / streptomycin (10,000 µg/ml)

2.1.6 Kits

Dual-Luciferase® Reporter (DLR™) Assay System	Promega, Mannheim, Germany
GE Healthcare illustra™ GFX™ PCR DNA and Gel Band Purification Kit	GE Healthcare Europe, Freiburg, Germany
GenElute™ Mammalian Total RNA Miniprep Kit	Sigma-Aldrich, Munich, Germany
PureYield™ Plasmid Midiprep Kit	Promega, Mannheim, Germany
PureYield™ RNA Midiprep System	Promega, Mannheim, Germany
RNeasy Mini Kit	QIAGEN, Hilden, Germany
Wizard® Plus SV Minipreps DNA Purification System	Promega, Mannheim, Germany
Wizard® SV Gel and PCR Clean Up Kit	Promega, Mannheim, Germany

2.1.7 Enzymes

DNA-free™ DNA Removal Kit	Ambion/Invitrogen, Karlsruhe, Germany
GoTaq® Green Master Mix	Promega, Mannheim, Germany
KAPA SYBR® FAST Universal Kit	Kapa Biosystems, Wilmington, USA
M-MLV Reverse Transcriptase	Promega, Mannheim, Germany
Proteinase K	Merck Millipore, Darmstadt, Germany
Q5® High-Fidelity DNA Polymerase	New England BioLabs, Frankfurt, Germany

RNAse free DNase I	Roche, Penzberg, Germany
SP6 RNA Polymerase	Promega, Mannheim, Germany
T3 RNA Polymerase	Promega, Mannheim, Germany
T4 DNA Ligase	Promega, Mannheim, Germany
T7 RNA Polymerase	Promega, Mannheim, Germany
USB® FideliTaqTM PCR Master Mix (2X)	Affimetrix, Cleveland, USA

Name	**Recognition Site**	**Source**
EcoRI	G▼AATT C C TTAA▲G	*Escherichia coli* RY 13
HindIII	A▼AGCT T T TCGA▲A	*Haemophilus influenzae* Rd
NotI	GC▼GGCC GC CG CCGG▲CG	*Nocardia otitidis-caviarum*
SpeI	A▼CTAG T T GATC▲A	*Sphaerotilus natans* ATCC 13923
XhoI	C▼TCGA G G AGCT▲C	*Xanthomonas holcicola*

Table 1: Restriction endonucleases used in this study
All enzymes were concentrated at 10 U/µl, purchased from Promega (Mannheim, Germany), and stored at -20 °C.

2.1.8 Standard size ladders

BenchTop DNA Ladder, 100 bp / 1 kb	Promega, Mannheim, Germany
peqGOLD Protein-Marker V	PeqLab, Erlangen, Germany
Precision Plus Protein™ Dual Color Standards	BioRad, München, Germany

2.1.9 Oligonucleotides

hAXIN fwd	5'- TCTCCAGGCGAACGAGCCAG -3'
hAXIN rev	5'- ACTGGCCGATTCTTCCTTAG -3'

hLGR5 fwd	5'- ACCAACTGCATCCTAAACTG -3'
hLGR5 rev	5'- ACCGAGTTTCACCTCAGCTC -3'

Table 2: RNA-in situ hybridization (ISH) — probe generation from cDNA

T3	5'- GCAATTAACCCTCACTAAAGG -3'
T7	5'- TAATACGACTCACTATAGGG -3'
SP6	5'- ATTTAGGTGACACTATAG -3'

Table 3: RNA-in situ hybridization (ISH) — screening primers

mSox17 fwd	5'- TTGCCGAACACACAAAAGGAG -3'
mSox17 rev	5'- TGGAGGTGCTGCTCACTGTAAC -3'
Cre fwd	5'- CCTGGAAAATGCTTCTGTCCG -3'
Cre rev	5'- CAGGGTGTTATAAGCAATCCC -3'

Table 4: Primers for mouse genotyping

hRNF43 fwd	5'- CCTGTGTGTGCCATCTGTCT -3'
hRNF43 rev	5'- GCAAGTCCGATGCTGATGTA -3'
hGAPDH fwd	5'- GAAGGTGAAGGTCGGAGT -3'
hGAPDH rev	5'- GAAGATGGTGATGGGATTTC -3'

Table 5: Primers for qRT-PCR

2.1.10 Plasmids

Transient overexpression experiments		
pcDNA™4/TO	Mammalian Expression Vector for RNF43 constructs with CMV promoter, TetO2 sites, and Zeocin resistance; EcoRV – NotI cloning site	Invitrogen, Karlsruhe, Germany
RNF43 (wt)	RNF43 wild type, full-length; FLAG-tag; inserted by PCR subcloning using EcoRV – NotI restriction sites	(Loregger et al. 2015)
RNF43H292R	RNF43 with mutated RING domain (H292R + H295R), full-length; mutations introduced by site-directed mutagenesis using internal primers; FLAG-tag; inserted by PCR subcloning using EcoRV – NotI restriction sites	(Loregger et al. 2015)

Table 6: Plasmids for transient overexpression experiments

RNA-in situ hybridization (ISH)		
pCMV-SPORT6	Generation of in situ hybridization probes; T7 and SP6 promoter; CMV promoter; ampicillin resistance	Invitrogen, Karlsruhe, Germany
pGEM-T	Generation of in situ hybridization probes; T7 and SP6 promoter; ampicillin resistance	Promega, Mannheim, Germany

TOP/FOP luciferase reporter assay		
TOPFlash	ten wild-type binding sites for TCF/LEF; ampicillin resistance	(van de Wetering et al. 1997)
FOPFlash	ten mutated binding sites for TCF/LEF; ampicillin resistance	(van de Wetering et al. 1997)
Renilla	CMV promoter; ampicillin resistance	Promega, Mannheim, Germany

2.1.11 RNA-probes

Probe	**Insert (GenBank)**	**Vector**	**RE**	**Poly**	**Length**	**Origin**
hAXIN2	NM_004655, nt 2243-2960	pGEM-T	SpeI	T7	718	PCR from cDNA
hLGR5	NM_003667, nt 20-1018	pGEM-T	NotI	T7	508	PCR from cDNA
hOLFM4	NM_006418.4, nt 19-1886	pCR®4-TOPO®	HindIII	T3	1191	kindly provided by H. Clevers, Utrecht

hRNF43	NM_017763.4, nt 3824-4402	pOTB7	HindIII	T7	691	IMAGp958B231316Q
hSOX17	NM_022454.3, nt 1407-1825	pT7T3D-PacI	XhoI	T3	418	IMAGp998M071822Q
mAxin2	NM_015732.4, nt 3472-4256	pT7T3D-PacI	NotI	T7	798	IMAGp998A039161Q
mOlfm4	NM_001030294.1, nt 643-1458	pBluescript II SK(+)	NotI	T7	800	kindly provided by Hans Clevers, Utrecht
mRnf43	NM_172448, nt 2701-4267	pCMV-Sport6	EcoRI	T7	1567	subcloned from RZPD: DKFZp781H0392Q3
mSox17	NM_011441.5, nt 2535-3616	pT7T3D-PacI	HindIII	T7	1081	IMAGp998H098336Q

Table 7: RNA-in situ hybridization probes
nt= nucleotides; RE= Restriction enzyme to linearize plasmid for anti-sense probe; Poly= RNA Polymerase to transcribe anti-sense probe; Length in base pairs; origin= I.M.A.G.E. EST clone (imagens GmbH, Berlin, Germany; now Source Bioscience) or as stated otherwise.

2.1.12 Antibodies

Primary antibodies		
Anti-β-Actin, monoclonal mouse, 8H10D10	WB 1:5000	New England BioLabs, Frankfurt, Germany
Anti-Calnexin, rabbit polyclonal, H-70	WB 1:1000	Santa Cruz, Heidelberg, Germany

Anti-CDC5L, rabbit polyclonal	WB 1:500	Sigma-Aldrich, Munich, Germany
Anti-β-Catenin, monoclonal mouse, 14/Beta-Catenin	WB 1:1000 IF 1:300 IHC 1:400	BD Bioscience, Heidelberg, Germany
Anti-non-phospho-β-Catenin (Ser33/37/Thr41), polyclonal rabbit	WB 1:1000	Cell Signaling Technology, Leiden, Netherlands
Anti-phospho-β-Catenin (Ser33/37/Thr41), polyclonal rabbit	WB 1:1000	Cell Signaling Technology, Leiden, Netherlands
Anti-FLAG®, monoclonal mouse, M2	WB 1:1000 IF 1:300 IP 1:170	Sigma-Aldrich, Munich, Germany
Anti-FLAG®, polyclonal rabbit	IF 1:300	Sigma-Aldrich, Munich, Germany
Anti-HA, polyclonal rabbit	IF 1:300	Sigma-Aldrich, Munich, Germany
Anti-mouse-IgG	IP 1:170	Santa Cruz, Heidelberg, Germany
Anti-rabbit-IgG	IP 1:170	Santa Cruz, Heidelberg, Germany
Anti-Ki67, monoclonal mouse, MIB-1	IHC 1:150	Dako, Glostrup, Denmark
Anti-RNF43, polyclonal rabbit	WB 1:500	LifeSpan BioSciences, Seattle, USA
Anti-RNF43, polyclonal rabbit	IHC 1:1000	Atlas Antibodies AB, Bromma, Sweden
Anti-RNF43, rat monoclonal, 8D6	WB 1:500	M. Grandl (our group) & E. Kremmer, TUM
Anti-TCF4, mouse monoclonal, 6H5-3	IHC 1:300	Merck Millipore, Darmstadt, Germany

Anti-TCF4, rabbit monoclonal, C9B9	WB 1:1000 IP 1:170	Cell Signaling Technology, Leiden, Netherlands
Anti-α-Tubulin, monoclonal mouse, B-7	WB 1:1000	Santa Cruz, Heidelberg, Germany

Table 8: Primary antibodies used in this study

Secondary antibodies — conjugated for Western Blot		
Anti-mouse IgG HRP Conjugate	WB 1:3000	Promega, Mannheim, Germany
Anti-rabbit IgG HRP Conjugate	WB 1:3000	Promega, Mannheim, Germany
Anti-rat IgG HRP Conjugate	WB 1:3000	Dako, Glostrup, Denmark

Table 9: Secondary antibodies — conjugated for Western Blot

Secondary antibodies — conjugated for Immunofluorescence		
Anti-mouse IgG, Alexa Fluor 488, polyclonal goat	IF 1:300	Invitrogen, Karlsruhe, Germany
Anti-rabbit IgG, Alexa Fluor 594, polyclonal chicken	IF 1:300	Invitrogen, Karlsruhe, Germany

Table 10: Secondary antibodies — conjugated for Immunofluorescence

Antibody — conjugated for in situ hybridization		
Anti-Digoxigenin-AP, Fab fragments	ISH 1:2000	Roche, Penzberg, Germany

2.1.13 Cell culture

Fetal Bovine Serum, heat inactivated (FBS/FCS)	Invitrogen, Karlsruhe, Germany
Gibco® DMEM	Invitrogen, Karlsruhe, Germany
Gibco® Optimem	Invitrogen, Karlsruhe, Germany
Gibco® PBS, pH 7.4, sterile	Invitrogen, Karlsruhe, Germany
Gibco® Trypan Blue Solution, 0.4%	Invitrogen, Karlsruhe, Germany

Gibco™ Penicillin-Streptomycin (10,000 U/ml)	Invitrogen, Karlsruhe, Germany
Trypsin / EDTA (0.04% / 0.03%)	Promo Cell, Heidelberg, Germany

2.1.14 Cell lines

AGS	gastric adenocarcinoma	ATCC® CRL-1739 (Barranco et al. 1983)
HCT116	colorectal carcinoma	ATCC® CCL-247 (Brattain et al. 1981)
KATOIII	gastric signet ring cell carcinoma	ATCC® HTB-103TM (Sekiguchi, Sakakibara, and Fujii 1978)
MKN45	poorly differentiated gastric adenocarcinoma	RCB1001 (Motoyama, Hojo, and Watanabe 1986)
MKN7	tubular gastric adenocarcinoma	RCB0999 (Motoyama, Hojo, and Watanabe 1986)
NCI-N87	well differentiated gastric adenocarcinoma	ATCC® CRL-5822 (Park et al. 1990)
NUGC4	gastric signet ring cell carcinoma	RCB1939 (Yokoyama et al. 1986)
ST23132	well differentiated gastric adenocarcinoma	(Vollmers et al. 1993)
ST2957	well differentiated gastric adenocarcinoma	(Vollmers et al. 1993)
ST3051	well differentiated gastric adenocarcinoma	(Vollmers et al. 1993)

Table 11: Human cancer cell lines used in this study.

2.1.15 Human Samples

Anonymized paraffin-embedded human tissue samples to include normal gastric and colonic mucosa, adenomas, and carcinomas were obtained from the archives of the

Institut für Pathologie, Klinikum Bayreuth, Germany, after approval of the local ethics committee.

Patients to be evaluated and treated for the GAPPS phenotype were enrolled into an institutional review board approved protocol (CCR NCI-09-0079) including written informed consent covering genetic testing and use of obtained tissue samples for research.

2.1.16 Mouse models

2.1.16.1 Conditional mouse model *Sox17* $^{fl/fl}$

Sox17 $^{fl/fl}$ mice were originally constructed by Dr. Sean J. Morrison's group at University of Michigan, now UT Southwestern (Kim, Saunders, and Morrison 2007) to investigate transcriptional programs of fetal and adult hematopoietic stem cells. The *Sox17* gene was targeted by a 'targeting vector' containing the *Sox17* coding sequence flanked by loxP sites as well as a FRT flanked neomycin cassette for subsequent positive selection. Then Flp-recombinase was used to remove the neo cassette. LoxP sites were placed such that they did not disturb any potential conserved regulatory elements. Upon recombination of loxP sites the entire coding sequence of *Sox17* is removed.

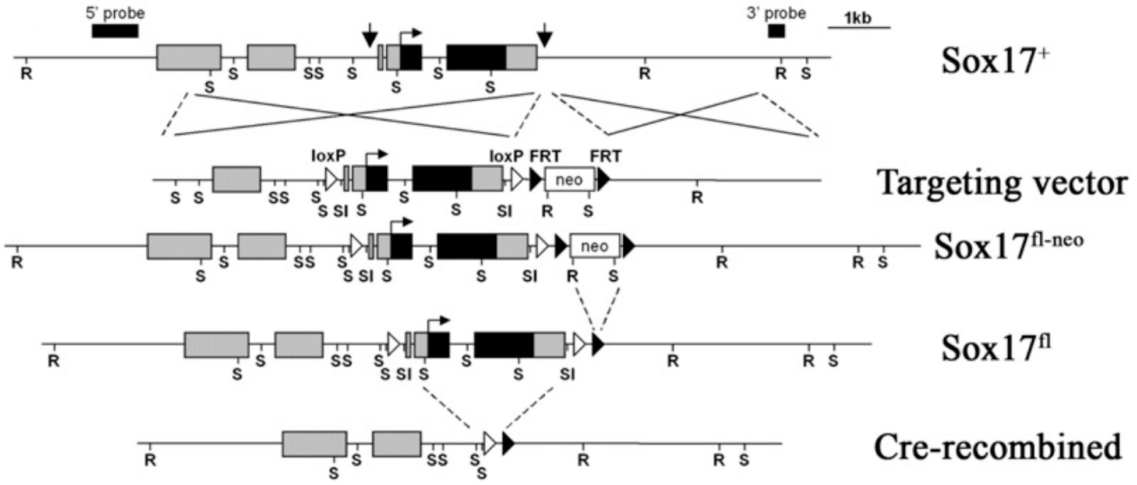

Figure 4: Generation of Sox17 $^{fl/fl}$ mice.
Fl= flanked by LoxP sites; loxP= LoxP sequence; Frt= flippase recognition target; neo= neomycin cassette; black boxes= coding sequence of *Sox17*. Adapted with permission from Kim, Saunders, and Morrison 2007. Copyright 2007 Elsevier.

2.1.16.2 Conditional mouse model *Cdh1* $^{fl/fl}$

Cdh1 $^{fl/fl}$ mice were created by Prof. Rolf Kemler's group at the Max Planck Institute of Immunobiology and Epigenetics, Freiburg to study E-cadherin's function in lactating mouse mammary gland (Boussadia et al. 2002). Exons 6-10 of the *Cdh1* gene are flanked by loxP sites and removed upon Cre-recombination.

2.1.16.3 Conditional mouse model *Hsp60* $^{fl/fl}$

Hsp60 $^{fl/fl}$ mice were created by Taconic-Artemis (Cologne, Germany) in close consultation with Prof. Dirk Haller's group (ZIEL — Institute for Food & Health, TUM). The construct contains loxP sites flanking exons 4-8 of the *Hsp60* gene, thereby removing the coding sequence for the chaperone's ATPase domain upon Cre mediated recombination (Berger et al. 2016).

2.1.16.4 Cre expressing mice — *Villin*-Cre and *Villin*-Cre-ER^{T2}

In all breedings, care was taken to maintain Cre mouse lines in a hemizygous state for the Cre transgene. The *villin* promoter was shown to exhibit exclusive activity in small and large intestinal mucosa and epithelia of proximal renal tubules (Pinto et al. 1999). It was used to serve as tissue specific promoter to drive Cre recombinase expression (el Marjou et al. 2004). *Vil*-Cre was shown to induce durable recombination in small and large intestine, indicating that intestinal progenitor cells were also targeted. The *vil*-Cre is constitutively transcribed from E9 in visceral endoderm and E12.5 in the intestinal epithelium.

To control the timing of recombination, a tamoxifen inducible Cre-ER^{T2} was put under the promoter of villin: *vil*-Cre-ER^{T2}. Tamoxifen can be administered via different routes, e.g. intraperitoneal injections (like in collaborative project Schneider et al. 2010) or fed in the form of pellets (like in collaborative project Berger et al. 2016) and only then Cre is expressed and induces recombination.

2.1.17 Software

Axiovision 4.8	Carl Zeiss, Oberkochen, Germany
BioRad CFX Manager	BioRad Laboratories, Munich, Germany
ChemoStar analysis software	INTAS Science Imaging Instruments, Göttingen, Germany
Fiji 1.0	imagej.net
GIMP 2.8.22	www.gimp.org
LAF-AS	Leica Biosystems, Nußloch, Germany
Microsoft Excel for Mac 15.41	Microsoft Germany, Munich, Germany
Microsoft PowerPoint for Mac 15.41	Microsoft Germany, Munich, Germany
Microsoft Word for Mac 15.41	Microsoft Germany, Munich, Germany
Molecular Imager Gel Doc XR+System	BioRad Laboratories, Munich, Germany
NanoDrop ND-1000 V38.1	Thermo Scientific, Karlsruhe, Germany
Photoshop CS6	Adobe Systems, San Jose, USA
Prism 5	GraphPad Software, La Jolla, USA
QuPath 0.1.2	qupath.github.io (Bankhead et al. 2017)

2.2 Microbiological methods

2.2.1 Sterilization of consumables, glassware, solutions, media, and S2 waste

Autoclavable consumables, glassware, self-made solutions, and media as well as S2 laboratory waste were steam sterilized at a minimum of 121 °C at 2 bar for at least 20 min. If non-autoclavable media or solutions needed to be sterilized, filters of 0.45 µm or 0.20 µm pore size were employed to eliminate bacteria or viruses, respectively.

2.2.2 Culture and storage of E. coli strains

E. coli chemically competent cells (e.g. DH5α) and transformed E. coli cells were grown in LB broth media with antibiotics at 37 °C and 150 rpm on a bacterial incubation shaker overnight. Antibiotics were added according to specific plasmid-encoded antibiotic resistance genes (e.g. 100 µg/ml Ampicillin, 25 µg/ml Chloramphenicol, or 25 µg/ml Kanamycin) from a 1000:1 stock solution. After bacterial growth was visually confirmed by turbidity of LB broth media, the bacterial suspension was centrifuged for 5 min at 5000 rpm, and the supernatant decanted. The bacterial pellet was carefully resuspended in remaining minimal volumes of media by pipetting, plated on LB agar plates with corresponding antibiotics, and grown overnight at 37 °C.

Next day, single colonies were picked and regrown in 5 ml (e.g. for DNA Mini preparation or colony PCR) or 100 ml (e.g. DNA Midi preparation) of LB broth media containing appropriate antibiotics.

Glycerol stocks of competent cells were prepared for long-term storage. 800 µl of overnight bacterial culture grown in LB broth media with corresponding antibiotics were thoroughly mixed by pipetting with 200 µl of 80% glycerol. (The pipet tip can be trimmed with sterile scissors to allow for easier mixing.) The glycerol stock was immediately dipped in liquid nitrogen and transferred to a -80 °C freezer for long-term storage.

2.2.3 Transformation of chemical competent cells

A 50 µl aliquot of chemical competent cells (e.g. E. coli DH5α) was retrieved from storage at -80 °C, thawed on ice, mixed with 100 ng of plasmid DNA, and incubated on ice for 10 min. The cells were exposed to a heat shock of 42 °C for 45 sec and immediately put back on ice to cool down for 5 min. 900 µl of 37 °C warm LB medium without antibiotics were added and cells incubated on a bacterial shaker at 37 °C for 60 min to allow for transcription of plasmid-encoded antibiotic resistance genes. Subsequently, the bacterial suspension was centrifuged at 4500 rpm for 10 min at room temperature and the supernatant decanted. The bacterial pellet was carefully resuspended in remaining minimal volumes of media by pipetting, plated on LB agar plates with corresponding antibiotics, and grown overnight at 37 °C.

2.3 Molecular biological methods

2.3.1 Plasmid DNA preparation from overnight cultures

Depending on the need of downstream applications either Mini or Midi preps were performed with input overnight culture volumes of 5 ml or 100 ml, respectively. Bacteria were harvested by centrifugation at 4000 rpm for 5 min. The supernatant was discharged and subsequent steps performed using the Wizard® Plus SV Minipreps DNA Purification System (Promega) and PureYield™ Plasmid Midiprep Kit (Promega), which are silica membrane-based systems, according to the manufacturer's instructions. In brief, transformed bacteria were thoroughly resuspended, lysed, and treated with an alkaline protease solution. This was followed by centrifugation, transfer of cleared lysate onto columns, washing, and endotoxin removal steps. The Miniprep was exclusively performed by micro centrifugation whereas the Midiprep was achieved by vacuum using Promega's vacuum pump, vacuum manifold, and Eluator™ Vacuum Elution Device. Nuclease-free water was warmed to 65 °C before applying to elution columns in order to achieve higher DNA yields. DNA was eluted in 30-50 µl nuclease-free water for Minipreps or 400-600 µl for Midipreps. Volumes were adjusted depending on specific downstream needs and expected yields. DNA concentration was measured with the

NanoDrop instrument (Thermo Scientific). Isolated plasmid DNA was stored at 4 °C for short-term usage or at -20 °C long-term.

At times, it was necessary to further purify or concentrate the recovered plasmid DNA. Ice-cold 100% Isopropanol was added at 0.6-0.7 volumes for precipitation of purified plasmid. Optionally the mix was stored at -20 °C overnight. Next, maximum speed centrifugation was carried out in a pre-cooled centrifuge at -4 °C. The pellet was washed at least once in 70% ethanol, resuspended, and again centrifuged. Ethanol was carefully and completely removed. Residual ethanol was vaporized either at room temperature or briefly at 37 °C on a thermo mixer. The pellet was resuspended in 30 µl of nuclease-free water.

2.3.2 RNA isolation from mammalian cell lines

Total RNA was isolated from a wide range of gastric cancer cell lines (**Table 11**) to determine the basal expression of RNF43. Cell lines were seeded at $3x10^5$ cells in 6-well plates and incubated overnight at 37 °C. Growth and viability were judged by microscopic examination before proceeding with cell lysis. For adherent cell lines, medium was removed and cells were washed in 1x PBS. After 1-2 min of incubation in 300 µl of lysis buffer, which contained guanidine thiocyanate and 2-mercaptoethanol to inactivate RNases, cells were lysed with cell scrapers. Cells growing in suspension where pelleted by centrifugation for 5 min at 300 × g and resuspended in lysis buffer. The resulting cell lysates were further processed with the GenElute™ Mammalian Total RNA Miniprep Kit (Sigma-Aldrich) according to the manufacturer's instructions. In brief, cellular debris was removed using a filtration column. The flow-through was mixed with equal amounts of 70% ethanol and loaded onto a silica-based binding column. After three washing steps, RNA was eluted in 30 µl of RNase-free water and stored at -80 °C until further use.

2.3.3 DNA digestion of RNA preparations

Carried-over contaminating genomic DNA was removed from RNA preparations using the DNAfree™ kit (Ambion) following the manufacturer's instructions. RNA samples were mixed with 0.1 volume of 10X DNase I Buffer and 1 µl of rDNase I followed by incubation at 37 °C for 25 min. DNase Inactivation Reagent was added at 0.1 volumes to

inhibit rDNase I and remove divalent cations from the sample. After incubation for 2 min samples were centrifuged at 13,000 rpm and the supernatant fraction transferred into a fresh microcentrifuge tube.

2.3.4 Assessing nucleic acid concentration and purity

DNA and RNA concentrations were assessed with a NanoDrop ND-1000 spectrophotometer (Thermo Scientific) loading a sample of 1.5 µl plasmid DNA or RNA. Absorbance was measured at a wavelength of 260 nm (A260) and 280 nm (A280). Sample concentrations were provided based on the measurement at 260 nm. The ratio of sample absorbance at 260 nm to 280 nm was given as a surrogate of DNA and RNA purity. Ratios in the range of 1.8-2.0 would indicate a good sample with very little protein contamination.

2.3.5 Reverse Transcription

For cDNA synthesis, total RNA of cultured cells was reverse-transcribed with M-MLV (Moloney Murine Leukemia Virus) Reverse Transcriptase, RNase H Minus, point mutant (Promega) following the manufacturer's instructions. 1 µg of RNA and 1 µl of random primers (150 ng/µl) were mixed in a final volume of 14 µl (filled up with RNase-free water). This RNA-primer mix was incubated at 70 °C for 5 min and then immediately placed on ice for 5 min. Then 5 µl M-MLV RT 5X Reaction Buffer, 1.25 µl of PCR Nucleotide Mix (dNTP), and of 1 µl M-MLV RT (H–) enzyme were added with nuclease-free water to a final volume of 25 µl. cDNA synthesis was carried out at RT for 10 min followed by 50 °C for 50 min. The reaction was inactivated by heating to 70 °C for 15 min. The resulting cDNA was stored at -20 °C. The identical reaction mix without M-MLV RT (H–) enzyme was run as a negative control to monitor possible carryover of DNA.

2.3.6 Quantitative Real-time PCR (qRT-PCR)

Quantitative Real-time PCR was performed to determine the levels of baseline *RNF43* expression (primer sequences in **Table 5**) using the KAPA SYBR® FAST qPCR

Universal Master Mix (Kapa Biosystems), which includes an engineered Taq DNA polymerase to reduce non-specific products like primer-dimers, and SYBR Green I, a fluorescent dye that emits a signal upon binding of double-stranded DNA. qRT-PCR was carried out on a BioRad CFX384 system (BioRad).

The reaction mix per well was optimized to require less reagent input and contained 5 µl of KAPA SYBR® FAST qPCR Master Mix (2x), 0.5 µl of each forward and reverse primer [10 µM], and 4 µl of cDNA template [50 ng/µl]. All samples were run in triplicates. Additionally, reverse transcriptase-free and template-free samples were assessed as negative controls in each run.

The PCR reaction was started with an enzyme activation step at 95 °C for 3 min, followed by 40 cycles of denaturation at 95 °C for 15 sec, annealing at 60 °C for 10 sec, and melting curve analysis in 0.5 °C steps per sec from 60-95 °C. The instrument was halted at 12 °C. *RNF43* expression was normalized to expression of the housekeeping gene *GAPDH* using the ΔCT method (Livak and Schmittgen 2001):

relative mRNA expression = $2^{\Delta CT\ (RNF43\text{-}GAPDH)}$

2.3.7 Gel electrophoresis

Agarose gel electrophoresis was used to separate DNA fragments based on their size. Gels were prepared freshly by heating and dissolving 1-2% (w/v) agarose in 1x TAE in a microwave. Once it was visually confirmed that the agarose had completely dissolved, the solution was cooled down under running tap water. 5 µl Roti®-Safe were added to 100 ml of agarose solution before it was poured into a gel chamber. A gel comb to create sample loading pockets was placed into the hardening gel. Once firmness was achieved, the comb was carefully removed, the gel transferred into an electrophoresis chamber and submerged into 1x TAE buffer. 6x loading dye was added to samples before transferring them into the gel pockets. Electrophoresis was carried out at 90-100 V for 30-70 min depending on DNA fragment size and agarose concentration.

Illumination with ultraviolet light of a wavelength of 302 nm enabled detection of DNA fragments. Gel imaging was performed with the Gel Doc™ XR+ Gel Documentation System (BioRad Laboratories).

For extraction, DNA fragments were cut with DNA Pick-up Tips (SLG) and subsequently purified with the Wizard® SV Gel and PCR Clean Up Kit (Promega) according to the

manufacturer's instructions. DNA was eluted in 30 µl of nuclease-free water and stored at -20 °C.

2.3.8 Restriction digest of DNA

Plasmid DNA and PCR fragments were digested with restriction endonucleases supplied by Promega (**Table 1**). Typically, 1 µg of DNA was mixed with 10x Buffer, and 10 units of restriction enzyme(s) to a total volume of 20 µl to 50 µl. Restriction enzymes were kept on ice, added last to the reaction mix, and thoroughly mixed by pipetting up and down. Incubation was carried out at 37 °C on a thermoshaker for 1 h, if needed longer. Completeness of digestion was verified by agarose gel electrophoresis and digestion products extracted and purified as needed with the illustra GFX PCR DNA and Gel Band Purification Kit (GE Healthcare) following the manufacturer's instructions.

2.3.9 Colony PCR

Transformed bacteria were screened by Colony PCR for the presence and orientation of respective inserts. Usually a pair of one insert specific primer and one of two primers on opposing sides of the multiple cloning site were used (**Table 3**). Single colonies of transformed. E. coli bacteria where picked with a sterile pipette tip which was then swirled in 20 µl of nuclease free water. 5 µl of that suspension were subsequently used as a template for PCR. A master mix of 12.5 µl (GoTaq® Green Master Mix, Promega), each 1 µl forward and reverse primer [10 µM], and 5.5 µl nuclease free water was prepared and the bacterial solution added. PCR was performed following standard conditions: an extended initial denaturation to destroy bacteria and release plasmid DNA at 95 °C for 5 min, followed by 36 cycles of denaturation at 95 °C for 30 sec, annealing at 56 °C for 30 sec, and extension at 72 °C for 2 min. This was followed by a final extension at 72 °C for 5 min and a final hold at 12 °C.

Resulting PCR products were subjected to agarose gel electrophoresis which provided a convenient readout to determine presence and size of the cloned insert.

2.3.10 Sanger sequencing

Sequences of all purchased plasmids and self-made constructs were verified by commercial Sanger sequencing services (MWG Eurofins, Ebersberg). Samples were prepared according to the company's instructions with a plasmid DNA concentration of 50-100 ng/µl in a total sample volume of 15 µl. If none of the company's provided sequencing primers was suitable, 30 pmol of an own sequencing primer were added.

2.4 Cell culture methods

2.4.1 Culturing of cell lines

A list of cell lines used can be found in **Table 11**. Routinely, cells were grown in cell culture flasks of 25 cm^2 or 75 cm^2 in 7 ml or 13 ml of DMEM — Dulbecco's Modified Eagle Medium (Gibco®, Invitrogen), supplemented with 10% Fetal Calf Serum (Thermo Scientific), 1x Penicillin-Streptomycin (Gibco®, Invitrogen), and grown at 37 °C in an atmosphere of 5% CO_2 and 90% humidity. Cells were monitored daily for vitality and growth and routinely monitored by PCR for mycoplasma contamination.
Before reaching confluence, cells were split at 1:5-10 and subcultured. Media was removed and cells were washed in 5 ml of DPBS — Dulbecco's phosphate-buffered saline (Gibco®, Invitrogen), followed by trypsinization with 1.0 ml of 0.25% Trypsin-EDTA (Promo Cell) at 37 °C and 5% CO_2 for approximately 10 min and longer if needed. Cells were detached and collected by applying repeat washes of 6 ml of DMEM/10% FCS that also stopped the trypsinization reaction. The solution was centrifuged in a 15 ml falcon tube at 1000 rpm for 5 min, the supernatant discarded, and the pellet resuspended in 5 ml DMEM/10% FCS. A fraction of that volume, typically 0.5-1 ml, was transferred to a new cell culture flask and remaining cells were used for subsequent experiments or appropriately disposed.

2.4.2 Cell counting

Cells were manually counted using a Neubauer cell counting chamber/hemocytometer. After trypsinizing cells, 10 µl of cell suspension were mixed with 90 µl of the vital stain

Trypan blue (Gibco®, Invitrogen) that is able to penetrate cell membranes of dead cells and thereby selectively stain those. The cell counting chamber was thoroughly cleaned with 70% ethanol, air dried, and 10 µl of the Trypan blue cell suspension were evenly applied. Its four large peripheral quarters were counted under the microscope using a tally counter and only taking into account cells that are within the quadrants or sitting on the top and left lines. The mean cell number of unstained and thereby vital cells was calculated and multiplied by 10^4 to provide the number of cells per ml since the chamber's volume is 0.1mm (depth) x 1 mm^2 (grid area) which equals 0.1 mm^3 or 0.1 µl. Because cells were initially diluted at 1:10 in Trypan blue, a final multiplication by 10 provided the number of cells in the original cell suspension.

2.4.3 Freezing and thawing of cell lines

To preserve cells at low passage numbers cells were grown, aliquoted, frozen, and stored in liquid nitrogen at -190 °C. This was repeated once initial stocks were being consumed. Cell lines were grown and trypsinized before reaching confluence, centrifuged at 1000 rpm for 5 min, and the pellet resuspended in 9 ml of fresh DMEM/10% FCS + P/S. Subsequently 900 µl of cell suspension were added to Nalgene™ cryotubes (Thermo Scientific) prefilled with ice-cold 100 µl DMSO (dimethyl sulfoxide). This allowed for preparation of ten aliquots, which were frozen in a stepwise fashion, initially left on ice for a few minutes, then transferred to a freezer at -80 °C, and ultimately after 1-3 days moved into liquid nitrogen at -190 °C.

To thaw cell lines, 10 ml of DMEM/10% FCS were pre-heated to 37 °C in 15 ml falcon tubes. Cells in cryotubes were partially thawed in a water bath at 37 °C and immediately transferred to pre-heated media. Cells were pelleted at 1000 rpm for 5 min, resuspended in 1 ml of cell culture medium, and seeded into 25 cm^2 cell culture flasks prepared with 6 ml of medium.

2.4.4 Paraffin cell pellets

First, cells were grown in 10 cm^2 cell culture dishes and washed once with 1x PBS. Next, 1-5 ml of PBS were added, cells gently scraped to avoid cell lysis, and transferred to several microcentrifuge tubes. Centrifugation was performed at 1200 rpm for 5 min. If

resulting pellet size was in excess of 50 µl it was resuspended and distributed over more microcentrifuge tubes. PBS was decanted and 4% PFA added. After a centrifugation step at 1200 rpm for 5 min the pellets were fixed in 4% PFA for at least 48 h at RT. Next, PFA was removed and pellets were dehydrated by incubation in 1 ml of 50%, 70%, 96%, and absolute ethanol for at least 1 h at RT. Incubation in absolute ethanol was performed three times and left overnight. To maintain pellet integrity as best as possible a centrifugation step after each ethanol exchange was added at 1500 rpm for 1 min. The following day, 1 ml of xylene was added, incubated for 2 h, and changed at least three times. About half of xylene was removed. The pellet was transferred with the remaining xylene into a metallic embedding cassette. Liquid paraffin was added followed by incubation at 65 °C overnight. Next day, the liquid paraffin was exchanged and the metallic embedding cassette put on ice while making sure that the pellet was evenly aligned at the bottom of the well as the paraffin hardened. Subsequently, the paraffin block was removed from the metallic embedding cassette and cut at 3.5 µm for immunohistochemical staining.

2.5 Protein biochemical methods

2.5.1 Protein complex immunoprecipitation (Co-IP)

For protein complex immunoprecipitation (Co-IP), AGS cells were seeded in 10 cm^2 cell culture dishes and grown to 70-90% confluence in DMEM/10% FCS without antibiotics. Then they were transiently transfected with 6 µg empty vector control (pcDNA4/TO) or FLAG-tagged RNF43 using the Lipofectamine® 2000 reagent (Invitrogen) according to the manufacturer's instructions.

After two days, cells were washed in PBS, chilled on ice, and lysed with 900 µl of NP-40 lysis buffer. Pre-clearing of cells was achieved by adding 50 µl of protein agarose A beads followed by incubation for 2 h at 4 °C on a rotating wheel. This was repeated once after a centrifugation step at maximum speed at 4 °C for 2 min.

1/10 of these raw lysates were set aside as controls, mixed with 3x SDS buffer, and frozen at -20 °C.

Next, raw lysates were transferred to fresh microcentrifuge tubes. Antibodies specific to the protein to be precipitated were added and samples incubated on a rotating wheel at 4 °C overnight. Subsequently, 50 µl of Protein agarose A were added and incubated for

at least 4 h at 4 °C on a rotating wheel. This was followed by centrifugation at 6000 rpm for 3 min at 4 °C. Supernatants were removed and Protein agarose A beads were thoroughly washed — 3x with lysis buffer and 2x with sterile PBS. Ultimately, 100 µl of 1x SDS buffer were added, lysates sub-boiled at 95 °C for 5 min, and frozen at -20 °C.

2.5.2 Subcellular fractionation

Subcellular fractionation separates nuclear, membranous and cytoplasmic compartments by differential centrifugation also using ultracentrifugation. To preserve integrity of samples all centrifuges should be pre-cooled and operated at 4 °C and samples should be kept on ice as much as possible. For optimal results a large number of cells is needed. Cells were therefore grown in 10 cm^2 cell culture plates in 10 ml DMEM/10% FCS at 37 °C overnight. Cells were harvested and counted to make sure that more than 1x 10^6 cells were collected before proceeding. Cells were washed in PBS and split into 1x10^6 cell aliquots followed by centrifugation at 3000 rpm for 5 min. The resulting pellet was resuspended in 100 µl CLB buffer with protease inhibitors (Protease Inhibitors Set and Pefabloc, Roche) and kept on ice for 5 min. Dissociation of cells was achieved by using glass dounce tissue grinders and douncing cells 50 times. Subsequently, the homogenate was centrifuged at 3000 rpm for 5 min at 4 °C.

The resulting supernatant (S1; membranes and cytoplasm) was taken off and stored in a new microcentrifuge tube on ice for later processing.

The remaining cell pellet (P1; nuclear fraction) was resuspended in 800 µl of TSE buffer with protease inhibitors and dounced 30 times followed by centrifugation at 3000 rpm for 5 min at 4 °C. The supernatant was discarded and the pellet washed in 800 µl of TSE buffer. After repeated centrifugation at 3000 rpm for 5 min at 4 °C the supernatant was discarded and the pellet was eluted in 100 µl of RIPA buffer with protease inhibitors and 0.1% SDS. 50 µl of 3x SDS were added to the sample followed by sub-boiling at 95 °C for 5 min. This sample containing the nuclear fraction was then stored at -20 °C.

Then the previously set-aside S1 fraction was further processed. First, it was ultracentrifuged at 39,000 g for 15 min at 4 °C. Only the top 100 µl of the supernatant (S2; cytoplasmic fraction) were mixed with 50 µl of 3x SDS, sub-boiled at 95 °C for 5 min, and stored at -20 °C. The pellet (P2; membranes) was resuspended in 50 µl of 1x SDS, sub-boiled at 95 °C for 5 min, and stored at -20 °C.

2.5.3 Western blot

2.5.3.1 Preparation of cell lysates

Cancer cell lines were seeded at 5 x 10^5 cells/well in 6-well plates, either transiently transfected with 0.5 µg of plasmid DNA with Lipofectamine 2000 or non-transfected. Growth medium was removed, cells washed in 1x PBS, and 100 µl of 1x SDS lysis buffer were added before cells were detached with a cell scraper. The lysate was transferred to 1.5 ml microcentrifuge tubes. Cells were either sonicated for 5 min in a chilled ultrasonic water bath (Transsonic T460, Elma Schmidbauer) or sonicated with an ultrasonic homogenizer (Sonoplus UW 2070, BANDELIN electronic; amplitude 30%, 10 sec) while on ice. The samples were sub-boiled at 95 °C for 5 min on a thermoshaker, cooled down on ice, briefly spun down, and loaded onto the polyacrylamide gel or frozen at -20 °C.

2.5.3.2 SDS-polyacrylamide gel electrophoresis (SDS-PAGE)

SDS-PAGE was used to separate proteins by molecular weight. Samples were run on polyacrylamide gels of 8-12% depending on protein size of interest. Separating and stacking gels were hand-made (see **2.1.4**). First, the separating gel solution was prepared and poured into a Novex® gel cassette (Invitrogen) and covered with isopropanol to prevent drying-out and to assure an even interface. After 1 h of polymerization the isopropanol was poured-off, the stacking gel solution added, and a gel comb carefully inserted while avoiding the creation of bubbles. After 1 h of polymerization the gels were wrapped in water-soaked paper towels, sealed in plastic bags, and stored at 4 °C for future use if not immediately used. Gels without combs were mounted in the XCell SureLock™ Mini-Cell Electrophoresis System (Invitrogen) which was filled to the top with 1x SDS running buffer. Samples were loaded into gel pockets with a Hamilton syringe. Usually electrophoresis was performed at 150 V and max. 300 mA for 1 h.

2.5.3.3 Western blot: Semi-dry or wet transfer

Proteins were blotted to nitrocellulose membranes (Whatman) by semi-dry or wet transfer. Semi-dry transfer was performed with the Trans-Blot® SD Semi-Dry Transfer

Cell (BioRad Laboratories) at 90 mA/cm^2 for 100 min in transfer buffer. Wet transfer was performed with the XCell II™ Blot Module (Invitrogen) at 2.5 mA/cm^2 for 60 min in transfer buffer. The efficacy of protein transfer was assessed by reversible staining with Ponceau S that was washed off by several rinses in water. Also, bands of the protein standard were marked with pencil on the membrane.

Unspecific binding sites were blocked by incubation in 1x TBS-T (TBS with 0.1% Tween 20) with 5% fat-free milk powder (BioRad Laboratories) at RT for at least 1 h. The membrane was briefly rinsed in TBS-T to removed excess blocking solution. The primary antibodies (**Table 8**) were diluted in 5% BSA in TBS-T and membranes were incubated at 4 °C overnight. Next day, membranes were washed three times in TBS-T for each 10 min. Secondary HRP (horseradish peroxidase)-conjugated antibodies (Table 9) were diluted in 1x TBS-T with 5% fat-free milk powder and membranes were incubated at RT for 1 h. Subsequently, membranes were washed six times in TBS-T for each 10 min.

About 2 ml of either Pierce™ ECL Western Blotting Substrate (Thermo Scientific) or if signal was weak SuperSignal™ West Pico PLUS Chemiluminescent Substrate (Thermo Scientific) were applied to the membranes. After incubation for 5 min in the dark, detection was either conventionally by x-ray films (Kodak) and the Curix 60 film processor (Agfa) or digitally with the CHEMOCAM Imager 3.2 (INTAS Science Imaging Instruments).

If additional proteins needed to be detected on the same membrane, membranes were stripped by incubation in Restore™ Western Blot Stripping Buffer (Thermo Scientific) for 15 min on a slowly-turning laboratory rocker after a brief wash in TBS-T. Stripping buffer was removed by three washes in TBS-T for each 10 min. The membranes were blocked again in 1x TBS-T with 5% fat-free milk powder at RT for at least 1 h and steps as outlined above repeated.

2.6 TOP/FOP luciferase reporter assay

AGS, HCT116, and MKN45 were seeded in 24-well plates at 10^5 cells / well in DMEM with 10% FCS + Penicillin-Streptomycin and incubated overnight at 37 °C and 5% CO_2. Different amounts of expression plasmids (RNF43-wt, RNF43-H292, or empty vector control; **Table 6**) were used with appropriate amounts of empty vector added to ensure that an equal amount of DNA was transfected.

In addition, cells were simultaneously cotransfected with two reporter plasmids. First, either 100 ng of pTOPFlash or pFOPFlash reporter gene plasmids kindly provided by Mark van de Wetering were added. The TOP/FOP assay was designed to assess signaling activity of the canonical Wnt pathway through its downstream transcription factor TCF4 (van de Wetering et al. 1997, Korinek et al. 1997). pTOPFlash contains ten wild-type binding sites for TCF/LEF (5'-CCTTTGATC-3') upstream of a Firefly luciferase under a minimal c-fos promoter. In parallel, pFOPFlash is run as a negative control with ten mutated binding sites for TCF/LEF (5'-CCTTTGGCC-3') to evaluate unspecific background luciferase activity.

To better account for experimental variations like transfection efficiency, proliferation, or cell viability but also technical issues like pipetting errors or incomplete cell lysis 10 ng of pCMV-Renilla, a reporter plasmid with Renilla luciferase under the control of the CMV promoter (Promega) were transfected. All experimental conditions were carried out in duplicates.

Cells were transiently transfected using the Lipofectamine® 2000 reagent (Invitrogen) according to the manufacturer's instructions. In brief, respective plasmid DNA (usually 100 ng of TOPFlash, 10 ng of FOPFlash, and variable amounts of experimental plasmid and empty vector) was diluted in 50 µl of minimal medium, Opti-MEM® I (Gibco®, Invitrogen) and gently mixed. In parallel, 1 µl of Lipofectamine® 2000 was diluted in 49 µl of Opti-MEM® I and incubated for 5 min at RT. DNA and Lipofectamine dilutions were mixed carefully at 1:1 to a total volume of 100 µl. This mix was incubated for 20 min at RT. Culture medium of cells was replaced with 100 µl Opti-MEM® I before 100 µl of DNA-Lipofectamine complexes were added in a drop-wise fashion directly to the cells. Cells were incubated overnight at 37 °C and 5% CO_2. Next day, 300 µl of fresh Opti-MEM® I was added.

After 48 h of incubation at 37 °C and 5% CO_2, cells were washed twice in 1x PBS, and excess fluid was carefully removed. Activities of Firefly and Renilla luciferases were measured using the Dual-Luciferase® Reporter Assay System (Promega) according to the manufacturer's instructions.

In brief, 100 µl of Passive Lysis Buffer (Promega) were added followed by at least 30 min incubation on a rocking platform. If needed the lysed cells could be stored at -20 °C for a few weeks. Occasionally, this step was performed to enhance cell lysis. Only after visual confirmation of cell lysis, 20 µl of lysate were transferred to a 96-well white round-bottom plate and protected from light exposure by wrapping in aluminum foil.

Assay readout was obtained on an Orion Microplate Luminometer (Berthold) equipped with an automated pipetting system. First, the substrate of the Firefly luciferase is added and the resulting luminescent signal measured. Next a reagent containing a quencher for the Firefly luciferase and the substrate for the Renilla luciferase is added followed by measurement of Renilla luciferase activity.

For each duplicate, Firefly luciferase activity was normalized to Renilla luciferase activity. The mean of the normalized duplicates was calculated and activities of pTOPFlash and pFOPFlash reporter constructs were reported as normalized relative light units compared to the mean normalized value of empty pTOPFlash vectors controls.

2.7 Immunofluorescence

AGS, HCT116, and MKN45 were transiently transfected with 500 ng of plasmid DNA with the Lipofectamine® 2000 reagent (Invitrogen) according to the manufacturer's instructions and grown directly on coverslips emerged in 500 µl of DMEM/10% FCS without antibiotics in 12-well plates overnight.

Media was removed, cells washed once in 1x PBS, followed by fixation and permeabilization in an ice-cold 1:1 mixture of methanol/acetone for 15 min. Methanol/acetone was removed and cells were washed three times in 1x PBS.

To decrease antibody binding to nonspecific epitopes, cells were blocked with IF blocking buffer for 15 min at RT. IF blocking buffer was removed. The primary antibodies were diluted in wash solution 1 (**Table 8**). 40 µl of antibody mix were applied to Parafilm (Bemis Company) in a drop-wise fashion, coverslips with adherent cells were put face down, and incubation was carried out in a humidified chamber at 4 °C overnight. Next day, cells were washed three times in wash solution 1 followed by incubation with the fluorochrome-conjugated secondary antibodies diluted in wash solution 1 (**Table 10**) for 60 min at RT in a light-tight box. The following steps were carried out with minimal light exposure to avoid fluorochrome fading.

This was followed by three washes in wash solution 2. Coverslips with adherent cells were mounted with Vectashield, a DAPI containing mounting media (Vector Laboratories) and flipped on glass coverslips (Menzel Gläser).

Confocal microscopy (Leica SP5) was usually performed immediately or after storage of up to 3 days at -20 °C.

2.8 Murine husbandry

2.8.1 Genotyping

For genotyping, about 2 mm of mouse tail tips at age 3-4 weeks were clipped and mice were numbered with ear punches. To each tip, 500 µl of Laird's Buffer (Laird et al. 1991) mixed with proteinase K (Merck Millipore) at 100 µg/ml were added. Tips were digested overnight at 56 °C in a thermoshaker at 750 rpm. Next day, samples were centrifuged at 15,000 rpm for 5 min at RT. The supernatant was transferred to a fresh microcentrifuge tube prefilled with 500 µl of isopropanol and inverted several times. Visible threads of DNA were fished with a sterile pipet tip and care was taken to transfer as little isopropanol as possible into a fresh tube of 200 µl nuclease free water. DNA was eluted on a thermoshaker at 37 °C, 250 rpm for several hours.
Genotyping PCR (primers in **Table 4**) was carried out with an initial denaturation step at 94 °C for 5 min, followed by 35 cycles of 94 °C for 30 sec, 58 °C (Cre) or 60 °C (Sox17) for 30 sec, and 72 °C for 30 sec. A final elongation step of 10 min at 72 °C was added.

2.8.2 Necropsy and tissue processing

Mice were mated overnight and a plug check was performed the next morning. When positive, this was regarded as embryonic day E0.5. Pregnant mice were sacrificed at indicated time points, killed by cervical dislocation, and embryos were extracted from the uterus and killed. Adult mice were killed by cervical dislocation.
Once mice were sacrificed, stomach, small intestine, and colon were immediately removed and separated from each other. To clean out luminal contents organs were gently flushed with ice-cold PBS using a subcutaneous syringe (25-gauge needle) and kept on Petri dishes placed on ice. Organs were longitudinally opened and intestines were rolled with the mucosa facing outwards in a so called ‘Swiss roll’ (Moolenbeek and Ruitenberg 1981). Tissues were fixed in 4% PFA overnight at 4 °C and for a maximum of 2 days to avoid overfixation. Tissues were then run on a tissue processor following a standard dehydration and paraffinization protocol (ASP 300 S, Leica Microsystems) and subsequently embedded in a paraffin block using a Leica tissue embedding station.

2.8.3 Ethics statement

The maintenance and breeding of mouse lines and all experiments were approved by the Committee on Animal Health and Care of the local government body of the state of Upper Bavaria (Regierung von Oberbayern; TVA 12-12 and TVA 214-13 for Berger et al. 2016, TVA 087/09 for Schneider et al. 2010, and TVA 55.2.1.54-2532-160-12 for own experiments) and performed in strict compliance with the EEC recommendations for the care and use of laboratory animals (European Communities Council Directive of 24 November 1986 (86/609/EEC)).

2.9 Histological methods

2.9.1 Hematoxylin and eosin stain (H&E)

FFPE tissues were cut at 3 µm, mounted on SuperFrost™ Plus slides (Menzel-Gläser), and baked in a hybridization oven at 60 °C for 20 min. This was followed by a standard protocol of deparaffinization in Roticlear® (Carl Roth) for three times 10 min and rehydration by rinsing in absolute ethanol twice for 10 min, and descending dilutions of ethanol (90%, 70%, 50%) and dH_2O for each 5 min. Slides were stained with 5% hematoxylin (Morphisto) for 6 min, followed by a quick rinse in tap water, and staining with 1% eosin (Morphisto) for 6 min. Excess staining solution was washed off with tap water and slides were dehydrated in ascending dilutions of ethanol (50%, 70%, 90%) for each 1 min, twice in absolute ethanol for 5 min, and three times in Roticlear® (Carl Roth) for 5 min. Slides were mounted with DPX mounting medium for histology (Sigma-Aldrich).

2.9.2 RNA in situ hybridization (ISH)

RNA in situ hybridization (ISH) is a great tool to visualize mRNA expression in tissue sections if no antibody is available to detect the protein of interest. This technique is widely used in developmental biology and had a multitude of adaptions and improvements over almost 50 years. The laboratory of Prof. Dr. Hans Clevers has adapted the procedure to work particularly well in formalin-fixed paraffin embedded tissue

sections of human and murine intestines and ISH was essentially performed as described (Gregorieff and Clevers 2015).

2.9.2.1 Probes

To detect the mRNA of interest specific complementary RNA probes (riboprobes) needed to be generated. An anti-sense and a sense probe were generated where the anti-sense probe binds to the (sense) mRNA and the sense probe should not bind and thereby serves as a negative control.

To this end, run-off in vitro transcription was performed. Vectors with viral RNA polymerase promoters (T3/ T7/ SP6) at opposing sides of the multiple cloning site (MCS) were used. cDNA of the target mRNA was either reversely transcribed from RNA (**Table 2**) or obtained through an I.M.A.G.E. clone (imaGenes GmbH, Berlin, Germany; now Source Bioscience) and cloned into the MCS (**Table 7**). Preferentially the 3' untranslated region was included in the probe design given its potentially lower homology to other genes.

Linearized plasmids as templates for run-off in vitro transcription were generated using restriction enzymes so that the viral RNA polymerase promoter (T3/ T7/ SP6) would be followed by the nucleotide sequence to be transcribed. The RNA polymerase would then fall off at the end of the sequence where the restriction enzyme had cut. During transcription digoxigenin-UTP will be incorporated for about every 3rd uracil which subsequently can be detected by alkaline phosphatase (AP) coupled anti-digoxigenin antibodies.

10 µg of plasmid DNA were digested with 30 units of restriction enzyme and 10 µl of restriction enzyme buffer (10x) in a total volume of 100 µl RNAse free water. After incubation for 3 h at 37 °C the digested DNA was cleaned up with the illustra GFX PCR DNA and Gel Band Purification Kit (GE Healthcare) according to the manufacturer's instructions and eluted in only 10 µl of RNAse free water. Next, 1% agarose gel electrophoresis of 2 µl digested DNA, 3 µl H_2O, and 1 µl of 6x DNA Gel Loading Dye (Thermo Scientific) was run to confirm complete linearization.

2.9.2.2 In vitro transcription

In vitro transcription was set up in the following order in a 1.5 ml microcentrifuge tube: 7.5 µl of nuclease free water, 2 µl of linearized template DNA (~ 1-2 µg of DNA), 4 µl of transcription buffer, 5 x (Promega), 2 µl of DTT 0.1 M (Promega), 2 µl of DIG RNA Labeling Mix, 10 x (Roche), 1 µl of RNasin® Ribonuclease Inhibitor (Promega), and 1.5 µl of T3/T7/SP6 RNA polymerase (Promega). After incubation for more than 2 h at 37 °C, the sample was incubated with 1 µl of RNAse free DNase I (Roche) for 15 min at 37 °C.

It is paramount that the following steps are performed under RNAse free conditions to avoid inadvertent degradation of the RNA probe. Gloves have to be worn at all times and surfaces should be sprayed and wiped with RNase AWAY™ surface decontaminant (Thermo Scientific). Dedicated RNAse free pipettors are encouraged and nuclease-free pipette tips with aerosol filters have to be used. Further it is advisable to work as quickly as possible. Therefore, one should have ice, dry ice, and all tubes including the final tubes for permanent storage ready and labeled.

The RNA probe was purified using RNeasy Mini Kit (QIAGEN) following the manufacturer's instructions. Elution was carried out in a final volume of 50 µl RNAse free water and the probe was immediately put on ice.

1.5 µl of probe were set aside to be quantified using the NanoDrop ND-1000 spectrophotometer (Thermo Scientific). 2 µl of probe were set aside to be run with 8 µl of RNA Sample Loading Buffer (Sigma-Aldrich) and 2 µl of Orange DNA Loading Dye, 6X (Thermo Scientific) on a denaturing agarose gel (50 ml of 1% agarose in 1x TAE + 1 ml formaldehyde + 1.5 µl ethidium bromide). Before these quality control assays were run, an equal volume of RNAse/DNAse free formamide (Sigma-Aldrich) was added to the remaining 47 µl of probe, which was immediately placed on dry ice and subsequently stored at -80 °C.

2.9.2.3 RNA hybridization

Preparation for in situ RNA hybridization starts days before the actual experiment. All stock solutions and reagents, ideally all buffers, and sufficient amounts of DEPC (diethyl pyrocarbonate)-treated water need to be available. Hellendahl staining jars made of glass were baked at 200 °C overnight while wrapped in aluminium foil to inactivate RNAses.

The day before in situ hybridization formalin-fixed paraffin-embedded (FFPE) human and murine paraffin blocks were cut at a thickness of 8-10 µm, picked up onto SuperFrost™ Plus slides (Menzel-Gläser), and baked in a hybridization oven at 70 °C overnight.

The next day, tissue sections were deparaffinized by three rounds of fresh xylene (AppliChem) or the less toxic Roticlear® (Carl Roth) for each 5 min. This was followed by rehydration in a descending ethanol series of absolute (twice), 75%, 50%, and 25% ethanol for each 5 min at RT and two rinses in DEPC-treated H_2O. Ethanol absolute for molecular biology (AppliChem) was used to prepare the dilutions. Of note, it is of utmost importance that slides never dry out throughout the entire procedure. While performing these steps the hybridization oven should be set to 68 °C with a sufficiently large beaker cup of ddH_20 to establish an H_2O-saturated atmosphere. Further, water baths should be set to 37 °C and 70 °C and 4% PFA should be prepared freshly which takes a long time to dissolve (heat to 70 °C in water bath, add a few drops of NaOH, followed by frequent agitation). Tissue sections were pretreated with 0.2 N hydrochloric acid (HCl) for 15 min at RT. Next sections were incubated with proteinase K (30 µg/ml; Merck Millipore) in PBS at 37 °C for 20 min (time variable depending on tissue type). Afterwards, samples were rinsed with 0.2% glycine (dissolved in PBS immediately before use) and twice with PBS. Tissue sections underwent postfixation for 10 min with 4% PFA and samples were subsequently rinsed twice with PBS. Acetic anhydride treatment (0.1 M triethanolamine (pH 8) mixed with 0.25% acetic anhydride in DEPC-treated H_2O, prepared right before usage followed by vigorous shaking) was carried out twice for 5 min. Samples were rinsed twice with PBS and twice with 5x SSC (pH 4.5).

For prehybridization and hybridization an improvised hybridization chamber was created by placing slides horizontally in a plastic microscopy slide storage box. Paper towels were folded, soaked in 5x SSC / 50% formamide, and placed at the bottom of the chamber to create a humid atmosphere. During hybridization steps, small stripes cut from Parafilm (Bemis Company) were placed on top of the slides, thereby floating on pre-/ hybridization solution to prevent drying out of samples. In addition, for the 24-72 h hybridization, boxes were placed in sealable plastic bags and excess air was removed by a laboratory vacuum pump. For prehybridization, 400 µl of hybridization solution were carefully pipetted on top of the samples ensuring that all tissue is covered and incubated at 68 °C for at least 1 h. For hybridization, usually 3 µl of probe (quickly thawed from stocks at -80 °C and denatured at 95 °C for 5 min) were diluted in 100 µl of hybridization solution which were

added to the 400 µl already on the slide. Hybridization was allowed to take place at 68 °C for 24-72 h.

Post hybridization washes started with dipping excess hybridization solution off slides and a rinse in 2x SSC (pH 4.5) followed by three washes for each 25 min in 50% formamide / 2 x SSC (pH 4.5) at 65 °C or adapted empirically for best results (preheat solution in water bath to ensure constant stringency of washes). Slides were rinsed five times in TBST (TBS + 0.1% Tween20) and placed back into the hybridization chamber, now humidified with TBST-soaked paper towels. Samples were covered in 400 µl of blocking solution for at least 30 min at RT before 100 µl of anti-Digoxigenin-AP, Fab fragments (1:2000; Roche) were added in a drop-wise fashion. Incubation was carried out overnight at 4 °C.

The next day, slides were rinsed 5-7x in TBST followed by 2-3 rinses in NTM. A NBT/BCIP Ready-to-Use Tablet (Roche) was diluted in 10 ml of water and 500 µl were added to each slide. For most probes slides were kept in the dark and incubated overnight at RT. But for probes producing a strong signal the incubation times was shortened to as little as 30 min and slides were left in PBS until processed with the remaining slides.

The next day, slides were rinsed twice in PBS and coverslips mounted with Kaiser's glycerol gelatine (Merck) which is an aqueous mounting agent thus avoiding xylene containing mounting media that may lead to crystal formations of the color precipitates (NBT/BCIP, manufacturer’s recommendation).

2.9.3 Immunohistochemistry (IHC)

Stains for murine KI-67 (rat anti-mouse KI-67, Dako, Hamburg, Germany) were performed by A. Sendelhofert (Pathologisches Institut, LMU München). In brief, antigen retrieval was achieved by sub-boiling sections for 20 min at 95 °C in 10 mM sodium citrate buffer (pH 6.0, 10 mM) and antigen detection was performed with the Vectastain ABC-Kit Elite Rat. DAB (Dako) was used as chromogen. Slides were counterstained with hematoxylin.

Stains for human KI-67 and β-catenin were performed with clinically validated antibodies at Pathologisches Institut, LMU München.

2.9.3.1 Immunohistochemistry for RNF43

Tissue sections were cut at 4 µm and underwent the standard protocol of deparaffinization and rehydration outlined in the hematoxylin and eosin staining procedure. To expose epitopes previously masked in the process of tissue fixation, heat induced epitope retrieval (HIER) was performed by boiling slides in 0.01 M sodium citrate (pH 6) for 5 min in a domestic stainless-steel pressure cooker placed on a hot plate. Sodium citrate was preheated, slides added to the boiling buffer, and the lid closed tightly. This was followed by a slow cooldown for 30 min at RT. Next, slides were rinsed in dH_20, assembled in a Sequenza™ Slide Rack and Coverplate™ system (Thermo Scientific), and washed twice with PBS.

Endogenous peroxidases were blocked by incubation with 150 µl of 3% hydrogen peroxide for 10 min (freshly prepared from 30% stock, diluted in dH_2O). Slides were rinsed twice in dH_2O and once in TBS-T (0.1% (v/v) Tween 20 in 1x TBS). Sections were blocked with 150 µl of 5% goat serum (Cell Signaling Technology) diluted in TBS-T for 1 h at RT.

After trying antibodies of various different suppliers RNF43 (HPA008079, Atlas Antibodies AB) gave the best results for the detection of endogenous RNF43. The RNF43 antibody was diluted at 1:1000 in SignalStain® Antibody Diluent (Cell Signaling Technology) and 150 µl of antibody solution were applied to sections and incubated overnight at 4 °C.

Next morning, slides were warmed to RT for 10 min and rinsed four times in 0.1% TBS-T. Subsequently, a secondary anti-rabbit IgG HRP (horseradish peroxidase)-conjugated antibody (Promega) was diluted 1:200 in SignalStain® Antibody Diluent. 150 µl were applied to each slide and incubated for 1 h at RT. This was followed by four rinses in 0.1% TBS-T (take care to periodically discard the flow-through). SignalStain® DAB Substrate (Cell Signaling Technology) was added and slides were incubated for 7 min at RT while periodically checking sections to make sure no grossly evident over-staining occurs. The slide rack was disassembled and slides were transferred to dH_2O. Sections were briefly counterstained with 5% hematoxylin (Morphisto) for 1 min to yield only a faint nuclear stain since immunohistochemistry for RNF43 also labels the nucleus. After rinsing slides under running tap water, they were dehydrated as outlined in the hematoxylin and eosin staining procedure and mounted with DPX mounting medium for histology (Sigma-Aldrich).

>sp|Q68DV7|RNF43_HUMAN E3 ubiquitin-protein ligase RNF43 OS=Homo sapiens GN=RNF43 PE=1 SV=1

MSGGHQLQLAALWPWLLMATLQAGFGRTGLVLAAAVESERSAEQKAIIRVIPLKMDPTGKLNLTLEGVFAGVAEITP
AEGKLMQSHPLYLCNASDDDNLEPGFISIVKLESPRRAPRPCLSLASKARMAGERGASAVLFDITEDRAAAEQLQQP
LGLTWPVVLIWGNDAEKLMEFVYKNQKAHVRIELKEPPAWPDYDVWILMTVVGTIFVIILASVLRIRCRPRHSRPDP
LQQRTAWAISQLATRRYQASCRQARGEWPDSGSSCSSAPV**CAICLEEFSEGQELRVISCLHEFHRNCVDPWLHQHRT**
CPLCMFNITEGDSFSQSLGPSRSYQEPGRRLHLIRQHPGHAHYHLPAAYLLGPSRSAVARPPRPGPFLPSQEPGMGP
RHHRFPRAAHPRAPGEQQRLAGAQHPYAQGWGLSHLQSTSQHPAACPVPLRRARPPDSSGSGESYCTERSGYLADGP
ASDSSSGPCHGSSSDSVVNCTDISLQGVHGSSSTFCSSLSSDFDPLVYCSPKGDPQRVDMQPSVTSRPRSLDSVVPT
GETQVSSHVHYHRHRHHHYKKRFQWHGRKPGPETGVPQSRPPIPRTQPQPEPPSPDQQVTRSNSAAPSGRLSNPQCP
RALPEPAPGPVDASSICPSTSSLFNLQKSSLSARHPQRKRRGGPSEPTPGSRPQDATVHPACQIFPHYTPSVAYPWS
PEAHPLICGPPGLDKRLLPETPGPCYSNSQPVWLCLTPRQPLEPHPPGEGPSEWSSDTAEGRPCPYPHCQVLSAQPG
SEEELEELCEQAV

signal peptide; **ZINC FINGER domain;** R and G truncating mutations
Immunogen: anti-RNF43 (HPA008079, Atlas Antibodies AB) and (8D6, rat sera).

Figure 5: Anti-RNF43 (HPA008079 and 8D6) still bind to most truncated RNF43 proteins. Isoform 1 — 'canonical' sequence of RNF43 (Length: 783bp, Mass: 85.722 kDa), derived from http://www.uniprot.org/uniprot/Q68DV7.RNF43; signal peptide is underlined, ZINC FINGER domain in bold; R and G indicate positions of most mutations that were truncating at p.Gly659fs (41.7-48% of cases) and p.Arg117fs (8.3-12% of cases) (Giannakis et al. 2014); in grey and black background are the immunogens used to raise anti-RNF43 HPA008079 and 8D6, respectively.

2.9.3.2 Evaluation

Slides were digitally scanned with the Olympus Virtual Slide System VS120 (Olympus). RNF43 immunohistochemistry was semiquantitatively scored by assigning an H-score (Ishibashi et al. 2003) which takes into account proportions and respective staining intensities and gives more weight to more intensely stained tumor cell populations. Possible results range from 0-300.

H score = 1 × (proportion of cells stained at 1+ intensity) +
2 × (proportion of cells stained at 2+ intensity) +
3 × (proportion of cells stained at 3+ intensity)

KI-67 proliferative index assessed by immunohistochemistry was calculated as number of positive tumor cells / number of total tumor cells and was therefore presented as percent positive cells.

2.10 Statistical analysis

Results are presented as mean ± SD of at least three biologically independent experiments, unless denoted differently. Statistical analysis of normally distributed data was performed using Student's t-test. A result was considered statistically significant when $p \leq 0.05$.

Genotyping results of pubs of *Sox17*$^{fl/fl}$ to *Villin*-Cre matings were assessed for statistical significance with the online chi-squared test of independence. (http://www.socscistatistics.com/tests/chisquare2/Default2.aspx; accessed January 3rd 2018).

3 Results

The Wnt/β-catenin pathway plays an important role in gastrointestinal tumorigenesis but also in homeostasis. It was shown that knocking out the Wnt effector Tcf-4 in a mouse model led to loss of intestinal regenerative capacity and was not compatible with life (Korinek et al. 1998). Therefore, targeting the Wnt/β-catenin itself is not a viable approach in treating human cancers.

With the intention of identifying Wnt target genes that are instrumental in tumorigenesis but dispensable in homeostasis, gene expression arrays were performed of normal mucosa vs. adenomas of a conditional mouse model of intestinal tumorigenesis Ahcre^{+}; *APC* $^{fl/fl}$ (Sansom et al. 2004) and human colorectal carcinomas/adenomas (Van der Flier et al. 2007). Around 200 overexpressed genes were selected in preliminary work by Prof. M. Gerhard based on structural prediction or published literature indicating that they might be worthwhile therapeutic targets (transcription factors, kinases, role in development, proliferation, cell cycle control, transmembrane receptors, ZINC/RING finger proteins). Consecutively, in situ hybridization was performed on murine and human tissues to identify deregulated genes that were expressed exclusively in the crypt and/or tumor. Most of these genes could further be identified as direct Wnt target genes by the presence of TCF4 binding sites discovered by whole genome CHIP with TCF4 specific antibodies (Hatzis et al. 2008).

Of these, I chose to investigate Sox17, Axin2, and Rnf43 and analyze their roles in more detail in different aspects of Wnt/β-catenin signaling.

Some of the results presented herein are published:

Schneider MR, Dahlhoff M, Horst D, Hirschi B, Trülzsch K, Müller-Höcker J, Vogelmann R, Allgäuer M, Gerhard M, Steininger S, Wolf E, Kolligs FT.
A key role for E-cadherin in intestinal homeostasis and Paneth cell maturation.
PLoS One. 2010 Dec 14;5(12):e14325.

Loregger A, Grandl M, Mejías-Luque R, Allgäuer M, Degenhart K, Haselmann V, Oikonomou C, Hatzis P, Janssen KP, Nitsche U, Gradl D, van den Broek O, Destree O,

Ulm K, Neumaier M, Kalali B, Jung A, Varela I, Schmid RM, Rad R, Busch DH, Gerhard M.
The E3 ligase RNF43 inhibits Wnt signaling downstream of mutated β-catenin by sequestering TCF4 to the nuclear membrane.
Sci Signal. 2015 Sep 8;8(393):ra90.

McDuffie LA, Sabesan A, Allgaeuer M, Xin L, Koh C, Heller T, Davis JL, Raffeld M, Miettinen M, Quezado M, Rudloff U.
β-Catenin activation in fundic gland polyps, gastric cancer and colonic polyps in families afflicted by 'gastric adenocarcinoma and proximal polyposis of the stomach' (GAPPS).
J Clin Pathol. 2016 Sep;69(9):826-33.

Berger E, Rath E, Yuan D, Waldschmitt N, Khaloian S, Allgäuer M, Staszewski O, Lobner EM, Schöttl T, Giesbertz P, Coleman OI, Prinz M, Weber A, Gerhard M, Klingenspor M, Janssen KP, Heikenwalder M, Haller D.
Mitochondrial function controls intestinal epithelial stemness and proliferation.
Nat Commun. 2016 Oct 27;7:13171.

3.1 The Wnt/β-catenin pathway in gastrointestinal development

3.1.1 *Sox17* shows crypt-restricted expression and is upregulated in tumors

In order to learn more about the biological function of Sox17, I wanted to visualize its spatial expression in murine and human intestinal samples. Of particular interest would be a suprabasal/stem cell expression within the crypts and/or expression in tumors. One study found *Sox17* to be expressed in normal gut epithelium but reduced in adenomas of *APC* $^{min/+}$ mice (Sinner et al. 2007). Whereas in another study, *Sox17* was found to be induced in gastric tumors developing in *K19*-Wnt1/C2mE mice and in human gastrointestinal adenomas (Du et al. 2009) but downregulated by promoter methylation in the course of malignant progression (Zhang et al. 2008). Since no reliable antibodies were available to be used with regular IHC procedures, I resorted to in situ hybridization for detection of *Sox17* mRNA.

Chromogenic RNA-in situ hybridization (ISH) for murine *Sox17* weakly labeled epithelial cells at the base of the crypt in murine small intestine (**Figure 6 A**) demonstrating low amounts of *Sox17* mRNA transcripts. Expression of *Sox17* was upregulated in aberrant crypt foci of *APC* $^{min/+}$ mice (**Figure 6 B**) and in adenoma developing in *APC* $^{min/+}$ mice (**Figure 6 C**).

Human *SOX17* mRNA transcripts could be visualized in a similar fashion at the base of human colonic crypts (**Figure 6 D**). *SOX17* was more abundant in human colonic adenocarcinoma than in normal colonic mucosa (**Figure 6 E, F**).

Thus, in both mouse and human, *SOX17* showed low levels of expression in intestinal and colonic crypts under physiological conditions and was upregulated in tumorigenesis.

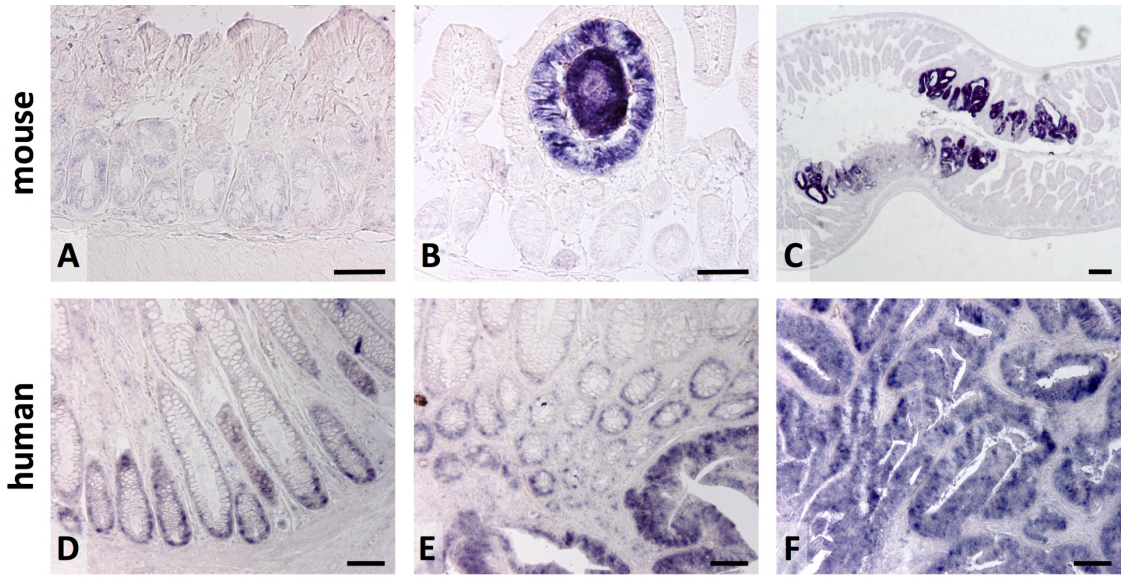

Figure 6: Expression of murine and human *SOX17* in intestine.
Riboprobes against murine and human *SOX17* mRNA transcripts were detected by chromogenic RNA-in situ hybridization in sections of murine normal small intestinal mucosa (A), aberrant crypt focus of *APC* $^{min/+}$ mouse (B), small intestinal adenoma developing in an *APC* $^{min/+}$ mouse (C), human normal colonic mucosa (D), colonic mucosa to adenocarcinoma transition (E), and colonic adenocarcinoma (F). Scale bars indicate 100 µm (A, B, D, E, F) and 200 µm (C).

3.1.2 Conditional knockout of *Sox17* in murine intestinal epithelium is inconsequential for intestinal development

Sox17 was shown to be integral for proper formation of definitive endoderm (Hudson et al. 1997, Sinner et al. 2004) and its deletion in a knockout mouse model led to defective mid- and hindgut development at E8.5-9.5 (Kanai-Azuma et al. 2002).

In order to study the role of Sox17 at later stages of intestinal development and homeostasis, a conditional knockout mouse model of Sox17 (*Sox17* $^{fl/fl}$) was obtained (Kim, Saunders, and Morrison 2007). The entire coding sequence of *Sox17* was removed upon Cre mediated recombination of flanking loxP sites.

To achieve tissue specific deletion in the intestinal epithelium, *Sox17* $^{fl/fl}$ mice were crossed with *Villin*-cre mice harboring transgenic Cre recombinase under the *Villin* promoter (el Marjou et al. 2004). In this mouse model, Cre mediated recombination was reported to occur in visceral endoderm at E9 and by E12.5 in the epithelial lining of small and large intestine. Renal cortex was the only other site were recombination events monitored by reporter gene beta-galactosidase were detected (el Marjou et al. 2004).

Genotypes were determined by PCR (**Figure 7**). *Sox17* floxed alleles could be distinguished from *Sox17* wild type based on the size of PCR products (480 bp vs.

350 bp). PCR for Cre recombinase yielded a product when present and was otherwise negative. Positive and negative controls were run with all genotyping reactions.

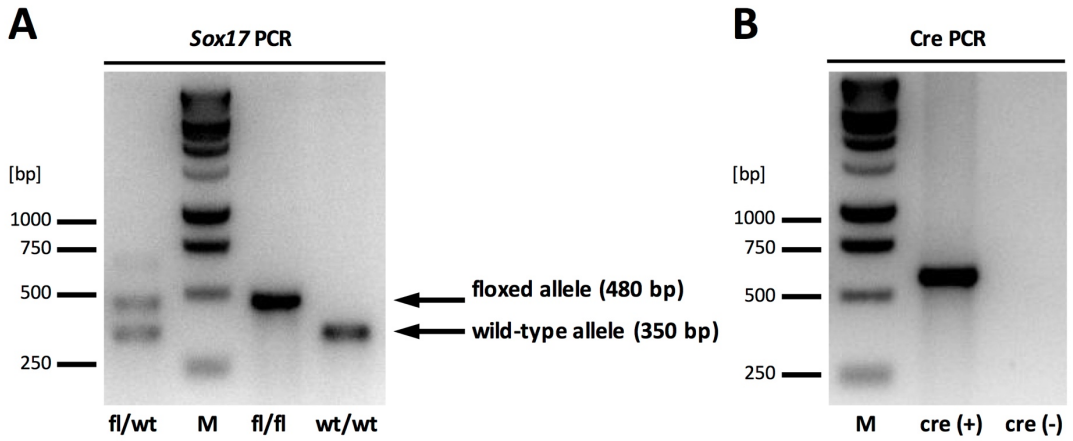

Figure 7: Genotyping of *Sox17* $^{fl/fl}$ and *Villin*-Cre mice.
Genotyping PCR products run on agarose gels. Three representative examples of *Sox17* mice are shown (A) and two mice genotyped for Cre recombinase (B). fl = *Sox17* allele "flanked by LoxP sites"; wt = *Sox17* wild type allele; M = marker. Y-axis indicates DNA length in base pairs.

All four possible genotype combinations occurred among pubs of *Sox17* $^{fl/fl}$ to *Villin*-Cre matings (**Table 12**). There was no statistically significant difference in encountered genotypes by chi-squared test (p=0.41), indicating that deletion of *Sox17* in intestinal epithelial cells did not lead to intrauterine demise.

n=51	*Sox17* $^{fl/wt}$	*Sox17* $^{fl/fl}$	
cre +	14 (27,5%)	5 (9,8%)	37,3 %
cre -	20 (39,2%)	12 (23,5%)	62,7 %
	66,7 %	33,3 %	100 %

Table 12: Genotypes of pubs of *Sox17* $^{fl/fl}$ to *Villin*-Cre matings.
Numbers of live-born pubs of *Sox17* $^{fl/fl}$ to *Villin*-Cre matings. Relative percentages of all live-born pubs are given in brackets. fl = *Sox17* allele "flanked by LoxP sites"; wt = *Sox17* wild type allele.

To monitor for effects of intestinal epithelium specific deletion of *Sox17* starting with *Villin*-Cre recombinase activity on E12.5, pregnant mice were sacrificed on days 13, 14, 16, and 17 post conception corresponding to embryonic days E13.5, E14.5, E16.5, and E17.5. Embryos were retrieved, genotyped, and histologically processed.

Microscopic evaluation of *Villin*-cre^{+}; *Sox17* $^{fl/fl}$ embryos confirmed regular intestinal development at E13.5 (**Figure 8 A**) and E14.5 (**Figure 8 B**). Sections of stomach and esophagus did not reveal any abnormalities at E14.5, E16.5, and E17.5 (**Figure 8 C-E**) but changes would not be expected since *Villin*-Cre did not show any recombination activity in the stomach (el Marjou et al. 2004).

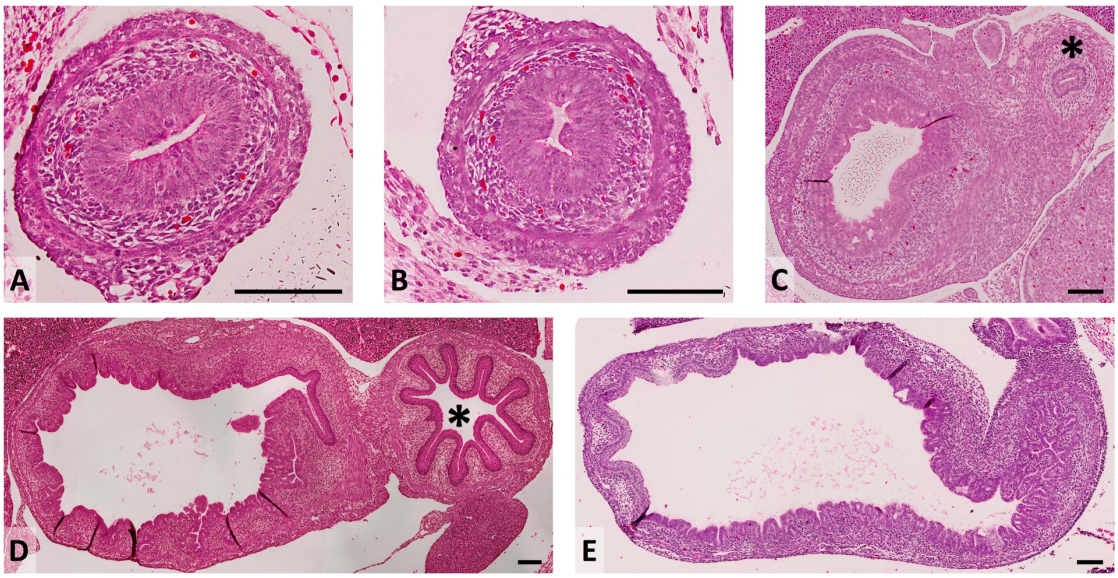

Figure 8: Regular development of gastrointestinal tract in *Villin*-cre^{+}; *Sox17* $^{fl/fl}$ embryos. Cross sections of small intestines of *Villin*-cre^{+}; *Sox17* $^{fl/fl}$ embryos at E13.5 (A) and E14.5 (B). Cross sections of stomach at E14.5 (C), E16.5 (D), and E17.5 (E). Asterisk marks esophagus. H&E stain. Scale bars indicate 100 µm.

Comparison of small intestines in *Villin*-cre^{-}; *Sox17* $^{fl/fl}$ and *Villin*-cre^{+}; *Sox17* $^{fl/fl}$ embryos at E16.5 (**Figure 9 A, B**) and E17.5 (**Figure 9 C, D**) revealed regular development of intestine and pancreas.

There were no morphologically discernible features nor a significant decrease in viability between *Sox17* $^{fl/fl}$ mice and mice with a *Villin*-cre mediated knockout of *Sox17* indicating that deletion of Sox17 in later endoderm formation is inconsequential for intestinal development.

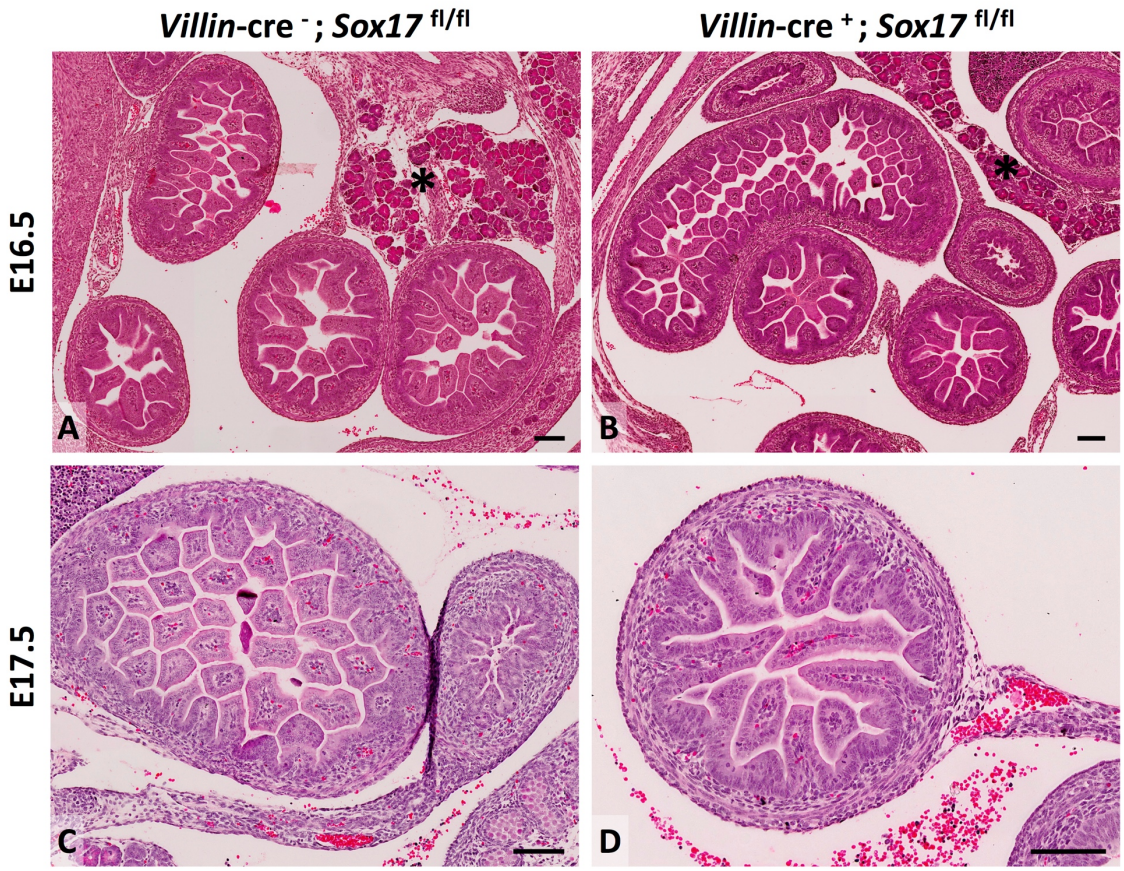

Figure 9: No morphological difference in small intestinal development of *Villin*-cre^{-} ; *Sox17* $^{fl/fl}$ and *Villin*-cre^{+} ; *Sox17* $^{fl/fl}$ embryos.
Cross sections of small intestines of *Villin*-cre^{-} ; *Sox17* $^{fl/fl}$ embryos at E16.5 (A) and E17.5 (C) and *Villin*-cre^{+} ; *Sox17* $^{fl/fl}$ embryos at E16.5 (B) and E17.5 (D). Asterisk marks pancreas. H&E stain. Scale bars indicate 100 µm.

Since *Sox17* deletion did not affect intestinal organogenesis I wanted to assess whether there were any alterations in postnatal intestinal homeostasis. Litters were genotyped and sacrificed at 4 weeks of age. Sections of stomach (**Figure 10 A, C**) showed regularly formed gastric oxyntic/fundic mucosa without any pathological changes. Proliferative activity (**Figure 10 B, D**) was restricted to the neck of gastric glands and did not significantly differ between *Sox17* $^{fl/fl}$ mice with or without *Villin*-cre recombinase. Again, changes in stomach would not be expected since *Villin*-cre recombinase is not active there.

Small intestine showed intact villous architecture without any pathological changes (**Figure 10 E, G**). Proliferative activity by KI-67 was seen to be restricted to the crypts (**Figure 10 F, H**). Additionally, lymphocytes within the submucosa of the villi were labeled. There was no noticeable difference between *Sox17* $^{fl/fl}$ mice with or without *Villin*-cre recombinase.

Colonic sections revealed regularly formed colonic crypts (**Figure 10 I, K**) with crypt-restricted proliferation (**Figure 10 J, L**). Again, no difference between *Sox17* $^{fl/fl}$ mice with or without *Villin*-cre recombinase was seen.

Overall, *Villin*-cre^{+} ; *Sox17* $^{fl/fl}$ mice did not display any abnormal histomorphological phenotype, but showed regular intestinal development and architecture.

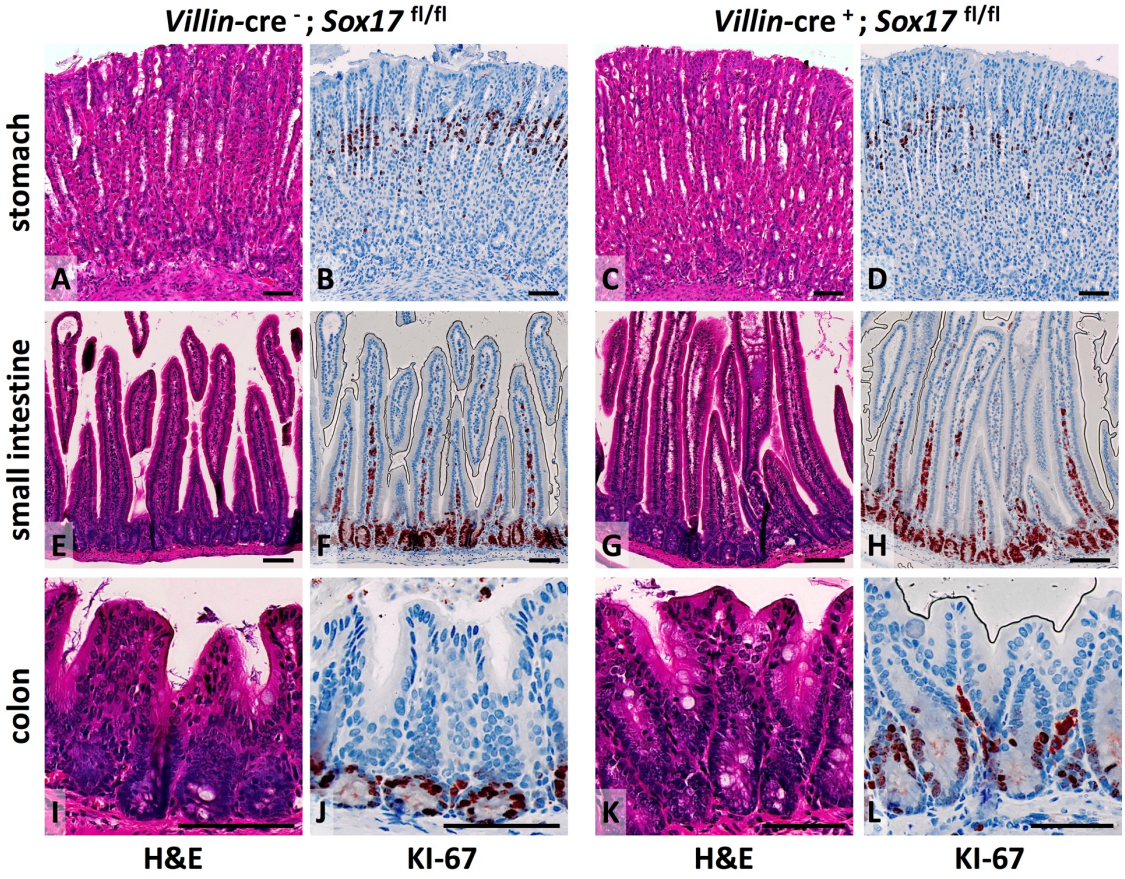

Figure 10: No morphological difference in adult gastrointestinal tract of *Villin*-cre^{-} ; *Sox17* $^{fl/fl}$ and *Villin*-cre^{+} ; *Sox17* $^{fl/fl}$ adult mice.
Comparison of sections of stomach (A-D), small intestine (E-H), and colon (I-L) in *Villin*-cre^{-} ; *Sox17* $^{fl/fl}$ mice (A, B, E, F, I, J) and *Villin*-cre^{+} ; *Sox17* $^{fl/fl}$ mice (C, D, G, H, K, L). H&E stain and immunohistochemistry for KI-67. Scale bars indicate 100 µm.

3.2 The Wnt/β-catenin pathway in gastrointestinal stemness and homeostasis

The intestinal epithelium is exposed to mechanical, chemical, and infectious stressors. To preserve its integrity, it undergoes constant, rapid renewal – in the mouse every 3-5 days – and this process is largely driven by the Wnt/β-catenin pathway (Fevr et al. 2007, van Es, Haegebarth, et al. 2012). Early studies in the 40ties established that intestinal crypts were the origin of the intestinal self-renewal capacity (Friedman 1945). In the 70ties, crypt base columnar (CBC) cells interspersed between Paneth cells were suggested to be the stem cells of the intestine (Cheng and Leblond 1974). More recently, microarray experiments of crypts and colon cancers turned up *Lgr5* as being overexpressed in both. Subsequently, it was found to show restricted expression in CBC, which were then shown in *in vivo* lineage tracking experiments to represent adult intestinal stem cells (Barker et al. 2007).

3.2.1 Challenges in detection of intestinal stem cell markers

When studying intestinal physiology in experimental mouse models and in human disease it is of particular interest to highlight stem cells. One caveat is that Lgr5 is expressed at very low levels. Antibodies for LGR5 are not well established. In addition, detection is hampered by low protein expression which has led some investigators to increase the sensitivity by using fluorescence amplification systems (Yamazaki et al. 2015). In situ hybridization that was used in the original paper (Barker et al. 2007) also remains a challenge as acknowledged by the authors themselves. This led to the identification of Olfm4 as a surrogate marker for $Lgr5^{+}$ stem cells (van der Flier, Haegebarth, et al. 2009, Schuijers et al. 2014). Nevertheless, it should be mentioned that its validity has been questioned in human colon and colon cancer as it was found to mark a larger proportion of cells including some of the transit amplifying cells (Ziskin et al. 2013).

Despite many iterations and modifications of staining parameters, chromogenic RNA-in situ hybridization for human *LGR5* (**Figure 11 A**) and murine *Lgr5* (not shown) remained challenging to perform with at best marginally above background staining. The sense-control probe for *LGR5* (**Figure 11 B**) showed no specific staining indicating that the

faint staining for human *LGR5* (**Figure 11 A**) in fact represented a valid signal. In the murine intestine (**Figure 14 A**), hybridization to *Olfm4* produced a strong and robust signal at the position of CBC cells. However, hybridization to *OLFM4* (**Figure 11 C**) in the human intestine yielded a strong and robust signal at the position of CBC but also stained additional cells further up the crypt-villus axis underscoring the notion that *OLFM4* might not be an ideal surrogate for $Lgr5^{+}$ stem cells in human tissues (Ziskin et al. 2013). The dot-like positivity distributed randomly along the villi is a technical artifact occasionally seen in ISH.

Figure 11: Establishing chromogenic RNA-in situ hybridization for *LGR5* and *OLFM4*. Riboprobe against *LGR5* mRNA transcript (A), *LGR5* sense-control probe (B), and *OLFM4* (C) in sections of normal human small intestinal mucosa. Scale bars indicate 200 µm.

3.2.2 A key role for E-cadherin in intestinal homeostasis and Paneth cell maturation

This collaborative project (Schneider et al. 2010) with Prof. Frank T. Kolligs' group and others (Department of Medicine II, Klinikum Großhadern and Gene Center, University of Munich) was investigating the role of E-cadherin — an integral protein to form adherens junctions between epithelial cells — in intestinal homeostasis and Paneth cell maturation.

E-cadherin's intracellular binding partners include β-catenin, an integral component of the Wnt/β-catenin pathway. Wnt signaling was further described as being involved in maturation and positioning of Paneth cells (Schneider et al. 2010, Pinto et al. 2003, Bastide et al. 2007). A knockout of β-catenin (Ireland et al. 2004) or its target gene *EphB3* led to mispositioning of Paneth cells along the crypt-villus axis (Batlle et al. 2002). E-cadherin was found to be downregulated in patients with inflammatory bowel disease and contribute to pathogenesis (Jankowski et al. 1998, Gassler et al. 2001, Kucharzik et

al. 2001, Bruewer, Samarin, and Nusrat 2006). Since E-cadherin is important in cell-cell adhesion, it was found to be downregulated or substituted by N-cadherin contributing to epithelial to mesenchymal transition with enhanced invasiveness and potential metastasis, a hallmark of cancer (Halbleib and Nelson 2006, Islam et al. 1996). Prior to this study E-cadherin's function in the small intestine had not been directly investigated (Hermiston and Gordon 1995, Smalley-Freed et al. 2010).

The *Cdh1* gene was therefore conditionally knocked-out in intestinal epithelial cells by mating homozygous *Cdh1* $^{fl/fl}$ mice (Boussadia et al. 2002), in which exons 6-10 of the gene encoding E-cadherin are flanked by loxP sites, with an intestinal epithelial cell-specific, tamoxifen-inducible cre mouse (Villin-cre-ER^{T2}).

Mice undergoing an intensive schedule of tamoxifen administrations on days 1-5 (short-time model) suffered of hemorrhagic diarrhea and required euthanasia. To study the long-term effects of E-cadherin deficiency a milder protocol of tamoxifen induction on days 1, 2, 5, and 8 was applied (long-time model). Immunohistochemistry confirmed largely lost staining for E-cadherin apart from scattered cells at the crypt bottoms (Schneider et al. 2010).

The expression of Wnt target genes was also analyzed in these mice. Wild type mice showed staining for *Axin2* in crypts of proximal (**Figure 12 A**) and distal (**Figure 12 E**) small intestine. *Villin*-cre-ER^{T2}; *Cdh1* $^{fl/fl}$ mice in the short-time model (E-cadherin deficient) did not show any staining for *Axin2* at day 4 (**Figure 12 B, F**) pointing to a marked reduction of Wnt signaling activity at the bottom of the crypts. Staining was reduced in the attenuated long-time recombination model (E-cadherin partially deficient) on day 12 (**Figure 12 C, G**), and close to normal at day 20 (**Figure 12 D, H**).

In either model, *Axin2* positive cells were only encountered at the crypt base but not in other regions of the villi, where mispositioned Paneth cells were detected by immunohistochemical stains, indicating that no active Wnt signaling took place in those. This was confirmed by membranous, non-nuclear staining for β-catenin.

Olfm4 mRNA levels followed a similar course. Wild type mice showed strong staining at the base of the crypts of proximal (**Figure 13 A**) and distal (**Figure 13 E**) small intestine staining CBC cells.

Villin-cre-ER^{T2}; *Cdh1* $^{fl/fl}$ mice in the short-time model did not show any staining for stem cell marker *Olfm4* at day 4 (**Figure 13 B, F**) indicating a potential loss of stemness. Staining of CBC was comparatively weak in the long-time model on day 12 (**Figure 13 C, G**) but close to normal at day 20 (**Figure 13 D, H**).

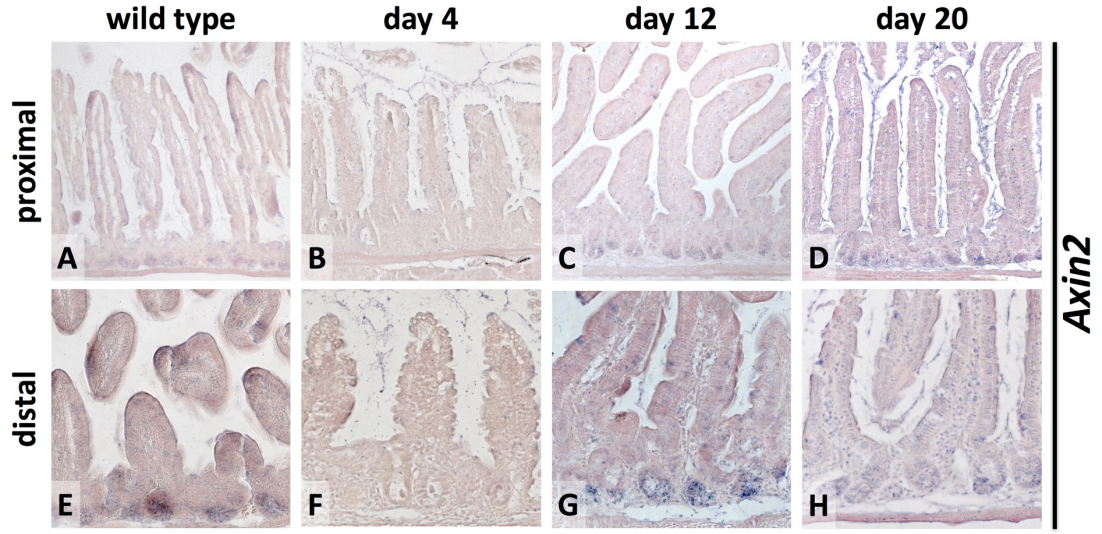

Figure 12: Expression of *Axin2*, a Wnt target gene, as a surrogate marker of Wnt/β-catenin pathway activity in *Villin*-cre-ER^{T2}; *Cdh1* $^{fl/fl}$ mice.
Chromogenic RNA-in situ hybridization for *Axin2* in wild type and E-cadherin deficient mice (short-time model, sacrificed at day 4 post tamoxifen administration) and E-cadherin partially deficient mice (long-time model, sacrificed at day 12 and day 20) of proximal (A-D) and distal (E-H) small intestine. Photomicrographs taken at 100x (A-D) and 200x (E-H) original magnification.

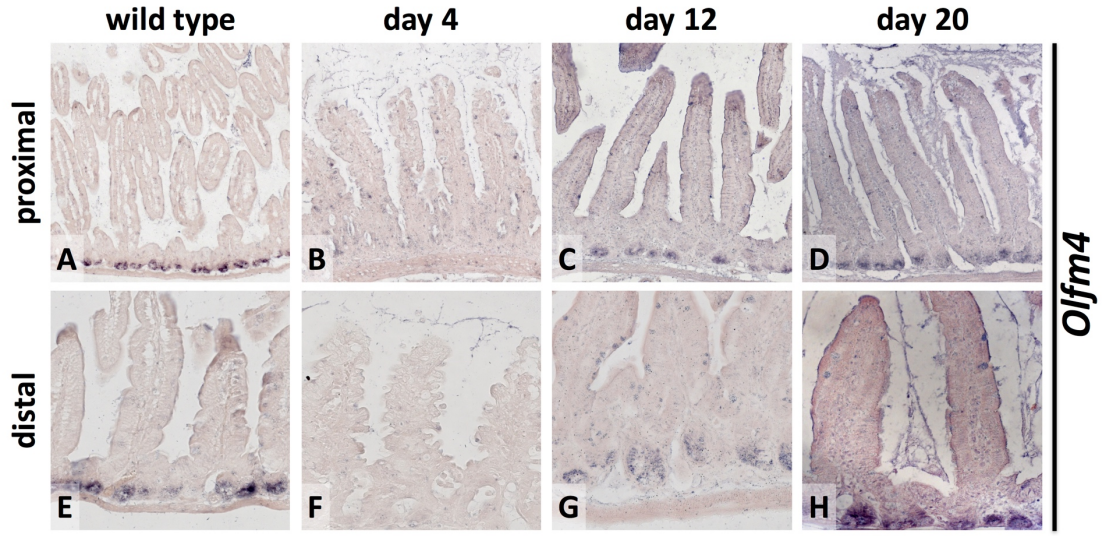

Figure 13: Expression of *Olfm4* in *Villin*-cre-ER^{T2}; *Cdh1* $^{fl/fl}$ mice.
Chromogenic RNA-in situ hybridization for *Olfm4* in wild type and E-cadherin deficient mice (short-time model, sacrificed at day 4 post tamoxifen administration) and E-cadherin partially deficient mice (long-time model, sacrificed at day 12 and day 20) of proximal (A-D) and distal (E-H) small intestine. Photomicrographs taken at 100x (A-D) and 200x (E-H) original magnification.

This collaborative project showed that knockout of E-cadherin resulted in loss of adherens junctions and desmosomes, which led to epithelial cell apoptosis followed by cell shedding. Paneth cells and goblet cells did not mature properly, were misplaced, and reduced in numbers. Active Wnt signaling — as would be seen in mature Paneth cells —

assessed by ISH for *Axin2* and IHC for β-catenin was not evident in these precursors. *Olfm4* expression was absent in the short-time model indicating loss of CBC or an impaired stemness program. In the long-time model, staining was restricted to CBC while misplaced Paneth or goblet cells did not show any expression of *Olfm4*.

3.2.3 Mitochondrial function controls intestinal epithelial stemness and proliferation

This collaborative project (Berger et al. 2016) with Prof. Dirk Haller's group (ZIEL—Institute for Food & Health, TUM) was addressing the role of mitochondrial chaperone HSP60 in the regulation of intestinal homeostasis. To this end, a conditional knockout mouse model (*Hsp60* $^{fl/fl}$) was created. Upon recombination of loxP sites, integral regions of the *Hsp60* gene were deleted resulting in absence of the HSP60 protein.
Breeding with intestinal epithelial cell (IEC)-specific, tamoxifen-inducible cre mice (*Villin*-cre-ER^{T2}) resulted in severe wasting necessitating euthanasia of mice at day 2 after cessation of tamoxifen feeding.

Cre recombinase under the *Villin* promoter is known to not be consistently expressed in all IEC (Madison et al. 2002). On occasion, single IEC could therefore escape deletion of *Hsp60* and give rise to hyper-proliferative HSP60-positive crypt foci ("escaper crypts"). In order to delineate the cellular origin of these nodules and to investigate the status of Wnt/β-catenin signaling, sections of small intestines of *Hsp60* $^{fl/fl}$ and *Hsp60* $^{\Delta/\Delta\ IEC}$ mice were subjected to chromogenic RNA-in situ hybridization for *Olfm4* (**Figure 14 A**) and *Axin2* (**Figure 14 B**).
In *Hsp60* $^{fl/fl}$ mice, *Olfm4* expression recapitulated the normal, regular expression in wild type mice with strong, uniform, crypt-restricted staining (**Figure 14 A, left**). In contrast, *Hsp60* $^{\Delta/\Delta\ IEC}$ mice showed only moderate crypt-restricted staining, most notably in only a reduced number of crypts (**Figure 14 A, right**).
Expression levels of *Axin2* showed similar characteristics. *Hsp60* $^{fl/fl}$ mice revealed regular staining for *Axin2* in all small intestinal crypts (**Figure 14 B, left**) whereas *Hsp60* $^{\Delta/\Delta\ IEC}$ mice did only show inconsistent crypt labeling for *Axin2* (**Figure 14 B, right**).

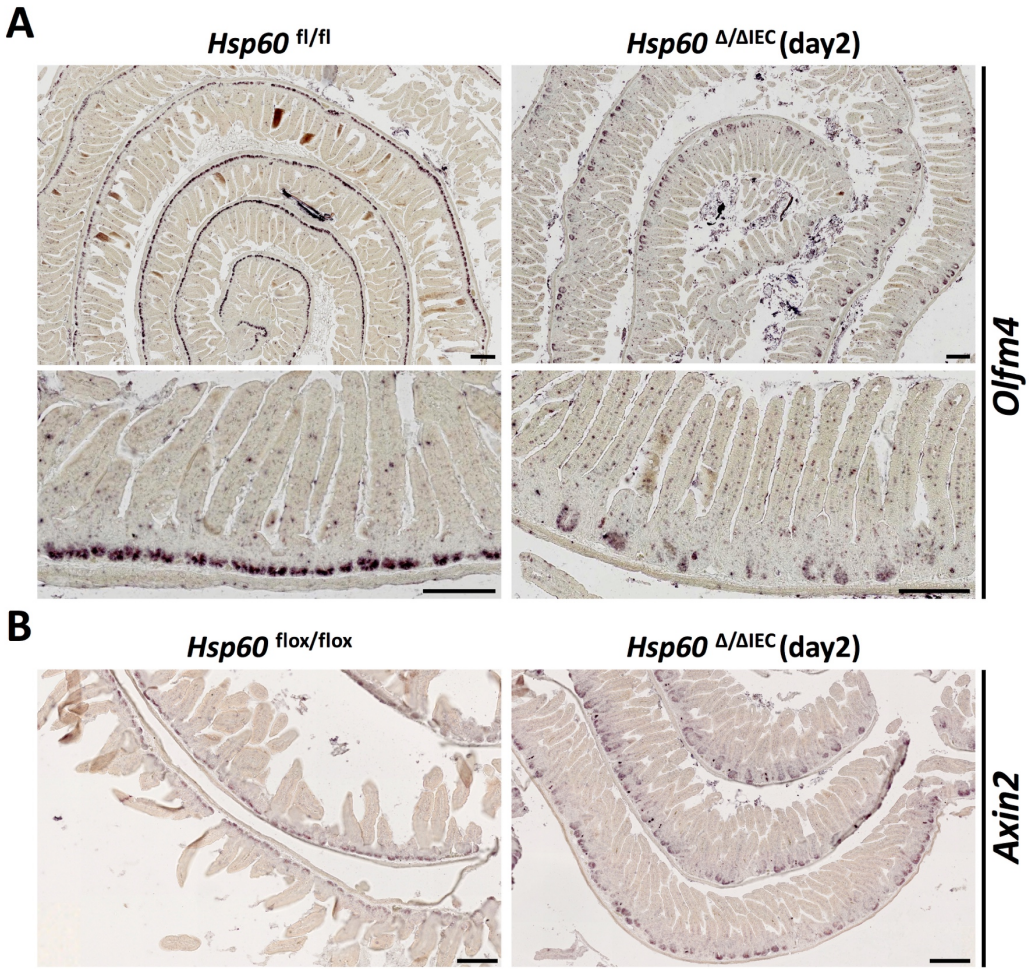

Figure 14: Overview of expression of intestinal stem cell marker *Olfm4* and Wnt target gene *Axin2* in small intestines of *Hsp60* $^{fl/fl}$ and *Hsp60* $^{\Delta/\Delta IEC}$ mice.
Chromogenic RNA-in situ hybridization for *Olfm4* (A) and *Axin2* (B) in *Hsp60* $^{fl/fl}$ and *Hsp60* $^{\Delta/\Delta IEC}$ mice (at day 2 post tamoxifen administration). Scale bars indicate 250 µm.

Hyper-proliferative HSP60-positive crypt foci ("escaper crypts") expressed *Olfm4* indicating that expanding *Olfm4*$^{+}$ stem cells gave rise to these crypt-based nodules. *Olfm4* was not detected in adjacent hypo-proliferative crypts. The dot plot (**Figure 15**) illustrates the significant loss of *Olfm4* expressing crypts in knockout animals.

Olfm4 served as a surrogate marker for *Lgr5*$^{+}$ stem cells indicated by the fact that mRNA expression levels detected by qRT–PCR of both *Olfm4* and *Lgr5* were markedly reduced comparing *Hsp60* $^{\Delta/\Delta IEC}$ to *Hsp60* $^{fl/fl}$ mice (Berger et al. 2016).

This shows that depletion of HSP60 led to widespread loss of stemness in intestinal crypts.

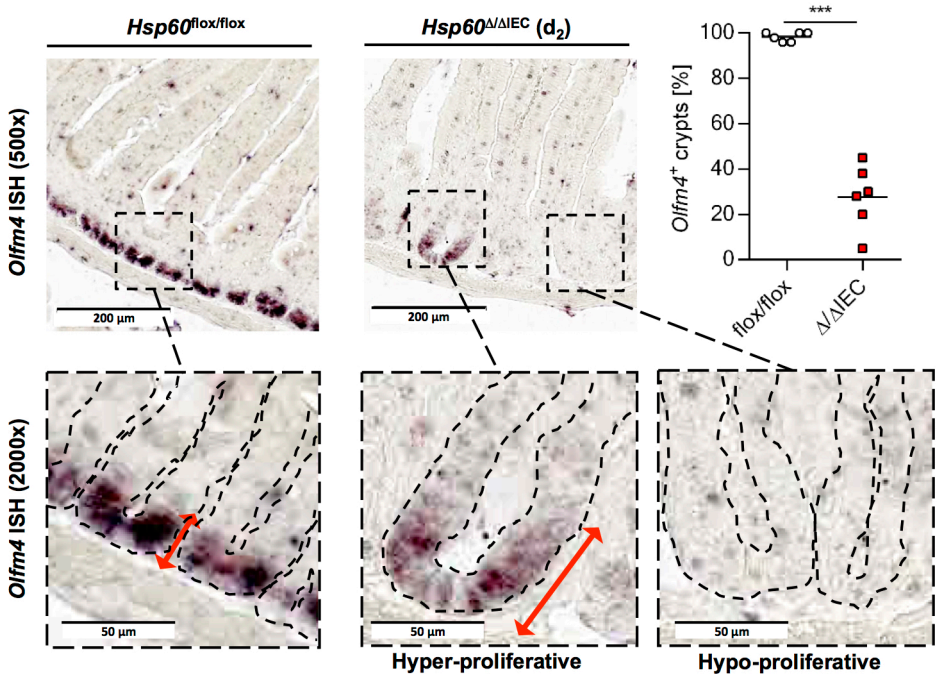

Figure 15: Quantification and extent of expression of *Olfm4* in small intestines of *Hsp60* $^{fl/fl}$ and *Hsp60* $^{\Delta/\Delta IEC}$ mice.
Representative regions from Figure 14 of chromogenic RNA-in situ hybridization for *Olfm4* in *Hsp60* $^{fl/fl}$ and *Hsp60* $^{\Delta/\Delta IEC}$ mice (at day 2 post tamoxifen administration). Proportion of *Olfm4*$^{+}$ crypts in each 6 mice per genotype is given in dot plot. *** $p<0.001$. Contours of crypt epithelial cells are outlined by dotted lines. Red arrows illustrate extent of *Olfm4* expression. Scale bars indicate 200 µm (top images) and 50 µm (bottom images).
Reprinted under Creative Commons Attribution 4.0 International License (CC BY) from Berger et al. 2016. Copyright 2016 by the authors.

Wnt signaling is known to be essential for maintaining stemness and homeostasis of the intestinal epithelium. Paralleling the loss of *Olfm4*, in situ hybridization confirmed concomitant loss of expression of Wnt target gene *Axin2*. In contrast to the majority of hypo-proliferative crypts, *Axin2* expression was maintained and even expanded in hyper-proliferative crypts. This indicates that Wnt signaling plays a functional role in causing hyper-proliferation and long-term regeneration of intestinal epithelium.

Of note, hyper-proliferative crypts/nodules were not observed with an intestinal stem cell specific knockout (*Lgr5*-EGFP-ires-cre-ER^{T2}), which suggests that it was not the loss of intestinal stem cells but rather paracrine (Wnt) signaling from HSP60-deficient IEC that led to hyper-proliferative nodules.

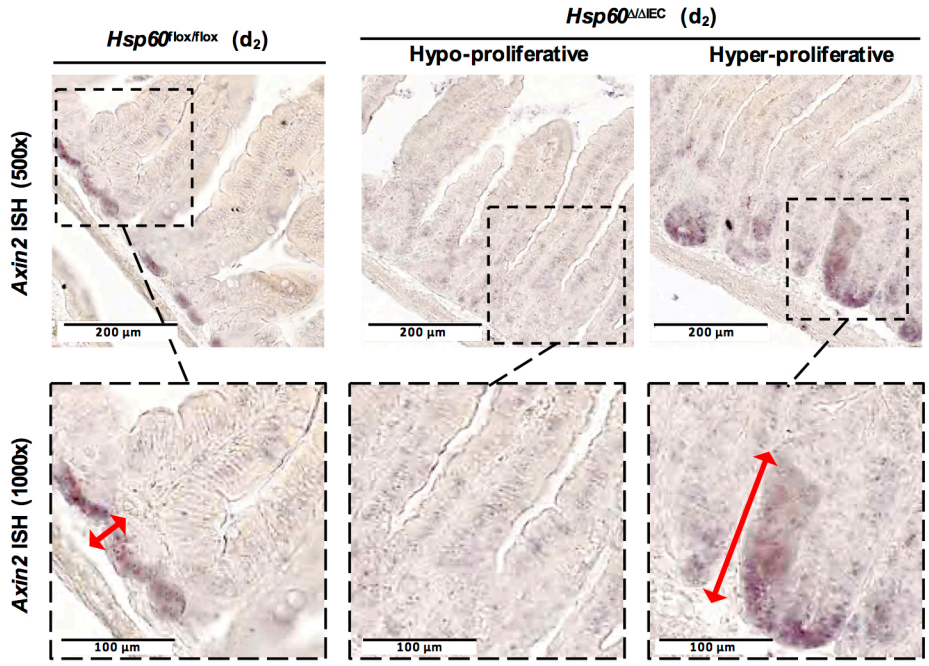

Figure 16: Expression of Wnt target gene *Axin2* in small intestines of *Hsp60* $^{fl/fl}$ and *Hsp60* $^{\Delta/\Delta\ IEC}$ mice.

Representative regions from Figure 14 of chromogenic RNA-in situ hybridization for Wnt target gene *Axin2* in *Hsp60* $^{fl/fl}$ and *Hsp60* $^{\Delta/\Delta\ IEC}$ mice (at day 2 post tamoxifen administration). Red arrows illustrate extent of *Axin2* expression. Scale bars indicate 200 µm (top images) and 100 µm (bottom images).

Reprinted under Creative Commons Attribution 4.0 International License (CC BY) from Berger et al. 2016. Copyright 2016 by the authors.

3.3 The Wnt/β-catenin pathway in gastrointestinal carcinogenesis

3.3.1 RNF43 and its role in intestinal carcinogenesis

As a first step to gain additional insight into the function of RNF43, its spatial expression in murine and human tissues was investigated. Due to the lack of a good, commercially available antibody at the beginning of the project, chromogenic RNA-in situ hybridization was initially employed. Once various antibodies for application on human tissue became available and after rigorous testing and tweaking of reaction parameters, a reliable and valid antibody could be used for further studies.

3.3.1.1 Rnf43 shows crypt-restricted expression in murine intestine and upregulation in tumorigenesis

Since many published studies on Wnt signaling and more specifically RNF43 were carried out in mouse models, I started out investigating *Rnf43* expression in mice, both wild type and the *APC* $^{min/+}$ mouse model that is characterized by the development of ten to hundreds of benign adenomatous polyps in the small intestine (Moser, Pitot, and Dove 1990).

Chromogenic RNA-in situ hybridization (ISH) for *Rnf43* yielded a blue precipitate at the base of the crypt (**Figure 17 A**) indicating expression of *Rnf43*. In contrast to immunohistochemical stains there is staining of the entire cytoplasm and no specific compartments can be delineated since mRNA is detected. In our hands, when staining normal mucosa, many genes show relatively low staining intensities that might just be slightly above background staining. Therefore, negative controls are essential which were run in parallel and were consistently negative. Again, scattered blue dots represent an artifact.

Rnf43 expression in adenoma of *APC* $^{min/+}$ mice (**Figure 17 B**) was markedly increased in comparison to the normal weak expression at the base of the crypt. There was a sharp demarcation between regular mucosa with only weak staining in the crypts and uniformly, positively stained adenomatous tissue.

Olfm4 expression was much stronger (**Figure 17 C**) which is why it is used as a robust marker to highlight intestinal stem cells located at the bottom of the crypt. *Axin2* (**Figure 17 D**) as a target gene of the canonical Wnt pathway was uniformly expressed throughout the tumor and at the base of crypts although barely perceivable.

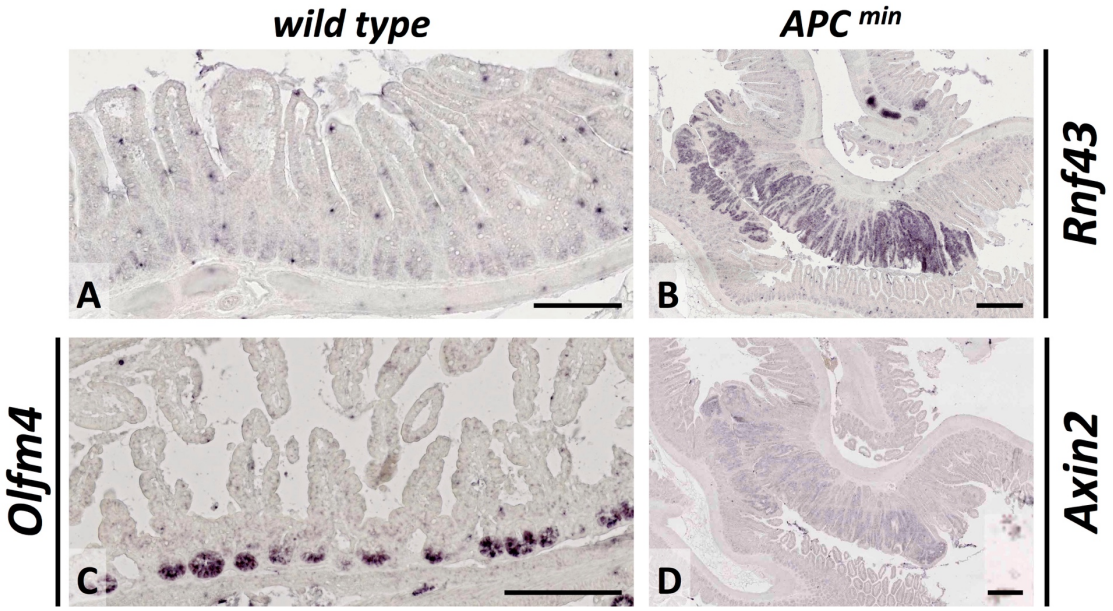

Figure 17: Expression of *Rnf43* in murine intestine by chromogenic RNA-in situ hybridization.
Riboprobes against *Rnf43* (A, B), *Olfm4* (C), and *Axin2* (D) mRNA transcripts in sections of normal small intestinal mucosa (A, C) and small intestinal adenoma developing in an *APC* $^{min/+}$ mouse (B, D). Scale bars indicate 200 µm (A, C) and 400 µm (B, D).

3.3.1.2 RNF43 shows crypt-restricted, nuclear expression and is overexpressed in human colorectal adenomas and carcinomas

Since our ultimate goal is to better understand human disease, I next investigated RNF43 expression in anonymized human FFPE tissue samples.

Chromogenic RNA-in situ hybridization for *RNF43* was performed with a probe that is oriented anti-sense to the endogenous mRNA transcript (**Figure 18 A, C**). In parallel a sense-oriented control probe was run (**Figure 18 B, D**).
The section of adenocarcinoma showed strong and uniform staining for *RNF43* in neoplastic epithelial cells (**Figure 18 A**) while the control (**Figure 18 B**) was entirely negative. *RNF43* was detected at the base of the crypts but with a lower intensity

compared to the staining in tumor (**Figure 18 C**). The control probe did not yield any specific staining (**Figure 18 D**).

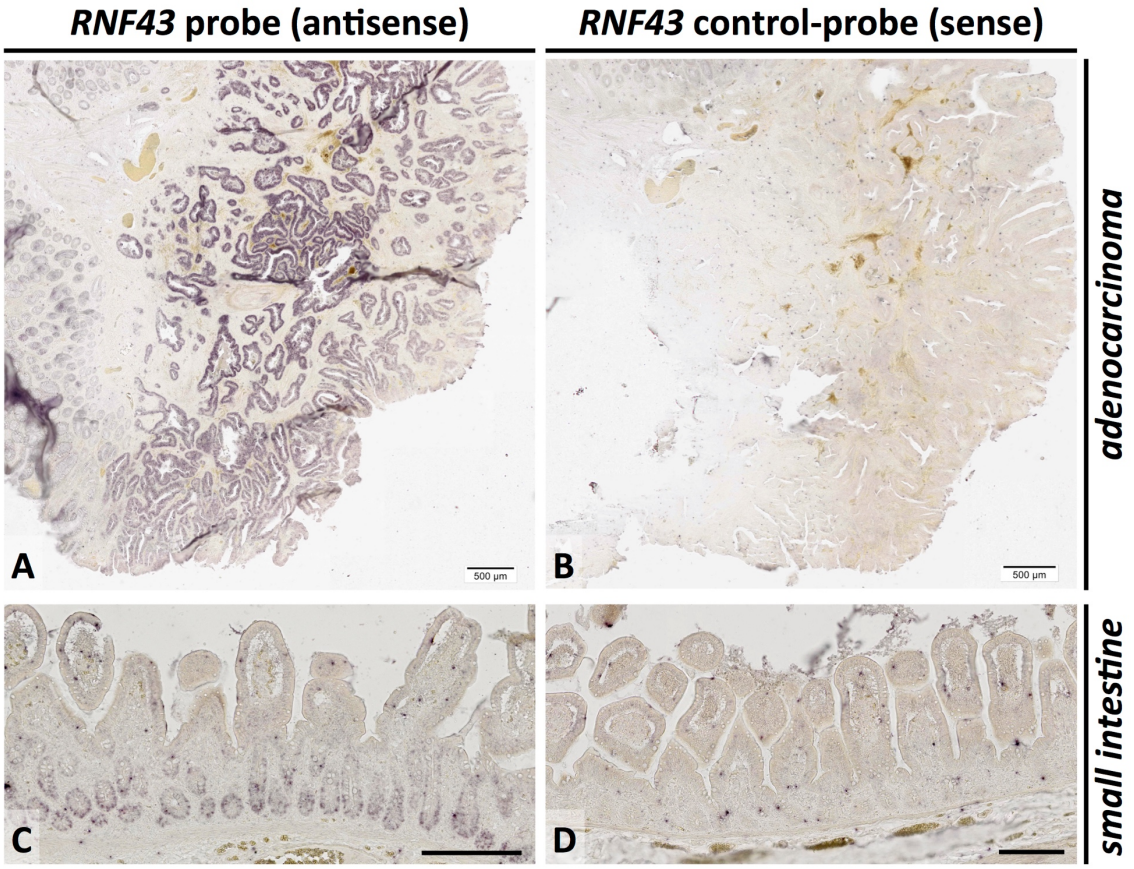

Figure 18: Establishing chromogenic RNA-in situ hybridization for *RNF43*.
Riboprobe against *RNF43* mRNA transcripts (A, C) and sense-control probe (B, D) in sections of human colorectal adenocarcinoma (A, B) and normal human small intestinal mucosa (C, D). Scale bars indicate 500 µm (A, B) and 250 µm (C, D).

Once in situ hybridization was established I wanted to investigate the expression pattern of *RNF43* in normal healthy colon and colonic carcinogenesis from adenoma to adenocarcinoma (**Figure 19**). *RNF43* expression was detected in small intestinal and colonic crypts. *RNF43* expression was even more pronounced in colonic adenoma and adenocarcinoma. In comparison *OLFM4* staining showed much stronger staining in small intestinal and colonic crypts. *OLFM4* was uniformly expressed in neoplastic epithelia of colonic adenoma but only in scattered areas of colonic adenocarcinoma.

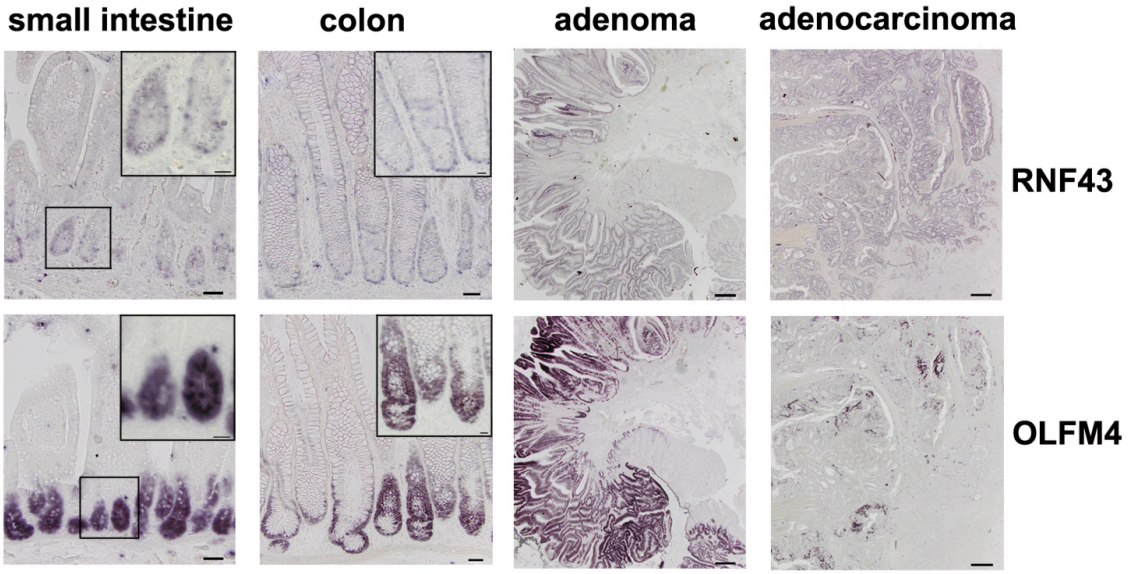

Figure 19: Chromogenic RNA-in situ hybridization for *RNF43* and *OLFM4*.
Riboprobe against *RNF43* and *OLFM4* mRNA transcripts in sections of normal human small intestine and colon, as well as colonic adenoma and adenocarcinoma. Scale bars indicate 50 µm (small intestine and colon), 500 µm (colonic adenoma and adenocarcinoma), and 20 µm (insets). Reprinted with permission from Loregger et al. 2015. Copyright 2015 AAAS.

In situ hybridization for *RNF43* could successfully be established for murine and human intestine. Nevertheless, detection of protein expression has additional advantages such as determining subcellular localization, being more robust on clinical FFPE material, a quicker turnaround time, and most importantly yielding more relevant information since mRNA expression by ISH does not necessarily equate to protein expression.
Out of different antibodies tested, RNF43 (HPA008079, Atlas Antibodies AB), which was developed for and used in the Human Protein Atlas (available from www.proteinatlas.org (Uhlen et al. 2015)) turned out to yield strong yet clean nuclear staining which was in line with data obtained through other experimental approaches (immunofluorescence, nuclear fractionation).

Immunohistochemical staining required significant tweaking of parameters including antigen retrieval solution (low pH of 6.0 and high pH 9.0), boiling time, antibody dilutions (1:250, 1:500, and 1:1000) and primary antibody incubation time. Dilutions of primary antibody were most critical since a low dilution like 1:250 (**Figure 20 A**) yielded labeling of many epithelial cells and also chronic inflammatory infiltrates in the submucosa. Using a dilution of 1:500 (**Figure 20 B**) and even better, but with reduced overall sensitivity at 1:1000 (**Figure 20 C**) led to increased specificity with reduced background staining.

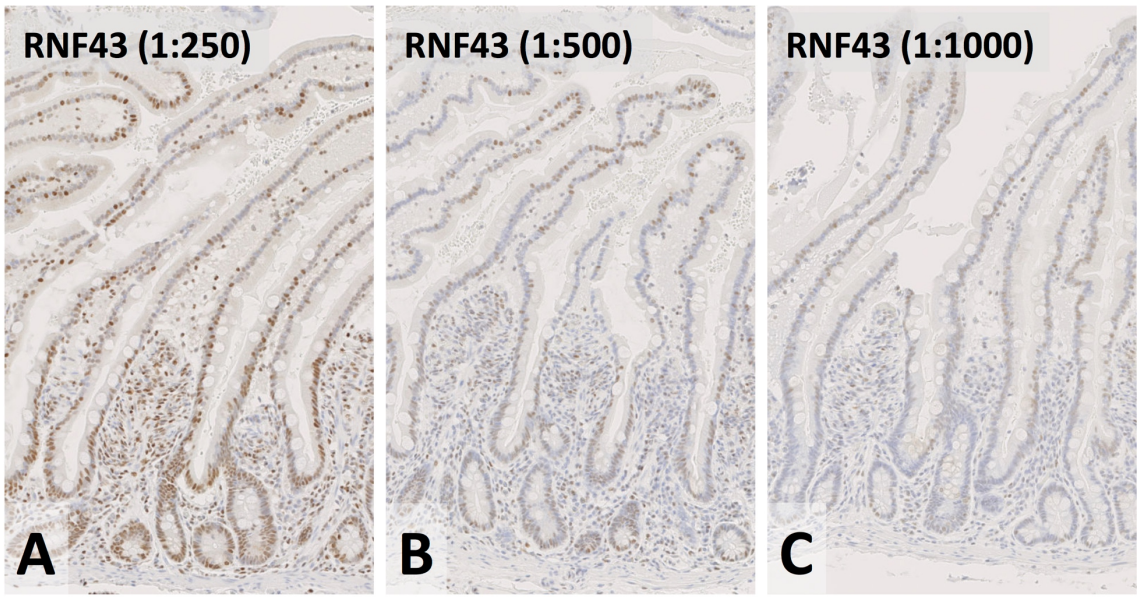

Figure 20: Establishing immunohistochemistry for RNF43.
Immunohistochemical staining of normal small intestinal mucosa with 1:250 (A), 1:500 (B), and 1:1000 (C) dilutions of primary antibody against RNF43 (HPA008079, Atlas Antibodies AB). 100x original magnification.

After further optimization, immunohistochemistry revealed crypt restricted expression of RNF43 in sections of human small intestine (**Figure 21 A, B**). Of note, the staining pattern was nuclear providing additional insight into the subcellular localization of RNF43. Staining of colonic adenocarcinoma (**Figure 21 C, D**) showed strong and diffuse nuclear staining throughout the tumor.

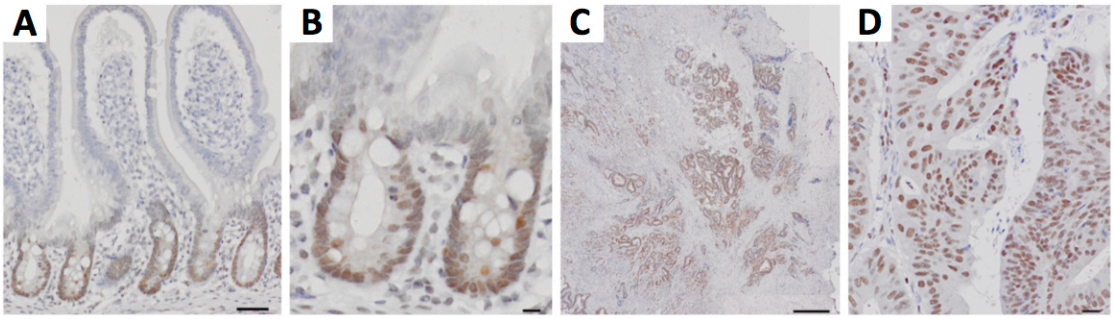

Figure 21: RNF43 shows crypt-restricted, nuclear expression and is overexpressed in human colorectal carcinogenesis.
RNF43 expression detected by immunohistochemistry in human small intestine (A, B) and colonic adenocarcinoma (C, D). Scale bars indicate 20 µm (B, D), 50 µm (A), and 500 µm (C). Adapted with permission from Loregger et al. 2015. Copyright 2015 AAAS.

3.3.1.3 RNF43 inhibits Wnt/β-catenin signaling in colon cancer cells

RNF43 showed crypt-specific expression, in stem cells and transit amplifying cells and was upregulated in colorectal tumorigenesis, both processes which are known to be driven by enhanced Wnt/β-catenin signaling (Krausova and Korinek 2014). In addition, RNF43 was found to be a direct target gene of the Wnt/β-catenin pathway (Hatzis et al. 2008). Therefore, I wanted to see whether overexpression of RNF43 in HCT116, which have mutated RNF43 (**Table 14**), would influence Wnt/β-catenin pathway activity. In addition, a RING-mutant RNF43^{H292R} was also investigated.

Transient transfection with *RNF43* caused a decrease of TOPFlash luciferase activity albeit not in a dose dependent manner in this experiment (**Figure 22**). Transfection with the mutant *RNF43*^{H292R} led to enhanced TOPFlash luciferase activity, FOPFlash luciferase activity served as a negative control and showed low level background luciferase activity.

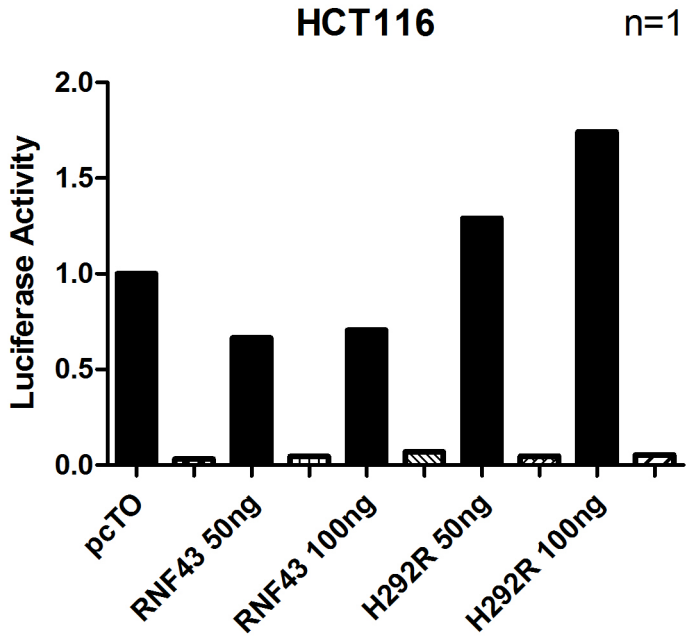

Figure 22: Wnt/β-catenin signaling activity after overexpression of RNF43 and mutant RNF43^{H292R}.
TOP/FOP luciferase reporter assay in HCT116 human colon carcinoma cell line transiently transfected with empty vector control (pcDNA4/TO) and indicated amounts of wild type or mutant *RNF43* (*RNF43*^{H292R}) expression plasmids. One representative experiment is shown. (Firefly) Luciferase normalized to renilla luciferase and values expressed normalized to empty vector control (pcDNA4/TO) luciferase activity. Solid bars: TOPFlash; shaded bars: FOPFlash.

This experiment illustrated that RNF43 suppresses Wnt/β-catenin signaling while RNF43^{H292R} causes a transactivation of Wnt/β-catenin signaling. Additional experiments to characterize RNF43's function in colon cancer were carried out by A. Loregger and M. Grandl (Loregger et al. 2015).

3.3.2 GAPPS — an example of Wnt-driven gastric carcinogenesis

This collaborative project (McDuffie et al. 2016) with Dr. Udo Rudloff's group (Thoracic and Gastrointestinal Oncology Branch, National Cancer Institute, NIH) was investigating gastric adenocarcinoma and proximal polyposis of the stomach (GAPPS), an autosomal-dominant cancer syndrome predisposing affected individuals to develop more than 100 fundic gland polyps (FGP) in the gastric fundus and corpus with sparing of the antrum (**Figure 23**). Although most sporadic FGP are benign, these syndromic FGP have a propensity to develop high grade dysplasia and progress to invasive carcinoma.

The genetic basis of GAPPS was only recently identified as point mutations in promoter 1B of *APC* (Li et al. 2016). *APC* is widely known to be mutated in patients with another cancer-predisposition syndrome — familial adenomatous polyposis (FAP) coli. Interestingly, GAPPS patients were found to develop FGP but usually no syndromic polyps in the intestine (Worthley et al. 2012).

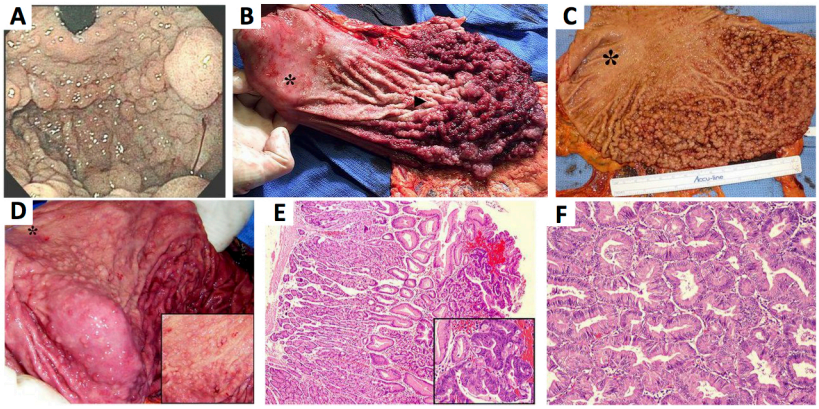

Figure 23: Endoscopic, macroscopic, and histopathological findings in patients afflicted by GAPPS.
Upper endoscopy, retroflexed view, to show polyposis involving the gastric fundus (A). Gastrectomy specimens of three patients (B, C, D) illustrating the classical phenotype: polyposis of gastric fundus, cardia, and corpus with sparing of the antrum (asterisk). Fundic gland polyp with high-grade dysplasia (E) (H&E, 100x original magnification, inset 200x). Early, well-differentiated gastric adenocarcinoma, intestinal-type (F) (H&E, 200x original magnification).
Adapted with permission from McDuffie et al. 2016. Copyright 2016 BMJ Publishing Group Ltd.

I had the chance to study the pathology of members of two GAPPS families. To investigate whether GAPPS is linked to an increased incidence of colonic polyps, family members at risk where compared to family members exhibiting the GAPPS phenotype. 9 GAPPS patients and 6 unaffected family members underwent colonoscopy, which revealed colonic pathology in 7 GAPPS patients and in none of the unaffected family members.

Positive nuclear staining for β-catenin in fundic gland polyp (**Figure 24 D**), gastric adenocarcinoma (**Figure 24 E**), and colonic adenoma (**Figure 24 F**) confirm the role of active Wnt/β-catenin signaling in these pre-neoplastic and neoplastic processes.

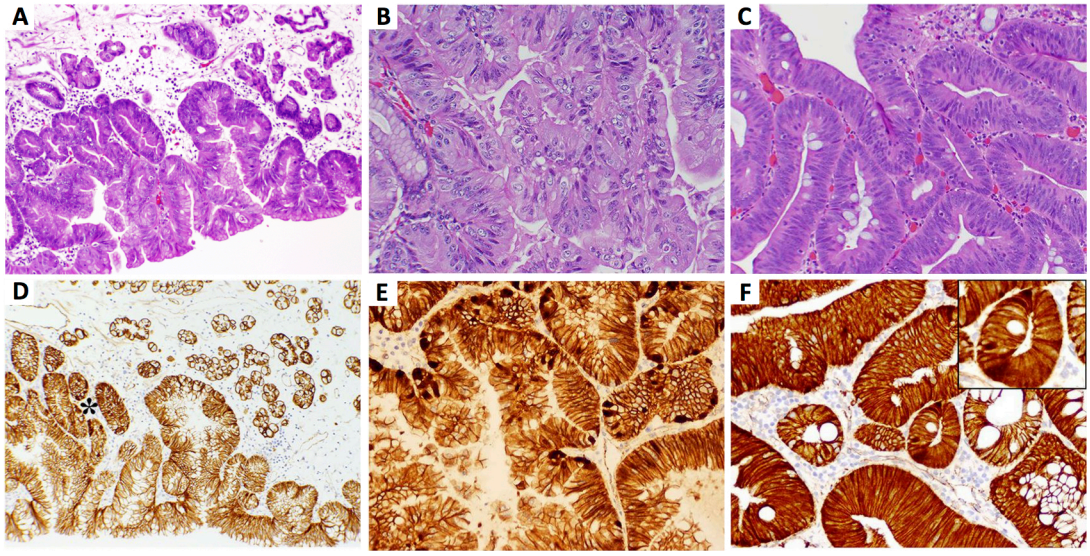

Figure 24: Wnt/β-catenin pathway activation assessed by immunohistochemistry for β-catenin in patients afflicted by GAPPS.
H&E stains of fundic gland polyp (A), gastric adenocarcinoma (B), and colonic adenoma (C) in patients afflicted by GAPPS. Corresponding immunohistochemistry for β-catenin (D-F). Area of nuclear β-catenin expression (asterisk). 100x original magnification (A, D), 200× (B, C, E, F).
Adapted with permission from McDuffie et al. 2016. Copyright 2016 BMJ Publishing Group Ltd.

3.3.3 RNF43 and its role in gastric carcinogenesis

The Wnt/β-catenin pathway plays a role in a subset of sporadic and syndromic gastric cancers (like GAPPS). Since RNF43 was shown to be a Wnt target gene and negative regulator of the Wnt/β-catenin pathway in colon cancer, I wanted to investigate its role in gastric cancer since at that time there was no data published on RNF43 in gastric cancer.

3.3.3.1 *RNF43* is highly mutated in gastric tumors

The publicly available cBioPortal provided by Memorial Sloan Kettering Cancer Center (MSKCC) is an elegant tool to query a multitude of genomic cancer studies including The Cancer Genome Atlas (TCGA) for genetic alterations.

A search for *RNF43* across sequencing datasets of gastrointestinal neoplasms (**Figure 25**) showed that the most prevalent genetic changes were mutations followed by amplifications, deletions, and fusions.

While *RNF43* was most frequently altered in pancreatic neoplasms (IPMN, MCN), there were three subtypes of gastric cancer among the top ten tumor entities with most *RNF43* alterations: mucinous stomach adenocarcinoma, tubular stomach adenocarcinoma, and stomach adenocarcinoma, not otherwise specified. The alteration frequency for these was in excess of 10% of sequenced cases thereby constituting a substantial patient population given how common gastric cancer is.

Therefore, it was deemed prudent to further investigate the role of RNF43 in gastric carcinogenesis.

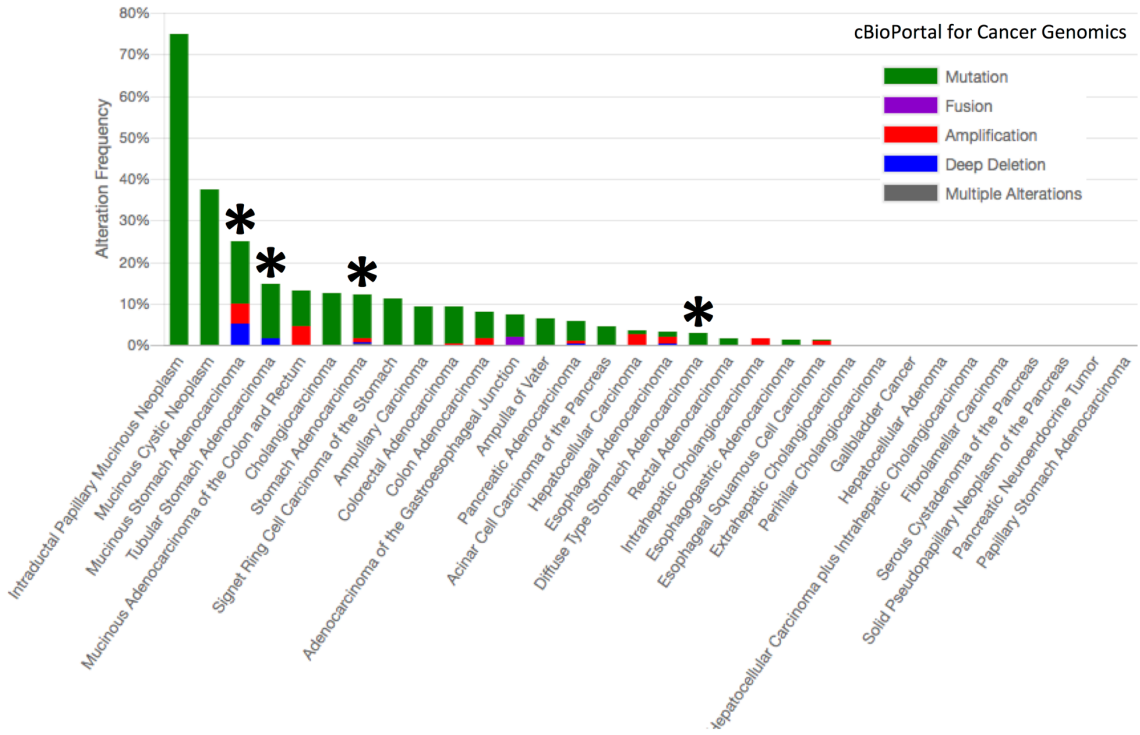

Figure 25: Genetic alterations of *RNF43* across gastrointestinal neoplasms (cBioPortal). Summary and visualization of genetic alteration data on *RNF43* derived from 38 studies of gastrointestinal neoplasms (Giannakis et al. 2016, Chen et al. 2015, Seshagiri et al. 2012, Cancer Genome Atlas Research Network et al. 2017, Janjigian et al. 2018, Brannon et al. 2014, Song et al. 2014, Dulak et al. 2013, Cancer Genome Atlas Research 2014, Kakiuchi et al. 2014, Lin et al. 2014, Wang et al. 2011, Cancer Genome Atlas 2012, Wang et al. 2014, Gingras et al. 2016, Chan-

On et al. 2013, Ong et al. 2012, Li et al. 2014, Jiao et al. 2013, Pilati et al. 2014, Schulze et al. 2015, Ahn et al. 2014, Fujimoto et al. 2012, Jiao et al. 2014, Wu et al. 2011, Cao et al. 2013, Biankin et al. 2012, Bailey et al. 2016, Witkiewicz et al. 2015, Jiao et al. 2011, Scarpa et al. 2017, Yaeger et al. 2018) and provisional TCGA datasets of Colorectal Adenocarcinoma, Cholangiocarcinoma, Esophageal Carcinoma, Liver Hepatocellular Carcinoma, Pancreatic Adenocarcinoma, and Stomach Adenocarcinoma provided by the cBioPortal (Cerami et al. 2012, Gao et al. 2013) (http://www.cbioportal.org; accessed December 19th 2017). Gastric cancer subtypes are indicated (asterisk).

3.3.3.2 Expression of RNF43 in the human stomach

Since RNF43 was upregulated in colorectal carcinomas the question was whether the same held true for gastric cancers, especially in the context of abundant genetic alterations. So far, expression of RNF43 in healthy stomach has not been assessed and only one study compared a collective of gastric tumors but with suboptimal immunohistochemical staining results (Niu et al. 2015).

Sections of morphologically normal oxyntic/fundic gastric mucosa showed nuclear staining restricted to parietal cells (**Figure 26**), which was uniform ranging from strong (4 cases) to moderate (5 cases). Sections that just contained antral mucosa and thereby no parietal cells (3 cases) were negative. Four cases also showed additional weak-moderate nuclear staining in mucous cells of gastric pits.
Morphologically normal appearing mucosa in sections adjacent to tumors showed nuclear staining restricted to parietal cells, which was mostly strong and diffuse (10 cases), strong but only focal (2 cases), and moderate and focal (1 case).
Overall, parietal cells showed strong and diffuse nuclear staining for RNF43 with occasional, weaker staining of other epithelial cells.

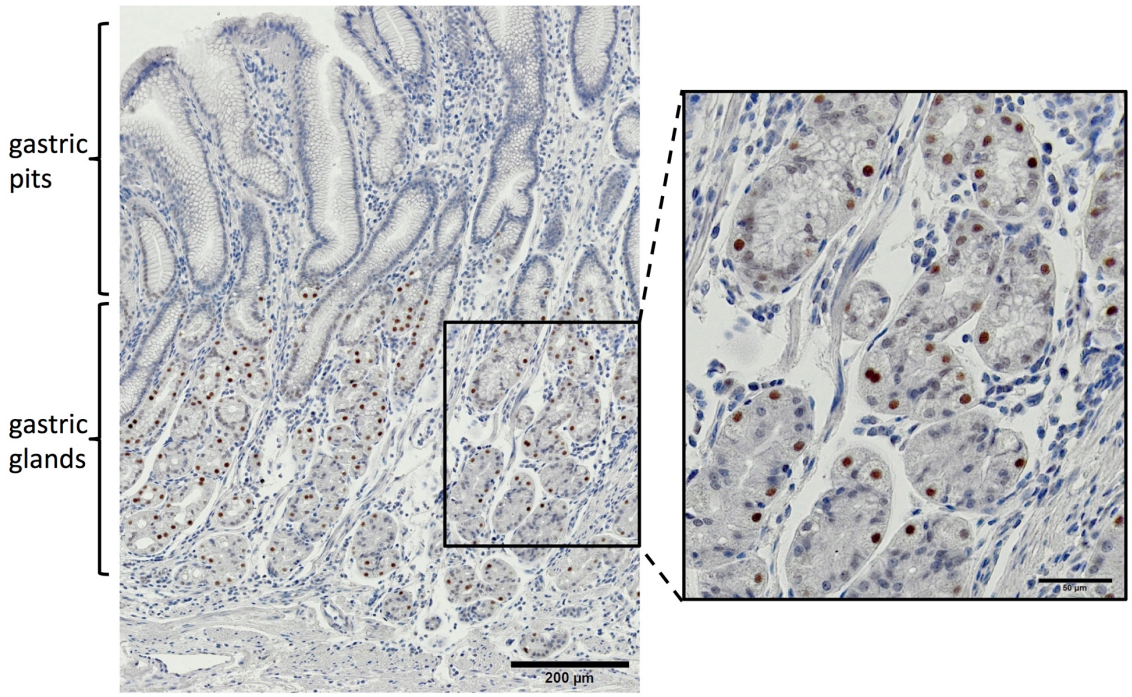

Figure 26: RNF43 is expressed in parietal cells of oxyntic/fundic glands.
RNF43 expression assessed by immunohistochemistry for RNF43 (HPA008079, Atlas Antibodies AB). Mucosal compartments with superficially located, mucin producing gastric pits and deeper gastric glands are labeled. Scale bars indicate 200 µm (large image) and 50 µm (inset).

Nine tissue sections bearing tumor had adjacent areas of intestinal metaplasia available for evaluation. KI-67, a marker for proliferation, showed increased proliferation in glands of intestinal metaplasia in comparison to adjacent normal oxyntic/fundic glands (**Figure 27**). β-catenin expression was uniformly membranous, non-nuclear and therefore not indicating active Wnt/β-catenin pathway signaling. In all nine cases, glands of intestinal metaplasia did not reveal RNF43 expression by immunohistochemistry whereas adjacent oxyntic/fundic mucosa showed strong and diffuse staining for RNF43 restricted to parietal cells.

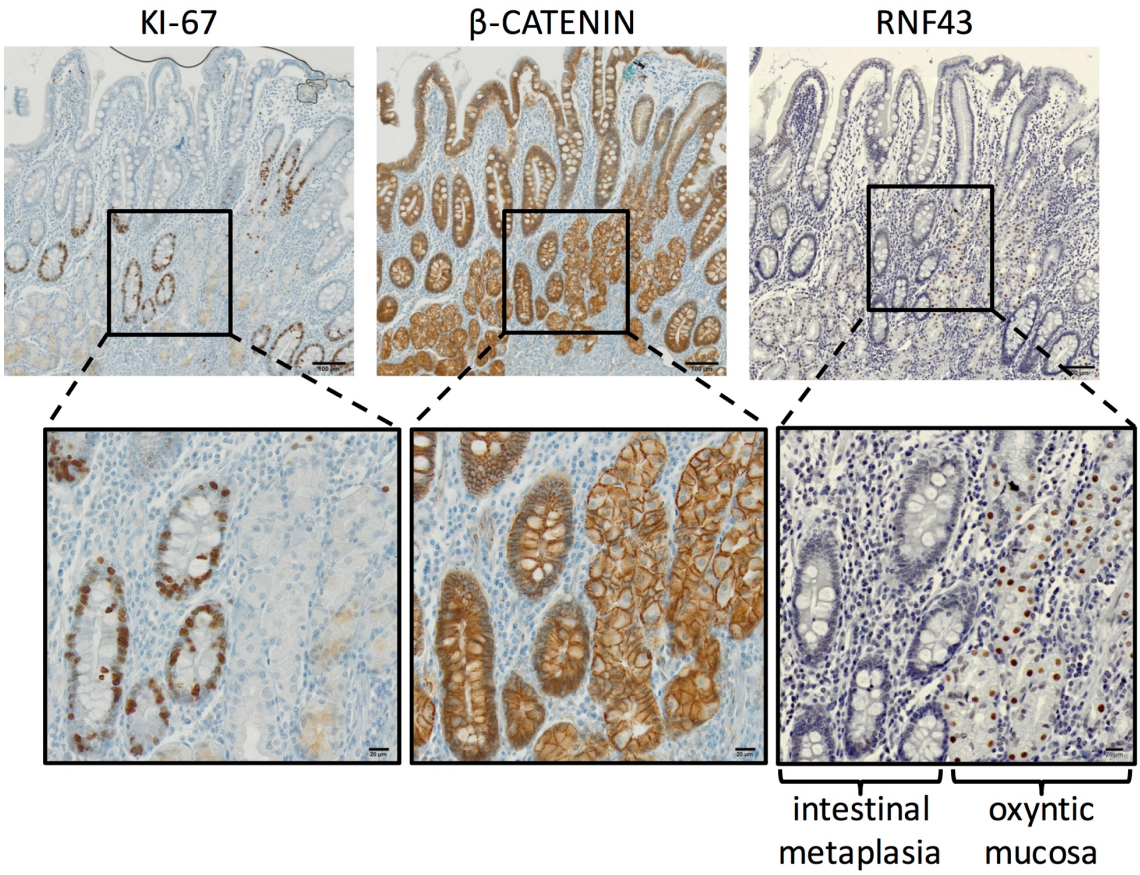

Figure 27: RNF43 is not expressed in areas of intestinal metaplasia.
KI-67, β-catenin, and RNF43 (HPA008079, Atlas Antibodies AB) expression assessed by immunohistochemistry. Areas of intestinal metaplasia and regular oxyntic/fundic mucosa are labeled. Scale bars indicate 100 µm (top row) and 20 µm (bottom row).

A collective of 26 cases of anonymized paraffin-embedded tissue samples of gastric adenocarcinomas was assembled from the archives of the Institut für Pathologie, Klinikum Bayreuth, Germany (**Table 13**).

Average age at time of surgery was 80.0 years (range 42-92) and sexes were equally distributed (13 female, 13 male). Histology according to the Lauren Classification was intestinal type (17/26), diffuse type (5/26), and mixed type (4/26). Tumor grade was G1 (4/26), G2 (9/26), G3 (11/26), and G4 (2/26). Primary tumor size/extent was mostly T1 (20/26), followed by T2 (5/26), and T4 (1/26). Regional lymph node status was largely N0 (20/26) with a few cases of N1 (2/26), N2 (1/26), N3 (2/26), and undetermined lymph node status NX (1/26). Clinical stage was Stage I (23/26) and Stage IV (3/26). Reported or pathologically confirmed *H. pylori* status was positive (20/26), ex-positive (4/26), negative (1/26), and unknown (1/26).

The cases were immunohistochemically stained for KI-67, β-catenin, and RNF43 (HPA008079, Atlas Antibodies AB). Proliferative index by KI-67 immunohistochemistry

was on average 48% (range 10-99%). Immunohistochemistry for β-catenin revealed membranous staining in most cases (21/26) and nuclear staining in a subset (5/26). RNF43 staining of tumor cells was assessed both in intensity and proportion of tumor cells stained and H-scores were calculated. Most cases did not show any positive staining (19/26), some showed moderate staining (4/26), and a few (3/26) exhibited strong nuclear staining for RNF43.

RNF43 expression levels (H-scores) did not correlate with any of the aforementioned parameters.

#	Age	Sex	Type	Grade	pT	pN	Stage	H. pylori	KI-67 (%)	β-CATENIN	RNF43				
											0	+	++	+++	H-score
1	72	M	I&D	G3	T2	N3	IV	+	20	m	10	30	30	30	180
2	42	M	D	G4	T2	N3	IV	+	60	m	50	10	30	10	100
3	75	M	I	G1	T1	N0	I	+ (ex)	30	m	50	0	50	0	100
4	76	F	I	G2	T1	N0	I	+ (ex)	40	n (>90%)	75	5	20	0	45
5	67	F	D	G3	T1	N0	I	+	30	m	80	5	10	5	40
6	70	M	I	G2	T1	N0	I	+ (ex)	10	m	80	20	0	0	20
7	71	F	D	G3	T1	N0	Ia	+	10	m	90	0	10	0	20
8	77	M	I	G2	T2	N0	Ib	+	50	n (5%)	100	0	0	0	0
9	88	F	I	G2	T1	N0	I	+	60	m	100	0	0	0	0
10	75	M	I&D	G3	T1	N0	I	+	20	m	100	0	0	0	0
11	92	F	I	G3	T2	N0	Ib	+	99	m	100	0	0	0	0
12	84	M	I	G3	T4	N2	IV	+	30	m	100	0	0	0	0
13	73	M	I	G2	T1	N0	Ia	+	90	m	100	0	0	0	0
14	80	M	I	G2	T1	N0	Ia	+	20	m	100	0	0	0	0
15	57	M	I&D	G3	T1	N0	Ia	+ (ex)	80	m	100	0	0	0	0
16	76	M	I	G2	T1	N0	I	+	80	m	100	0	0	0	0
17	78	F	I	G2	T1	N0	I	+	90	m	100	0	0	0	0
18	79	F	I	G3	T1	N0	I	?	20	n (5%)	100	0	0	0	0
19	79	F	I	G1	T1	N0	Ia	+	20	m	100	0	0	0	0
20	52	M	D	G3	T1	N1	Ib	+	10	m	100	0	0	0	0
21	65	M	I	G3	T1	N0	Ia	+	30	n (10%)	100	0	0	0	0
22	72	F	I	G1	T1	N0	Ia	-	90	n (1%)	100	0	0	0	0
23	63	F	I&D	G3	T1	N1	I	+	60	m	100	0	0	0	0
24	52	F	I	G1	T1	NX	I	+	60	m	100	0	0	0	0
25	70	F	I	G2	T1	N0	I	+	60	m	100	0	0	0	0
26	60	F	D	G4	T2	N0	Ia	+	80	m	100	0	0	0	0

Table 13: Characteristics of gastric cancer collective and results of immunohistochemical stains for KI-67, β-catenin, and RNF43.

26 cases of gastric adenocarcinoma with details on age (in years), sex (m=male, f=female), type according to Lauren Classification (I=intestinal, D=diffuse, I&D=intestinal and diffuse/mixed), histopathological grade, pT (histopathologically determined tumor size/extent), pN (histopathologically determined regional lymph node status), stage (overall clinical stage), *H. pylori* infection status ([+]=positive histopathology/clinical testing; [+(ex)]=prior positive histopathology/test result, now negative; [-]=negative histopathology/clinical testing), KI-67 proliferative index assessed by immunohistochemistry, β-catenin expression (m=membranous, n=nuclear with percentage of positive tumor cells), RNF43 expression categorized according to intensities ([0]=negative/no staining; [+]=minimal staining; [++]=moderate staining; [+++]=strong staining) with percentage of positive tumor cells, and resulting H-score.

Figure 28 shows photomicrographs of 3 cases that exhibited positive staining for RNF43: A well-differentiated tubular adenocarcinoma (**Figure 28 A; case #3 in Table 13**) with a proliferative index of 30% (KI-67), membranous staining for β-catenin, and moderate staining for RNF43 in 50% of tumor cells. A moderately-differentiated intestinal type adenocarcinoma (**Figure 28 B; case #4 in Table 13**) with a proliferative index of 40% (KI-67), nuclear staining for β-CATENIN (> 90% of tumor cells), and minimal (5% of tumor cells) to moderate (20% of tumor cells) staining for RNF43. A poorly-differentiated mixed (intestinal and diffuse) type adenocarcinoma (**Figure 28 C; case #1 in Table 13**) with a proliferative index of 20% (KI-67), membranous staining for β-catenin, and minimal (30% of tumor cells), moderate (30% of tumor cells), and strong (30% of tumor cells) staining for RNF43.

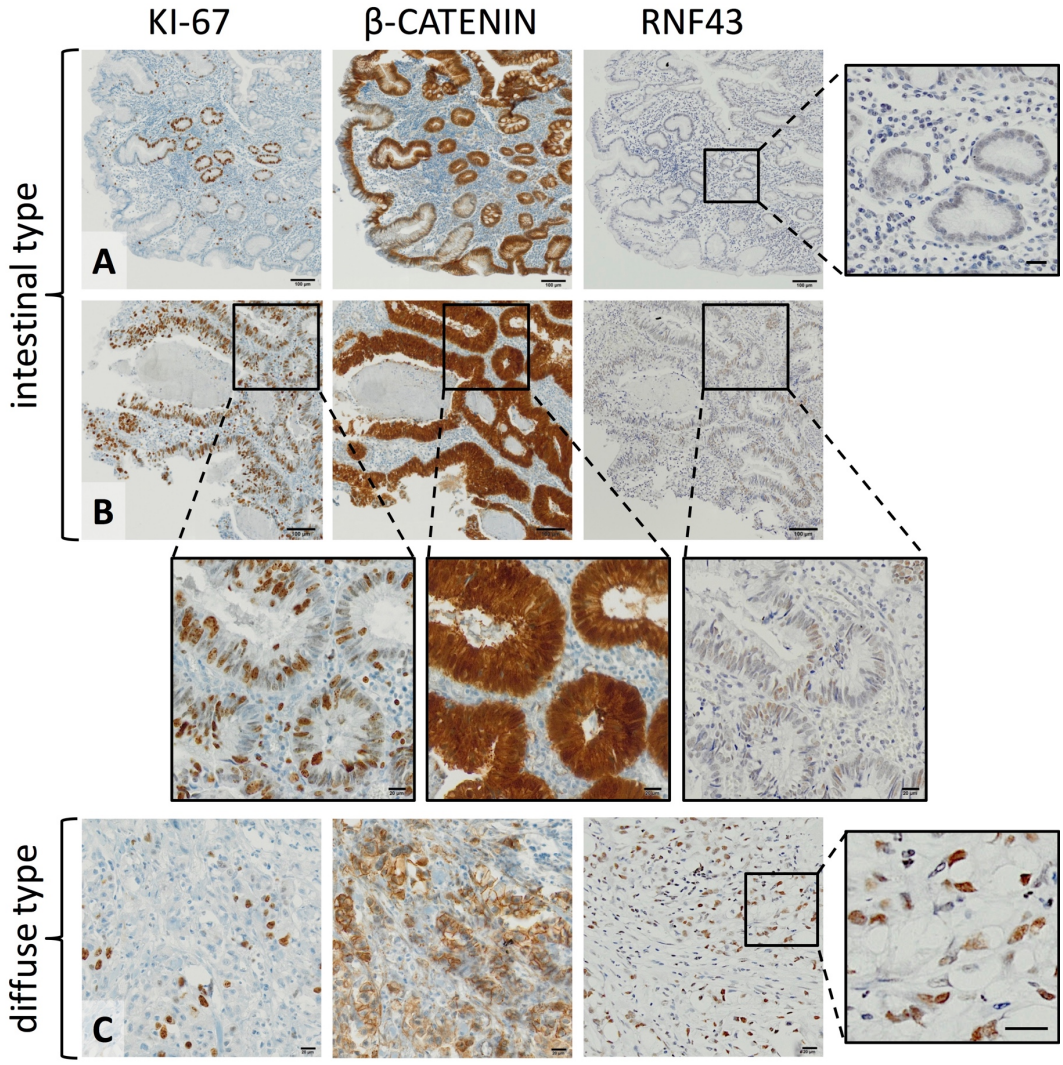

Figure 28: RNF43 is expressed in a minority of gastric adenocarcinomas.
KI-67, β-catenin, and RNF43 (HPA008079, Atlas Antibodies AB) expression assessed by immunohistochemistry. Two cases of intestinal type (A, B) and one case of diffuse type gastric adenocarcinoma (C) are shown. Scale bars indicate 100 µm (A, B) and 20 µm (C, all insets).

3.3.3.3 *RNF43* is expressed in human gastric cancer cell lines

The publicly available Cancer Cell Line Encyclopedia (CCLE) provided by the Broad Institute is a good resource to investigate mRNA expression levels across a large set of cancer cell lines. This can serve as a good starting point to assess the relevance of a gene of interest for a specific type of tumor.

A query for *RNF43* (**Figure 29**) showed that gastric cancer cell lines exhibited the second highest mRNA expression levels by RNA sequencing and Affymetrix microarrays, only to be trumped by colorectal cancer cell lines indicating that *RNF43* likely is of some relevance in gastric cancer.

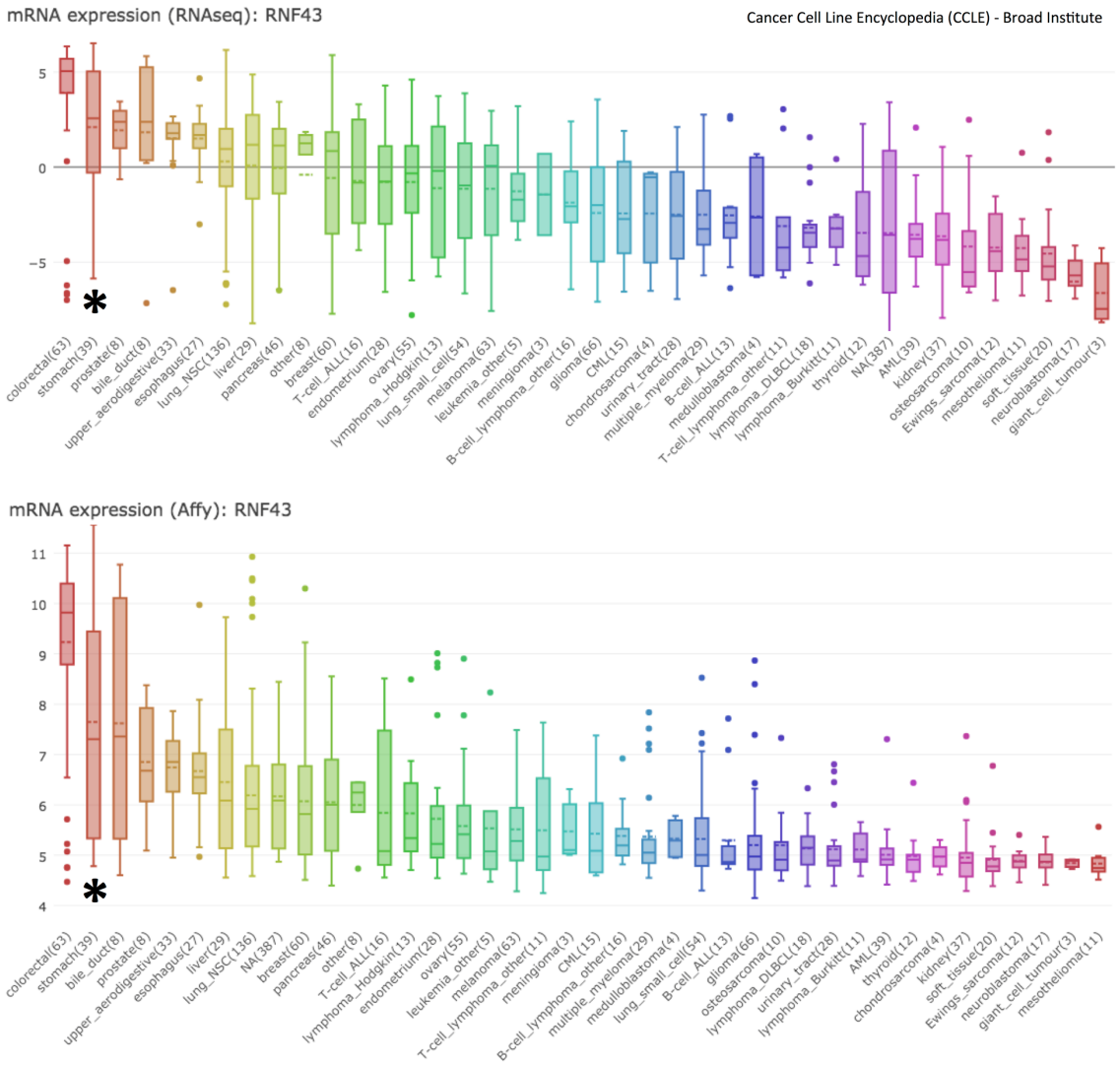

Figure 29: Gastric cancer cell lines exhibit high levels of *RNF43* mRNA expression in comparison to other human cancer cell lines (CCLE).
Summary and visualization of *RNF43* mRNA expression levels assessed through RNAseq (RNA sequencing) and Affy (Affymetrix microarrays) across 1457 cancer cell lines. Obtained from the Cancer Cell Line Encyclopedia (CCLE) provided by the Broad Institute

(https://portals.broadinstitute.org/ccle; accessed December 19th 2017). Gastric cancer cell lines (n=39) are indicated (asterisk). Dashed line within box represents the mean.

To specifically interrogate mRNA levels of RNF43 in our available gastric cancer cell lines, I ran two independent qRT-PCRs (**Figure 30**) on 8 gastric cancer cell lines. Both experiments showed comparable results. *RNF43* transcripts could be detected in all cell lines. KATOIII, NUGC4, ST2957, ST3051, and ST23132 showed higher expression levels than AGS, MKN45, and MKN7.

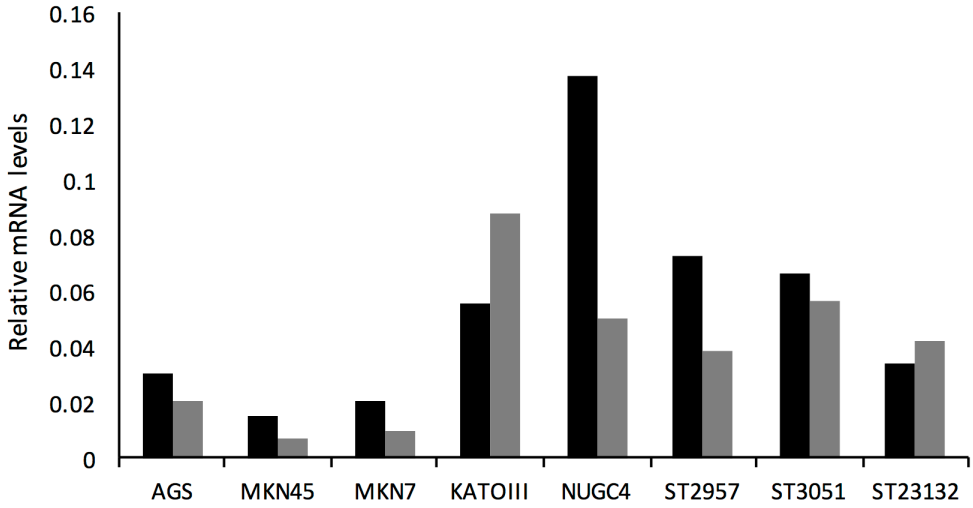

Figure 30: *RNF43* is expressed at variable levels in human gastric cancer cell lines.
Relative mRNA expression levels of *RNF43* in eight gastric cancer cell lines normalized to expression of housekeeping gene *GAPDH*. Data of two independent experiments are shown indicated by black and grey bars.

RNF43 protein expression was investigated in lysates of eight gastric cancer cell lines (**Figure 31**). First, a commercially available polyclonal antibody raised in rabbit against a peptide of RNF43 (LS-C102008, LifeSpan BioSciences) was applied and yielded some prominent bands between 70-95 kDa despite apparent background staining. RNF43 has four predicted isoforms (http://www.uniprot.org; accessed January 1st 2018) with molecular weights of 85.7 kDa ('canonical' sequence), 81.2 kDa, 72.1 kDa, and 95.0 kDa. Therefore, some of the observed bands might be due to the detection of these isoforms. But they might also represent an off-target effect since polyclonal antibodies detect multiple epitopes of the peptide used for immunization leading to a higher chance of cross-reactivity with homologous proteins.

Next, a monoclonal antibody "8D6" (derived from immunizing rats and creating hybridomas; screened and validated by M. Grandl, our group) was applied. In all cell lines, there was only a single band detected at about 95 kDa.

Both antibodies detected RNF43 protein in all cell lines. Most cell lines appeared to express comparable amounts of RNF43 by western blot. AGS and KATOIII showed lower levels of RNF43 since with both antibodies band intensities were weaker, despite at least average amounts of loaded cell lysates when judging by β-actin intensities. NUGC4 also showed lower levels but giving potentially lower amounts of loaded cell lysates by β-actin intensity this is difficult to state with certainty.

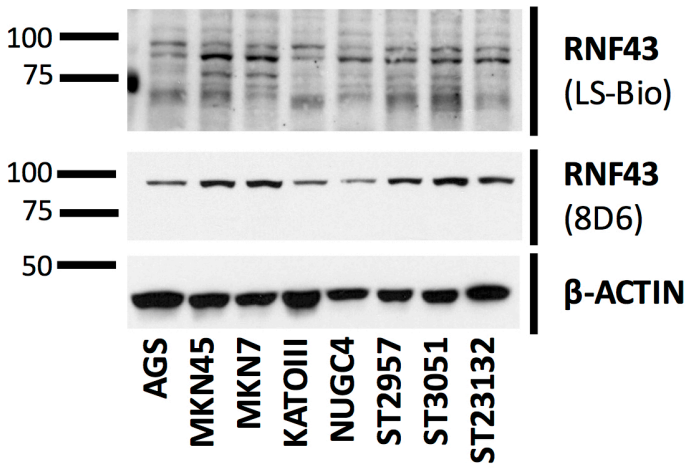

Figure 31: Protein expression of RNF43 in human gastric cancer cell lines.
Protein expression of RNF43 in eight gastric cancer cell lines by western blot. A commercially available polyclonal antibody against RNF43 (LS-C102008, LifeSpan BioSciences) and a monoclonal antibody derived from rat hybridomas "8D6" (validated by M. Grandl, our group) were run in parallel. β-actin served as loading control. A representative experiment is shown. Numbers on y-axis indicate molecular weight in kilodaltons.

3.3.3.4 Basal Wnt signaling activity in gastric cancer cell lines

Nuclear translocation of β-catenin – also the immunohistochemical hallmark of active Wnt/β-catenin signaling – associated with mutations rendering it resistant to phosphorylation, has been reported in up to one third of gastric cancers (Clements et al. 2002, Ebert et al. 2002, Cheng et al. 2004).

Cytoplasmic levels of β-catenin are tightly regulated. In the absence of active Wnt signaling, β-catenin is phosphorylated by glycogen synthase kinase 3 (GSK-3) and casein kinase 1α (CK1α) in a complex with APC and Axin. This marks it for subsequent degradation via the ubiquitin–proteasome pathway (Angers and Moon 2009). Therefore, one can assess Wnt/β-catenin pathway activity by investigating the phosphorylation status of its key mediator β-catenin.

To this end, three different antibodies for the detection of different forms of β-catenin were used (**Figure 32**) with expected bands at a molecular weight of 92 kDa. The phosphorylated form of β-catenin was detected with an antibody specific for phosphorylation at Ser33, Ser37, and Thr41, residues that are phosphorylated to mark β-catenin for degradation. The non-phosphorylated, active form of β-catenin, which is dephosphorylated on Ser33, Ser37, and Thr41 was detected with a different phosphorylation site specific antibody. Lastly, an antibody detecting total β-catenin irrespective of phosphorylation status was used.
Total β-catenin was detected in all cell lines at similar levels with the exception of NUGC4, which showed noticeably lower levels. Non-phosphorylated β-catenin was seen at comparable levels in all cell lines but absent in NUGC4 as was reported before (Nojima et al. 2007). On the western blot, two bands were visible but only the upper band was regarded as specific since a band was expected at 92 kDa as seen in the blot of total β-catenin. The western blot for phosphorylated β-catenin did not lead to as robust signals but showed slightly higher expression levels in AGS and NUGC4. All cell lines expressed comparable amounts of TCF4 by western blot, yet the presence of TCF4 itself does not signify active Wnt/β-catenin signaling.

In order to measure Wnt/β-catenin pathway activation in a functional assay, nine gastric cancer cell lines were transfected with TOPFlash or FOPFlash luciferase reporter plasmids (**Figure 33**). KATOIII showed the highest TOP/FOP luciferase activity, followed by AGS, N87, and MKN45. The remaining cell lines showed only rather low levels of basal activity.

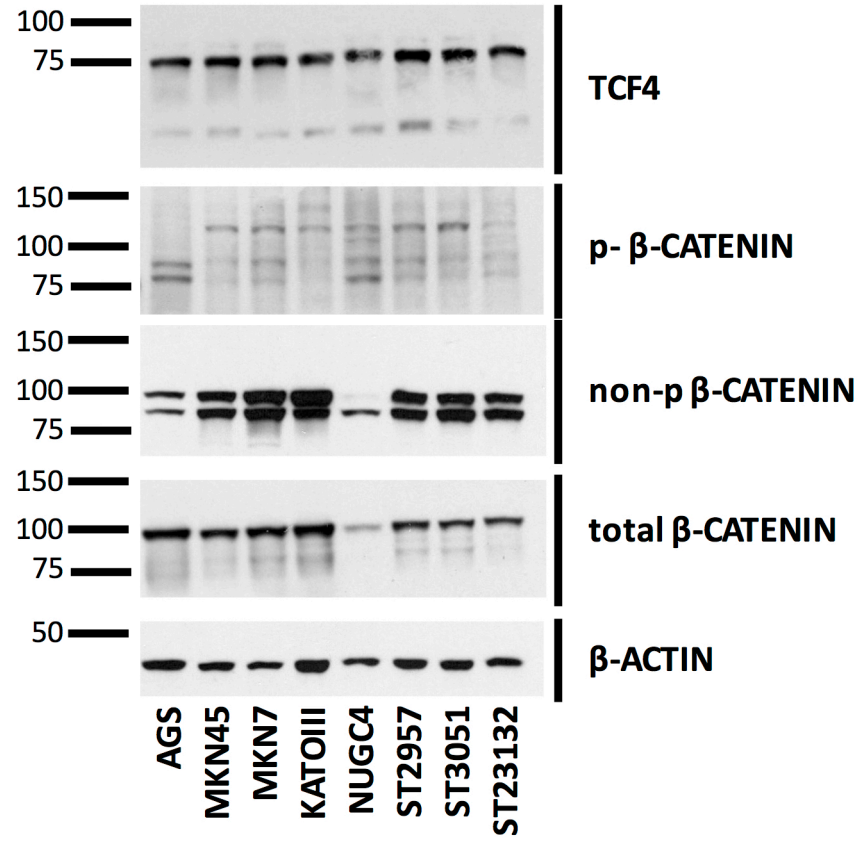

Figure 32: High levels of active/non-phosphorylated β-catenin in most human gastric cancer cell lines.
Protein expression of TCF4, phosphorylated, non-phosphorylated, and total β-CATENIN in eight gastric cancer cell lines by western blot. β-actin served as loading control. A representative experiment is shown. Numbers on y-axis indicate molecular weight in kilodaltons.

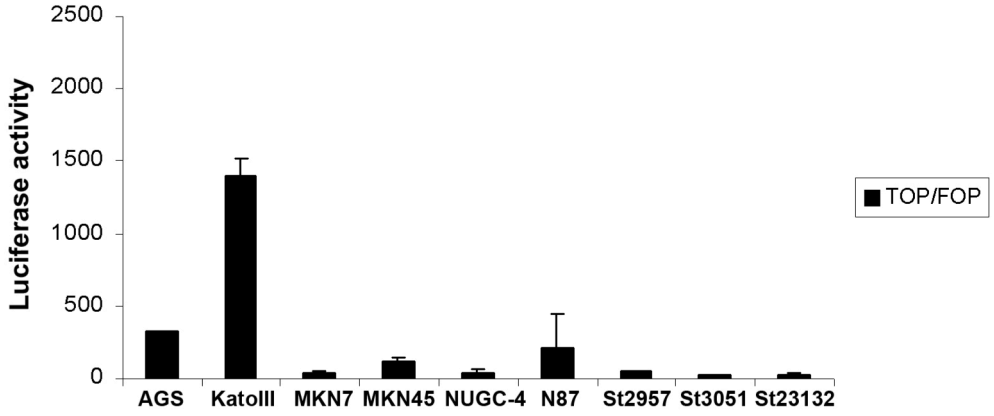

Figure 33: Some human gastric cancer cell lines exhibit increased levels of Wnt/β-catenin pathway activation.
TOP/FOP luciferase reporter assays in nine gastric cancer cell lines. TOPFlash luciferase activity was divided by FOPFlash luciferase activity after both were normalized to Renilla luciferase activity to control for transfection efficiency. Numbers on y-axis represent arbitrary units of luciferase activity.

3.3.3.5 *RNF43* is wild type in gastric cancer cell lines used

Next, I wanted to check whether the observed increased levels of Wnt/β-catenin pathway activation in gastric cancer cells were due to the presence of genetic mutations in key components of the pathway and whether RNF43 was mutated. **Table 14** lists all human cancer cell lines used in this study with mutational status of selected Wnt pathway components derived from the COSMIC database. AGS, MKN45, and to a lesser degree KATOIII and ST23132 were primarily used for *in vitro* experiments.

The AGS cell line was derived from a stomach adenocarcinoma, not otherwise specified and harbors a missense mutation in *CTNNB1*, the gene encoding β-catenin, leading to amino acid exchange G34E. This affects a ubiquitination target motif (Suarez et al. 2015) and renders the mutant protein resistant to degradation (Ganesan et al. 2008) leading to accumulation of β-catenin and thereby to an increased activation of the Wnt/β-catenin pathway (Caca et al. 1999).

MKN45 originates from a liver metastasis of a poorly differentiated adenocarcinoma and was not found to have mutations in *APC*, *CTNNB1*, or *RNF43*.

KATOIII was grown from a signet ring cell carcinoma causing a carcinomatous pleural effusion. No mutations in *APC*, *CTNNB1*, or *RNF43* were described. None of the cell lines harbored mutation in genes encoding GSK-3, CK1α, or Axin.

ST23132 was established from a well-differentiated gastric adenocarcinoma but no mutational data was available, most likely since these cell lines are not widely used.

HCT116, a colorectal cancer cell line used as control in some experiments, contains a mutant form of *CTNNB1* (c.131_133delCTT) removing amino acid Ser45, an important phosphorylation site for GSK-3β (Morin et al. 1997) leading to accumulation of β-catenin. It is also the only cell line in this study to harbor a mutation in *RNF43* (p.R117fs*41).

					COSMIC (cancer.sanger.ac.uk)		
Cell line	**Tumor**	**Site**	**Age**	**Sex**	***APC***	***CTNNB1***	***RNF43***
AGS	adenocarcinoma	stomach	54	f	wt	c.101G>A p.G34E substitution - missense	wt
MKN45	poorly differentiated adenocarcinoma	met. (liver)	62	f	wt	wt	wt
MKN7	tubular adenocarcinoma	met. (lymph node)	39	m	p.Y1179Y c.3537T>C silent	wt	wt
KATOIII	signet ring cell carcinoma	met. (pleural effusion)	55	m	wt	wt	wt
NUGC4	signet ring cell carcinoma	met. (lymph node)	35	f	wt	wt	wt
NCI-N87	well differentiated adenocarcinoma	met. (liver)	-	m	wt	wt	wt
ST23132	well differentiated adenocarcinoma	stomach	-	-	-	-	-
ST3051	well differentiated adenocarcinoma	stomach	-	-	-	-	-
ST2957	well differentiated adenocarcinoma	met. (lymph node)	-	-	-	-	-
HCT116	colorectal carcinoma	colon	adult	m	wt	p.S45del c.131_133delCTT deletion - in frame	p.R117fs*41 c.344delC deletion - frameshift

Table 14: *RNF43* is wild type in used gastric cancer cell lines.
Summary of nine gastric and one colonic (HCT116) cancer cell lines listing histological tumor type, site of procurement, patient demographics, and mutational status of selected Wnt/β-catenin pathway components (derived from https://www.lgcstandards-atcc.org; http://en.brc.riken.jp; http://cancer.sanger.ac.uk/cosmic (Forbes et al. 2017); all accessed December 18th 2017). wt = wild type allele.

3.3.3.6 RNF43 is expressed in the nucleus of gastric cancer cell lines

As discussed, RNF43 was shown to exhibit diverse functions from ubiquitinating frizzled receptors at the cell surface (Hao et al. 2012, Koo et al. 2012) to tethering TCF4 to the nuclear membrane (Loregger et al. 2015) and was further described to interact with various nuclear proteins (Sugiura, Yamaguchi, and Miyamoto 2008, Miyamoto, Sakurai, and Sugiura 2008, Shinada et al. 2011, Nailwal et al. 2015, Xie et al. 2015).

Immunohistochemistry for RNF43 on human samples showed a nuclear staining pattern (**Figure 21, Figure 26**). To provide additional *in vivo* evidence for its subcellular localization, I conducted confocal immunofluorescence as an initial experiment. Endogenous RNF43 could not be directly investigated due to the lack of a specific

antibody working with immunofluorescence at that time. Therefore FLAG-tagged RNF43 was transiently overexpressed.

Confocal immunofluorescence microscopy of AGS cells (**Figure 34**) showed FLAG-tagged RNF43 to be localized along the nuclear membrane and in a distribution reminiscent of the endoplasmic reticulum. β-catenin showed predominant nuclear and to a lesser degree cytoplasmic staining indicative of active Wnt/β-catenin signaling.

In MKN45 cells, FLAG-tagged RNF43 was found in a similar perinuclear distribution. β-catenin was not only seen in the nucleus but also along the cell membrane. The merged image clearly showed that signals of FLAG-tagged RNF43 and β-catenin did not overlap and that there was a spatial separation between the two signals. Since β-catenin is known to interact with E-cadherin at the cell membrane, it can be concluded that FLAG-tagged RNF43 did not localize to the cell membrane.

The HCT116 colonic carcinoma cell line that was run as a positive control showed similar staining patterns as MKN45.

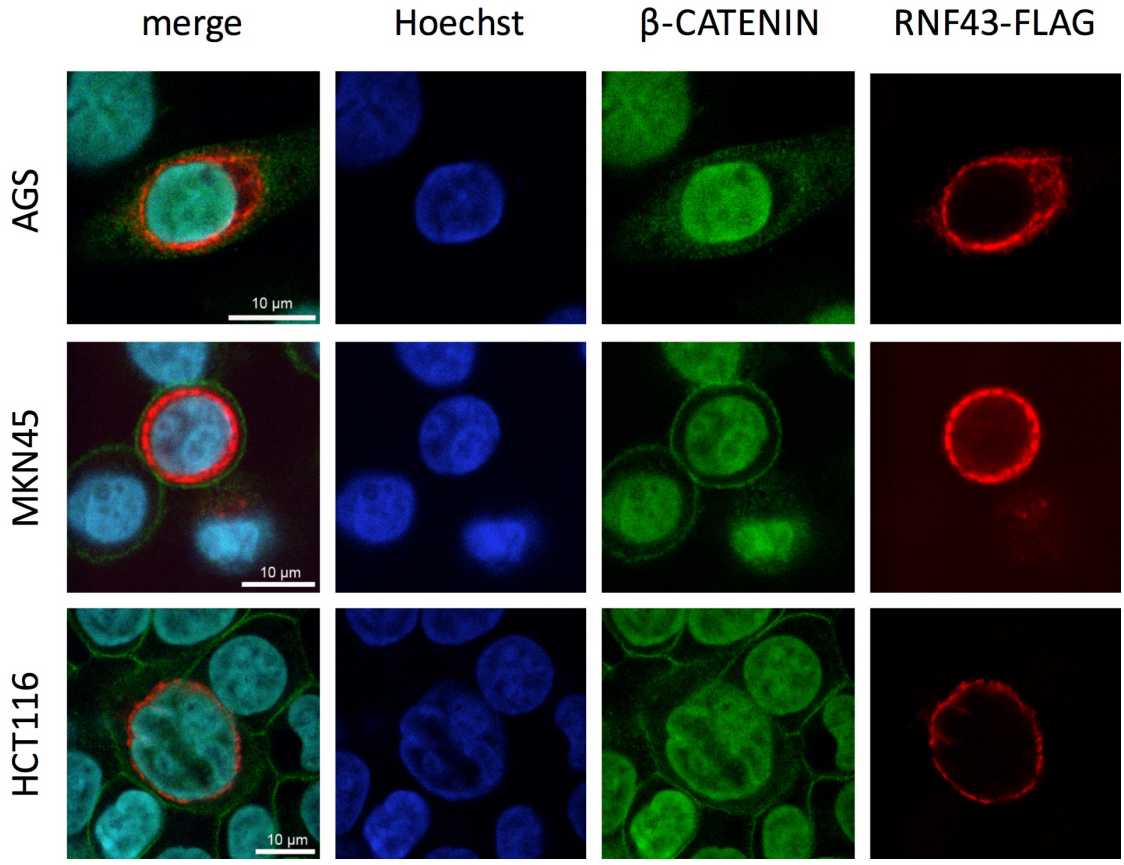

Figure 34: Transiently overexpressed RNF43 localizes to nuclear membrane and endoplasmic reticulum in gastric and colonic carcinoma cell lines.
Confocal immunofluorescence microscopy of FLAG-tagged RNF43 that was overexpressed in AGS, MKN45, and HCT116 cell lines. The Hoechst dye (blue) specifically bound to DNA and thereby highlighted the nucleus. Antibodies against β-CATENIN (green) and FLAG-tag (red) were applied. Scale bars indicate 10 µm.

In order to assess whether a mutation of the RING domain has an influence on subcellular localization, FLAG-tagged RING domain mutated RNF43^{H292R} was also transiently overexpressed.

Confocal immunofluorescence microscopy of AGS cells (**Figure 35**) showed FLAG-tagged RNF43^{H292R} to be localized in a similar distribution to RNF43 wt: along the nuclear membrane and in the distribution of the endoplasmic reticulum. β-catenin showed nuclear staining. In MKN45 and HCT116 cells FLAG-tagged RNF43^{H292R} was found in a similar perinuclear distribution. β-catenin staining was also not altered in comparison to transfection of RNF43 wt yielding nuclear and membranous staining. Again, the merged image clearly showed that the FLAG-tagged RNF43^{H292R} and β-catenin did not overlap.

Taken together, a mutation of the RING domain had no influence on subcellular localization of RNF43^{H292R} and yielded similar staining patterns as RNF43 wt.

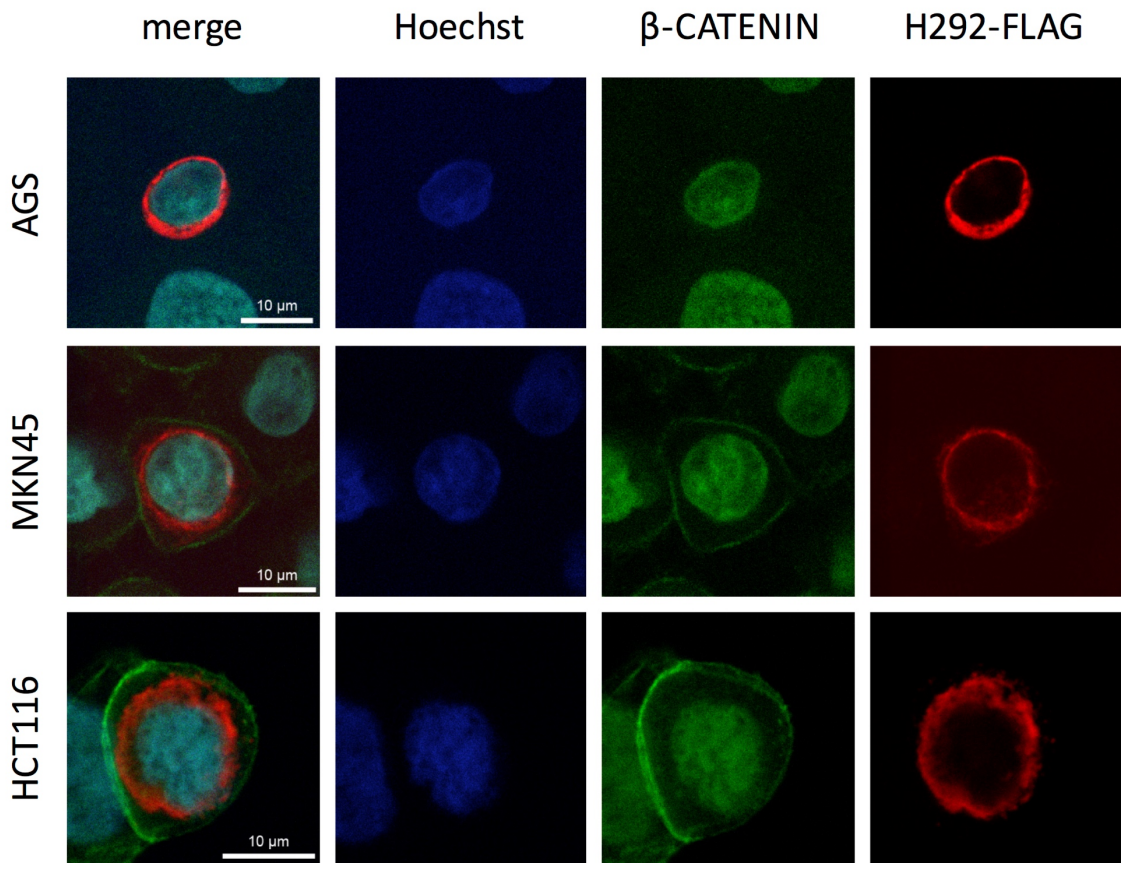

Figure 35: Transiently overexpressed mutant RNF43^{H292R} shows comparable expression patterns to wild type RNF43 in gastric and colonic carcinoma cell lines.
Confocal immunofluorescence microscopy of FLAG-tagged RING domain mutated RNF43^{H292R} that was overexpressed in AGS, MKN45, and HCT116 cell lines. The Hoechst dye (blue) specifically bound to DNA and thereby highlighted the nucleus. Antibodies against β-CATENIN (green) and FLAG-tag (red) were applied. Scale bars indicate 10 µm.

Since I could establish a working antibody for immunohistochemistry on human tissue FFPE samples, I thought to apply the same technique to FFPE cell pellets of gastric cancer cell lines to further substantiate the subcellular distribution of endogenous RNF43 which was wild type in the gastric cancer cell lines used (**Table 14**). This was important since confocal immunofluorescence experiments were carried out under overexpression of RNF43. Of note, this is also true for most of the aforementioned published studies.

RNF43 immunohistochemistry revealed a nuclear staining pattern in all four cell lines (**Figure 36**) with varying intensities and proportions of cells stained. ST23132 showed the highest proportion of labeled nuclei, followed by AGS, KATOIII, and MKN45, corroborating the results of confocal immunofluorescence experiments.

β-catenin was membranous, cytoplasmic, and nuclear in AGS and KATOIII, while it was mostly membranous in MKN45 and ST32132.

TCF4 showed nuclear staining with the largest proportion of cells stained in MKN45 and ST32132, followed by AGS and KATOIII.

Taken together, RNF43 showed nuclear distribution in all cell lines.

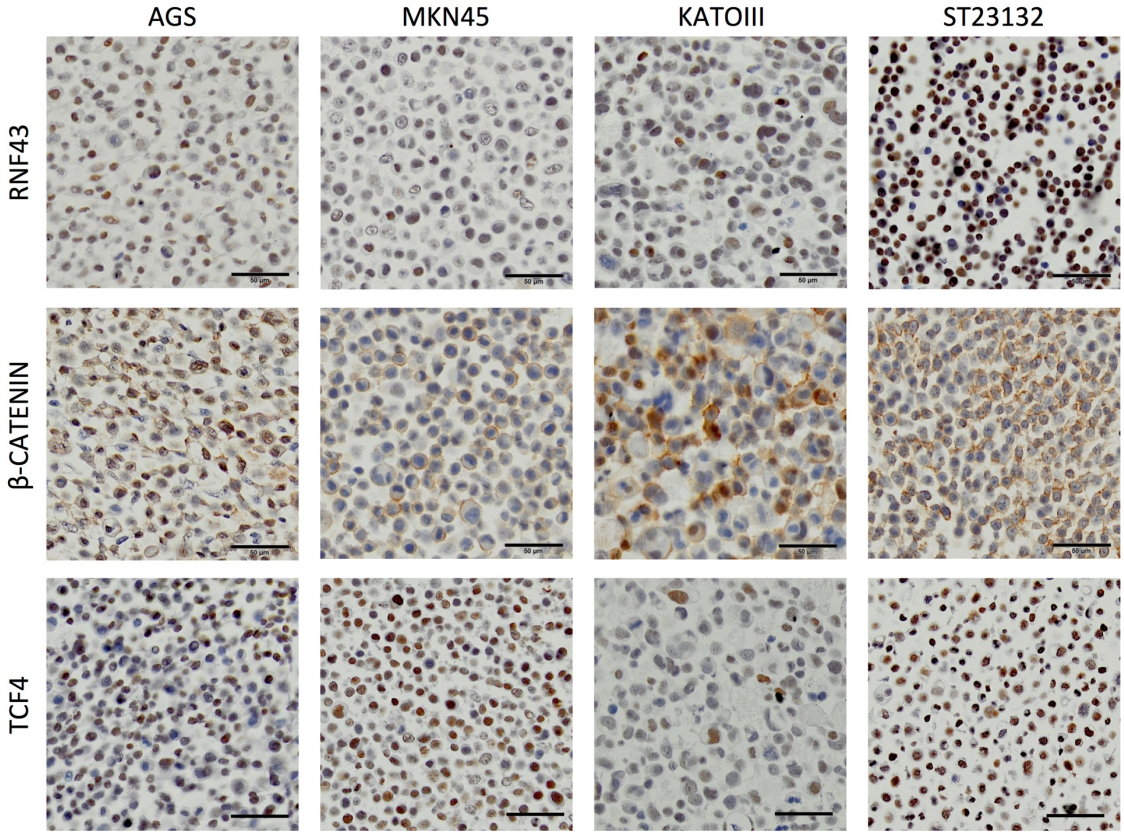

Figure 36: RNF43 shows strong nuclear expression in gastric cancer cell pellets.
FFPE cell pellets of gastric cancer cell lines AGS, MKN45, KATOIII, and ST23132 were prepared and immunohistochemistry for RNF43 (HPA008079, Atlas Antibodies AB), β-catenin, and TCF4 was performed. Scale bars indicate 50 µm.

Subcellular fractionation of four gastric cancer cell lines was performed to shed further light on the localization of endogenous RNF43.

The cleanest fractionation was achieved with ST23132 (**Figure 37**) and is thus described in more detail. CDC5L showed a strong band in the nuclear fraction and minor contaminations in the membranes and cytoplasm fractions. CALNEXIN showed strong bands in membranes and nuclear fractions indicating the presence of endoplasmic reticulum in both. α-TUBULIN was not detected in the nuclear fraction confirming the absence of cytoplasm, only to a small degree in the membranes fraction, and largely in the cytoplasm. β-actin showed strongest expression in the cytoplasm with some in the membranes fraction, but none in the nuclear fraction. RNF43 showed a strong band in the nuclear fraction. In light of the presence of endoplasmic reticulum marker CALNEXIN in the nuclear fraction it can be concluded that RNF43 is expressed in the nucleoplasm and/or endoplasmic reticulum in ST23132 cells.

AGS cells revealed a weak signal for RNF43 exclusively in the nuclear fraction as confirmed by the presence of CDC5L and absence of α-TUBULIN. Again, the nuclear fraction contained components of endoplasmic reticulum as evident by CALNEXIN. Interestingly, β-actin was detected in the nucleus (also for KATOIII and MKN45) which could represent either a (low level) contamination, which is a possibility given the abundance of β-actin, or could be real since β-actin was described to be present in the nucleoplasm (Olave, Reck-Peterson, and Crabtree 2002, McDonald et al. 2006).

KATOIII and MKN45 cells showed similar results with strong and moderately strong bands for RNF43 in the nuclear fraction, respectively. The nuclear fraction was characterized by presence of CDC5L and absence of α-TUBULIN. Only a weak band for CALNEXIN was detected indicating minimal amounts of endoplasmic reticulum.

Taken together it can be stated that endogenous RNF43 is expressed in the nucleus of gastric cancer cell lines and not at the cell membrane.

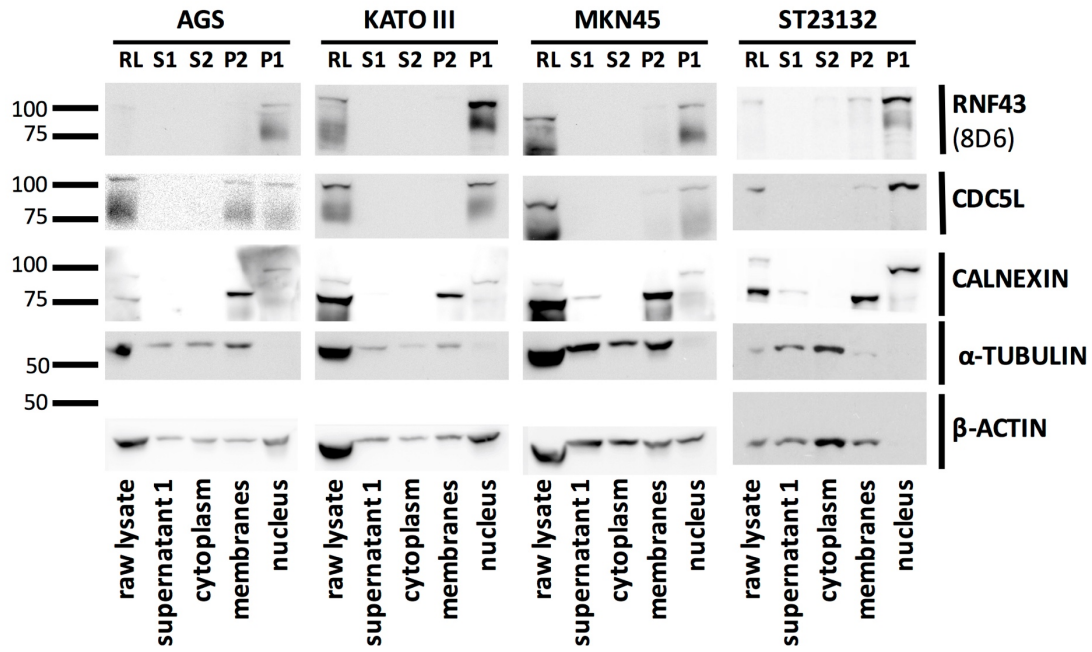

Figure 37: RNF43 is detected in the nuclear fraction of gastric cancer cell lines.
Subcellular fractionation of gastric cancer cell lines. RNF43 was detected with a monoclonal antibody derived from rat hybridomas "8D6" (established by M. Grandl, our group). The following markers were used to validate subcellular fractions: CDC5L (98 kDa; nuclear fraction), CALNEXIN (bands at 75-90 kDa; endoplasmic reticulum), and α-TUBULIN (55 kDa; cytoplasm, to a lesser degree membranes). β-actin served as a generic loading control. Representative experiments are shown. Numbers on y-axis indicate molecular weight in kilodaltons. RL=raw lysate; S1=supernatant 1 (cytoplasm+ membranes); S2=supernatant 2 (cytoplasm); P2=pellet 2 (membranes); P1= pellet 1 (nucleoplasm).

3.3.3.7 RNF43 does not inhibit Wnt/β-catenin signaling in gastric cancer cells

RNF43 was found to act in a negative feedback loop (Loregger et al. 2015) and suppress Wnt/β-catenin signaling in HCT116 colorectal cancer cells (**Figure 22**). Therefore, the question arose whether it would have a similar function in gastric cancer cells.

Transient overexpression of RNF43 in AGS (**Figure 38 A**) did not lead to a decrease of TOPFlash luciferase activity, unlike to what was observed in HCT116 colon cancer cells (**Figure 22**). Transfection of AGS with the RING domain mutated RNF43^{H292R} led to significantly enhanced TOPFlash luciferase activity at a higher dose of 250 ng.

Likewise, transient expression of RNF43 in MKN45 (**Figure 38 B**) did not lead to a decrease of TOPFlash luciferase activity. Transfection of MKN45 with the RING domain mutated RNF43^{H292R} led to significantly enhanced TOPFlash luciferase activity at a higher dose of 250 ng.

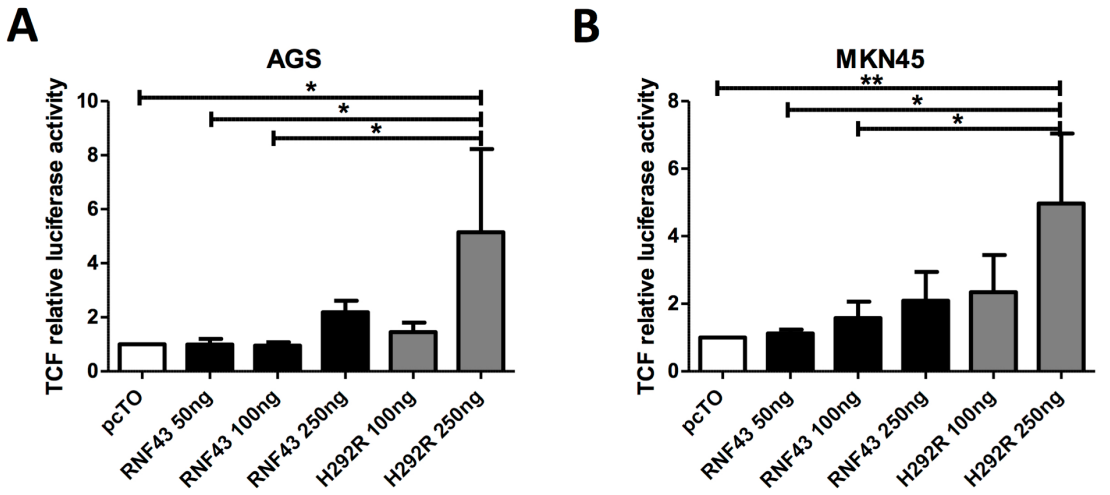

Figure 38: Wnt/β-catenin signaling activity after overexpression of RNF43 and mutant RNF43^{H292R} in AGS and MKN45.
TOP/FOP luciferase reporter assay of AGS (A) and MKN45 (B) human gastric carcinoma cell lines transiently transfected with empty vector control (pcDNA4/TO) and indicated amounts of *RNF43* and RING domain mutated *RNF43^{H292R}* expression plasmids. Results are presented as mean ± SD of three biologically independent experiments. (Firefly) Luciferase normalized to renilla luciferase and values expressed normalized to empty vector control (pcDNA4/TO) luciferase activity. Solid bars: TOPFlash; FOPFlash negative control was within background signal range, not shown. *$p \leq 0.05$; **$p \leq 0.01$ by Student's t-test.

3.3.3.8 RNF43 and TCF4 do not interact in gastric cancer cell lines

RNF43 was found to inhibit Wnt/β-catenin signaling in a negative feedback loop in colorectal cancer. While it has been proposed that this works via increased turnover of frizzled receptors – cell surface receptors for Wnt ligands – by ubiquitination (Hao et al. 2012, Koo et al. 2012), our group discovered that RNF43 inhibits Wnt signaling in colon cancer cell lines by sequestering TCF4 to the nuclear membrane (Loregger et al. 2015). RNF43 did not appear to be a regulator of Wnt/β-catenin signaling in the stomach since transient overexpression of RNF43 did not inhibit Wnt signaling in gastric cancer cell lines. To further substantiate this, I wanted to check whether any interaction between RNF43 and TCF4 occurs in gastric cancer cells.

By employing confocal immunofluorescence, I wanted to see whether there is colocalization of RNF43 and TCF4. Due to the lack of specific antibodies working with immunofluorescence at that time, HA-tagged TCF4 and FLAG-tagged RNF43 or RING domain mutated RNF43^{H292R} were transiently overexpressed.

Confocal immunofluorescence microscopy of AGS and MKN45 cells (**Figure 39**) showed FLAG-tagged RNF43 to be localized along the nuclear membrane and endoplasmic reticulum. HA-tagged TCF4 was localized to the nucleus exhibiting a punctate staining pattern. Similar findings were obtained with RING domain mutated RNF43^{H292R}.

To conclude, there was no alteration of the regular distribution of TCF4 (Cuilliere-Dartigues et al. 2006) in gastric cancer cell lines, unlike to our group's observations in colon cancer cell lines (Loregger et al. 2015).

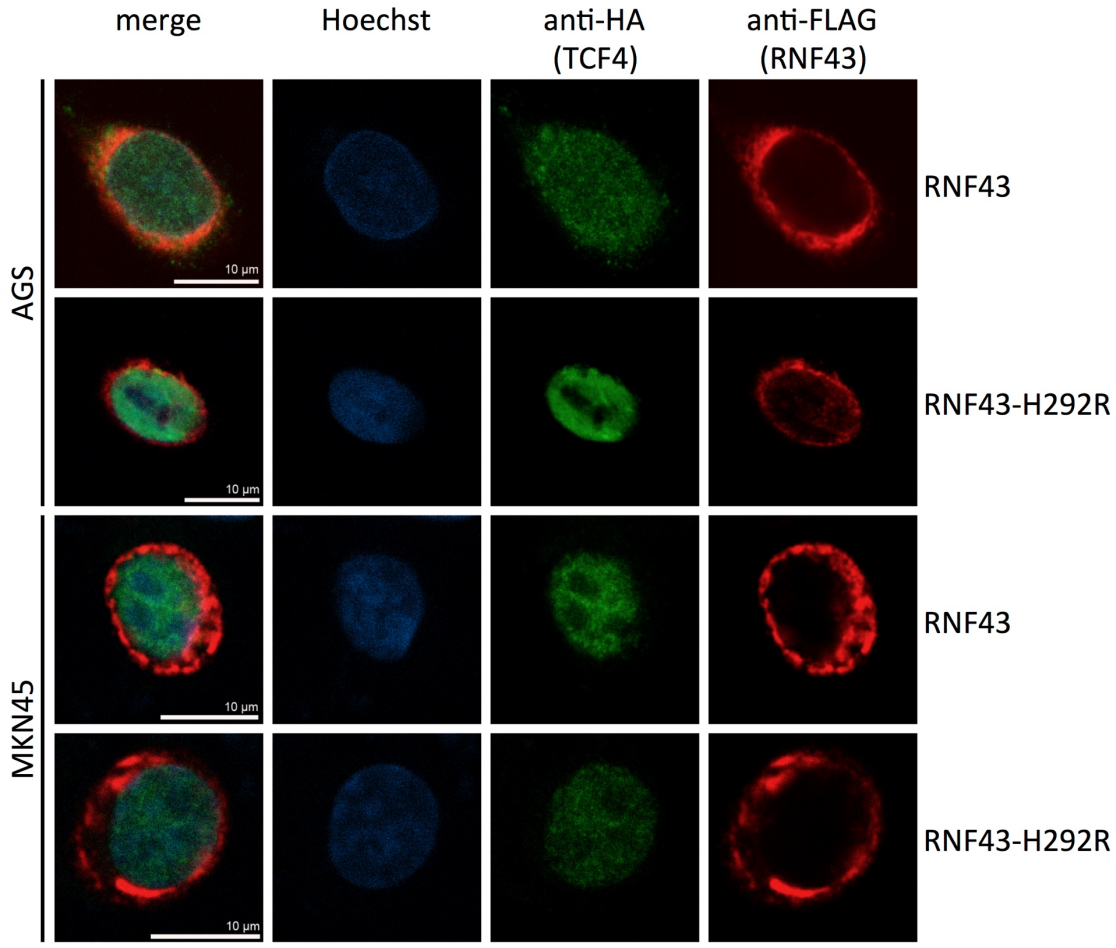

Figure 39: RNF43 and TCF4 do not colocalize in gastric cancer cell lines.
Confocal immunofluorescence microscopy of HA-tagged TCF4 and FLAG-tagged RNF43 or RING domain mutated RNF43^{H292R} which were transiently overexpressed in AGS and MKN45 cell lines. The Hoechst dye (blue) specifically bound to DNA and thereby highlighted the nucleus. Antibodies against HA-tag (green) and FLAG-tag (red) were applied. Scale bars indicate 10 µm.

To further investigate a possible interaction between RNF43 and TCF4, the AGS cell line was transiently transfected with FLAG-tagged RNF43 and protein complex immunoprecipitation (Co-IP) was performed.

Co-IP with anti-TCF4 (**Figure 40**) did not yield any detectable FLAG-tagged RNF43 but β-catenin as expected. Co-IP with anti-FLAG did not precipitate β-catenin, which also provided albeit weaker indirect evidence that it also did not bind TCF4.

To conclude, no direct interaction between β-catenin and overexpressed RNF43 could be shown in AGS cells. Further there was no evidence of an interaction between overexpressed RNF43 and TCF4 in AGS cells indicating that RNF43 might not play a role in gastric Wnt signaling but might fulfill other functions.

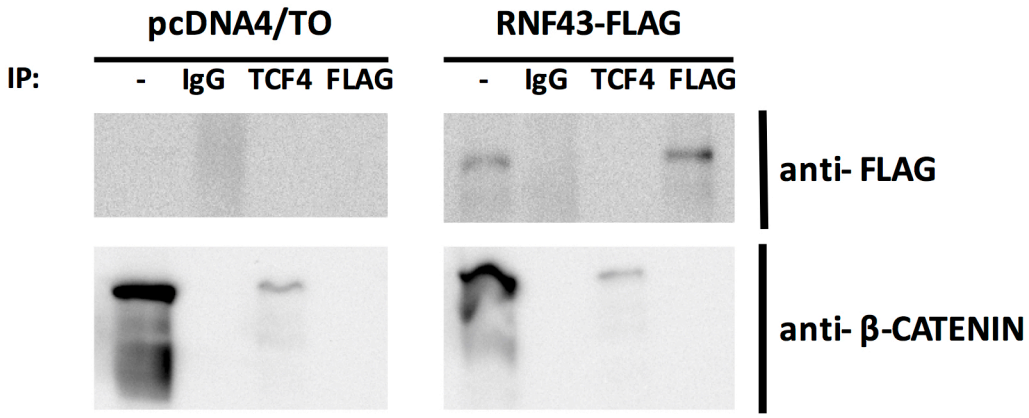

Figure 40: RNF43 and TCF4 do not interact in gastric cancer cell line AGS.
Protein complex immunoprecipitation (Co-IP) of AGS cell line which was transiently transfected with empty vector control (pcDNA4/TO) or FLAG-tagged RNF43. Co-IP with antibodies against IgG (isotope control), TCF4, and FLAG, followed by western blot. [-] = raw lysate.

4 Discussion

In the present thesis, I investigated the Wnt/β-catenin pathway in all its functional domains — development, homeostasis, and tumorigenesis. Setting out I looked into the role of *Sox17* in intestinal development by employing a mouse model with intestinal epithelium-specific knockout of *Sox17*. Through collaborative projects, I was involved in characterizing two conditional mouse models *Cdh1* $^{fl/fl}$ and *Hsp60* $^{fl/fl}$ — both of which showed a marked disturbance of intestinal homeostasis and also its key pathway, the Wnt/β-catenin pathway. Lastly, and most stimulating were the investigations around *RNF43*, a recently described negative regulator of Wnt/β-catenin signaling in colorectal cancer, which our group has also published on (Loregger et al. 2015). Building upon the findings in colorectal cancer I wanted to further explore RNF43's role in gastric cancer.

4.1 The Wnt/β-catenin pathway in gastrointestinal development

As outlined, *Sox17* was among those genes that were identified through microarray experiments to be upregulated in tumors of two mouse models (*APC* $^{min/+}$ and Ahcre^{+}; *APC* $^{fl/fl}$) and in human colorectal tumors (Van der Flier et al. 2007). It was found to be a target gene and negative regulator of Wnt/β-catenin signaling by interacting with β-catenin and TCF/LEF transcription factors (Sinner et al. 2004). Since then, several studies have confirmed its negative regulation of β-catenin levels and its tumor suppressive function in breast, lung, bile duct, and liver carcinomas (Fu et al. 2010, Yin et al. 2012, Merino-Azpitarte et al. 2017, Jia et al. 2010). In order to study Sox17, I first needed to establish a good tool for its detection and chose in situ hybridization (ISH).
Data on the expression of Sox17 in murine and human intestine during homeostasis and tumorigenesis had been conflicting and incomplete, mostly due to the absence of reliable antibodies for murine and human tissues. One group employed an antibody they had developed themselves for western blot (Sinner et al. 2004) and used for immunofluorescence before (Park et al. 2006). Their experiments revealed Sox17 to be expressed in the crypt and along the entire crypt-villus axis and downregulated in adenomas of *APC* $^{min/+}$ mice (Sinner et al. 2007). However, they did not use a conventional DAB-based detection system for immunohistochemistry but fluorescence

based signal detection (tyramide substrate amplification kit) that is usually used to amplify weak signals. This might indicate that their antibody was not ideally suited for IHC, yielding only weak signals, and there is a potential that unspecific staining was amplified. A later study showed, with a then commercially available antibody, that Sox17 was upregulated in gastric tumors developing in *K19-Wnt1/C2mE* mice, in intestinal adenomas of *Apc* $^{\Delta 716}$ mice, but down-regulated in invasive carcinomas of *cis-Apc*$^{\Delta 716}$ *Smad4* mice but they did not describe expression in normal intestinal mucosa (Du et al. 2009). Sox17 upregulation in adenomas and downregulation in early-invasive carcinomas of *APC* $^{min/+}$ mice was also confirmed in another microarray study (Paoni et al. 2003). In human colorectal tumorigenesis, SOX17 was found to be upregulated in gastrointestinal adenomas (Du et al. 2009) but downregulated by promoter hypermethylation in the course of malignant progression, indicating that SOX17 is able to antagonize Wnt signaling in early stages of tumor development but then tumor cells with epigenetically silenced *SOX17* gain a growth advantage (Zhang et al. 2008). *SOX17* was found to be hypermethylated in additional malignancies including breast cancer (Fu et al. 2010), lung cancer (Yin et al. 2012), cholangiocarcinoma (Goeppert et al. 2014, Merino-Azpitarte et al. 2017), and hepatocellular carcinoma (Jia et al. 2010).

Since Prof. M. Gerhard had successfully applied the versatile tool of chromogenic RNA-in situ hybridization (Gregorieff and Clevers 2015) during his postdoctoral work and we were lacking a working antibody for SOX17, I was implementing it in our laboratory. Here it bears notice that while ISH can be a powerful tool when one is lacking a specific antibody, it does quite often not produce as clear-cut results as one is used to see with IHC. Furthermore, while I was successful in implementing some self-designed and published RNA-probes, there were many more attempts targeting other genes that were unfruitful.

In the mouse, *Sox17* was weakly expressed at the base of the crypts and most notably upregulated in aberrant crypt foci and adenomas developing in *APC* $^{min/+}$ mice which was in line with some studies (Du et al. 2009, Paoni et al. 2003) but conflicting with the first mentioned study (Sinner et al. 2007).

In human tissue samples, I could detect *SOX17* expression at the base of colonic crypts but also to be overexpressed in human colorectal tumors. This is in contrast to findings that SOX17 was downregulated by promoter CpG island hypermethylation in 100% of colorectal cancer cell lines, 86% of adenomas, and all stage I and II and 89% of stage III colorectal cancers investigated (Zhang et al. 2008, Voorham et al. 2013). In breast cancer,

hypermethylation of *SOX17* promoter CpG islands was associated with higher clinical stage and lymph node metastases but still occurred in about 60-80% of cases (Fu et al. 2010). As noted, it is plausible that SOX17 as a Wnt-antagonist is silenced in the course of tumor progression. A study on hepatocellular carcinoma showed that cases with promoter CpG island hypermethylation were associated with enhanced Wnt signaling activity as seen by nuclear accumulation of β-catenin on immunohistochemistry (Jia et al. 2010). The observed difference of my ISH results to published data might be a matter of sample size since I only investigated *SOX17* expression in a few cases of colon cancer and not in a well-stratified cohort. A larger collective might have resulted in a number of cases with loss of SOX17 expression.
Only after I had concluded my investigations into SOX17 expression, a more reliable yet still not ideal antibody became available which was used for investigating seminomas (personal communication with the authors) (Bode et al. 2011, Weissferdt et al. 2015).

Sox17 was shown to be key for definitive endoderm formation and to act as a negative feedback loop on Wnt signaling, but no one had studied the effect of a Sox17 knockout on later stages of intestinal development and homeostasis (Hudson et al. 1997, Sinner et al. 2004). A *Sox17* knockout mouse model led to defective mid- and hindgut development at E8.5-9.5 (Kanai-Azuma et al. 2002) prohibiting the study of Sox17 at later stages of intestinal development and homeostasis. To avoid this lethal phenotype, I obtained a conditional knockout mouse model — *Sox17*$^{fl/fl}$ (Kim, Saunders, and Morrison 2007) and crossed it with transgenic *Villin*-cre mice (el Marjou et al. 2004) to achieve recombination restricted to the epithelial lining of small and large intestine by E12.5. Cre recombinase under the *Villin* promoter has been shown to be expressed in all epithelial cells of the intestine including stem cells (Madison et al. 2002, el Marjou et al. 2004). Initial breedings led to the impression of a lethal phenotype since no *villin*-cre $^{+}$; *Sox17*$^{fl/f}$ pubs were encountered. This prompted me to analyzed embryos in utero but no developmental differences were found. As additional breedings were conducted, homozygous knockout mice (*villin*-cre $^{+}$; *Sox17*$^{fl/fl}$) were born at the expected mendelian ratios. To see whether deletion of *Sox17* would cause a phenotype after several weeks into life, I studied the gastrointestinal tract of 4-week old mice but could not see any morphological differences or changes in proliferation. In retrospect, I would also assess mice at later time points since changes could be quite subtle after only 4 weeks.

A study published after my experiments on Sox17 sheds new light onto the here described findings. The group of Prof. H. Lickert created a mouse model (*Sox17*-mCherry) in which the fluorescent reporter gene mCherry is fused to the open reading frame of *Sox17*, thereby allowing tracking of Sox17 expression (Burtscher et al. 2012). While its previously identified expression in early endoderm development could be confirmed, it was found that by E12.5 Sox17 was only expressed in endothelia of intestinal vessels but not the intestinal epithelial cells themselves. The same group further established this in another knock-in mouse model — *Sox17* ^{CreERT2}. The stop codon of *Sox17* was replaced with a 2A sequence followed by CreER^{T2} which results in expression of a bicistronic mRNA and translation of equal amounts of Sox17 and Cre under the promoter of *Sox17* (Engert et al. 2013). These mice were bred to *Rosa26*-Cre reporter lines that express β-galactosidase upon Cre-mediated excision of a stop cassette. While administration of tamoxifen at E7.0 resulted in lacZ staining of all endoderm-derived organs including intestinal epithelium, administration of tamoxifen at E9.0 only stained mesoderm derived structures including blood vessels within the intestinal wall but not intestinal epithelial cells. Unfortunately, these two studies did not further investigate Sox17 expression after birth. Assuming that Sox17 is not re-expressed in intestinal epithelial cells under physiologic conditions, it is not surprising that deletion of *Sox17* by *Villin*-cre –mediated recombination at E12.5 did not cause an abnormal phenotype.

In light of these new data one might also question the rather weak, crypt-based expression of *Sox17* detected by ISH. However, since ISH detects mRNA, *Sox17* might still be expressed at the mRNA level but not actively translated into protein. These new data also raise the question whether the mouse is an adequate model to study the function of SOX17 since in human I found it to be prominently expressed in intestinal crypts.

4.2 The Wnt/β-catenin pathway in gastrointestinal stemness and homeostasis

Though the project on *Sox17* already touched upon Wnt/β-catenin in intestinal homeostasis, the two collaborative projects of characterizing *Cdh1* $^{fl/fl}$ (Schneider et al. 2010) and *Hsp60*$^{fl/fl}$ (Berger et al. 2016) conditional mouse models primarily addressed intestinal homeostasis in the context of Wnt/β-catenin signaling. Interestingly, both genes are involved or affect mechanisms of altered homeostasis in patients with inflammatory bowel disease (IBD).

E-cadherin was found to be downregulated in IBD and to contribute to its pathogenesis (Jankowski et al. 1998, Gassler et al. 2001, Kucharzik et al. 2001, Bruewer, Samarin, and Nusrat 2006). HSP60 deficiency leads to mitochondrial unfolded protein response (MT-UPR) that results in mitochondrial dysfunction, which was shown to play a role in intestinal inflammation and repair (Treton et al. 2011, Waldschmitt et al. 2014). In addition, MT-UPR was linked to endoplasmic reticulum unfolded protein response (ER-UPR) which was shown to be involved in the pathogenesis of IBD (Shkoda et al. 2007, Kaser et al. 2008, Treton et al. 2011).

In both studies, adult and phenotypically healthy mice were subjected to sudden intestinal epithelium-specific gene deletion by tamoxifen administration. This led to a marked hemorrhagic diarrhea (Schneider et al. 2010) and severe wasting (Berger et al. 2016) necessitating euthanasia in both cases. I contributed with my expertise in performing in situ hybridization to characterize parts of these phenotypes by assessing expression of intestinal stem cell marker *Olfm4* (Schuijers et al. 2014) and Wnt target gene *Axin2* (Jho et al. 2002).

Currently, two intestinal stem cell populations are described. Crypt base columnar (CBC) cells interspersed between Paneth cells and cells residing at the +4 position that might represent a quiescent pool of stem cells recruited during repair (Beumer and Clevers 2016). CBC are characterized by expression of marker Lgr5 but only at low levels, posing technical difficulties to detection by both IHC (Yamazaki et al. 2015) and ISH (Barker et al. 2007). This led to the validation of Olfm4 as a surrogate marker for $Lgr5^{+}$ stem cells in mice (van der Flier, Haegebarth, et al. 2009, Schuijers et al. 2014). Olfm4 was also used as a surrogate in humans but was found to mark a larger proportion of intestinal crypt cells including some of the transit amplifying cells questioning its validity as a stem cell marker in humans (Ziskin et al. 2013).

Axin2 is a target gene and also a negative regulator of the Wnt pathway (Yan et al. 2001, Jho et al. 2002, Lustig et al. 2002). By assessing its expression one can infer active Wnt/β-catenin signaling and it might be the optimal promoter to construct Wnt reporter mouse models (Nusse 2018). Another method is immunohistochemistry to check for nuclear/cytoplasmic expression of β-catenin indicating active signaling.

Tamoxifen induced recombination in *Villin*-cre-ER^{T2}; *Cdh1* $^{fl/fl}$ led to loss of E-cadherin expression, with resulting impairment of adherens junctions and desmosomes, causing increased epithelial cell apoptosis and shedding. An intense short-time model of tamoxifen induced recombination (E-cadherin deficient) led to hemorrhagic diarrhea and

required euthanasia. On a molecular level, ISH for *Axin2* revealed absence of physiological Wnt signaling at the bottom of the crypts. This was paralleled by loss of staining for *Olfm4* indicating a loss of stemness. In a less intense "long-term" induction protocol (resulting in partial E-cadherin deficiency), mice were less symptomatic, allowing for a longer period of investigation into altered homeostasis. *Axin2* showed reduced expression at day 12 but regained close to normal levels at day 20 which was identical to staining for *Olfm4*. Of note, *Axin2* and *Olfm4* positive cells were only encountered at the crypt base but not in other regions of the villi, where mispositioned Paneth cells were detected by immunohistochemical stains. This indicates that either the correct position/microenvironment is important for Wnt signaling in and maturation of Paneth cells or it is proper anchoring by E-cadherin.

After *villin*-Cre mediated abrogation of *HSP60* expression, *HSP60* deficient crypt intestinal epithelial cells were found to release Wnt signaling enhancer R-spondin-1 and HSP60 deficient Paneth cells secreted Wnt signaling protein Wnt-10a (Berger et al. 2016). In addition, occasional hyperproliferative crypt-based nodules were identified. By ISH I could show overexpression of *Axin2* in these nodules indicating active Wnt signaling. Adjacent crypts did not reveal any staining showing that Wnt signaling had ceased there. Staining for *Olfm4* revealed that these nodules expressed *Olfm4,* implying that they arose from intestinal stem cells. Since these nodules were of stem cell origin but only occurred in a minority of crypts it was concluded that they originated from stem cells that did not undergo *villin*-cre mediated recombination of the *Hsp60* locus ("escaper crypts").

Repopulation by residual intestinal stem cells was described in response to radiation injury (Hua et al. 2012) and in studies similar to the current one in which essential genes like *Ascl2*, *c-Myc*, or *TCF4* were acutely deleted by inducible Cre-mediated recombination (Muncan et al. 2006, van der Flier, van Gijn, et al. 2009, van Es, Haegebarth, et al. 2012).

4.3 The Wnt/β-catenin pathway in gastrointestinal carcinogenesis

Studies by The Cancer Genome Atlas Research Network (TCGA) showed that the Wnt/β-catenin pathway was altered in greater than 9 of 10 cases of colorectal cancer, mostly due to biallelic inactivations of *APC* or activating mutations of *CTNNB1*, the gene coding β-catenin (Cancer Genome Atlas 2012). Initially, no significant number of *RNF43*

mutations was found, but later two independent patient cohorts (Nurses' Health Study (NHS) and the Health Professionals Follow-Up Study (HPFS)) showed mutations in 18.9% of cases which prompted careful reanalysis of TCGA datasets, revealing that around 1/5 of cases harbored *RNF43* mutations, half of which were truncating frameshift mutations (Giannakis et al. 2014).

Although Wnt/β-catenin signaling is not as prominent in the pathogenesis of gastric cancer, some studies described activation in around 30% of gastric carcinomas (Park et al. 1999, Clements et al. 2002), and nuclear localization of β-catenin by immunohistochemistry was found to be associated with gastric cancer progression (Miyazawa et al. 2000). Furthermore, mutations and loss of heterozygosity in *APC* were detected in 18% and 21% of cases, respectively (Tahara 2004), implying an important role for Wnt signaling in gastric carcinogenesis. The TCGA showed that in gastric adenocarcinoma, *RNF43* alterations were mostly found in two subtypes — non-hypermutated and hypermutated gastric cancers. In non-hypermutated gastric cancers, frameshift and non-sense mutations of *APC* (7% of cases) and *RNF43* (3% of cases) and missense mutations of *CTNNB1* (4% of cases) were found. 33% of hypermutated gastric cancers showed frameshift mutations of *RNF43* but there was no significant number of *APC* or *CTNNB1* mutated cases (Cancer Genome Atlas Research 2014). A high number of *RNF43* mutations, 62.5% of which were truncating, was found in 54.6% of MSI-H (microsatellite instability-high) versus 4.8% of MSI-L (microsatellite instability-low) gastric adenocarcinomas in another study (Wang et al. 2014). It is noteworthy, that cases with MSI-H showed a marked enrichment for RNF43 mutations and it might be that RNF43 is involved in the pathogenesis of these highly mutated tumors. In fact, there was one publication associating RNF43 with DNA damage response (Gala et al. 2014) and other RNF proteins were also described to be involved in DNA repair and remodeling (Takagi et al. 2005, Mailand et al. 2007, Campbell et al. 2012, Bohgaki et al. 2013, Nakada 2016).

RNF43 was shown to be a target gene of the Wnt signaling pathway (Takahashi et al. 2014, Loregger et al. 2015) and it was attributed contradictory roles in colorectal carcinogenesis. In early reports, it was described as an oncogene (Yagyu et al. 2004, Miyamoto, Sakurai, and Sugiura 2008) but more recently it was shown by us and others to exhibit tumor suppressive properties (Koo et al. 2012, Loregger et al. 2015). Despite a

high frequency of genetic alterations nothing on its function in gastric cancer was published at the beginning of my investigations.

At first, I contributed to our studies of RNF43 in colorectal cancer. Since initially there was no good antibody available, I designed an in situ hybridization probe for both murine and human *RNF43*. ISH revealed crypt-restricted expression in murine intestine and upregulation in tumors developing in APC $^{min/+}$ mice, which showed Wnt activation by positive staining for Wnt target gene *Axin2*. Results on human tissue were similar. *RNF43* was expressed in the crypt compartment including intestinal stem cells showing comparable expression patterns to *OLFM4*, a surrogate stem cell marker which in the meantime has come under some scrutiny since its expression is more extensive including also transit amplifying cells (Ziskin et al. 2013). *RNF43* was found to be overexpressed in human adenomas and colorectal cancers, which is in line with previously published studies in mouse and human (Lin et al. 2002, Yagyu et al. 2004, Van der Flier et al. 2007). Since the mainstay for cancer diagnostics is immunohistochemistry, a major effort was to identify an antibody which could be used for detecting RNF43 in FFPE sections. IHC is more robust and also yields additional information on subcellular protein location plus of course, detects the protein and not only mRNA. Anti-RNF43 (HPA008079, Atlas Antibodies AB) turned out to be working quite well for IHC after extended optimization. In human colon, it yielded crypt-restricted, nuclear staining and extensively stained nuclei of human colorectal adenomas and carcinomas. Since *RNF43* is a target gene of Wnt signaling it was not surprising to observe its overexpression in colorectal tumorigenesis, which is Wnt driven in the majority of cases. In light of many truncating mutations one might wonder why the antibody still recognized RNF43 in colorectal carcinoma. A sequence analysis reveals that the immunogen used to raise anti-RNF43 (HPA008079, Atlas Antibodies AB) is not affected by the most common (truncating frameshift) mutations at p.Gly659fs (41.7-48% of cases) but only by p.Arg117fs (8.3-12%of cases) (Giannakis et al. 2014) (**Figure 5**). Some of the remaining 40-50% of mutations, that are distributed along the entire open reading frame (Loregger et al. 2015), might cause loss of immunoreactivity and it would be interesting to compare expression of RNF43 by immunohistochemistry to mutational status to see whether an immunohistochemical stain could have any diagnostic or clinical use.

Next, I investigated the expression of RNF43 in healthy human stomach, which until very recently was not looked at before. One study described cytoplasmic and nuclear expression of RNF43 in epithelial cells of the lower 1/3 to 1/2 of the gastric mucosa but

did not observe restriction to specific epithelial cell types (Gao et al. 2017). Interestingly, I found that RNF43 stained almost exclusively parietal cells of fundic/oxyntic gastric mucosa, which can morphologically be recognized by their comparatively large size, centrally placed nucleus, and finely granular cytoplasm. These cells are known to produce hydrochloric acid (HCl) and release intrinsic factor. Hydrochloric acid denatures ingested proteins and activates pepsinogen. Intrinsic factor aids in the absorption of vitamin B12 and its deficiency e.g. due to loss of parietal cells in autoimmune/atrophic gastritis leads to pernicious anemia. Exclusive expression of RNF43 in parietal cells could be explained by higher Wnt activity in these cells. However, accumulation of nuclear β-catenin in parietal cells was not observed. Not much is known about Wnt signaling and its influence on gastric homeostasis but the general concept is that the gastric mucosa — unlike intestinal mucosa — does not rely on constant Wnt signaling. In fact, it appears that repression of Wnt signaling is a requirement for organogenesis of stomach and lung as to avoid the default of intestinal differentiation under influence of Wnt/β-catenin (Verzi and Shivdasani 2008). In contrast to that, a recent study showed that Wnt signaling was essential to induce formation of fundic epithelium (with parietal cells) and not antral epithelium (without parietal cells) when creating gastric organoids from human pluripotent stem cells (hPSCs) and that high-Wnt and high-FGF (Fibroblast Growth Factor) culture medium was necessary to maintain fundic glands (McCracken et al. 2017). Areas of intestinal metaplasia, often regarded as a precancerous lesion, did not stain for RNF43. A small collective of mostly stage I gastric adenocarcinomas revealed staining in about a quarter of cases. Comparing other parameters, one can see that these positive cases comprised a pretty heterogeneous group and no correlation could be drawn. Interestingly, RNF43 expression was mostly associated with membranous staining for β-catenin indicating absence of active Wnt signaling. Since the mutational status of RNF43 in our collective was not known, it is possible that RNF43 was either not expressed or not recognized by our antibody due to the presence of mutations. There are two other studies that assessed RNF43 expression by IHC in gastric cancer. In the first study, 77 cases of gastric carcinoma and matched normal mucosa were assessed by IHC with an antibody yielding cytoplasmic staining for RNF43 (ab129401, Abcam) (Niu et al. 2015). In contrast to my set of cases, their collective comprised more advanced patients, as 75% were poorly differentiated tumors and included mostly cases at stage II (39%) and stage III (40%). Interestingly, RNF43-negative patients experienced shorter survival. It was further found that RNF43 expression was downregulated in tumors compared to

normal tissue especially with less differentiated tumors, increasing depth of invasion, and local lymph node metastases. Another study showed by transcriptome sequencing that RNF43 was significantly upregulated in adenomas and subsequently downregulated in carcinomas (Min et al. 2016). A randomly chosen set of 19 early gastric cancers was stained by IHC (again ab129401, Abcam) and loss of staining was evident in 80% of cases that harbored frameshift mutation Gly659fs. Since the antibody is no longer available, I could not check against which part of RNF43 it was raised and whether frameshift mutation Gly659fs would abrogate its binding site while the RNF43 protein is still expressed. As discussed at the beginning of this section, *RNF43* was found to be mutated in up to 30% of certain molecular subtypes of gastric cancer. A survey of 38 published datasets using the cBio portal revealed that gastric cancer is among the gastrointestinal neoplasms with the highest rate of genetic *RNF43* alterations ranging from less than 5% for diffuse type gastric cancer up to 25% for mucinous stomach adenocarcinoma, which might be one explanation why only a smaller fraction of my cases stained for RNF43 by IHC.

In order to study the function of RNF43 *in vivo*, I conducted a baseline assessment of gastric cancer cell lines available in our laboratory. qRT-PCR showed that *RNF43* transcripts could be detected in all cell lines, which was in agreement with the Cancer Cell Line Encyclopedia (CCLE) that showed mRNA levels of *RNF43* to be second highest among all cancer cell lines. The presence of RNF43 protein in all cell lines could be confirmed by both using a commercially available polyclonal antibody and monoclonal antibody “8D6” which M. Grandl from our group had established from immunized rats. The monoclonal antibody 8D6 appeared to only recognize isoform 4 of RNF43 at 95 kDA but showed robust performance and very little background. While the commercial antibody (LS-C102008, LifeSpan BioSciences) might recognize all 4 different isoforms it also showed increased background staining and did not show as robust performance. A search in the COSMIC databank revealed that none of the gastric cancer cells lines that I used and had sequencing data available, harbored mutations in *RNF43* and thereby of course also none of the described truncating frameshift mutations (Giannakis et al. 2014, Wang et al. 2014) which could interfere with protein detection by antibodies in IHC or western blot.

Further queries on the COSMIC databank did not bring up any mutations in Wnt/β-catenin pathway components *Axin*, *CK1α*, or *GSK-3*. *APC* showed a silent mutation in MKN7. Only AGS harbored a missense mutation in *CTNNB1*, the gene encoding

β-catenin, leading to amino acid exchange G34E which renders it resistant to degradation causing its accumulation and thereby increased activation of the Wnt/β-catenin pathway (Caca et al. 1999, Ganesan et al. 2008).

Our group and others showed that RNF43 inhibits Wnt signaling in colon cancer cell lines, which show high levels of Wnt signaling activity. Since I only found AGS cells to be mutated in a key component of the Wnt/β-catenin pathway, I wanted to investigate what the overall Wnt signaling activity was in the gastric cell lines I had available. This information was helpful when I decided which cell lines to use for subsequent functional assays.

At first, I assessed basal Wnt signaling activity by western blot with phosphorylation specific antibodies for β-catenin. Non-phosphorylated β-catenin, which represents the 'active' form that does not undergo proteasomal degradation, was seen at comparable levels in all cell lines but absent in NUGC4 as was reported before (Nojima et al. 2007). Higher amounts of non-phosphorylated β-catenin appeared to correlate with higher amounts of RNF43, which would make sense given the fact that *RNF43* is a target gene of Wnt signaling. However, differences in band intensities were subtle and there is always a risk that unequal loading of protein lysates is not fully accounted for by comparing β-actin intensities. Along that line, it needs to be said that at least in my small collective of gastric cancers, IHC for β-catenin and RNF43 did not show a positive correlation, which is in contrast to observations in colon cancer where we showed that a knockdown of β-catenin led to a significant reduction of *RNF43* mRNA expression (Loregger et al. 2015). One explanation might be that RNF43 could have still been expressed but maybe not detected anymore by IHC due to mutations interfering with antibody binding.

Most gastric cancer cell lines showed rather low Wnt activity by TOP/FOP assay but KATOIII, followed by AGS, N87, and MKN45 showed the highest activities, which is in line with published data (Nojima et al. 2007). While I did not analyze colon cancer cell lines in parallel, it has been shown that TOP/FOP luciferase activity of AGS is comparable to HCT116 and KATOIII showed higher activity closer to that of SW480 (Caca et al. 1999).

RNF43 has been ascribed different functions and correspondingly was detected in various subcellular compartments. RNF43 and its homologue ZNRF3 were prominently published to be localized at the cell membrane and promoting turnover of Wnt-receptors, which currently is the most widely accepted function and localization of RNF43 (Hao et al. 2012, Koo et al. 2012). However, RNF43 was also described to interact with several

nuclear proteins (Sugiura, Yamaguchi, and Miyamoto 2008, Miyamoto, Sakurai, and Sugiura 2008, Nailwal et al. 2015), suggested to be involved in DNA damage response (Gala et al. 2014), and shown by us to suppress Wnt signaling by tethering TCF4 to the nuclear membrane (Loregger et al. 2015), all functions that would imply a nuclear localization.

Studies so far have mostly investigated RNF43 under conditions of artificial overexpression since an antibody for detection of endogenous protein was lacking. Therefore, I also conducted overexpression experiments initially and used confocal immunofluorescence microscopy to detect FLAG-tagged RNF43 or the RING domain mutated RNF43^{H292R} which both localized along the nuclear membrane/the nuclear envelope and in a distribution reminiscent of the endoplasmic reticulum and clearly not at the cell membrane as published (Hao et al. 2012, Koo et al. 2012). But overexpression does not adequately recapitulate endogenous protein levels, which is further complicated when an expression plasmid with strong CMV promoter is used like here. As it is nicely outlined in a review article on transient overexpression (Gibson, Seiler, and Veitia 2013), one needs to be careful not to fall victim to interpreting artifacts like aggregation of overexpressed proteins, aggregation of fluorophore-tags, or subcellular mislocalization as real. Therefore, it is most important to study expression of endogenous RNF43 protein, which has been done by our group in colon cancer (Loregger et al. 2015) while others have employed overexpression systems (Hao et al. 2012, Koo et al. 2012).

IHC for RNF43 turned out to be another method to elucidate RNF43's subcellular localization. Human tissue samples showed clear and strong nuclear staining. Nuclear staining by IHC was observed by some (Sakamoto et al. 2015) while others detected cytoplasmic and nuclear staining (Bond et al. 2016, Gao et al. 2017). It needs to be addressed that the stain was nuclear and not perinuclear as seen in immunofluorescence. This might be attributable to the fact that confocal microscopy allows imaging of thinner layers, while in conventional IHC one is looking at 3.5 µm thick sections and so perinuclear stains might appear to involve the entire nucleoplasm. In addition, IHC might more easily overstain the entire nucleus. On the other hand, overexpressed protein might have localized to the ER in large amounts and generated high intensities of fluorescence when detected by fluorophore coupled anti-FLAG antibodies. This in turn might have led to decreasing the sensitivity of microscope settings leading to possible lower intensities of nuclear staining not being perceived.

I also applied IHC to cell pellets obtained from non-transfected gastric cancer cell lines and could confirm nuclear localization of RNF43. AGS and KATOIII showed nuclear and cytoplasmic staining for β-catenin which was in line with observed increased TOP/FOP luciferase activity and activating β-catenin mutations in AGS.

In order to further substantiate the subcellular localization of endogenous RNF43 by a biochemical approach, I conducted subcellular fractionation with differential centrifugation of AGS, KATOIII, MKN45, and ST23132. Experiments showed that endogenous RNF43 was expressed in the nucleus of gastric cancer cell lines and not at the cell membrane, which was in line with an early study of overexpressed RNF43 (Sugiura, Yamaguchi, and Miyamoto 2008) and its described interactions with various nuclear proteins and a suggested role in DNA damage response based on an UV-irradiation experiment. The question arises why RNF43 was described in different localizations and attributed various functions. The antibodies and tags I used for detection of RNF43 were located towards or at the C-terminal end, respectively. This is also where two nuclear localization sequences are encoded. A N-terminally located ectodomain was described to interact with R-spondin proteins and frizzled receptors at the cell surface. One could speculate that RNF43 is either enzymatically cleaved and one part goes to the nucleus whereas the other part goes to the cell membrane or that post-translational modifications direct it to different compartments.

Our group had worked out that RNF43 acted in a negative feedback loop and suppressed Wnt/β-catenin signaling in colorectal cancer by sequestering TCF4 to the nuclear membrane (Loregger et al. 2015). Thus, I wondered whether it would have a similar function in gastric cancer cells. KATOIII showed the highest Wnt signaling activity of tested gastric cancer cell lines by TOP/FOP luciferase assay. Therefore, they would have been a good model system to assess suppression of Wnt signaling by RNF43. However, transfection efficiency and TOP/FOP assays were technically suboptimal due to a substantial amount of KATOIII cells growing in suspension. AGS and MKN45 still showed above average Wnt signaling activity plus AGS is known to harbor an activating mutation in CTNNB1 rendering β-catenin resistant to degradation. However, I did not observe any significant suppression of Wnt/β-catenin signaling in AGS or MKN45 upon overexpression of RNF43 despite many iterations and variations. In contrast, RING-mutant $RNF43^{H292R}$ caused significant transactivation of Wnt/β-catenin signaling at higher doses thereby turning tumor suppressor RNF43 to acting as an oncogene. The COSMIC database did not list any mutations for *RNF43* in AGS and MKN45. It is

possible that I did not see an inhibition of Wnt/β-catenin signaling as cells already had wild type *RNF43* and adding additional copies by overexpression did not increase its inhibitory function. This is in line with observations made in pancreatic cancer cell lines where expression of wild-type RNF43 blocked proliferation of cells harboring mutant RNF43 but not wild-type RNF43 (Jiang et al. 2013)
Since I did not see a suppression of Wnt signaling by overexpression of RNF43, it was not surprising that I could not repeat observations our group has made in colorectal cancer (Loregger et al. 2015). There was no colocalization of overexpressed RNF43 and TCF4 by confocal immunofluorescence microscopy nor co-precipitation by protein complex immunoprecipitation in gastric cancer cell lines.

In order to further explore the function of endogenous RNF43, different attempts were made to generate a stable lentiviral-mediated knockdown of RNF43 over several months. At the end of my experimental work, this approach was not successful but was further pursued in the lab. Of note, RNF43 was later shown in our lab to have tumor suppressive functions and it was also shown by others that RNF43 inhibits gastric cancer cell proliferation, promotes apoptosis, impairs stemness of gastric cancer stem cells, decreases chemoresistance, attenuates tumorigenicity *in vivo*, and downregulates Wnt target genes (Niu et al. 2015, Gao et al. 2017).

4.4 Conclusion

In this work, I could expand the current body of knowledge of Wnt/β-catenin signaling in its various facets.

By specifically knocking out Wnt/β-catenin antagonist Sox17 in the intestinal epithelium and not noticing an abnormal phenotype, I could show that Sox17 does not appear to have a role in intestinal epithelium under physiologic conditions, which was subsequently indirectly confirmed by the demonstration that Sox17 is not expressed in intestinal epithelium of the mouse.

The contribution of Wnt/β-catenin signaling to intestinal homeostasis and restoration thereof could be demonstrated in two conditional mouse models *Cdh1* $^{fl/fl}$ and *Hsp60* $^{fl/fl}$, where in situ hybridization enabled detection of Wnt target gene *Axin2* and stem cell marker *Olfm4*.

By establishing in situ hybridization and immunohistochemistry for RNF43 I could further characterize its expression in human and murine gastrointestinal tissue samples. A databank search of published studies revealed that *RNF43* was highly mutated in gastric cancers and that cell lines showed high expression of RNF43 which I could confirm by qRT-PCR and western blot. Only about one quarter of gastric tumors revealed positive staining for RNF43 by IHC and I could detect strong nuclear staining of parietal cells in normal gastric mucosa. I could demonstrate by IHC of tissue samples and cell pellets as well as subcellular fractionation that endogenous RNF43 was expressed in the nucleus of human tissue samples and gastric cancer cell lines. In contrast to our prior findings in colon cancer, I did not see a suppression of Wnt/β-catenin signaling upon transient overexpression of RNF43 nor could I demonstrate a colocalization or co-immunoprecipitation of RNF43 and TCF4. The RING-mutant RNF43^{H292R} still demonstrate transactivation of the Wnt/β-catenin pathway. To conclude, I could detect the endogenous RNF43 in the nucleus of gastric cancer cells but did not detect Wnt/β-catenin pathway inhibition by additional overexpression of RNF43. RNF43 might carry-out different biological functions based on its subcellular distribution and tissue.

4.5 Outlook

To characterize the function of endogenous RNF43, the generation of knockdown and/or knockout cells is necessary. Notably, these models have more recently been established in our lab by using specific short hairpin (sh)RNAs as well as by CRISPR/Cas9 mediated knockout. Proliferation, colony formation, and invasion assays have allowed us to confirm RNF43's tumor suppressive function in colon and gastric cancer cells. In addition, the introduction of mutations in cells or human gastric organoids will further help to understand how mutations in RNF43 contribute to gastrointestinal tumorigenesis. The introduction of a Tag into the endogenous locus of RNF43 by CRISPR/Cas9 would be a good strategy to confirm the subcellular localization of RNF43 and to identify interaction partners until better antibodies against RNF43 are established.
To further characterize the function and the impact of mutations on endogenous proteins the generation of animal models is of great importance. Therefore, two mouse models were created. One to study the effect of RNF43 loss of function by introducing a 57-base pair long deletion in the RING domain, the other one to study the effect of Wnt transactivating RING-mutant $Rnf43^{H292R/H295R}$. These two animal models are currently being analyzed not only under basal conditions, but also after challenge with inflammatory agents, since inflammation highly contributes to the development of tumors of the gastrointestinal tract.

Together these strategies will contribute to determine whether RNF43 is important to maintain gastrointestinal homeostasis and to understand how mutations so frequently observed in human tumors disrupt it.

5 Reference list

Aberle, H., A. Bauer, J. Stappert, A. Kispert, and R. Kemler. 1997. "beta-catenin is a target for the ubiquitin-proteasome pathway." *EMBO J* 16 (13):3797-804. doi: 10.1093/emboj/16.13.3797.

Abraham, S. C., B. Nobukawa, F. M. Giardiello, S. R. Hamilton, and T. T. Wu. 2000. "Fundic gland polyps in familial adenomatous polyposis: neoplasms with frequent somatic adenomatous polyposis coli gene alterations." *Am J Pathol* 157 (3):747-54. doi: 10.1016/S0002-9440(10)64588-9.

Ahn, S. M., S. J. Jang, J. H. Shim, D. Kim, S. M. Hong, C. O. Sung, D. Baek, F. Haq, A. A. Ansari, S. Y. Lee, S. M. Chun, S. Choi, H. J. Choi, J. Kim, S. Kim, S. Hwang, Y. J. Lee, J. E. Lee, W. R. Jung, H. Y. Jang, E. Yang, W. K. Sung, N. P. Lee, M. Mao, C. Lee, J. Zucman-Rossi, E. Yu, H. C. Lee, and G. Kong. 2014. "Genomic portrait of resectable hepatocellular carcinomas: implications of RB1 and FGF19 aberrations for patient stratification." *Hepatology* 60 (6):1972-82. doi: 10.1002/hep.27198.

Angers, S., and R. T. Moon. 2009. "Proximal events in Wnt signal transduction." *Nat Rev Mol Cell Biol* 10 (7):468-77. doi: 10.1038/nrm2717.

Bailey, P., D. K. Chang, K. Nones, A. L. Johns, A. M. Patch, M. C. Gingras, D. K. Miller, A. N. Christ, T. J. Bruxner, M. C. Quinn, C. Nourse, L. C. Murtaugh, I. Harliwong, S. Idrisoglu, S. Manning, E. Nourbakhsh, S. Wani, L. Fink, O. Holmes, V. Chin, M. J. Anderson, S. Kazakoff, C. Leonard, F. Newell, N. Waddell, S. Wood, Q. Xu, P. J. Wilson, N. Cloonan, K. S. Kassahn, D. Taylor, K. Quek, A. Robertson, L. Pantano, L. Mincarelli, L. N. Sanchez, L. Evers, J. Wu, M. Pinese, M. J. Cowley, M. D. Jones, E. K. Colvin, A. M. Nagrial, E. S. Humphrey, L. A. Chantrill, A. Mawson, J. Humphris, A. Chou, M. Pajic, C. J. Scarlett, A. V. Pinho, M. Giry-Laterriere, I. Rooman, J. S. Samra, J. G. Kench, J. A. Lovell, N. D. Merrett, C. W. Toon, K. Epari, N. Q. Nguyen, A. Barbour, N. Zeps, K. Moran-Jones, N. B. Jamieson, J. S. Graham, F. Duthie, K. Oien, J. Hair, R. Grutzmann, A. Maitra, C. A. Iacobuzio-Donahue, C. L. Wolfgang, R. A. Morgan, R. T. Lawlor, V. Corbo, C. Bassi, B. Rusev, P. Capelli, R. Salvia, G. Tortora, D. Mukhopadhyay, G. M. Petersen, Initiative Australian Pancreatic Cancer Genome, D. M. Munzy, W. E. Fisher, S. A. Karim, J. R. Eshleman, R. H. Hruban, C. Pilarsky, J. P. Morton, O. J. Sansom, A. Scarpa, E. A. Musgrove, U. M. Bailey, O. Hofmann, R. L. Sutherland, D. A. Wheeler, A. J. Gill, R. A. Gibbs, J. V. Pearson, N. Waddell, A. V. Biankin, and S. M. Grimmond. 2016. "Genomic analyses identify molecular subtypes of pancreatic cancer." *Nature* 531 (7592):47-52. doi: 10.1038/nature16965.

Bang, Y. J., E. Van Cutsem, A. Feyereislova, H. C. Chung, L. Shen, A. Sawaki, F. Lordick, A. Ohtsu, Y. Omuro, T. Satoh, G. Aprile, E. Kulikov, J. Hill, M. Lehle, J. Ruschoff, Y. K. Kang, and G. A. Trial Investigators To. 2010. "Trastuzumab in combination with chemotherapy versus chemotherapy alone for treatment of HER2-positive advanced gastric or gastro-oesophageal junction cancer (ToGA): a phase 3, open-label, randomised controlled trial." *Lancet* 376 (9742):687-97. doi: 10.1016/S0140-6736(10)61121-X.

Bankhead, P., M. B. Loughrey, J. A. Fernandez, Y. Dombrowski, D. G. McArt, P. D. Dunne, S. McQuaid, R. T. Gray, L. J. Murray, H. G. Coleman, J. A. James, M. Salto-Tellez, and P. W. Hamilton. 2017. "QuPath: Open source software for

digital pathology image analysis." *Sci Rep* 7 (1):16878. doi: 10.1038/s41598-017-17204-5.

Barker, N., J. H. van Es, J. Kuipers, P. Kujala, M. van den Born, M. Cozijnsen, A. Haegebarth, J. Korving, H. Begthel, P. J. Peters, and H. Clevers. 2007. "Identification of stem cells in small intestine and colon by marker gene Lgr5." *Nature* 449 (7165):1003-7. doi: 10.1038/nature06196.

Barranco, S. C., C. M. Townsend, Jr., C. Casartelli, B. G. Macik, N. L. Burger, W. R. Boerwinkle, and W. K. Gourley. 1983. "Establishment and characterization of an in vitro model system for human adenocarcinoma of the stomach." *Cancer Res* 43 (4):1703-9.

Bartley, A. N., M. K. Washington, C. B. Ventura, N. Ismaila, C. Colasacco, A. B. Benson, 3rd, A. Carrato, M. L. Gulley, D. Jain, S. Kakar, H. J. Mackay, C. Streutker, L. Tang, M. Troxell, and J. A. Ajani. 2016. "HER2 Testing and Clinical Decision Making in Gastroesophageal Adenocarcinoma: Guideline From the College of American Pathologists, American Society for Clinical Pathology, and American Society of Clinical Oncology." *Arch Pathol Lab Med* 140 (12):1345-1363. doi: 10.5858/arpa.2016-0331-CP.

Bass, A. J., M. S. Lawrence, L. E. Brace, A. H. Ramos, Y. Drier, K. Cibulskis, C. Sougnez, D. Voet, G. Saksena, A. Sivachenko, R. Jing, M. Parkin, T. Pugh, R. G. Verhaak, N. Stransky, A. T. Boutin, J. Barretina, D. B. Solit, E. Vakiani, W. Shao, Y. Mishina, M. Warmuth, J. Jimenez, D. Y. Chiang, S. Signoretti, W. G. Kaelin, Jr., N. Spardy, W. C. Hahn, Y. Hoshida, S. Ogino, R. A. DePinho, L. Chin, L. A. Garraway, C. S. Fuchs, J. Baselga, J. Tabernero, S. Gabriel, E. S. Lander, G. Getz, and M. Meyerson. 2011. "Genomic sequencing of colorectal adenocarcinomas identifies a recurrent VTI1A-TCF7L2 fusion." *Nat Genet* 43 (10):964-968. doi: 10.1038/ng.936.

Bastide, P., C. Darido, J. Pannequin, R. Kist, S. Robine, C. Marty-Double, F. Bibeau, G. Scherer, D. Joubert, F. Hollande, P. Blache, and P. Jay. 2007. "Sox9 regulates cell proliferation and is required for Paneth cell differentiation in the intestinal epithelium." *J Cell Biol* 178 (4):635-48. doi: 10.1083/jcb.200704152.

Batlle, E., J. T. Henderson, H. Beghtel, M. M. van den Born, E. Sancho, G. Huls, J. Meeldijk, J. Robertson, M. van de Wetering, T. Pawson, and H. Clevers. 2002. "Beta-catenin and TCF mediate cell positioning in the intestinal epithelium by controlling the expression of EphB/ephrinB." *Cell* 111 (2):251-63.

Behrens, J., B. A. Jerchow, M. Wurtele, J. Grimm, C. Asbrand, R. Wirtz, M. Kuhl, D. Wedlich, and W. Birchmeier. 1998. "Functional interaction of an axin homolog, conductin, with beta-catenin, APC, and GSK3beta." *Science* 280 (5363):596-9.

Behrens, J., J. P. von Kries, M. Kuhl, L. Bruhn, D. Wedlich, R. Grosschedl, and W. Birchmeier. 1996. "Functional interaction of beta-catenin with the transcription factor LEF-1." *Nature* 382 (6592):638-42. doi: 10.1038/382638a0.

Berger, E., E. Rath, D. Yuan, N. Waldschmitt, S. Khaloian, M. Allgauer, O. Staszewski, E. M. Lobner, T. Schottl, P. Giesbertz, O. I. Coleman, M. Prinz, A. Weber, M. Gerhard, M. Klingenspor, K. P. Janssen, M. Heikenwalder, and D. Haller. 2016. "Mitochondrial function controls intestinal epithelial stemness and proliferation." *Nat Commun* 7:13171. doi: 10.1038/ncomms13171.

Beumer, J., and H. Clevers. 2016. "Regulation and plasticity of intestinal stem cells during homeostasis and regeneration." *Development* 143 (20):3639-3649. doi: 10.1242/dev.133132.

Biankin, A. V., N. Waddell, K. S. Kassahn, M. C. Gingras, L. B. Muthuswamy, A. L. Johns, D. K. Miller, P. J. Wilson, A. M. Patch, J. Wu, D. K. Chang, M. J. Cowley, B. B. Gardiner, S. Song, I. Harliwong, S. Idrisoglu, C. Nourse, E. Nourbakhsh, S.

Manning, S. Wani, M. Gongora, M. Pajic, C. J. Scarlett, A. J. Gill, A. V. Pinho, I. Rooman, M. Anderson, O. Holmes, C. Leonard, D. Taylor, S. Wood, Q. Xu, K. Nones, J. L. Fink, A. Christ, T. Bruxner, N. Cloonan, G. Kolle, F. Newell, M. Pinese, R. S. Mead, J. L. Humphris, W. Kaplan, M. D. Jones, E. K. Colvin, A. M. Nagrial, E. S. Humphrey, A. Chou, V. T. Chin, L. A. Chantrill, A. Mawson, J. S. Samra, J. G. Kench, J. A. Lovell, R. J. Daly, N. D. Merrett, C. Toon, K. Epari, N. Q. Nguyen, A. Barbour, N. Zeps, Initiative Australian Pancreatic Cancer Genome, N. Kakkar, F. Zhao, Y. Q. Wu, M. Wang, D. M. Muzny, W. E. Fisher, F. C. Brunicardi, S. E. Hodges, J. G. Reid, J. Drummond, K. Chang, Y. Han, L. R. Lewis, H. Dinh, C. J. Buhay, T. Beck, L. Timms, M. Sam, K. Begley, A. Brown, D. Pai, A. Panchal, N. Buchner, R. De Borja, R. E. Denroche, C. K. Yung, S. Serra, N. Onetto, D. Mukhopadhyay, M. S. Tsao, P. A. Shaw, G. M. Petersen, S. Gallinger, R. H. Hruban, A. Maitra, C. A. Iacobuzio-Donahue, R. D. Schulick, C. L. Wolfgang, R. A. Morgan, R. T. Lawlor, P. Capelli, V. Corbo, M. Scardoni, G. Tortora, M. A. Tempero, K. M. Mann, N. A. Jenkins, P. A. Perez-Mancera, D. J. Adams, D. A. Largaespada, L. F. Wessels, A. G. Rust, L. D. Stein, D. A. Tuveson, N. G. Copeland, E. A. Musgrove, A. Scarpa, J. R. Eshleman, T. J. Hudson, R. L. Sutherland, D. A. Wheeler, J. V. Pearson, J. D. McPherson, R. A. Gibbs, and S. M. Grimmond. 2012. "Pancreatic cancer genomes reveal aberrations in axon guidance pathway genes." *Nature* 491 (7424):399-405. doi: 10.1038/nature11547.

Blaser, M. J., G. I. Perez-Perez, H. Kleanthous, T. L. Cover, R. M. Peek, P. H. Chyou, G. N. Stemmermann, and A. Nomura. 1995. "Infection with Helicobacter pylori strains possessing cagA is associated with an increased risk of developing adenocarcinoma of the stomach." *Cancer Res* 55 (10):2111-5.

Bode, P. K., A. Barghorn, F. R. Fritzsche, M. O. Riener, G. Kristiansen, A. Knuth, and H. Moch. 2011. "MAGEC2 is a sensitive and novel marker for seminoma: a tissue microarray analysis of 325 testicular germ cell tumors." *Mod Pathol* 24 (6):829-35.

Bohgaki, M., T. Bohgaki, S. El Ghamrasni, T. Srikumar, G. Maire, S. Panier, A. Fradet-Turcotte, G. S. Stewart, B. Raught, A. Hakem, and R. Hakem. 2013. "RNF168 ubiquitylates 53BP1 and controls its response to DNA double-strand breaks." *Proc Natl Acad Sci U S A* 110 (52):20982-7. doi: 10.1073/pnas.1320302111.

Bond, C. E., D. M. McKeone, M. Kalimutho, M. L. Bettington, S. A. Pearson, T. D. Dumenil, L. F. Wockner, M. Burge, B. A. Leggett, and V. L. Whitehall. 2016. "RNF43 and ZNRF3 are commonly altered in serrated pathway colorectal tumorigenesis." *Oncotarget* 7 (43):70589-70600. doi: 10.18632/oncotarget.12130.

Boussadia, O., S. Kutsch, A. Hierholzer, V. Delmas, and R. Kemler. 2002. "E-cadherin is a survival factor for the lactating mouse mammary gland." *Mech Dev* 115 (1-2):53-62.

Boutros, M., and C. Niehrs. 2016. "Sticking Around: Short-Range Activity of Wnt Ligands." *Dev Cell* 36 (5):485-6. doi: 10.1016/j.devcel.2016.02.018.

Bowles, J., G. Schepers, and P. Koopman. 2000. "Phylogeny of the SOX family of developmental transcription factors based on sequence and structural indicators." *Dev Biol* 227 (2):239-55. doi: 10.1006/dbio.2000.9883.

Brannon, A. R., E. Vakiani, B. E. Sylvester, S. N. Scott, G. McDermott, R. H. Shah, K. Kania, A. Viale, D. M. Oschwald, V. Vacic, A. K. Emde, A. Cercek, R. Yaeger, N. E. Kemeny, L. B. Saltz, J. Shia, M. I. D'Angelica, M. R. Weiser, D. B. Solit, and M. F. Berger. 2014. "Comparative sequencing analysis reveals high genomic

concordance between matched primary and metastatic colorectal cancer lesions." *Genome Biol* 15 (8):454. doi: 10.1186/s13059-014-0454-7.

Brattain, M. G., W. D. Fine, F. M. Khaled, J. Thompson, and D. E. Brattain. 1981. "Heterogeneity of malignant cells from a human colonic carcinoma." *Cancer Res* 41 (5):1751-6.

Bruewer, M., S. Samarin, and A. Nusrat. 2006. "Inflammatory bowel disease and the apical junctional complex." *Ann N Y Acad Sci* 1072:242-52. doi: 10.1196/annals.1326.017.

Buchanan, D. D., M. Clendenning, L. Zhuoer, J. R. Stewart, S. Joseland, S. Woodall, J. Arnold, K. Semotiuk, M. Aronson, S. Holter, S. Gallinger, M. A. Jenkins, K. Sweet, F. A. Macrae, I. M. Winship, S. Parry, C. Rosty, and Study Genetics of Colonic Polyposis. 2017. "Lack of evidence for germline RNF43 mutations in patients with serrated polyposis syndrome from a large multinational study." *Gut* 66 (6):1170-1172. doi: 10.1136/gutjnl-2016-312773.

Buczacki, S. J., H. I. Zecchini, A. M. Nicholson, R. Russell, L. Vermeulen, R. Kemp, and D. J. Winton. 2013. "Intestinal label-retaining cells are secretory precursors expressing Lgr5." *Nature* 495 (7439):65-9. doi: 10.1038/nature11965.

Burtscher, I., W. Barkey, M. Schwarzfischer, F. J. Theis, and H. Lickert. 2012. "The Sox17-mCherry fusion mouse line allows visualization of endoderm and vascular endothelial development." *Genesis* 50 (6):496-505. doi: 10.1002/dvg.20829.

Caca, K., F. T. Kolligs, X. Ji, M. Hayes, J. Qian, A. Yahanda, D. L. Rimm, J. Costa, and E. R. Fearon. 1999. "Beta- and gamma-catenin mutations, but not E-cadherin inactivation, underlie T-cell factor/lymphoid enhancer factor transcriptional deregulation in gastric and pancreatic cancer." *Cell Growth Differ* 10 (6):369-76.

Campbell, S. J., R. A. Edwards, C. C. Leung, D. Neculai, C. D. Hodge, S. Dhe-Paganon, and J. N. Glover. 2012. "Molecular insights into the function of RING finger (RNF)-containing proteins hRNF8 and hRNF168 in Ubc13/Mms2-dependent ubiquitylation." *J Biol Chem* 287 (28):23900-10. doi: 10.1074/jbc.M112.359653.

Cancer Genome Atlas, Network. 2012. "Comprehensive molecular characterization of human colon and rectal cancer." *Nature* 487 (7407):330-7. doi: 10.1038/nature11252.

Cancer Genome Atlas Research, Network. 2014. "Comprehensive molecular characterization of gastric adenocarcinoma." *Nature* 513 (7517):202-9. doi: 10.1038/nature13480.

Cancer Genome Atlas Research Network, University Analysis Working Group: Asan, B. C. Cancer Agency, Brigham, Hospital Women's, Institute Broad, University Brown, University Case Western Reserve, Institute Dana-Farber Cancer, University Duke, Centre Greater Poland Cancer, School Harvard Medical, Biology Institute for Systems, K. U. Leuven, Clinic Mayo, Center Memorial Sloan Kettering Cancer, Institute National Cancer, Hospital Nationwide Children's, University Stanford, Alabama University of, Michigan University of, Carolina University of North, Pittsburgh University of, Rochester University of, California University of Southern, M. D. Anderson Cancer Center University of Texas, Washington University of, Institute Van Andel Research, University Vanderbilt, University Washington, Institute Genome Sequencing Center: Broad, Louis Washington University in St, B. C. Cancer Agency Genome Characterization Centers, Institute Broad, School Harvard Medical, University Sidney Kimmel Comprehensive Cancer Center at Johns Hopkins, Carolina University of North, Center University of Southern California Epigenome, M. D. Anderson Cancer Center University of Texas, Institute Van Andel Research, Institute Genome Data Analysis Centers: Broad, University Brown, School Harvard Medical, Biology

Institute for Systems, Center Memorial Sloan Kettering Cancer, Cruz University of California Santa, M. D. Anderson Cancer Center University of Texas, Consortium Biospecimen Core Resource: International Genomics, Hospital Research Institute at Nationwide Children's, Services Tissue Source Sites: Analytic Biologic, Center Asan Medical, Bioscience Asterand, Hospital Barretos Cancer, BioreclamationIvt, Clinic Botkin Municipal, School Chonnam National University Medical, System Christiana Care Health, Cureline, University Duke, University Emory, University Erasmus, Medicine Indiana University School of, Moldova Institute of Oncology of, Consortium International Genomics, Invidumed, Hamburg Israelitisches Krankenhaus, Medicine Keimyung University School of, Center Memorial Sloan Kettering Cancer, Goyang National Cancer Center, Bank Ontario Tumour, Centre Peter MacCallum Cancer, School Pusan National University Medical, School Ribeirao Preto Medical, Hospital St. Joseph's, Center Medical, University St. Petersburg Academic, Bank Tayside Tissue, Dundee University of, Center University of Kansas Medical, Michigan University of, Hill University of North Carolina at Chapel, Medicine University of Pittsburgh School of, M. D. Anderson Cancer Center University of Texas, University Disease Working Group: Duke, Center Memorial Sloan Kettering Cancer, Institute National Cancer, M. D. Anderson Cancer Center University of Texas, Medicine Yonsei University College of, Csra Inc Data Coordination Center, and Health Project Team: National Institutes of. 2017. "Integrated genomic characterization of oesophageal carcinoma." *Nature* 541 (7636):169-175. doi: 10.1038/nature20805.

Cao, Y., Z. Gao, L. Li, X. Jiang, A. Shan, J. Cai, Y. Peng, Y. Li, X. Jiang, X. Huang, J. Wang, Q. Wei, G. Qin, J. Zhao, X. Jin, L. Liu, Y. Li, W. Wang, J. Wang, and G. Ning. 2013. "Whole exome sequencing of insulinoma reveals recurrent T372R mutations in YY1." *Nat Commun* 4:2810. doi: 10.1038/ncomms3810.

Capelle, L. G., N. C. Van Grieken, H. F. Lingsma, E. W. Steyerberg, W. J. Klokman, M. J. Bruno, H. F. Vasen, and E. J. Kuipers. 2010. "Risk and epidemiological time trends of gastric cancer in Lynch syndrome carriers in the Netherlands." *Gastroenterology* 138 (2):487-92. doi: 10.1053/j.gastro.2009.10.051.

Cavallo, R. A., R. T. Cox, M. M. Moline, J. Roose, G. A. Polevoy, H. Clevers, M. Peifer, and A. Bejsovec. 1998. "Drosophila Tcf and Groucho interact to repress Wingless signalling activity." *Nature* 395 (6702):604-8. doi: 10.1038/26982.

Cerami, E., J. Gao, U. Dogrusoz, B. E. Gross, S. O. Sumer, B. A. Aksoy, A. Jacobsen, C. J. Byrne, M. L. Heuer, E. Larsson, Y. Antipin, B. Reva, A. P. Goldberg, C. Sander, and N. Schultz. 2012. "The cBio cancer genomics portal: an open platform for exploring multidimensional cancer genomics data." *Cancer Discov* 2 (5):401-4. doi: 10.1158/2159-8290.CD-12-0095.

Chan-On, W., M. L. Nairismagi, C. K. Ong, W. K. Lim, S. Dima, C. Pairojkul, K. H. Lim, J. R. McPherson, I. Cutcutache, H. L. Heng, L. Ooi, A. Chung, P. Chow, P. C. Cheow, S. Y. Lee, S. P. Choo, I. B. Tan, D. Duda, A. Nastase, S. S. Myint, B. H. Wong, A. Gan, V. Rajasegaran, C. C. Ng, S. Nagarajan, A. Jusakul, S. Zhang, P. Vohra, W. Yu, D. Huang, P. Sithithaworn, P. Yongvanit, S. Wongkham, N. Khuntikeo, V. Bhudhisawasdi, I. Popescu, S. G. Rozen, P. Tan, and B. T. Teh. 2013. "Exome sequencing identifies distinct mutational patterns in liver fluke-related and non-infection-related bile duct cancers." *Nat Genet* 45 (12):1474-8. doi: 10.1038/ng.2806.

Chang, H. R., S. Nam, M. C. Kook, K. T. Kim, X. Liu, H. Yao, H. R. Jung, R. Lemos, Jr., H. H. Seo, H. S. Park, Y. Gim, D. Hong, I. Huh, Y. W. Kim, D. Tan, C. G. Liu, G. Powis, T. Park, H. Liang, and Y. H. Kim. 2016. "HNF4alpha is a

therapeutic target that links AMPK to WNT signalling in early-stage gastric cancer." *Gut* 65 (1):19-32. doi: 10.1136/gutjnl-2014-307918.

Chen, B., M. E. Dodge, W. Tang, J. Lu, Z. Ma, C. W. Fan, S. Wei, W. Hao, J. Kilgore, N. S. Williams, M. G. Roth, J. F. Amatruda, C. Chen, and L. Lum. 2009. "Small molecule-mediated disruption of Wnt-dependent signaling in tissue regeneration and cancer." *Nat Chem Biol* 5 (2):100-7. doi: 10.1038/nchembio.137.

Chen, K., D. Yang, X. Li, B. Sun, F. Song, W. Cao, D. J. Brat, Z. Gao, H. Li, H. Liang, Y. Zhao, H. Zheng, M. Li, J. Buckner, S. D. Patterson, X. Ye, C. Reinhard, A. Bhathena, D. Joshi, P. S. Mischel, C. M. Croce, Y. M. Wang, S. Raghavakaimal, H. Li, X. Lu, Y. Pan, H. Chang, S. Ba, L. Luo, W. K. Cavenee, W. Zhang, and X. Hao. 2015. "Mutational landscape of gastric adenocarcinoma in Chinese: implications for prognosis and therapy." *Proc Natl Acad Sci U S A* 112 (4):1107-12. doi: 10.1073/pnas.1422640112.

Chen, W., J. H. Weisburger, E. S. Fiala, T. E. Spratt, S. G. Carmella, D. Chen, and S. S. Hecht. 1996. "Gastric carcinogenesis: 2-chloro-4-methylthiobutanoic acid, a novel mutagen in salted, pickled Sanma hiraki fish, or similarly treated methionine." *Chem Res Toxicol* 9 (1):58-66. doi: 10.1021/tx9500585.

Cheng, H., and C. P. Leblond. 1974. "Origin, differentiation and renewal of the four main epithelial cell types in the mouse small intestine. V. Unitarian Theory of the origin of the four epithelial cell types." *Am J Anat* 141 (4):537-61. doi: 10.1002/aja.1001410407.

Cheng, X. X., Y. Sun, X. Y. Chen, K. L. Zhang, Q. Y. Kong, J. Liu, and H. Li. 2004. "Frequent translocalization of beta-catenin in gastric cancers and its relevance to tumor progression." *Oncol Rep* 11 (6):1201-7.

Clements, W. M., J. Wang, A. Sarnaik, O. J. Kim, J. MacDonald, C. Fenoglio-Preiser, J. Groden, and A. M. Lowy. 2002. "beta-Catenin mutation is a frequent cause of Wnt pathway activation in gastric cancer." *Cancer Res* 62 (12):3503-6.

Clevers, H. 2013. "The intestinal crypt, a prototype stem cell compartment." *Cell* 154 (2):274-84. doi: 10.1016/j.cell.2013.07.004.

Correa, P. 1988. "A human model of gastric carcinogenesis." *Cancer Res* 48 (13):3554-60.

Cristescu, R., J. Lee, M. Nebozhyn, K. M. Kim, J. C. Ting, S. S. Wong, J. Liu, Y. G. Yue, J. Wang, K. Yu, X. S. Ye, I. G. Do, S. Liu, L. Gong, J. Fu, J. G. Jin, M. G. Choi, T. S. Sohn, J. H. Lee, J. M. Bae, S. T. Kim, S. H. Park, I. Sohn, S. H. Jung, P. Tan, R. Chen, J. Hardwick, W. K. Kang, M. Ayers, D. Hongyue, C. Reinhard, A. Loboda, S. Kim, and A. Aggarwal. 2015. "Molecular analysis of gastric cancer identifies subtypes associated with distinct clinical outcomes." *Nat Med* 21 (5):449-56. doi: 10.1038/nm.3850.

Cuilliere-Dartigues, P., J. El-Bchiri, A. Krimi, O. Buhard, P. Fontanges, J. F. Flejou, R. Hamelin, and A. Duval. 2006. "TCF-4 isoforms absent in TCF-4 mutated MSI-H colorectal cancer cells colocalize with nuclear CtBP and repress TCF-4-mediated transcription." *Oncogene* 25 (32):4441-8. doi: 10.1038/sj.onc.1209471.

Daniels, D. L., and W. I. Weis. 2005. "Beta-catenin directly displaces Groucho/TLE repressors from Tcf/Lef in Wnt-mediated transcription activation." *Nat Struct Mol Biol* 12 (4):364-71. doi: 10.1038/nsmb912.

Davidson, G., W. Wu, J. Shen, J. Bilic, U. Fenger, P. Stannek, A. Glinka, and C. Niehrs. 2005. "Casein kinase 1 gamma couples Wnt receptor activation to cytoplasmic signal transduction." *Nature* 438 (7069):867-72. doi: 10.1038/nature04170.

de Lau, W., N. Barker, T. Y. Low, B. K. Koo, V. S. Li, H. Teunissen, P. Kujala, A. Haegebarth, P. J. Peters, M. van de Wetering, D. E. Stange, J. E. van Es, D. Guardavaccaro, R. B. Schasfoort, Y. Mohri, K. Nishimori, S. Mohammed, A. J.

Heck, and H. Clevers. 2011. "Lgr5 homologues associate with Wnt receptors and mediate R-spondin signalling." *Nature* 476 (7360):293-7. doi: 10.1038/nature10337.

de Lau, W., W. C. Peng, P. Gros, and H. Clevers. 2014. "The R-spondin/Lgr5/Rnf43 module: regulator of Wnt signal strength." *Genes Dev* 28 (4):305-16. doi: 10.1101/gad.235473.113.

Deng, N., L. K. Goh, H. Wang, K. Das, J. Tao, I. B. Tan, S. Zhang, M. Lee, J. Wu, K. H. Lim, Z. Lei, G. Goh, Q. Y. Lim, A. L. Tan, D. Y. Sin Poh, S. Riahi, S. Bell, M. M. Shi, R. Linnartz, F. Zhu, K. G. Yeoh, H. C. Toh, W. P. Yong, H. C. Cheong, S. Y. Rha, A. Boussioutas, H. Grabsch, S. Rozen, and P. Tan. 2012. "A comprehensive survey of genomic alterations in gastric cancer reveals systematic patterns of molecular exclusivity and co-occurrence among distinct therapeutic targets." *Gut* 61 (5):673-84. doi: 10.1136/gutjnl-2011-301839.

Dow, L. E., K. P. O'Rourke, J. Simon, D. F. Tschaharganeh, J. H. van Es, H. Clevers, and S. W. Lowe. 2015. "Apc Restoration Promotes Cellular Differentiation and Reestablishes Crypt Homeostasis in Colorectal Cancer." *Cell* 161 (7):1539-1552. doi: 10.1016/j.cell.2015.05.033.

Du, Y. C., H. Oshima, K. Oguma, T. Kitamura, H. Itadani, T. Fujimura, Y. S. Piao, T. Yoshimoto, T. Minamoto, H. Kotani, M. M. Taketo, and M. Oshima. 2009. "Induction and down-regulation of Sox17 and its possible roles during the course of gastrointestinal tumorigenesis." *Gastroenterology* 137 (4):1346-57. doi: 10.1053/j.gastro.2009.06.041.

Dulak, A. M., S. E. Schumacher, J. van Lieshout, Y. Imamura, C. Fox, B. Shim, A. H. Ramos, G. Saksena, S. C. Baca, J. Baselga, J. Tabernero, J. Barretina, P. C. Enzinger, G. Corso, F. Roviello, L. Lin, S. Bandla, J. D. Luketich, A. Pennathur, M. Meyerson, S. Ogino, R. A. Shivdasani, D. G. Beer, T. E. Godfrey, R. Beroukhim, and A. J. Bass. 2012. "Gastrointestinal adenocarcinomas of the esophagus, stomach, and colon exhibit distinct patterns of genome instability and oncogenesis." *Cancer Res* 72 (17):4383-93. doi: 10.1158/0008-5472.CAN-11-3893.

Dulak, A. M., P. Stojanov, S. Peng, M. S. Lawrence, C. Fox, C. Stewart, S. Bandla, Y. Imamura, S. E. Schumacher, E. Shefler, A. McKenna, S. L. Carter, K. Cibulskis, A. Sivachenko, G. Saksena, D. Voet, A. H. Ramos, D. Auclair, K. Thompson, C. Sougnez, R. C. Onofrio, C. Guiducci, R. Beroukhim, Z. Zhou, L. Lin, J. Lin, R. Reddy, A. Chang, R. Landrenau, A. Pennathur, S. Ogino, J. D. Luketich, T. R. Golub, S. B. Gabriel, E. S. Lander, D. G. Beer, T. E. Godfrey, G. Getz, and A. J. Bass. 2013. "Exome and whole-genome sequencing of esophageal adenocarcinoma identifies recurrent driver events and mutational complexity." *Nat Genet* 45 (5):478-86. doi: 10.1038/ng.2591.

Ebert, M. P., G. Fei, S. Kahmann, O. Muller, J. Yu, J. J. Sung, and P. Malfertheiner. 2002. "Increased beta-catenin mRNA levels and mutational alterations of the APC and beta-catenin gene are present in intestinal-type gastric cancer." *Carcinogenesis* 23 (1):87-91.

el Marjou, F., K. P. Janssen, B. H. Chang, M. Li, V. Hindie, L. Chan, D. Louvard, P. Chambon, D. Metzger, and S. Robine. 2004. "Tissue-specific and inducible Cre-mediated recombination in the gut epithelium." *Genesis* 39 (3):186-93. doi: 10.1002/gene.20042.

El-Omar, E. M., M. Carrington, W. H. Chow, K. E. McColl, J. H. Bream, H. A. Young, J. Herrera, J. Lissowska, C. C. Yuan, N. Rothman, G. Lanyon, M. Martin, J. F. Fraumeni, Jr., and C. S. Rabkin. 2000. "Interleukin-1 polymorphisms associated

with increased risk of gastric cancer." *Nature* 404 (6776):398-402. doi: 10.1038/35006081.

Engert, S., I. Burtscher, B. Kalali, M. Gerhard, and H. Lickert. 2013. "The Sox17CreERT2 knock-in mouse line displays spatiotemporal activation of Cre recombinase in distinct Sox17 lineage progenitors." *Genesis* 51 (11):793-802. doi: 10.1002/dvg.22714.

Ensembl. 2017. "ENSG00000108375 (RNF43); http://www.ensembl.org; accessed 14th Feb 2018."

Farin, H. F., I. Jordens, M. H. Mosa, O. Basak, J. Korving, D. V. Tauriello, K. de Punder, S. Angers, P. J. Peters, M. M. Maurice, and H. Clevers. 2016. "Visualization of a short-range Wnt gradient in the intestinal stem-cell niche." *Nature* 530 (7590):340-3. doi: 10.1038/nature16937.

Fearon, E. R., and B. Vogelstein. 1990. "A genetic model for colorectal tumorigenesis." *Cell* 61 (5):759-67.

Ferlay, J., I. Soerjomataram, R. Dikshit, S. Eser, C. Mathers, M. Rebelo, D. M. Parkin, D. Forman, and F. Bray. 2015. "Cancer incidence and mortality worldwide: Sources, methods and major patterns in GLOBOCAN 2012." *Int J Cancer* 136 (5):E359-86. doi: 10.1002/ijc.29210.

Fevr, T., S. Robine, D. Louvard, and J. Huelsken. 2007. "Wnt/beta-catenin is essential for intestinal homeostasis and maintenance of intestinal stem cells." *Mol Cell Biol* 27 (21):7551-9. doi: 10.1128/MCB.01034-07.

Finch, P. W., X. He, M. J. Kelley, A. Uren, R. P. Schaudies, N. C. Popescu, S. Rudikoff, S. A. Aaronson, H. E. Varmus, and J. S. Rubin. 1997. "Purification and molecular cloning of a secreted, Frizzled-related antagonist of Wnt action." *Proc Natl Acad Sci U S A* 94 (13):6770-5.

Forbes, S. A., D. Beare, H. Boutselakis, S. Bamford, N. Bindal, J. Tate, C. G. Cole, S. Ward, E. Dawson, L. Ponting, R. Stefancsik, B. Harsha, C. Y. Kok, M. Jia, H. Jubb, Z. Sondka, S. Thompson, T. De, and P. J. Campbell. 2017. "COSMIC: somatic cancer genetics at high-resolution." *Nucleic Acids Res* 45 (D1):D777-D783. doi: 10.1093/nar/gkw1121.

Forman, D., and V. J. Burley. 2006. "Gastric cancer: global pattern of the disease and an overview of environmental risk factors." *Best Pract Res Clin Gastroenterol* 20 (4):633-49. doi: 10.1016/j.bpg.2006.04.008.

Fox, J. G., C. A. Dangler, M. T. Whary, W. Edelman, R. Kucherlapati, and T. C. Wang. 1997. "Mice carrying a truncated Apc gene have diminished gastric epithelial proliferation, gastric inflammation, and humoral immunity in response to Helicobacter felis infection." *Cancer Res* 57 (18):3972-8.

Friedman, N. B. 1945. "Cellular Dynamics in the Intestinal Mucosa: The Effect of Irradiation on Epithelial Maturation and Migration." *J Exp Med* 81 (6):553-8.

Fu, D. Y., Z. M. Wang, Chen Li, B. L. Wang, Z. Z. Shen, W. Huang, and Z. M. Shao. 2010. "Sox17, the canonical Wnt antagonist, is epigenetically inactivated by promoter methylation in human breast cancer." *Breast Cancer Res Treat* 119 (3):601-12. doi: 10.1007/s10549-009-0339-8.

Fujimoto, A., Y. Totoki, T. Abe, K. A. Boroevich, F. Hosoda, H. H. Nguyen, M. Aoki, N. Hosono, M. Kubo, F. Miya, Y. Arai, H. Takahashi, T. Shirakihara, M. Nagasaki, T. Shibuya, K. Nakano, K. Watanabe-Makino, H. Tanaka, H. Nakamura, J. Kusuda, H. Ojima, K. Shimada, T. Okusaka, M. Ueno, Y. Shigekawa, Y. Kawakami, K. Arihiro, H. Ohdan, K. Gotoh, O. Ishikawa, S. Ariizumi, M. Yamamoto, T. Yamada, K. Chayama, T. Kosuge, H. Yamaue, N. Kamatani, S. Miyano, H. Nakagama, Y. Nakamura, T. Tsunoda, T. Shibata, and H. Nakagawa. 2012. "Whole-genome sequencing of liver cancers identifies

etiological influences on mutation patterns and recurrent mutations in chromatin regulators." *Nat Genet* 44 (7):760-4. doi: 10.1038/ng.2291.

Funayama, N., F. Fagotto, P. McCrea, and B. M. Gumbiner. 1995. "Embryonic axis induction by the armadillo repeat domain of beta-catenin: evidence for intracellular signaling." *J Cell Biol* 128 (5):959-68.

Furukawa, T., Y. Kuboki, E. Tanji, S. Yoshida, T. Hatori, M. Yamamoto, N. Shibata, K. Shimizu, N. Kamatani, and K. Shiratori. 2011. "Whole-exome sequencing uncovers frequent GNAS mutations in intraductal papillary mucinous neoplasms of the pancreas." *Sci Rep* 1:161. doi: 10.1038/srep00161.

Gala, M. K., Y. Mizukami, L. P. Le, K. Moriichi, T. Austin, M. Yamamoto, G. Y. Lauwers, N. Bardeesy, and D. C. Chung. 2014. "Germline mutations in oncogene-induced senescence pathways are associated with multiple sessile serrated adenomas." *Gastroenterology* 146 (2):520-9. doi: 10.1053/j.gastro.2013.10.045.

Ganesan, K., T. Ivanova, Y. Wu, V. Rajasegaran, J. Wu, M. H. Lee, K. Yu, S. Y. Rha, H. C. Chung, B. Ylstra, G. Meijer, K. O. Lian, H. Grabsch, and P. Tan. 2008. "Inhibition of gastric cancer invasion and metastasis by PLA2G2A, a novel beta-catenin/TCF target gene." *Cancer Res* 68 (11):4277-86. doi: 10.1158/0008-5472.CAN-07-6517.

Gao, J., B. A. Aksoy, U. Dogrusoz, G. Dresdner, B. Gross, S. O. Sumer, Y. Sun, A. Jacobsen, R. Sinha, E. Larsson, E. Cerami, C. Sander, and N. Schultz. 2013. "Integrative analysis of complex cancer genomics and clinical profiles using the cBioPortal." *Sci Signal* 6 (269):pl1. doi: 10.1126/scisignal.2004088.

Gao, Y., A. Cai, H. Xi, J. Li, W. Xu, Y. Zhang, K. Zhang, J. Cui, X. Wu, B. Wei, and L. Chen. 2017. "Ring finger protein 43 associates with gastric cancer progression and attenuates the stemness of gastric cancer stem-like cells via the Wnt-beta/catenin signaling pathway." *Stem Cell Res Ther* 8 (1):98. doi: 10.1186/s13287-017-0548-8.

Gassler, N., C. Rohr, A. Schneider, J. Kartenbeck, A. Bach, N. Obermuller, H. F. Otto, and F. Autschbach. 2001. "Inflammatory bowel disease is associated with changes of enterocytic junctions." *Am J Physiol Gastrointest Liver Physiol* 281 (1):G216-28. doi: 10.1152/ajpgi.2001.281.1.G216.

Gavin, B. J., J. A. McMahon, and A. P. McMahon. 1990. "Expression of multiple novel Wnt-1/int-1-related genes during fetal and adult mouse development." *Genes Dev* 4 (12B):2319-32.

Giannakis, M., E. Hodis, X. Jasmine Mu, M. Yamauchi, J. Rosenbluh, K. Cibulskis, G. Saksena, M. S. Lawrence, Z. R. Qian, R. Nishihara, E. M. Van Allen, W. C. Hahn, S. B. Gabriel, E. S. Lander, G. Getz, S. Ogino, C. S. Fuchs, and L. A. Garraway. 2014. "RNF43 is frequently mutated in colorectal and endometrial cancers." *Nat Genet* 46 (12):1264-6. doi: 10.1038/ng.3127.

Giannakis, M., X. J. Mu, S. A. Shukla, Z. R. Qian, O. Cohen, R. Nishihara, S. Bahl, Y. Cao, A. Amin-Mansour, M. Yamauchi, Y. Sukawa, C. Stewart, M. Rosenberg, K. Mima, K. Inamura, K. Nosho, J. A. Nowak, M. S. Lawrence, E. L. Giovannucci, A. T. Chan, K. Ng, J. A. Meyerhardt, E. M. Van Allen, G. Getz, S. B. Gabriel, E. S. Lander, C. J. Wu, C. S. Fuchs, S. Ogino, and L. A. Garraway. 2016. "Genomic Correlates of Immune-Cell Infiltrates in Colorectal Carcinoma." *Cell Rep*. doi: 10.1016/j.celrep.2016.03.075.

Gibson, T. J., M. Seiler, and R. A. Veitia. 2013. "The transience of transient overexpression." *Nat Methods* 10 (8):715-21. doi: 10.1038/nmeth.2534.

Gingras, M. C., K. R. Covington, D. K. Chang, L. A. Donehower, A. J. Gill, M. M. Ittmann, C. J. Creighton, A. L. Johns, E. Shinbrot, N. Dewal, W. E. Fisher, Initiative Australian Pancreatic Cancer Genome, C. Pilarsky, R. Grutzmann, M.

J. Overman, N. B. Jamieson, G. Van Buren, 2nd, J. Drummond, K. Walker, O. A. Hampton, L. Xi, D. M. Muzny, H. Doddapaneni, S. L. Lee, M. Bellair, J. Hu, Y. Han, H. H. Dinh, M. Dahdouli, J. S. Samra, P. Bailey, N. Waddell, J. V. Pearson, I. Harliwong, H. Wang, D. Aust, K. A. Oien, R. H. Hruban, S. E. Hodges, A. McElhany, C. Saengboonmee, F. R. Duthie, S. M. Grimmond, A. V. Biankin, D. A. Wheeler, and R. A. Gibbs. 2016. "Ampullary Cancers Harbor ELF3 Tumor Suppressor Gene Mutations and Exhibit Frequent WNT Dysregulation." *Cell Rep* 14 (4):907-919. doi: 10.1016/j.celrep.2015.12.005.

Goentoro, L., and M. W. Kirschner. 2009. "Evidence that fold-change, and not absolute level, of beta-catenin dictates Wnt signaling." *Mol Cell* 36 (5):872-84. doi: 10.1016/j.molcel.2009.11.017.

Goeppert, B., C. Konermann, C. R. Schmidt, O. Bogatyrova, L. Geiselhart, C. Ernst, L. Gu, N. Becker, M. Zucknick, A. Mehrabi, M. Hafezi, F. Klauschen, A. Stenzinger, A. Warth, K. Breuhahn, M. Renner, W. Weichert, P. Schirmacher, C. Plass, and D. Weichenhan. 2014. "Global alterations of DNA methylation in cholangiocarcinoma target the Wnt signaling pathway." *Hepatology* 59 (2):544-54. doi: 10.1002/hep.26721.

Goldstein, B., H. Takeshita, K. Mizumoto, and H. Sawa. 2006. "Wnt signals can function as positional cues in establishing cell polarity." *Dev Cell* 10 (3):391-6. doi: 10.1016/j.devcel.2005.12.016.

Gonzalez, C. A., P. Jakszyn, G. Pera, A. Agudo, S. Bingham, D. Palli, P. Ferrari, H. Boeing, G. del Giudice, M. Plebani, F. Carneiro, G. Nesi, F. Berrino, C. Sacerdote, R. Tumino, S. Panico, G. Berglund, H. Siman, O. Nyren, G. Hallmans, C. Martinez, M. Dorronsoro, A. Barricarte, C. Navarro, J. R. Quiros, N. Allen, T. J. Key, N. E. Day, J. Linseisen, G. Nagel, M. M. Bergmann, K. Overvad, M. K. Jensen, A. Tjonneland, A. Olsen, H. B. Bueno-de-Mesquita, M. Ocke, P. H. Peeters, M. E. Numans, F. Clavel-Chapelon, M. C. Boutron-Ruault, A. Trichopoulou, T. Psaltopoulou, D. Roukos, E. Lund, B. Hemon, R. Kaaks, T. Norat, and E. Riboli. 2006. "Meat intake and risk of stomach and esophageal adenocarcinoma within the European Prospective Investigation Into Cancer and Nutrition (EPIC)." *J Natl Cancer Inst* 98 (5):345-54. doi: 10.1093/jnci/djj071.

Gotoda, T. 2007. "Endoscopic resection of early gastric cancer." *Gastric Cancer* 10 (1):1-11. doi: 10.1007/s10120-006-0408-1.

Gregorieff, A., and H. Clevers. 2015. "In Situ Hybridization to Identify Gut Stem Cells." *Curr Protoc Stem Cell Biol* 34:2F 1 1-11. doi: 10.1002/9780470151808.sc02f01s34.

Gregorieff, A., R. Grosschedl, and H. Clevers. 2004. "Hindgut defects and transformation of the gastro-intestinal tract in Tcf4(-/-)/Tcf1(-/-) embryos." *EMBO J* 23 (8):1825-33. doi: 10.1038/sj.emboj.7600191.

Gregorieff, A., D. Pinto, H. Begthel, O. Destree, M. Kielman, and H. Clevers. 2005. "Expression pattern of Wnt signaling components in the adult intestine." *Gastroenterology* 129 (2):626-38. doi: 10.1016/j.gastro.2005.06.007.

Groden, J., A. Thliveris, W. Samowitz, M. Carlson, L. Gelbert, H. Albertsen, G. Joslyn, J. Stevens, L. Spirio, M. Robertson, and et al. 1991. "Identification and characterization of the familial adenomatous polyposis coli gene." *Cell* 66 (3):589-600.

Group, Gastric, K. Oba, X. Paoletti, Y. J. Bang, H. Bleiberg, T. Burzykowski, N. Fuse, S. Michiels, S. Morita, Y. Ohashi, J. P. Pignon, P. Rougier, J. Sakamoto, D. Sargent, M. Sasako, K. Shitara, A. Tsuburaya, E. Van Cutsem, and M. Buyse. 2013. "Role of chemotherapy for advanced/recurrent gastric cancer: an

individual-patient-data meta-analysis." *Eur J Cancer* 49 (7):1565-77. doi: 10.1016/j.ejca.2012.12.016.

Guilford, P., J. Hopkins, J. Harraway, M. McLeod, N. McLeod, P. Harawira, H. Taite, R. Scoular, A. Miller, and A. E. Reeve. 1998. "E-cadherin germline mutations in familial gastric cancer." *Nature* 392 (6674):402-5. doi: 10.1038/32918.

Halbleib, J. M., and W. J. Nelson. 2006. "Cadherins in development: cell adhesion, sorting, and tissue morphogenesis." *Genes Dev* 20 (23):3199-214. doi: 10.1101/gad.1486806.

Hansford, S., P. Kaurah, H. Li-Chang, M. Woo, J. Senz, H. Pinheiro, K. A. Schrader, D. F. Schaeffer, K. Shumansky, G. Zogopoulos, T. A. Santos, I. Claro, J. Carvalho, C. Nielsen, S. Padilla, A. Lum, A. Talhouk, K. Baker-Lange, S. Richardson, I. Lewis, N. M. Lindor, E. Pennell, A. MacMillan, B. Fernandez, G. Keller, H. Lynch, S. P. Shah, P. Guilford, S. Gallinger, G. Corso, F. Roviello, C. Caldas, C. Oliveira, P. D. Pharoah, and D. G. Huntsman. 2015. "Hereditary Diffuse Gastric Cancer Syndrome: CDH1 Mutations and Beyond." *JAMA Oncol* 1 (1):23-32. doi: 10.1001/jamaoncol.2014.168.

Hao, H. X., Y. Xie, Y. Zhang, O. Charlat, E. Oster, M. Avello, H. Lei, C. Mickanin, D. Liu, H. Ruffner, X. Mao, Q. Ma, R. Zamponi, T. Bouwmeester, P. M. Finan, M. W. Kirschner, J. A. Porter, F. C. Serluca, and F. Cong. 2012. "ZNRF3 promotes Wnt receptor turnover in an R-spondin-sensitive manner." *Nature* 485 (7397):195-200. doi: 10.1038/nature11019.

Hartgrink, H. H., E. P. Jansen, N. C. van Grieken, and C. J. van de Velde. 2009. "Gastric cancer." *Lancet* 374 (9688):477-90. doi: 10.1016/S0140-6736(09)60617-6.

Hatzis, P., L. G. van der Flier, M. A. van Driel, V. Guryev, F. Nielsen, S. Denissov, I. J. Nijman, J. Koster, E. E. Santo, W. Welboren, R. Versteeg, E. Cuppen, M. van de Wetering, H. Clevers, and H. G. Stunnenberg. 2008. "Genome-wide pattern of TCF7L2/TCF4 chromatin occupancy in colorectal cancer cells." *Mol Cell Biol* 28 (8):2732-44. doi: 10.1128/MCB.02175-07.

He, T. C., A. B. Sparks, C. Rago, H. Hermeking, L. Zawel, L. T. da Costa, P. J. Morin, B. Vogelstein, and K. W. Kinzler. 1998. "Identification of c-MYC as a target of the APC pathway." *Science* 281 (5382):1509-12.

Heasman, J., A. Crawford, K. Goldstone, P. Garner-Hamrick, B. Gumbiner, P. McCrea, C. Kintner, C. Y. Noro, and C. Wylie. 1994. "Overexpression of cadherins and underexpression of beta-catenin inhibit dorsal mesoderm induction in early Xenopus embryos." *Cell* 79 (5):791-803.

Hermiston, M. L., and J. I. Gordon. 1995. "Inflammatory bowel disease and adenomas in mice expressing a dominant negative N-cadherin." *Science* 270 (5239):1203-7.

Hernandez, A. R., A. M. Klein, and M. W. Kirschner. 2012. "Kinetic responses of beta-catenin specify the sites of Wnt control." *Science* 338 (6112):1337-40. doi: 10.1126/science.1228734.

Higashi, H., R. Tsutsumi, S. Muto, T. Sugiyama, T. Azuma, M. Asaka, and M. Hatakeyama. 2002. "SHP-2 tyrosine phosphatase as an intracellular target of Helicobacter pylori CagA protein." *Science* 295 (5555):683-6. doi: 10.1126/science.1067147.

Hsieh, J. C., L. Kodjabachian, M. L. Rebbert, A. Rattner, P. M. Smallwood, C. H. Samos, R. Nusse, I. B. Dawid, and J. Nathans. 1999. "A new secreted protein that binds to Wnt proteins and inhibits their activities." *Nature* 398 (6726):431-6. doi: 10.1038/18899.

Hua, G., T. H. Thin, R. Feldman, A. Haimovitz-Friedman, H. Clevers, Z. Fuks, and R. Kolesnick. 2012. "Crypt base columnar stem cells in small intestines of mice are

radioresistant." *Gastroenterology* 143 (5):1266-76. doi: 10.1053/j.gastro.2012.07.106.

Huber, O., R. Korn, J. McLaughlin, M. Ohsugi, B. G. Herrmann, and R. Kemler. 1996. "Nuclear localization of beta-catenin by interaction with transcription factor LEF-1." *Mech Dev* 59 (1):3-10.

Hudson, C., D. Clements, R. V. Friday, D. Stott, and H. R. Woodland. 1997. "Xsox17alpha and -beta mediate endoderm formation in Xenopus." *Cell* 91 (3):397-405.

Huelsken, J., R. Vogel, V. Brinkmann, B. Erdmann, C. Birchmeier, and W. Birchmeier. 2000. "Requirement for beta-catenin in anterior-posterior axis formation in mice." *J Cell Biol* 148 (3):567-78.

Ikeda, S., S. Kishida, H. Yamamoto, H. Murai, S. Koyama, and A. Kikuchi. 1998. "Axin, a negative regulator of the Wnt signaling pathway, forms a complex with GSK-3beta and beta-catenin and promotes GSK-3beta-dependent phosphorylation of beta-catenin." *EMBO J* 17 (5):1371-84. doi: 10.1093/emboj/17.5.1371.

Ireland, H., R. Kemp, C. Houghton, L. Howard, A. R. Clarke, O. J. Sansom, and D. J. Winton. 2004. "Inducible Cre-mediated control of gene expression in the murine gastrointestinal tract: effect of loss of beta-catenin." *Gastroenterology* 126 (5):1236-46.

Ishibashi, H., T. Suzuki, S. Suzuki, T. Moriya, C. Kaneko, T. Takizawa, M. Sunamori, M. Handa, T. Kondo, and H. Sasano. 2003. "Sex steroid hormone receptors in human thymoma." *J Clin Endocrinol Metab* 88 (5):2309-17. doi: 10.1210/jc.2002-021353.

Ishikawa, T. O., Y. Tamai, Q. Li, M. Oshima, and M. M. Taketo. 2003. "Requirement for tumor suppressor Apc in the morphogenesis of anterior and ventral mouse embryo." *Dev Biol* 253 (2):230-46.

Islam, S., T. E. Carey, G. T. Wolf, M. J. Wheelock, and K. R. Johnson. 1996. "Expression of N-cadherin by human squamous carcinoma cells induces a scattered fibroblastic phenotype with disrupted cell-cell adhesion." *J Cell Biol* 135 (6 Pt 1):1643-54.

Jakubowska, A., K. Nej, T. Huzarski, R. J. Scott, and J. Lubinski. 2002. "BRCA2 gene mutations in families with aggregations of breast and stomach cancers." *Br J Cancer* 87 (8):888-91. doi: 10.1038/sj.bjc.6600562.

Janjigian, Y. Y., F. Sanchez-Vega, P. Jonsson, W. K. Chatila, J. F. Hechtman, G. Y. Ku, J. C. Riches, Y. Tuvy, R. Kundra, N. Bouvier, E. Vakiani, J. Gao, Z. J. Heins, B. E. Gross, D. P. Kelsen, L. Zhang, V. E. Strong, M. Schattner, H. Gerdes, D. G. Coit, M. Bains, Z. K. Stadler, V. W. Rusch, D. R. Jones, D. Molena, J. Shia, M. E. Robson, M. Capanu, S. Middha, A. Zehir, D. M. Hyman, M. Scaltriti, M. Ladanyi, N. Rosen, D. H. Ilson, M. F. Berger, L. Tang, B. S. Taylor, D. B. Solit, and N. Schultz. 2018. "Genetic Predictors of Response to Systemic Therapy in Esophagogastric Cancer." *Cancer Discov* 8 (1):49-58. doi: 10.1158/2159-8290.CD-17-0787.

Jankowski, J. A., F. K. Bedford, R. A. Boulton, N. Cruickshank, C. Hall, J. Elder, R. Allan, A. Forbes, Y. S. Kim, N. A. Wright, and D. S. Sanders. 1998. "Alterations in classical cadherins associated with progression in ulcerative and Crohn's colitis." *Lab Invest* 78 (9):1155-67.

Janssen, K. P., P. Alberici, H. Fsihi, C. Gaspar, C. Breukel, P. Franken, C. Rosty, M. Abal, F. El Marjou, R. Smits, D. Louvard, R. Fodde, and S. Robine. 2006. "APC and oncogenic KRAS are synergistic in enhancing Wnt signaling in intestinal tumor formation and progression." *Gastroenterology* 131 (4):1096-109. doi: 10.1053/j.gastro.2006.08.011.

Jho, E. H., T. Zhang, C. Domon, C. K. Joo, J. N. Freund, and F. Costantini. 2002. "Wnt/beta-catenin/Tcf signaling induces the transcription of Axin2, a negative regulator of the signaling pathway." *Mol Cell Biol* 22 (4):1172-83.

Jia, Y., Y. Yang, S. Liu, J. G. Herman, F. Lu, and M. Guo. 2010. "SOX17 antagonizes WNT/beta-catenin signaling pathway in hepatocellular carcinoma." *Epigenetics* 5 (8):743-9. doi: 10.4161/epi.5.8.13104.

Jiang, X., H. X. Hao, J. D. Growney, S. Woolfenden, C. Bottiglio, N. Ng, B. Lu, M. H. Hsieh, L. Bagdasarian, R. Meyer, T. R. Smith, M. Avello, O. Charlat, Y. Xie, J. A. Porter, S. Pan, J. Liu, M. E. McLaughlin, and F. Cong. 2013. "Inactivating mutations of RNF43 confer Wnt dependency in pancreatic ductal adenocarcinoma." *Proc Natl Acad Sci U S A* 110 (31):12649-54. doi: 10.1073/pnas.1307218110.

Jiao, Y., T. M. Pawlik, R. A. Anders, F. M. Selaru, M. M. Streppel, D. J. Lucas, N. Niknafs, V. B. Guthrie, A. Maitra, P. Argani, G. J. A. Offerhaus, J. C. Roa, L. R. Roberts, G. J. Gores, I. Popescu, S. T. Alexandrescu, S. Dima, M. Fassan, M. Simbolo, A. Mafficini, P. Capelli, R. T. Lawlor, A. Ruzzenente, A. Guglielmi, G. Tortora, F. de Braud, A. Scarpa, W. Jarnagin, D. Klimstra, R. Karchin, V. E. Velculescu, R. H. Hruban, B. Vogelstein, K. W. Kinzler, N. Papadopoulos, and L. D. Wood. 2013. "Exome sequencing identifies frequent inactivating mutations in BAP1, ARID1A and PBRM1 in intrahepatic cholangiocarcinomas." *Nat Genet* 45 (12):1470-1473. doi: 10.1038/ng.2813.

Jiao, Y., C. Shi, B. H. Edil, R. F. de Wilde, D. S. Klimstra, A. Maitra, R. D. Schulick, L. H. Tang, C. L. Wolfgang, M. A. Choti, V. E. Velculescu, L. A. Diaz, Jr., B. Vogelstein, K. W. Kinzler, R. H. Hruban, and N. Papadopoulos. 2011. "DAXX/ATRX, MEN1, and mTOR pathway genes are frequently altered in pancreatic neuroendocrine tumors." *Science* 331 (6021):1199-203. doi: 10.1126/science.1200609.

Jiao, Y., R. Yonescu, G. J. Offerhaus, D. S. Klimstra, A. Maitra, J. R. Eshleman, J. G. Herman, W. Poh, L. Pelosof, C. L. Wolfgang, B. Vogelstein, K. W. Kinzler, R. H. Hruban, N. Papadopoulos, and L. D. Wood. 2014. "Whole-exome sequencing of pancreatic neoplasms with acinar differentiation." *J Pathol* 232 (4):428-35. doi: 10.1002/path.4310.

Jin, L. H., Q. J. Shao, W. Luo, Z. Y. Ye, Q. Li, and S. C. Lin. 2003. "Detection of point mutations of the Axin1 gene in colorectal cancers." *Int J Cancer* 107 (5):696-9. doi: 10.1002/ijc.11435.

Jo, Y. S., M. S. Kim, J. H. Lee, S. H. Lee, C. H. An, and N. J. Yoo. 2015. "Frequent frameshift mutations in 2 mononucleotide repeats of RNF43 gene and its regional heterogeneity in gastric and colorectal cancers." *Hum Pathol* 46 (11):1640-6. doi: 10.1016/j.humpath.2015.07.004.

Kahn, M. 2014. "Can we safely target the WNT pathway?" *Nat Rev Drug Discov* 13 (7):513-32. doi: 10.1038/nrd4233.

Kakiuchi, M., T. Nishizawa, H. Ueda, K. Gotoh, A. Tanaka, A. Hayashi, S. Yamamoto, K. Tatsuno, H. Katoh, Y. Watanabe, T. Ichimura, T. Ushiku, S. Funahashi, K. Tateishi, I. Wada, N. Shimizu, S. Nomura, K. Koike, Y. Seto, M. Fukayama, H. Aburatani, and S. Ishikawa. 2014. "Recurrent gain-of-function mutations of RHOA in diffuse-type gastric carcinoma." *Nat Genet* 46 (6):583-7. doi: 10.1038/ng.2984.

Kakugawa, S., P. F. Langton, M. Zebisch, S. Howell, T. H. Chang, Y. Liu, T. Feizi, G. Bineva, N. O'Reilly, A. P. Snijders, E. Y. Jones, and J. P. Vincent. 2015. "Notum deacylates Wnt proteins to suppress signalling activity." *Nature* 519 (7542):187-192. doi: 10.1038/nature14259.

Kanai-Azuma, M., Y. Kanai, J. M. Gad, Y. Tajima, C. Taya, M. Kurohmaru, Y. Sanai, H. Yonekawa, K. Yazaki, P. P. Tam, and Y. Hayashi. 2002. "Depletion of definitive gut endoderm in Sox17-null mutant mice." *Development* 129 (10):2367-79.

Kaser, A., A. H. Lee, A. Franke, J. N. Glickman, S. Zeissig, H. Tilg, E. E. Nieuwenhuis, D. E. Higgins, S. Schreiber, L. H. Glimcher, and R. S. Blumberg. 2008. "XBP1 links ER stress to intestinal inflammation and confers genetic risk for human inflammatory bowel disease." *Cell* 134 (5):743-56. doi: 10.1016/j.cell.2008.07.021.

Kim, I., T. L. Saunders, and S. J. Morrison. 2007. "Sox17 dependence distinguishes the transcriptional regulation of fetal from adult hematopoietic stem cells." *Cell* 130 (3):470-83. doi: 10.1016/j.cell.2007.06.011.

Kim, K. A., M. Kakitani, J. Zhao, T. Oshima, T. Tang, M. Binnerts, Y. Liu, B. Boyle, E. Park, P. Emtage, W. D. Funk, and K. Tomizuka. 2005. "Mitogenic influence of human R-spondin1 on the intestinal epithelium." *Science* 309 (5738):1256-9. doi: 10.1126/science.1112521.

Kim, S. E., H. Huang, M. Zhao, X. Zhang, A. Zhang, M. V. Semonov, B. T. MacDonald, X. Zhang, J. Garcia Abreu, L. Peng, and X. He. 2013. "Wnt stabilization of beta-catenin reveals principles for morphogen receptor-scaffold assemblies." *Science* 340 (6134):867-70. doi: 10.1126/science.1232389.

Kinzler, K. W., M. C. Nilbert, L. K. Su, B. Vogelstein, T. M. Bryan, D. B. Levy, K. J. Smith, A. C. Preisinger, P. Hedge, D. McKechnie, and et al. 1991. "Identification of FAP locus genes from chromosome 5q21." *Science* 253 (5020):661-5.

Koo, B. K., M. Spit, I. Jordens, T. Y. Low, D. E. Stange, M. van de Wetering, J. H. van Es, S. Mohammed, A. J. Heck, M. M. Maurice, and H. Clevers. 2012. "Tumour suppressor RNF43 is a stem-cell E3 ligase that induces endocytosis of Wnt receptors." *Nature* 488 (7413):665-9. doi: 10.1038/nature11308.

Korinek, V., N. Barker, P. Moerer, E. van Donselaar, G. Huls, P. J. Peters, and H. Clevers. 1998. "Depletion of epithelial stem-cell compartments in the small intestine of mice lacking Tcf-4." *Nat Genet* 19 (4):379-83. doi: 10.1038/1270.

Korinek, V., N. Barker, P. J. Morin, D. van Wichen, R. de Weger, K. W. Kinzler, B. Vogelstein, and H. Clevers. 1997. "Constitutive transcriptional activation by a beta-catenin-Tcf complex in APC-/- colon carcinoma." *Science* 275 (5307):1784-7.

Kormish, J. D., D. Sinner, and A. M. Zorn. 2010. "Interactions between SOX factors and Wnt/beta-catenin signaling in development and disease." *Dev Dyn* 239 (1):56-68. doi: 10.1002/dvdy.22046.

Korswagen, H. C., M. A. Herman, and H. C. Clevers. 2000. "Distinct beta-catenins mediate adhesion and signalling functions in C. elegans." *Nature* 406 (6795):527-32. doi: 10.1038/35020099.

Krausova, M., and V. Korinek. 2014. "Wnt signaling in adult intestinal stem cells and cancer." *Cell Signal* 26 (3):570-9. doi: 10.1016/j.cellsig.2013.11.032.

Kucharzik, T., S. V. Walsh, J. Chen, C. A. Parkos, and A. Nusrat. 2001. "Neutrophil transmigration in inflammatory bowel disease is associated with differential expression of epithelial intercellular junction proteins." *Am J Pathol* 159 (6):2001-9. doi: 10.1016/S0002-9440(10)63051-9.

Kuhnert, F., C. R. Davis, H. T. Wang, P. Chu, M. Lee, J. Yuan, R. Nusse, and C. J. Kuo. 2004. "Essential requirement for Wnt signaling in proliferation of adult small intestine and colon revealed by adenoviral expression of Dickkopf-1." *Proc Natl Acad Sci U S A* 101 (1):266-71. doi: 10.1073/pnas.2536800100.

Kulak, O., H. Chen, B. Holohan, X. Wu, H. He, D. Borek, Z. Otwinowski, K. Yamaguchi, L. A. Garofalo, Z. Ma, W. Wright, C. Chen, J. W. Shay, X. Zhang, and L. Lum. 2015. "Disruption of Wnt/beta-Catenin Signaling and Telomeric Shortening Are Inextricable Consequences of Tankyrase Inhibition in Human Cells." *Mol Cell Biol* 35 (14):2425-35. doi: 10.1128/MCB.00392-15.

Kusserow, A., K. Pang, C. Sturm, M. Hrouda, J. Lentfer, H. A. Schmidt, U. Technau, A. von Haeseler, B. Hobmayer, M. Q. Martindale, and T. W. Holstein. 2005. "Unexpected complexity of the Wnt gene family in a sea anemone." *Nature* 433 (7022):156-60. doi: 10.1038/nature03158.

La Vecchia, C., E. Negri, S. Franceschi, and A. Gentile. 1992. "Family history and the risk of stomach and colorectal cancer." *Cancer* 70 (1):50-5.

Ladeiras-Lopes, R., A. K. Pereira, A. Nogueira, T. Pinheiro-Torres, I. Pinto, R. Santos-Pereira, and N. Lunet. 2008. "Smoking and gastric cancer: systematic review and meta-analysis of cohort studies." *Cancer Causes Control* 19 (7):689-701. doi: 10.1007/s10552-008-9132-y.

Laird, P. W., A. Zijderveld, K. Linders, M. A. Rudnicki, R. Jaenisch, and A. Berns. 1991. "Simplified mammalian DNA isolation procedure." *Nucleic Acids Res* 19 (15):4293.

Lammi, L., S. Arte, M. Somer, H. Jarvinen, P. Lahermo, I. Thesleff, S. Pirinen, and P. Nieminen. 2004. "Mutations in AXIN2 cause familial tooth agenesis and predispose to colorectal cancer." *Am J Hum Genet* 74 (5):1043-50. doi: 10.1086/386293.

Lauren, P. 1965. "The Two Histological Main Types of Gastric Carcinoma: Diffuse and So-Called Intestinal-Type Carcinoma. An Attempt at a Histo-Clinical Classification." *Acta Pathol Microbiol Scand* 64:31-49.

Lee, Y. C., T. H. Chen, H. M. Chiu, C. T. Shun, H. Chiang, T. Y. Liu, M. S. Wu, and J. T. Lin. 2013. "The benefit of mass eradication of Helicobacter pylori infection: a community-based study of gastric cancer prevention." *Gut* 62 (5):676-82. doi: 10.1136/gutjnl-2012-302240.

Li, J., S. L. Woods, S. Healey, J. Beesley, X. Chen, J. S. Lee, H. Sivakumaran, N. Wayte, K. Nones, J. J. Waterfall, J. Pearson, A. M. Patch, J. Senz, M. A. Ferreira, P. Kaurah, R. Mackenzie, A. Heravi-Moussavi, S. Hansford, T. R. M. Lannagan, A. B. Spurdle, P. T. Simpson, L. da Silva, S. R. Lakhani, A. D. Clouston, M. Bettington, F. Grimpen, R. A. Busuttil, N. Di Costanzo, A. Boussioutas, M. Jeanjean, G. Chong, A. Fabre, S. Olschwang, G. J. Faulkner, E. Bellos, L. Coin, K. Rioux, O. F. Bathe, X. Wen, H. C. Martin, D. W. Neklason, S. R. Davis, R. L. Walker, K. A. Calzone, I. Avital, T. Heller, C. Koh, M. Pineda, U. Rudloff, M. Quezado, P. N. Pichurin, P. J. Hulick, S. M. Weissman, A. Newlin, W. S. Rubinstein, J. E. Sampson, K. Hamman, D. Goldgar, N. Poplawski, K. Phillips, L. Schofield, J. Armstrong, C. Kiraly-Borri, G. K. Suthers, D. G. Huntsman, W. D. Foulkes, F. Carneiro, N. M. Lindor, S. L. Edwards, J. D. French, N. Waddell, P. S. Meltzer, D. L. Worthley, K. A. Schrader, and G. Chenevix-Trench. 2016. "Point Mutations in Exon 1B of APC Reveal Gastric Adenocarcinoma and Proximal Polyposis of the Stomach as a Familial Adenomatous Polyposis Variant." *Am J Hum Genet* 98 (5):830-842. doi: 10.1016/j.ajhg.2016.03.001.

Li, M., Z. Zhang, X. Li, J. Ye, X. Wu, Z. Tan, C. Liu, B. Shen, X. A. Wang, W. Wu, D. Zhou, D. Zhang, T. Wang, B. Liu, K. Qu, Q. Ding, H. Weng, Q. Ding, J. Mu, Y. Shu, R. Bao, Y. Cao, P. Chen, T. Liu, L. Jiang, Y. Hu, P. Dong, J. Gu, W. Lu, W. Shi, J. Lu, W. Gong, Z. Tang, Y. Zhang, X. Wang, Y. E. Chin, X. Weng, H. Zhang, W. Tang, Y. Zheng, L. He, H. Wang, Y. Liu, and Y. Liu. 2014. "Whole-exome

and targeted gene sequencing of gallbladder carcinoma identifies recurrent mutations in the ErbB pathway." *Nat Genet* 46 (8):872-6. doi: 10.1038/ng.3030.

Li, V. S., S. S. Ng, P. J. Boersema, T. Y. Low, W. R. Karthaus, J. P. Gerlach, S. Mohammed, A. J. Heck, M. M. Maurice, T. Mahmoudi, and H. Clevers. 2012. "Wnt signaling through inhibition of beta-catenin degradation in an intact Axin1 complex." *Cell* 149 (6):1245-56. doi: 10.1016/j.cell.2012.05.002.

Lickert, H., A. Kispert, S. Kutsch, and R. Kemler. 2001. "Expression patterns of Wnt genes in mouse gut development." *Mech Dev* 105 (1-2):181-4.

Lin, D. C., J. J. Hao, Y. Nagata, L. Xu, L. Shang, X. Meng, Y. Sato, Y. Okuno, A. M. Varela, L. W. Ding, M. Garg, L. Z. Liu, H. Yang, D. Yin, Z. Z. Shi, Y. Y. Jiang, W. Y. Gu, T. Gong, Y. Zhang, X. Xu, O. Kalid, S. Shacham, S. Ogawa, M. R. Wang, and H. P. Koeffler. 2014. "Genomic and molecular characterization of esophageal squamous cell carcinoma." *Nat Genet* 46 (5):467-73. doi: 10.1038/ng.2935.

Lin, Y. M., Y. Furukawa, T. Tsunoda, C. T. Yue, K. C. Yang, and Y. Nakamura. 2002. "Molecular diagnosis of colorectal tumors by expression profiles of 50 genes expressed differentially in adenomas and carcinomas." *Oncogene* 21 (26):4120-8. doi: 10.1038/sj.onc.1205518.

Liu, P., M. Wakamiya, M. J. Shea, U. Albrecht, R. R. Behringer, and A. Bradley. 1999. "Requirement for Wnt3 in vertebrate axis formation." *Nat Genet* 22 (4):361-5. doi: 10.1038/11932.

Liu, W., X. Dong, M. Mai, R. S. Seelan, K. Taniguchi, K. K. Krishnadath, K. C. Halling, J. M. Cunningham, L. A. Boardman, C. Qian, E. Christensen, S. S. Schmidt, P. C. Roche, D. I. Smith, and S. N. Thibodeau. 2000. "Mutations in AXIN2 cause colorectal cancer with defective mismatch repair by activating beta-catenin/TCF signalling." *Nat Genet* 26 (2):146-7. doi: 10.1038/79859.

Livak, K. J., and T. D. Schmittgen. 2001. "Analysis of relative gene expression data using real-time quantitative PCR and the 2(-Delta Delta C(T)) Method." *Methods* 25 (4):402-8. doi: 10.1006/meth.2001.1262.

Loh, K. M., R. van Amerongen, and R. Nusse. 2016. "Generating Cellular Diversity and Spatial Form: Wnt Signaling and the Evolution of Multicellular Animals." *Dev Cell* 38 (6):643-55. doi: 10.1016/j.devcel.2016.08.011.

Lopez-Garcia, C., A. M. Klein, B. D. Simons, and D. J. Winton. 2010. "Intestinal stem cell replacement follows a pattern of neutral drift." *Science* 330 (6005):822-5. doi: 10.1126/science.1196236.

Loregger, A., M. Grandl, R. Mejias-Luque, M. Allgauer, K. Degenhart, V. Haselmann, C. Oikonomou, P. Hatzis, K. P. Janssen, U. Nitsche, D. Gradl, O. van den Broek, O. Destree, K. Ulm, M. Neumaier, B. Kalali, A. Jung, I. Varela, R. M. Schmid, R. Rad, D. H. Busch, and M. Gerhard. 2015. "The E3 ligase RNF43 inhibits Wnt signaling downstream of mutated beta-catenin by sequestering TCF4 to the nuclear membrane." *Sci Signal* 8 (393):ra90. doi: 10.1126/scisignal.aac6757.

Lustig, B., B. Jerchow, M. Sachs, S. Weiler, T. Pietsch, U. Karsten, M. van de Wetering, H. Clevers, P. M. Schlag, W. Birchmeier, and J. Behrens. 2002. "Negative feedback loop of Wnt signaling through upregulation of conductin/axin2 in colorectal and liver tumors." *Mol Cell Biol* 22 (4):1184-93.

Ma, J. L., L. Zhang, L. M. Brown, J. Y. Li, L. Shen, K. F. Pan, W. D. Liu, Y. Hu, Z. X. Han, S. Crystal-Mansour, D. Pee, W. J. Blot, J. F. Fraumeni, Jr., W. C. You, and M. H. Gail. 2012. "Fifteen-year effects of Helicobacter pylori, garlic, and vitamin treatments on gastric cancer incidence and mortality." *J Natl Cancer Inst* 104 (6):488-92. doi: 10.1093/jnci/djs003.

MacDonald, B. T., K. Tamai, and X. He. 2009. "Wnt/beta-catenin signaling: components, mechanisms, and diseases." *Dev Cell* 17 (1):9-26. doi: 10.1016/j.devcel.2009.06.016.

Madison, B. B., L. Dunbar, X. T. Qiao, K. Braunstein, E. Braunstein, and D. L. Gumucio. 2002. "Cis elements of the villin gene control expression in restricted domains of the vertical (crypt) and horizontal (duodenum, cecum) axes of the intestine." *J Biol Chem* 277 (36):33275-83. doi: 10.1074/jbc.M204935200.

Mailand, N., S. Bekker-Jensen, H. Faustrup, F. Melander, J. Bartek, C. Lukas, and J. Lukas. 2007. "RNF8 ubiquitylates histones at DNA double-strand breaks and promotes assembly of repair proteins." *Cell* 131 (5):887-900. doi: 10.1016/j.cell.2007.09.040.

Majewski, I. J., I. Kluijt, A. Cats, T. S. Scerri, D. de Jong, R. J. Kluin, S. Hansford, F. B. Hogervorst, A. J. Bosma, I. Hofland, M. Winter, D. Huntsman, J. Jonkers, M. Bahlo, and R. Bernards. 2013. "An alpha-E-catenin (CTNNA1) mutation in hereditary diffuse gastric cancer." *J Pathol* 229 (4):621-9. doi: 10.1002/path.4152.

Mankaney, G., P. Leone, M. Cruise, L. LaGuardia, M. O'Malley, A. Bhatt, J. Church, and C. A. Burke. 2017. "Gastric cancer in FAP: a concerning rise in incidence." *Fam Cancer* 16 (3):371-376. doi: 10.1007/s10689-017-9971-3.

Mao, B., W. Wu, Y. Li, D. Hoppe, P. Stannek, A. Glinka, and C. Niehrs. 2001. "LDL-receptor-related protein 6 is a receptor for Dickkopf proteins." *Nature* 411 (6835):321-5. doi: 10.1038/35077108.

Mao, J., J. Wang, B. Liu, W. Pan, G. H. Farr, 3rd, C. Flynn, H. Yuan, S. Takada, D. Kimelman, L. Li, and D. Wu. 2001. "Low-density lipoprotein receptor-related protein-5 binds to Axin and regulates the canonical Wnt signaling pathway." *Mol Cell* 7 (4):801-9.

Markowitz, S. D., and M. M. Bertagnolli. 2009. "Molecular origins of cancer: Molecular basis of colorectal cancer." *N Engl J Med* 361 (25):2449-60. doi: 10.1056/NEJMra0804588.

Masciari, S., A. Dewanwala, E. M. Stoffel, G. Y. Lauwers, H. Zheng, M. I. Achatz, D. Riegert-Johnson, L. Foretova, E. M. Silva, L. Digianni, S. J. Verselis, K. Schneider, F. P. Li, J. Fraumeni, J. E. Garber, and S. Syngal. 2011. "Gastric cancer in individuals with Li-Fraumeni syndrome." *Genet Med* 13 (7):651-7. doi: 10.1097/GIM.0b013e31821628b6.

McCracken, K. W., E. Aihara, B. Martin, C. M. Crawford, T. Broda, J. Treguier, X. Zhang, J. M. Shannon, M. H. Montrose, and J. M. Wells. 2017. "Wnt/beta-catenin promotes gastric fundus specification in mice and humans." *Nature* 541 (7636):182-187. doi: 10.1038/nature21021.

McCrea, P. D., W. M. Brieher, and B. M. Gumbiner. 1993. "Induction of a secondary body axis in Xenopus by antibodies to beta-catenin." *J Cell Biol* 123 (2):477-84.

McDonald, D., G. Carrero, C. Andrin, G. de Vries, and M. J. Hendzel. 2006. "Nucleoplasmic beta-actin exists in a dynamic equilibrium between low-mobility polymeric species and rapidly diffusing populations." *J Cell Biol* 172 (4):541-52. doi: 10.1083/jcb.200507101.

McDuffie, L. A., A. Sabesan, M. Allgaeuer, L. Xin, C. Koh, T. Heller, J. L. Davis, M. Raffeld, M. Miettienen, M. Quezado, and U. Rudloff. 2016. "beta-Catenin activation in fundic gland polyps, gastric cancer and colonic polyps in families afflicted by 'gastric adenocarcinoma and proximal polyposis of the stomach' (GAPPS)." *J Clin Pathol* 69 (9):826-33. doi: 10.1136/jclinpath-2016-203746.

McMahon, A. P., and R. T. Moon. 1989. "Ectopic expression of the proto-oncogene int-1 in Xenopus embryos leads to duplication of the embryonic axis." *Cell* 58 (6):1075-84.

Merino-Azpitarte, M., E. Lozano, M. J. Perugorria, A. Esparza-Baquer, O. Erice, A. Santos-Laso, C. J. O'Rourke, J. B. Andersen, R. Jimenez-Aguero, A. Lacasta, M. D'Amato, O. Briz, N. Jalan-Sakrikar, R. C. Huebert, K. M. Thelen, S. A. Gradilone, A. M. Aransay, J. L. Lavin, M. G. Fernandez-Barrena, A. Matheu, M. Marzioni, G. J. Gores, L. Bujanda, J. J. G. Marin, and J. M. Banales. 2017. "SOX17 regulates cholangiocyte differentiation and acts as a tumor suppressor in cholangiocarcinoma." *J Hepatol* 67 (1):72-83. doi: 10.1016/j.jhep.2017.02.017.

Min, B. H., J. Hwang, N. K. Kim, G. Park, S. Y. Kang, S. Ahn, S. Ahn, S. Y. Ha, Y. K. Lee, R. Kushima, M. Van Vrancken, M. J. Kim, C. Park, H. Y. Park, J. Chae, S. S. Jang, S. J. Kim, Y. H. Kim, J. I. Kim, and K. M. Kim. 2016. "Dysregulated Wnt signalling and recurrent mutations of the tumour suppressor RNF43 in early gastric carcinogenesis." *J Pathol* 240 (3):304-314. doi: 10.1002/path.4777.

Miyaki, M., M. Konishi, R. Kikuchi-Yanoshita, M. Enomoto, T. Igari, K. Tanaka, M. Muraoka, H. Takahashi, Y. Amada, M. Fukayama, and et al. 1994. "Characteristics of somatic mutation of the adenomatous polyposis coli gene in colorectal tumors." *Cancer Res* 54 (11):3011-20.

Miyamoto, K., H. Sakurai, and T. Sugiura. 2008. "Proteomic identification of a PSF/p54nrb heterodimer as RNF43 oncoprotein-interacting proteins." *Proteomics* 8 (14):2907-10. doi: 10.1002/pmic.200800083.

Miyazawa, K., K. Iwaya, M. Kuroda, M. Harada, H. Serizawa, Y. Koyanagi, Y. Sato, Y. Mizokami, T. Matsuoka, and K. Mukai. 2000. "Nuclear accumulation of beta-catenin in intestinal-type gastric carcinoma: correlation with early tumor invasion." *Virchows Arch* 437 (5):508-13.

Molenaar, M., M. van de Wetering, M. Oosterwegel, J. Peterson-Maduro, S. Godsave, V. Korinek, J. Roose, O. Destree, and H. Clevers. 1996. "XTcf-3 transcription factor mediates beta-catenin-induced axis formation in Xenopus embryos." *Cell* 86 (3):391-9.

Morin, P. J., A. B. Sparks, V. Korinek, N. Barker, H. Clevers, B. Vogelstein, and K. W. Kinzler. 1997. "Activation of beta-catenin-Tcf signaling in colon cancer by mutations in beta-catenin or APC." *Science* 275 (5307):1787-90.

Moser, A. R., H. C. Pitot, and W. F. Dove. 1990. "A dominant mutation that predisposes to multiple intestinal neoplasia in the mouse." *Science* 247 (4940):322-4.

Motoyama, T., H. Hojo, and H. Watanabe. 1986. "Comparison of seven cell lines derived from human gastric carcinomas." *Acta Pathol Jpn* 36 (1):65-83.

Muncan, V., O. J. Sansom, L. Tertoolen, T. J. Phesse, H. Begthel, E. Sancho, A. M. Cole, A. Gregorieff, I. M. de Alboran, H. Clevers, and A. R. Clarke. 2006. "Rapid loss of intestinal crypts upon conditional deletion of the Wnt/Tcf-4 target gene c-Myc." *Mol Cell Biol* 26 (22):8418-26. doi: 10.1128/MCB.00821-06.

Murata-Kamiya, N., Y. Kurashima, Y. Teishikata, Y. Yamahashi, Y. Saito, H. Higashi, H. Aburatani, T. Akiyama, R. M. Peek, Jr., T. Azuma, and M. Hatakeyama. 2007. "Helicobacter pylori CagA interacts with E-cadherin and deregulates the beta-catenin signal that promotes intestinal transdifferentiation in gastric epithelial cells." *Oncogene* 26 (32):4617-26. doi: 10.1038/sj.onc.1210251.

Nailwal, H., S. Sharma, A. K. Mayank, and S. K. Lal. 2015. "The nucleoprotein of influenza A virus induces p53 signaling and apoptosis via attenuation of host ubiquitin ligase RNF43." *Cell Death Dis* 6:e1768. doi: 10.1038/cddis.2015.131.

Nakada, S. 2016. "Opposing roles of RNF8/RNF168 and deubiquitinating enzymes in ubiquitination-dependent DNA double-strand break response signaling and DNA-repair pathway choice." *J Radiat Res* 57 Suppl 1:i33-i40. doi: 10.1093/jrr/rrw027.

Niehrs, C. 2004. "Norrin and frizzled; a new vein for the eye." *Dev Cell* 6 (4):453-4.

Niehrs, C., and S. P. Acebron. 2012. "Mitotic and mitogenic Wnt signalling." *EMBO J* 31 (12):2705-13. doi: 10.1038/emboj.2012.124.

Niu, L., H. Z. Qin, H. Q. Xi, B. Wei, S. Y. Xia, and L. Chen. 2015. "RNF43 Inhibits Cancer Cell Proliferation and Could be a Potential Prognostic Factor for Human Gastric Carcinoma." *Cell Physiol Biochem* 36 (5):1835-46. doi: 10.1159/000430154.

Nojima, M., H. Suzuki, M. Toyota, Y. Watanabe, R. Maruyama, S. Sasaki, Y. Sasaki, H. Mita, N. Nishikawa, K. Yamaguchi, K. Hirata, F. Itoh, T. Tokino, M. Mori, K. Imai, and Y. Shinomura. 2007. "Frequent epigenetic inactivation of SFRP genes and constitutive activation of Wnt signaling in gastric cancer." *Oncogene* 26 (32):4699-713. doi: 10.1038/sj.onc.1210259.

Nusse, R., A. Brown, J. Papkoff, P. Scambler, G. Shackleford, A. McMahon, R. Moon, and H. Varmus. 1991. "A new nomenclature for int-1 and related genes: the Wnt gene family." *Cell* 64 (2):231.

Nusse, R., and H. Varmus. 2012. "Three decades of Wnts: a personal perspective on how a scientific field developed." *EMBO J* 31 (12):2670-84. doi: 10.1038/emboj.2012.146.

Nusse, R., and H. E. Varmus. 1982. "Many tumors induced by the mouse mammary tumor virus contain a provirus integrated in the same region of the host genome." *Cell* 31 (1):99-109.

Nusse, Roel. 2018. https://web.stanford.edu/group/nusselab/cgi-bin/wnt/reporters; accessed Jan 23rd 2018.

Odenbreit, S., J. Puls, B. Sedlmaier, E. Gerland, W. Fischer, and R. Haas. 2000. "Translocation of Helicobacter pylori CagA into gastric epithelial cells by type IV secretion." *Science* 287 (5457):1497-500.

Ogasawara, N., T. Tsukamoto, T. Mizoshita, K. Inada, X. Cao, Y. Takenaka, T. Joh, and M. Tatematsu. 2006. "Mutations and nuclear accumulation of beta-catenin correlate with intestinal phenotypic expression in human gastric cancer." *Histopathology* 49 (6):612-21. doi: 10.1111/j.1365-2559.2006.02560.x.

Ohnishi, N., H. Yuasa, S. Tanaka, H. Sawa, M. Miura, A. Matsui, H. Higashi, M. Musashi, K. Iwabuchi, M. Suzuki, G. Yamada, T. Azuma, and M. Hatakeyama. 2008. "Transgenic expression of Helicobacter pylori CagA induces gastrointestinal and hematopoietic neoplasms in mouse." *Proc Natl Acad Sci U S A* 105 (3):1003-8. doi: 10.1073/pnas.0711183105.

Olave, I. A., S. L. Reck-Peterson, and G. R. Crabtree. 2002. "Nuclear actin and actin-related proteins in chromatin remodeling." *Annu Rev Biochem* 71:755-81. doi: 10.1146/annurev.biochem.71.110601.135507.

OMIM. 2017. "612482 (RNF43); https://www.omim.org; accessed 13th Feb 2018."

Ong, C. K., C. Subimerb, C. Pairojkul, S. Wongkham, I. Cutcutache, W. Yu, J. R. McPherson, G. E. Allen, C. C. Ng, B. H. Wong, S. S. Myint, V. Rajasegaran, H. L. Heng, A. Gan, Z. J. Zang, Y. Wu, J. Wu, M. H. Lee, D. Huang, P. Ong, W. Chan-on, Y. Cao, C. N. Qian, K. H. Lim, A. Ooi, K. Dykema, K. Furge, V. Kukongviriyapan, B. Sripa, C. Wongkham, P. Yongvanit, P. A. Futreal, V. Bhudhisawasdi, S. Rozen, P. Tan, and B. T. Teh. 2012. "Exome sequencing of liver fluke-associated cholangiocarcinoma." *Nat Genet* 44 (6):690-3. doi: 10.1038/ng.2273.

Orford, K., C. Crockett, J. P. Jensen, A. M. Weissman, and S. W. Byers. 1997. "Serine phosphorylation-regulated ubiquitination and degradation of beta-catenin." *J Biol Chem* 272 (40):24735-8.

Oshima, H., A. Matsunaga, T. Fujimura, T. Tsukamoto, M. M. Taketo, and M. Oshima. 2006. "Carcinogenesis in mouse stomach by simultaneous activation of the Wnt signaling and prostaglandin E2 pathway." *Gastroenterology* 131 (4):1086-95. doi: 10.1053/j.gastro.2006.07.014.

Ozawa, M., H. Baribault, and R. Kemler. 1989. "The cytoplasmic domain of the cell adhesion molecule uvomorulin associates with three independent proteins structurally related in different species." *EMBO J* 8 (6):1711-7.

Paoni, N. F., M. W. Feldman, L. S. Gutierrez, V. A. Ploplis, and F. J. Castellino. 2003. "Transcriptional profiling of the transition from normal intestinal epithelia to adenomas and carcinomas in the APCMin/+ mouse." *Physiol Genomics* 15 (3):228-35. doi: 10.1152/physiolgenomics.00078.2003.

Park, J. G., H. Frucht, R. V. LaRocca, D. P. Bliss, Jr., Y. Kurita, T. R. Chen, J. G. Henslee, J. B. Trepel, R. T. Jensen, B. E. Johnson, and et al. 1990. "Characteristics of cell lines established from human gastric carcinoma." *Cancer Res* 50 (9):2773-80.

Park, K. S., J. M. Wells, A. M. Zorn, S. E. Wert, and J. A. Whitsett. 2006. "Sox17 influences the differentiation of respiratory epithelial cells." *Dev Biol* 294 (1):192-202. doi: 10.1016/j.ydbio.2006.02.038.

Park, W. S., R. R. Oh, J. Y. Park, S. H. Lee, M. S. Shin, Y. S. Kim, S. Y. Kim, H. K. Lee, P. J. Kim, S. T. Oh, N. J. Yoo, and J. Y. Lee. 1999. "Frequent somatic mutations of the beta-catenin gene in intestinal-type gastric cancer." *Cancer Res* 59 (17):4257-60.

Peifer, M., L. M. Pai, and M. Casey. 1994. "Phosphorylation of the Drosophila adherens junction protein Armadillo: roles for wingless signal and zeste-white 3 kinase." *Dev Biol* 166 (2):543-56. doi: 10.1006/dbio.1994.1336.

Pilati, C., E. Letouze, J. C. Nault, S. Imbeaud, A. Boulai, J. Calderaro, K. Poussin, A. Franconi, G. Couchy, G. Morcrette, M. Mallet, S. Taouji, C. Balabaud, B. Terris, F. Canal, V. Paradis, J. Y. Scoazec, A. de Muret, C. Guettier, P. Bioulac-Sage, E. Chevet, F. Calvo, and J. Zucman-Rossi. 2014. "Genomic profiling of hepatocellular adenomas reveals recurrent FRK-activating mutations and the mechanisms of malignant transformation." *Cancer Cell* 25 (4):428-41. doi: 10.1016/j.ccr.2014.03.005.

Pinto, D., A. Gregorieff, H. Begthel, and H. Clevers. 2003. "Canonical Wnt signals are essential for homeostasis of the intestinal epithelium." *Genes Dev* 17 (14):1709-13. doi: 10.1101/gad.267103.

Pinto, D., S. Robine, F. Jaisser, F. E. El Marjou, and D. Louvard. 1999. "Regulatory sequences of the mouse villin gene that efficiently drive transgenic expression in immature and differentiated epithelial cells of small and large intestines." *J Biol Chem* 274 (10):6476-82.

Plummer, M., S. Franceschi, J. Vignat, D. Forman, and C. de Martel. 2015. "Global burden of gastric cancer attributable to Helicobacter pylori." *Int J Cancer* 136 (2):487-90. doi: 10.1002/ijc.28999.

Plummer, M., L. J. van Doorn, S. Franceschi, B. Kleter, F. Canzian, J. Vivas, G. Lopez, D. Colin, N. Munoz, and I. Kato. 2007. "Helicobacter pylori cytotoxin-associated genotype and gastric precancerous lesions." *J Natl Cancer Inst* 99 (17):1328-34. doi: 10.1093/jnci/djm120.

Proffitt, K. D., B. Madan, Z. Ke, V. Pendharkar, L. Ding, M. A. Lee, R. N. Hannoush, and D. M. Virshup. 2013. "Pharmacological inhibition of the Wnt acyltransferase

PORCN prevents growth of WNT-driven mammary cancer." *Cancer Res* 73 (2):502-7. doi: 10.1158/0008-5472.CAN-12-2258.

Qian, D., C. Jones, A. Rzadzinska, S. Mark, X. Zhang, K. P. Steel, X. Dai, and P. Chen. 2007. "Wnt5a functions in planar cell polarity regulation in mice." *Dev Biol* 306 (1):121-33. doi: 10.1016/j.ydbio.2007.03.011.

Quintana, I., R. Mejias-Luque, M. Terradas, M. Navarro, V. Pinol, P. Mur, S. Belhadj, E. Grau, E. Darder, A. Solanes, J. Brunet, G. Capella, M. Gerhard, and L. Valle. 2018. "Evidence suggests that germline RNF43 mutations are a rare cause of serrated polyposis." *Gut*. doi: 10.1136/gutjnl-2017-315733.

Riggleman, B., P. Schedl, and E. Wieschaus. 1990. "Spatial expression of the Drosophila segment polarity gene armadillo is posttranscriptionally regulated by wingless." *Cell* 63 (3):549-60.

Rubinfeld, B., I. Albert, E. Porfiri, C. Fiol, S. Munemitsu, and P. Polakis. 1996. "Binding of GSK3beta to the APC-beta-catenin complex and regulation of complex assembly." *Science* 272 (5264):1023-6.

Rubinfeld, B., B. Souza, I. Albert, O. Muller, S. H. Chamberlain, F. R. Masiarz, S. Munemitsu, and P. Polakis. 1993. "Association of the APC gene product with beta-catenin." *Science* 262 (5140):1731-4.

Rugge, M., R. M. Genta, D. Y. Graham, F. Di Mario, L. G. Vaz Coelho, N. Kim, P. Malfertheiner, K. Sugano, V. Tsukanov, and P. Correa. 2016. "Chronicles of a cancer foretold: 35 years of gastric cancer risk assessment." *Gut* 65 (5):721-5. doi: 10.1136/gutjnl-2015-310846.

Ryland, G. L., S. M. Hunter, M. A. Doyle, S. M. Rowley, M. Christie, P. E. Allan, D. D. Bowtell, Group Australian Ovarian Cancer Study, K. L. Gorringe, and I. G. Campbell. 2013. "RNF43 is a tumour suppressor gene mutated in mucinous tumours of the ovary." *J Pathol* 229 (3):469-76. doi: 10.1002/path.4134.

Sakamoto, H., Y. Kuboki, T. Hatori, M. Yamamoto, M. Sugiyama, N. Shibata, K. Shimizu, K. Shiratori, and T. Furukawa. 2015. "Clinicopathological significance of somatic RNF43 mutation and aberrant expression of ring finger protein 43 in intraductal papillary mucinous neoplasms of the pancreas." *Mod Pathol* 28 (2):261-7. doi: 10.1038/modpathol.2014.98.

Sakamoto, Y., K. Hara, M. Kanai-Azuma, T. Matsui, Y. Miura, N. Tsunekawa, M. Kurohmaru, Y. Saijoh, P. Koopman, and Y. Kanai. 2007. "Redundant roles of Sox17 and Sox18 in early cardiovascular development of mouse embryos." *Biochem Biophys Res Commun* 360 (3):539-44. doi: 10.1016/j.bbrc.2007.06.093.

Sangiorgi, E., and M. R. Capecchi. 2008. "Bmi1 is expressed in vivo in intestinal stem cells." *Nat Genet* 40 (7):915-20. doi: 10.1038/ng.165.

Sansom, O. J., K. R. Reed, A. J. Hayes, H. Ireland, H. Brinkmann, I. P. Newton, E. Batlle, P. Simon-Assmann, H. Clevers, I. S. Nathke, A. R. Clarke, and D. J. Winton. 2004. "Loss of Apc in vivo immediately perturbs Wnt signaling, differentiation, and migration." *Genes Dev* 18 (12):1385-90. doi: 10.1101/gad.287404.

Sato, T., J. H. van Es, H. J. Snippert, D. E. Stange, R. G. Vries, M. van den Born, N. Barker, N. F. Shroyer, M. van de Wetering, and H. Clevers. 2011. "Paneth cells constitute the niche for Lgr5 stem cells in intestinal crypts." *Nature* 469 (7330):415-8. doi: 10.1038/nature09637.

Sato, T., R. G. Vries, H. J. Snippert, M. van de Wetering, N. Barker, D. E. Stange, J. H. van Es, A. Abo, P. Kujala, P. J. Peters, and H. Clevers. 2009. "Single Lgr5 stem cells build crypt-villus structures in vitro without a mesenchymal niche." *Nature* 459 (7244):262-5. doi: 10.1038/nature07935.

Scarpa, A., D. K. Chang, K. Nones, V. Corbo, A. M. Patch, P. Bailey, R. T. Lawlor, A. L. Johns, D. K. Miller, A. Mafficini, B. Rusev, M. Scardoni, D. Antonello, S.

Barbi, K. O. Sikora, S. Cingarlini, C. Vicentini, S. McKay, M. C. Quinn, T. J. Bruxner, A. N. Christ, I. Harliwong, S. Idrisoglu, S. McLean, C. Nourse, E. Nourbakhsh, P. J. Wilson, M. J. Anderson, J. L. Fink, F. Newell, N. Waddell, O. Holmes, S. H. Kazakoff, C. Leonard, S. Wood, Q. Xu, S. H. Nagaraj, E. Amato, I. Dalai, S. Bersani, I. Cataldo, A. P. Dei Tos, P. Capelli, M. V. Davi, L. Landoni, A. Malpaga, M. Miotto, V. L. Whitehall, B. A. Leggett, J. L. Harris, J. Harris, M. D. Jones, J. Humphris, L. A. Chantrill, V. Chin, A. M. Nagrial, M. Pajic, C. J. Scarlett, A. Pinho, I. Rooman, C. Toon, J. Wu, M. Pinese, M. Cowley, A. Barbour, A. Mawson, E. S. Humphrey, E. K. Colvin, A. Chou, J. A. Lovell, N. B. Jamieson, F. Duthie, M. C. Gingras, W. E. Fisher, R. A. Dagg, L. M. Lau, M. Lee, H. A. Pickett, R. R. Reddel, J. S. Samra, J. G. Kench, N. D. Merrett, K. Epari, N. Q. Nguyen, N. Zeps, M. Falconi, M. Simbolo, G. Butturini, G. Van Buren, S. Partelli, M. Fassan, Initiative Australian Pancreatic Cancer Genome, K. K. Khanna, A. J. Gill, D. A. Wheeler, R. A. Gibbs, E. A. Musgrove, C. Bassi, G. Tortora, P. Pederzoli, J. V. Pearson, N. Waddell, A. V. Biankin, and S. M. Grimmond. 2017. "Whole-genome landscape of pancreatic neuroendocrine tumours." *Nature* 543 (7643):65-71. doi: 10.1038/nature21063.

Schneider, M. R., M. Dahlhoff, D. Horst, B. Hirschi, K. Trulzsch, J. Muller-Hocker, R. Vogelmann, M. Allgauer, M. Gerhard, S. Steininger, E. Wolf, and F. T. Kolligs. 2010. "A key role for E-cadherin in intestinal homeostasis and Paneth cell maturation." *PLoS One* 5 (12):e14325. doi: 10.1371/journal.pone.0014325.

Schuijers, J., L. G. van der Flier, J. van Es, and H. Clevers. 2014. "Robust cre-mediated recombination in small intestinal stem cells utilizing the olfm4 locus." *Stem Cell Reports* 3 (2):234-41. doi: 10.1016/j.stemcr.2014.05.018.

Schulze, K., S. Imbeaud, E. Letouze, L. B. Alexandrov, J. Calderaro, S. Rebouissou, G. Couchy, C. Meiller, J. Shinde, F. Soysouvanh, A. L. Calatayud, R. Pinyol, L. Pelletier, C. Balabaud, A. Laurent, J. F. Blanc, V. Mazzaferro, F. Calvo, A. Villanueva, J. C. Nault, P. Bioulac-Sage, M. R. Stratton, J. M. Llovet, and J. Zucman-Rossi. 2015. "Exome sequencing of hepatocellular carcinomas identifies new mutational signatures and potential therapeutic targets." *Nat Genet* 47 (5):505-511. doi: 10.1038/ng.3252.

Sekiguchi, M., K. Sakakibara, and G. Fujii. 1978. "Establishment of cultured cell lines derived from a human gastric carcinoma." *Jpn J Exp Med* 48 (1):61-8.

Seshagiri, S., E. W. Stawiski, S. Durinck, Z. Modrusan, E. E. Storm, C. B. Conboy, S. Chaudhuri, Y. Guan, V. Janakiraman, B. S. Jaiswal, J. Guillory, C. Ha, G. J. Dijkgraaf, J. Stinson, F. Gnad, M. A. Huntley, J. D. Degenhardt, P. M. Haverty, R. Bourgon, W. Wang, H. Koeppen, R. Gentleman, T. K. Starr, Z. Zhang, D. A. Largaespada, T. D. Wu, and F. J. de Sauvage. 2012. "Recurrent R-spondin fusions in colon cancer." *Nature* 488 (7413):660-4. doi: 10.1038/nature11282.

Sharma, R. P., and V. L. Chopra. 1976. "Effect of the Wingless (wg1) mutation on wing and haltere development in Drosophila melanogaster." *Dev Biol* 48 (2):461-5.

Shinada, K., T. Tsukiyama, T. Sho, F. Okumura, M. Asaka, and S. Hatakeyama. 2011. "RNF43 interacts with NEDL1 and regulates p53-mediated transcription." *Biochem Biophys Res Commun* 404 (1):143-7. doi: 10.1016/j.bbrc.2010.11.082.

Shkoda, A., P. A. Ruiz, H. Daniel, S. C. Kim, G. Rogler, R. B. Sartor, and D. Haller. 2007. "Interleukin-10 blocked endoplasmic reticulum stress in intestinal epithelial cells: impact on chronic inflammation." *Gastroenterology* 132 (1):190-207. doi: 10.1053/j.gastro.2006.10.030.

Siegfried, E., T. B. Chou, and N. Perrimon. 1992. "wingless signaling acts through zeste-white 3, the Drosophila homolog of glycogen synthase kinase-3, to regulate engrailed and establish cell fate." *Cell* 71 (7):1167-79.

Sinner, D., J. J. Kordich, J. R. Spence, R. Opoka, S. Rankin, S. C. Lin, D. Jonatan, A. M. Zorn, and J. M. Wells. 2007. "Sox17 and Sox4 differentially regulate beta-catenin/T-cell factor activity and proliferation of colon carcinoma cells." *Mol Cell Biol* 27 (22):7802-15. doi: 10.1128/MCB.02179-06.

Sinner, D., S. Rankin, M. Lee, and A. M. Zorn. 2004. "Sox17 and beta-catenin cooperate to regulate the transcription of endodermal genes." *Development* 131 (13):3069-80. doi: 10.1242/dev.01176.

Smalley-Freed, W. G., A. Efimov, P. E. Burnett, S. P. Short, M. A. Davis, D. L. Gumucio, M. K. Washington, R. J. Coffey, and A. B. Reynolds. 2010. "p120-catenin is essential for maintenance of barrier function and intestinal homeostasis in mice." *J Clin Invest* 120 (6):1824-35. doi: 10.1172/JCI41414.

Smyth, E. C., M. Verheij, W. Allum, D. Cunningham, A. Cervantes, D. Arnold, and Esmo Guidelines Committee. 2016. "Gastric cancer: ESMO Clinical Practice Guidelines for diagnosis, treatment and follow-up." *Ann Oncol* 27 (suppl 5):v38-v49. doi: 10.1093/annonc/mdw350.

Snippert, H. J., L. G. van der Flier, T. Sato, J. H. van Es, M. van den Born, C. Kroon-Veenboer, N. Barker, A. M. Klein, J. van Rheenen, B. D. Simons, and H. Clevers. 2010. "Intestinal crypt homeostasis results from neutral competition between symmetrically dividing Lgr5 stem cells." *Cell* 143 (1):134-44. doi: 10.1016/j.cell.2010.09.016.

Song, Y., L. Li, Y. Ou, Z. Gao, E. Li, X. Li, W. Zhang, J. Wang, L. Xu, Y. Zhou, X. Ma, L. Liu, Z. Zhao, X. Huang, J. Fan, L. Dong, G. Chen, L. Ma, J. Yang, L. Chen, M. He, M. Li, X. Zhuang, K. Huang, K. Qiu, G. Yin, G. Guo, Q. Feng, P. Chen, Z. Wu, J. Wu, L. Ma, J. Zhao, L. Luo, M. Fu, B. Xu, B. Chen, Y. Li, T. Tong, M. Wang, Z. Liu, D. Lin, X. Zhang, H. Yang, J. Wang, and Q. Zhan. 2014. "Identification of genomic alterations in oesophageal squamous cell cancer." *Nature* 509 (7498):91-5. doi: 10.1038/nature13176.

Spence, J. R., A. W. Lange, S. C. Lin, K. H. Kaestner, A. M. Lowy, I. Kim, J. A. Whitsett, and J. M. Wells. 2009. "Sox17 regulates organ lineage segregation of ventral foregut progenitor cells." *Dev Cell* 17 (1):62-74. doi: 10.1016/j.devcel.2009.05.012.

Stevens, C. E., and C. P. Leblond. 1947. "Rate of renewal of the cells of the intestinal epithelium in the rat." *Anat Rec* 97 (3):373.

Stewart, BW, and CP Wild. 2015. *World Cancer Report 2014*: Lyon: International Agency for Research on Cancer.

Su, L. K., B. Vogelstein, and K. W. Kinzler. 1993. "Association of the APC tumor suppressor protein with catenins." *Science* 262 (5140):1734-7.

Suarez, M. I., D. Uribe, C. M. Jaramillo, G. Osorio, J. C. Perez, R. Lopez, S. Hoyos, P. Hainaut, P. Pineau, and M. C. Navas. 2015. "Wnt/beta-catenin signaling pathway in hepatocellular carcinomas cases from Colombia." *Ann Hepatol* 14 (1):64-74.

Sugiura, T., A. Yamaguchi, and K. Miyamoto. 2008. "A cancer-associated RING finger protein, RNF43, is a ubiquitin ligase that interacts with a nuclear protein, HAP95." *Exp Cell Res* 314 (7):1519-28. doi: 10.1016/j.yexcr.2008.01.013.

Tahara, E. 2004. "Genetic pathways of two types of gastric cancer." *IARC Sci Publ* (157):327-49.

Takagi, Y., C. A. Masuda, W. H. Chang, H. Komori, D. Wang, T. Hunter, C. A. Joazeiro, and R. D. Kornberg. 2005. "Ubiquitin ligase activity of TFIIH and the transcriptional response to DNA damage." *Mol Cell* 18 (2):237-43. doi: 10.1016/j.molcel.2005.03.007.

Takahashi, N., K. Yamaguchi, T. Ikenoue, T. Fujii, and Y. Furukawa. 2014. "Identification of two Wnt-responsive elements in the intron of RING finger

protein 43 (RNF43) gene." *PLoS One* 9 (1):e86582. doi: 10.1371/journal.pone.0086582.

Takeda, N., R. Jain, M. R. LeBoeuf, Q. Wang, M. M. Lu, and J. A. Epstein. 2011. "Interconversion between intestinal stem cell populations in distinct niches." *Science* 334 (6061):1420-4. doi: 10.1126/science.1213214.

Taupin, D., W. Lam, D. Rangiah, L. McCallum, B. Whittle, Y. Zhang, D. Andrews, M. Field, C. C. Goodnow, and M. C. Cook. 2015. "A deleterious RNF43 germline mutation in a severely affected serrated polyposis kindred." *Hum Genome Var* 2:15013. doi: 10.1038/hgv.2015.13.

TheEUROGAST-StudyGroup. 1993. "Epidemiology of, and risk factors for, Helicobacter pylori infection among 3194 asymptomatic subjects in 17 populations. The EUROGAST Study Group." *Gut* 34 (12):1672-6.

Thompson, C. A., A. DeLaForest, and M. A. Battle. 2018. "Patterning the gastrointestinal epithelium to confer regional-specific functions." *Dev Biol*. doi: 10.1016/j.ydbio.2018.01.006.

Thrasivoulou, C., M. Millar, and A. Ahmed. 2013. "Activation of intracellular calcium by multiple Wnt ligands and translocation of beta-catenin into the nucleus: a convergent model of Wnt/Ca2+ and Wnt/beta-catenin pathways." *J Biol Chem* 288 (50):35651-9. doi: 10.1074/jbc.M112.437913.

Tian, H., B. Biehs, S. Warming, K. G. Leong, L. Rangell, O. D. Klein, and F. J. de Sauvage. 2011. "A reserve stem cell population in small intestine renders Lgr5-positive cells dispensable." *Nature* 478 (7368):255-9. doi: 10.1038/nature10408.

Torre, L. A., R. L. Siegel, E. M. Ward, and A. Jemal. 2016. "Global Cancer Incidence and Mortality Rates and Trends--An Update." *Cancer Epidemiol Biomarkers Prev* 25 (1):16-27. doi: 10.1158/1055-9965.EPI-15-0578.

Treton, X., E. Pedruzzi, D. Cazals-Hatem, A. Grodet, Y. Panis, A. Groyer, R. Moreau, Y. Bouhnik, F. Daniel, and E. Ogier-Denis. 2011. "Altered endoplasmic reticulum stress affects translation in inactive colon tissue from patients with ulcerative colitis." *Gastroenterology* 141 (3):1024-35. doi: 10.1053/j.gastro.2011.05.033.

Tsai, J. H., J. Y. Liau, C. T. Yuan, Y. L. Lin, L. H. Tseng, M. L. Cheng, and Y. M. Jeng. 2016. "RNF43 Is an Early and Specific Mutated Gene in the Serrated Pathway, With Increased Frequency in Traditional Serrated Adenoma and Its Associated Malignancy." *Am J Surg Pathol* 40 (10):1352-9. doi: 10.1097/PAS.0000000000000664.

Tsugane, S. 2005. "Salt, salted food intake, and risk of gastric cancer: epidemiologic evidence." *Cancer Sci* 96 (1):1-6. doi: 10.1111/j.1349-7006.2005.00006.x.

Uhlen, M., L. Fagerberg, B. M. Hallstrom, C. Lindskog, P. Oksvold, A. Mardinoglu, A. Sivertsson, C. Kampf, E. Sjostedt, A. Asplund, I. Olsson, K. Edlund, E. Lundberg, S. Navani, C. A. Szigyarto, J. Odeberg, D. Djureinovic, J. O. Takanen, S. Hober, T. Alm, P. H. Edqvist, H. Berling, H. Tegel, J. Mulder, J. Rockberg, P. Nilsson, J. M. Schwenk, M. Hamsten, K. von Feilitzen, M. Forsberg, L. Persson, F. Johansson, M. Zwahlen, G. von Heijne, J. Nielsen, and F. Ponten. 2015. "Proteomics. Tissue-based map of the human proteome." *Science* 347 (6220):1260419. doi: 10.1126/science.1260419.

UniProtKB. 2017. "Q68DV7 (RNF43_HUMAN); http://www.uniprot.org; accessed 14th Feb 2018."

van Amerongen, R., C. Fuerer, M. Mizutani, and R. Nusse. 2012. "Wnt5a can both activate and repress Wnt/beta-catenin signaling during mouse embryonic development." *Dev Biol* 369 (1):101-14. doi: 10.1016/j.ydbio.2012.06.020.

van Amerongen, R., and R. Nusse. 2009. "Towards an integrated view of Wnt signaling in development." *Development* 136 (19):3205-14. doi: 10.1242/dev.033910.

van de Wetering, M., R. Cavallo, D. Dooijes, M. van Beest, J. van Es, J. Loureiro, A. Ypma, D. Hursh, T. Jones, A. Bejsovec, M. Peifer, M. Mortin, and H. Clevers. 1997. "Armadillo coactivates transcription driven by the product of the Drosophila segment polarity gene dTCF." *Cell* 88 (6):789-99.

van de Wetering, M., E. Sancho, C. Verweij, W. de Lau, I. Oving, A. Hurlstone, K. van der Horn, E. Batlle, D. Coudreuse, A. P. Haramis, M. Tjon-Pon-Fong, P. Moerer, M. van den Born, G. Soete, S. Pals, M. Eilers, R. Medema, and H. Clevers. 2002. "The beta-catenin/TCF-4 complex imposes a crypt progenitor phenotype on colorectal cancer cells." *Cell* 111 (2):241-50.

van der Flier, L. G., A. Haegebarth, D. E. Stange, M. van de Wetering, and H. Clevers. 2009. "OLFM4 is a robust marker for stem cells in human intestine and marks a subset of colorectal cancer cells." *Gastroenterology* 137 (1):15-7. doi: 10.1053/j.gastro.2009.05.035.

Van der Flier, L. G., J. Sabates-Bellver, I. Oving, A. Haegebarth, M. De Palo, M. Anti, M. E. Van Gijn, S. Suijkerbuijk, M. Van de Wetering, G. Marra, and H. Clevers. 2007. "The Intestinal Wnt/TCF Signature." *Gastroenterology* 132 (2):628-32. doi: 10.1053/j.gastro.2006.08.039.

van der Flier, L. G., M. E. van Gijn, P. Hatzis, P. Kujala, A. Haegebarth, D. E. Stange, H. Begthel, M. van den Born, V. Guryev, I. Oving, J. H. van Es, N. Barker, P. J. Peters, M. van de Wetering, and H. Clevers. 2009. "Transcription factor achaete scute-like 2 controls intestinal stem cell fate." *Cell* 136 (5):903-12. doi: 10.1016/j.cell.2009.01.031.

van Es, J. H., A. Haegebarth, P. Kujala, S. Itzkovitz, B. K. Koo, S. F. Boj, J. Korving, M. van den Born, A. van Oudenaarden, S. Robine, and H. Clevers. 2012. "A critical role for the Wnt effector Tcf4 in adult intestinal homeostatic self-renewal." *Mol Cell Biol* 32 (10):1918-27. doi: 10.1128/MCB.06288-11.

van Es, J. H., P. Jay, A. Gregorieff, M. E. van Gijn, S. Jonkheer, P. Hatzis, A. Thiele, M. van den Born, H. Begthel, T. Brabletz, M. M. Taketo, and H. Clevers. 2005. "Wnt signalling induces maturation of Paneth cells in intestinal crypts." *Nat Cell Biol* 7 (4):381-6. doi: 10.1038/ncb1240.

van Es, J. H., T. Sato, M. van de Wetering, A. Lyubimova, A. N. Yee Nee, A. Gregorieff, N. Sasaki, L. Zeinstra, M. van den Born, J. Korving, A. C. M. Martens, N. Barker, A. van Oudenaarden, and H. Clevers. 2012. "Dll1+ secretory progenitor cells revert to stem cells upon crypt damage." *Nat Cell Biol* 14 (10):1099-1104. doi: 10.1038/ncb2581.

van Ooyen, A., V. Kwee, and R. Nusse. 1985. "The nucleotide sequence of the human int-1 mammary oncogene; evolutionary conservation of coding and non-coding sequences." *EMBO J* 4 (11):2905-9.

Veeman, M. T., J. D. Axelrod, and R. T. Moon. 2003. "A second canon. Functions and mechanisms of beta-catenin-independent Wnt signaling." *Dev Cell* 5 (3):367-77.

Verzi, M. P., and R. A. Shivdasani. 2008. "Wnt signaling in gut organogenesis." *Organogenesis* 4 (2):87-91.

Vollmers, H. P., K. Stulle, J. Dammrich, M. Pfaff, T. Papadopoulos, C. Betz, K. Saal, and H. K. Muller-Hermelink. 1993. "Characterization of four new gastric cancer cell lines." *Virchows Arch B Cell Pathol Incl Mol Pathol* 63 (6):335-43.

Voorham, Q. J., J. Janssen, M. Tijssen, S. Snellenberg, S. Mongera, N. C. van Grieken, H. Grabsch, M. Kliment, B. J. Rembacken, C. J. Mulder, M. van Engeland, G. A. Meijer, R. D. Steenbergen, and B. Carvalho. 2013. "Promoter methylation of Wnt-antagonists in polypoid and nonpolypoid colorectal adenomas." *BMC Cancer* 13:603. doi: 10.1186/1471-2407-13-603.

Waldschmitt, N., E. Berger, E. Rath, R. B. Sartor, B. Weigmann, M. Heikenwalder, M. Gerhard, K. P. Janssen, and D. Haller. 2014. "C/EBP homologous protein inhibits tissue repair in response to gut injury and is inversely regulated with chronic inflammation." *Mucosal Immunol* 7 (6):1452-66. doi: 10.1038/mi.2014.34.

Wang, K., J. Kan, S. T. Yuen, S. T. Shi, K. M. Chu, S. Law, T. L. Chan, Z. Kan, A. S. Chan, W. Y. Tsui, S. P. Lee, S. L. Ho, A. K. Chan, G. H. Cheng, P. C. Roberts, P. A. Rejto, N. W. Gibson, D. J. Pocalyko, M. Mao, J. Xu, and S. Y. Leung. 2011. "Exome sequencing identifies frequent mutation of ARID1A in molecular subtypes of gastric cancer." *Nat Genet* 43 (12):1219-23. doi: 10.1038/ng.982.

Wang, K., S. T. Yuen, J. Xu, S. P. Lee, H. H. Yan, S. T. Shi, H. C. Siu, S. Deng, K. M. Chu, S. Law, K. H. Chan, A. S. Chan, W. Y. Tsui, S. L. Ho, A. K. Chan, J. L. Man, V. Foglizzo, M. K. Ng, A. S. Chan, Y. P. Ching, G. H. Cheng, T. Xie, J. Fernandez, V. S. Li, H. Clevers, P. A. Rejto, M. Mao, and S. Y. Leung. 2014. "Whole-genome sequencing and comprehensive molecular profiling identify new driver mutations in gastric cancer." *Nat Genet* 46 (6):573-82. doi: 10.1038/ng.2983.

Ward, M. H., and L. Lopez-Carrillo. 1999. "Dietary factors and the risk of gastric cancer in Mexico City." *Am J Epidemiol* 149 (10):925-32.

Wehrli, M., S. T. Dougan, K. Caldwell, L. O'Keefe, S. Schwartz, D. Vaizel-Ohayon, E. Schejter, A. Tomlinson, and S. DiNardo. 2000. "arrow encodes an LDL-receptor-related protein essential for Wingless signalling." *Nature* 407 (6803):527-30. doi: 10.1038/35035110.

Weissferdt, A., J. Rodriguez-Canales, H. Liu, J. Fujimoto, Wistuba, II, and C. A. Moran. 2015. "Primary mediastinal seminomas: a comprehensive immunohistochemical study with a focus on novel markers." *Hum Pathol* 46 (3):376-83. doi: 10.1016/j.humpath.2014.11.009.

Wells, J. M., and D. A. Melton. 1999. "Vertebrate endoderm development." *Annu Rev Cell Dev Biol* 15:393-410. doi: 10.1146/annurev.cellbio.15.1.393.

Willert, K., J. D. Brown, E. Danenberg, A. W. Duncan, I. L. Weissman, T. Reya, J. R. Yates, 3rd, and R. Nusse. 2003. "Wnt proteins are lipid-modified and can act as stem cell growth factors." *Nature* 423 (6938):448-52. doi: 10.1038/nature01611.

Witkiewicz, A. K., E. A. McMillan, U. Balaji, G. Baek, W. C. Lin, J. Mansour, M. Mollaee, K. U. Wagner, P. Koduru, A. Yopp, M. A. Choti, C. J. Yeo, P. McCue, M. A. White, and E. S. Knudsen. 2015. "Whole-exome sequencing of pancreatic cancer defines genetic diversity and therapeutic targets." *Nat Commun* 6:6744. doi: 10.1038/ncomms7744.

Wong, G. T., B. J. Gavin, and A. P. McMahon. 1994. "Differential transformation of mammary epithelial cells by Wnt genes." *Mol Cell Biol* 14 (9):6278-86.

Wood, L. D., D. W. Parsons, S. Jones, J. Lin, T. Sjoblom, R. J. Leary, D. Shen, S. M. Boca, T. Barber, J. Ptak, N. Silliman, S. Szabo, Z. Dezso, V. Ustyanksky, T. Nikolskaya, Y. Nikolsky, R. Karchin, P. A. Wilson, J. S. Kaminker, Z. Zhang, R. Croshaw, J. Willis, D. Dawson, M. Shipitsin, J. K. Willson, S. Sukumar, K. Polyak, B. H. Park, C. L. Pethiyagoda, P. V. Pant, D. G. Ballinger, A. B. Sparks, J. Hartigan, D. R. Smith, E. Suh, N. Papadopoulos, P. Buckhaults, S. D. Markowitz, G. Parmigiani, K. W. Kinzler, V. E. Velculescu, and B. Vogelstein. 2007. "The genomic landscapes of human breast and colorectal cancers." *Science* 318 (5853):1108-13. doi: 10.1126/science.1145720.

Wood, L. D., S. N. Salaria, M. W. Cruise, F. M. Giardiello, and E. A. Montgomery. 2014. "Upper GI tract lesions in familial adenomatous polyposis (FAP): enrichment of pyloric gland adenomas and other gastric and duodenal neoplasms." *Am J Surg Pathol* 38 (3):389-93. doi: 10.1097/PAS.0000000000000146.

Worthley, D. L., K. D. Phillips, N. Wayte, K. A. Schrader, S. Healey, P. Kaurah, A. Shulkes, F. Grimpen, A. Clouston, D. Moore, D. Cullen, D. Ormonde, D. Mounkley, X. Wen, N. Lindor, F. Carneiro, D. G. Huntsman, G. Chenevix-Trench, and G. K. Suthers. 2012. "Gastric adenocarcinoma and proximal polyposis of the stomach (GAPPS): a new autosomal dominant syndrome." *Gut* 61 (5):774-9. doi: 10.1136/gutjnl-2011-300348.

Wu, J., Y. Jiao, M. Dal Molin, A. Maitra, R. F. de Wilde, L. D. Wood, J. R. Eshleman, M. G. Goggins, C. L. Wolfgang, M. I. Canto, R. D. Schulick, B. H. Edil, M. A. Choti, V. Adsay, D. S. Klimstra, G. J. Offerhaus, A. P. Klein, L. Kopelovich, H. Carter, R. Karchin, P. J. Allen, C. M. Schmidt, Y. Naito, L. A. Diaz, Jr., K. W. Kinzler, N. Papadopoulos, R. H. Hruban, and B. Vogelstein. 2011. "Whole-exome sequencing of neoplastic cysts of the pancreas reveals recurrent mutations in components of ubiquitin-dependent pathways." *Proc Natl Acad Sci U S A* 108 (52):21188-93. doi: 10.1073/pnas.1118046108.

Xie, H., C. Xing, G. Cao, B. Wei, X. Xu, P. Song, L. Chen, H. Chen, S. Yin, L. Zhou, and S. Zheng. 2015. "Association of RNF43 with cell cycle proteins involved in p53 pathway." *Int J Clin Exp Pathol* 8 (11):14995-5000.

Xu, Q., Y. Wang, A. Dabdoub, P. M. Smallwood, J. Williams, C. Woods, M. W. Kelley, L. Jiang, W. Tasman, K. Zhang, and J. Nathans. 2004. "Vascular development in the retina and inner ear: control by Norrin and Frizzled-4, a high-affinity ligand-receptor pair." *Cell* 116 (6):883-95.

Yaeger, R., W. K. Chatila, M. D. Lipsyc, J. F. Hechtman, A. Cercek, F. Sanchez-Vega, G. Jayakumaran, S. Middha, A. Zehir, M. T. A. Donoghue, D. You, A. Viale, N. Kemeny, N. H. Segal, Z. K. Stadler, A. M. Varghese, R. Kundra, J. Gao, A. Syed, D. M. Hyman, E. Vakiani, N. Rosen, B. S. Taylor, M. Ladanyi, M. F. Berger, D. B. Solit, J. Shia, L. Saltz, and N. Schultz. 2018. "Clinical Sequencing Defines the Genomic Landscape of Metastatic Colorectal Cancer." *Cancer Cell* 33 (1):125-136 e3. doi: 10.1016/j.ccell.2017.12.004.

Yagyu, R., Y. Furukawa, Y. M. Lin, T. Shimokawa, T. Yamamura, and Y. Nakamura. 2004. "A novel oncoprotein RNF43 functions in an autocrine manner in colorectal cancer." *Int J Oncol* 25 (5):1343-8.

Yamazaki, M., A. Kato, Y. Zaitsu, T. Watanabe, M. Iimori, S. Funahashi, H. Kitao, H. Saeki, E. Oki, and M. Suzuki. 2015. "Intensive Immunofluorescence Staining Methods for Low Expression Protein: Detection of Intestinal Stem Cell Marker LGR5." *Acta Histochem Cytochem* 48 (5):159-64. doi: 10.1267/ahc.15019.

Yan, D., M. Wiesmann, M. Rohan, V. Chan, A. B. Jefferson, L. Guo, D. Sakamoto, R. H. Caothien, J. H. Fuller, C. Reinhard, P. D. Garcia, F. M. Randazzo, J. Escobedo, W. J. Fantl, and L. T. Williams. 2001. "Elevated expression of axin2 and hnkd mRNA provides evidence that Wnt/beta -catenin signaling is activated in human colon tumors." *Proc Natl Acad Sci U S A* 98 (26):14973-8. doi: 10.1073/pnas.261574498.

Yan, H. H. N., J. C. W. Lai, S. L. Ho, W. K. Leung, W. L. Law, J. F. Y. Lee, A. K. W. Chan, W. Y. Tsui, A. S. Y. Chan, B. C. H. Lee, S. S. K. Yue, A. H. Y. Man, H. Clevers, S. T. Yuen, and S. Y. Leung. 2017. "RNF43 germline and somatic mutation in serrated neoplasia pathway and its association with BRAF mutation." *Gut* 66 (9):1645-1656. doi: 10.1136/gutjnl-2016-311849.

Yan, K. S., L. A. Chia, X. Li, A. Ootani, J. Su, J. Y. Lee, N. Su, Y. Luo, S. C. Heilshorn, M. R. Amieva, E. Sangiorgi, M. R. Capecchi, and C. J. Kuo. 2012. "The intestinal stem cell markers Bmi1 and Lgr5 identify two functionally distinct populations." *Proc Natl Acad Sci U S A* 109 (2):466-71. doi: 10.1073/pnas.1118857109.

Yin, D., Y. Jia, Y. Yu, M. V. Brock, J. G. Herman, C. Han, X. Su, Y. Liu, and M. Guo. 2012. "SOX17 methylation inhibits its antagonism of Wnt signaling pathway in lung cancer." *Discov Med* 14 (74):33-40.

Yokoyama, I., T. Watanabe, M. Nishikimi, H. Ichihashi, T. Kondo, H. Takagi, and S. Sakuma. 1986. "Radioimmunoscintigraphy of human gastric carcinoma xenografts with 125I-labeled monoclonal antibody." *Jpn J Cancer Res* 77 (11):1114-21.

Yost, C., M. Torres, J. R. Miller, E. Huang, D. Kimelman, and R. T. Moon. 1996. "The axis-inducing activity, stability, and subcellular distribution of beta-catenin is regulated in Xenopus embryos by glycogen synthase kinase 3." *Genes Dev* 10 (12):1443-54.

Zebisch, M., and E. Y. Jones. 2015. "Crystal structure of R-spondin 2 in complex with the ectodomains of its receptors LGR5 and ZNRF3." *J Struct Biol* 191 (2):149-55. doi: 10.1016/j.jsb.2015.05.008.

Zeng, L., F. Fagotto, T. Zhang, W. Hsu, T. J. Vasicek, W. L. Perry, 3rd, J. J. Lee, S. M. Tilghman, B. M. Gumbiner, and F. Costantini. 1997. "The mouse Fused locus encodes Axin, an inhibitor of the Wnt signaling pathway that regulates embryonic axis formation." *Cell* 90 (1):181-92.

Zeng, X., K. Tamai, B. Doble, S. Li, H. Huang, R. Habas, H. Okamura, J. Woodgett, and X. He. 2005. "A dual-kinase mechanism for Wnt co-receptor phosphorylation and activation." *Nature* 438 (7069):873-7. doi: 10.1038/nature04185.

Zhang, W., S. C. Glockner, M. Guo, E. O. Machida, D. H. Wang, H. Easwaran, L. Van Neste, J. G. Herman, K. E. Schuebel, D. N. Watkins, N. Ahuja, and S. B. Baylin. 2008. "Epigenetic inactivation of the canonical Wnt antagonist SRY-box containing gene 17 in colorectal cancer." *Cancer Res* 68 (8):2764-72. doi: 10.1158/0008-5472.CAN-07-6349.

Ziskin, J. L., D. Dunlap, M. Yaylaoglu, I. K. Fodor, W. F. Forrest, R. Patel, N. Ge, G. G. Hutchins, J. K. Pine, P. Quirke, H. Koeppen, and A. M. Jubb. 2013. "In situ validation of an intestinal stem cell signature in colorectal cancer." *Gut* 62 (7):1012-23. doi: 10.1136/gutjnl-2011-301195.

6 List of figures and tables

Figures

Tables

7 Abbreviations

°C	degree Celsius
AAAS	American Association for the Advancement of Science
ab	antibody
ACF	aberrant crypt foci
amp	ampicillin
APC	adenomatous polyposis coli
APS	ammonium persulfate
bp	base pairs
BSA	bovine serum albumin
Ca^{2+}	calcium
CBC	crypt base columnar cells
CHIP	chromatin immunoprecipitation
CTNNB1	gene encoding β-catenin
DAB	diaminobenzidine
DAPI	4',6-diamidino-2-phenylindole
ddH2O	double-distilled water (i.e. Millipore purified water)
DEPC	diethyl pyrocarbonate
dH2O	distilled water
DIG	digoxigenin
DMEM	Dulbecco's Modified Eagle Medium
DMSO	dimethylsulfoxid
DNA	deoxyribonucleic acid
DTT	dithiothreitol
E	embryonic day
E. coli	Escherichia coli
EDTA	ethylenediaminetetraacetic acid
EST	expressed sequence tag
FCS	fetal calf serum
FFPE	formalin-fixed paraffin-embedded
floxed	'flanked by LoxP sites'
fwd	forward

fz	frizzled
g	gram
GAPPS	gastric adenocarcinoma and proximal polyposis of the stomach
GFP	green fluorescent protein
GSK-3β	glycogen synthase kinase 3 β
h	hour
H&E	hematoxylin and eosin stain
H_2O	water
H_2O_2	hydrogen peroxide
HCl	hydrogen chloride
HRP	horseradish peroxidase
IBD	inflammatory bowel disease
IEC	intestinal epithelial cell
IgG	immunoglobulin G
IHC	immunohistochemistry
IPMN	intraductal papillary mucinous neoplasm
ISH	RNA in situ hybridization
kB	kilo base
kDa	kilodalton
LGR5	leucine-rich repeat-containing G-protein coupled receptor 5
LMU	Ludwig Maximilian University of Munich
MCN	mucinous cystic neoplasm
mRNA	messenger RNA
µg	microgram
µl	microliter
µM	micromolar
µm	micrometer
n	number of replicates
NaOH	sodium hydroxide
nm	nanometer
OLFM4	olfactomedin 4
PBS	phosphate-buffered saline
PCR	polymerase chain reaction

PFA	paraformaldehyde
qRT-PCR	quantitative real-time PCR
rev	reverse
RING	really interesting new gene
RNA	ribonucleic acid
RNAse	ribonuclease
RNF	RING finger
RNF43	ring finger protein 43
rpm	revolutions per minute
RT	room temperature
SD	standard deviation
sec	second
SOX17	SRY-Box 17
TBS	tris-buffered saline
TCF	T cell factor
TCGA	The Cancer Genome Atlas Research Network
TEMED	tetramethylethylenediamine
TP53	tumor protein 53
TUM	Technical University of Munich
w/v	weight per volume
WB	western blot
wt	wild type
ZNRF3	zinc and ring finger 3

8 Publications

Schneider MR, Dahlhoff M, Horst D, Hirschi B, Trülzsch K, Müller-Höcker J, Vogelmann R, Allgäuer M, Gerhard M, Steininger S, Wolf E, Kolligs FT.
A key role for E-cadherin in intestinal homeostasis and Paneth cell maturation.
PLoS One. 2010 Dec 14;5(12):e14325.

Loregger A, Grandl M, Mejías-Luque R, Allgäuer M, Degenhart K, Haselmann V, Oikonomou C, Hatzis P, Janssen KP, Nitsche U, Gradl D, van den Broek O, Destree O, Ulm K, Neumaier M, Kalali B, Jung A, Varela I, Schmid RM, Rad R, Busch DH, Gerhard M.
The E3 ligase RNF43 inhibits Wnt signaling downstream of mutated β-catenin by sequestering TCF4 to the nuclear membrane.
Sci Signal. 2015 Sep 8;8(393):ra90.

McDuffie LA, Sabesan A, Allgaeuer M, Xin L, Koh C, Heller T, Davis JL, Raffeld M, Miettinen M, Quezado M, Rudloff U.
β-Catenin activation in fundic gland polyps, gastric cancer and colonic polyps in families afflicted by 'gastric adenocarcinoma and proximal polyposis of the stomach' (GAPPS).
J Clin Pathol. 2016 Sep;69(9):826-33.

Berger E, Rath E, Yuan D, Waldschmitt N, Khaloian S, Allgäuer M, Staszewski O, Lobner EM, Schöttl T, Giesbertz P, Coleman OI, Prinz M, Weber A, Gerhard M, Klingenspor M, Janssen KP, Heikenwalder M, Haller D.
Mitochondrial function controls intestinal epithelial stemness and proliferation.
Nat Commun. 2016 Oct 27;7:13171.

9 Acknowledgements

Basic scientific experimentation, now more than ever before, is not done in a vacuum but involves advice and help from many. Therefore, I would like to thank:

First off, Prof. Dr. med. Markus Gerhard who accepted me into his group for his enduring support and trust, for sharing his scientific and experimental advice, providing new ideas, guidance, enthusiasm and motivation.
Prof. Dr. med. Roland Schmid and Prof. Dr. med. Dirk Busch for providing an excellent and supportive environment for research at the II. Medical Clinic and Polyclinic and the Institute for Medical Microbiology, Immunology and Hygiene, respectively.

My mentors Prof. Dr. rer. nat. Andreas Jung and Prof. Dr. rer. nat. Klaus-Peter Janssen for constant support, encouragement, advice, and help over many years. Prof. Dr. Andreas Jung and LMU pathology's research immunohistochemistry facility for conducting stains on human and murine tissue samples. Prof. Dr. Klaus-Peter Janssen and his group for teaching and enabling me to perform subcellular fractionation experiments in his laboratory.
Prof. Dr. med. Michael Vieth, Director of the Institut für Pathologie of the Klinikum Bayreuth, for providing and characterizing gastric and colonic tissue samples.

Dr. Katrin Offe, Desislava Zlatanova, and Dr. med. vet. Nicole Abbrederis from the Medical Life Science and Technology Ph.D. program for providing guidance and excellent administrative support. The faculty and leadership of the program for creating and maintaining this outstanding opportunity for medical and basic science students. The program and medical faculty for funding my position and supplies through the Commission of Clinical Research (KKF).

Dr. Raquel Mejías-Luque as my direct mentor and supervisor in day-to-day laboratory experimentation and planning, for outstanding teaching, great scientific guidance, valuable technical advice, and constant encouragement that benefited so many in the laboratory.

Dr. rer. nat. Martina Grandl and Dr. rer. nat. Anke Loregger for investigating RNF43 in colon cancer and sharing their constructs and experience. Martina for sharing her broad and excellent training in laboratory experimentation and biochemistry.

Dr. rer. nat. Christian Bolz, Dr. rer. nat. Behnam Kalali, and Dr. rer. nat. Florian Anderl who were the early AG Gerhard when I joined. Thank you for openly accepting me, especially Christian for answering countless questions and introducing me to molecular biology. Behnam for help with DNA and PCR-related issues and sharing his excitement for constructs and mouse models. Jeannette Koch and Ina Sebald for providing technical assistance. The animal caretakers at the mouse facilities of the medical faculty for their work and expertise.
All former and current members of AG Gerhard for helping and encouraging each other. It has been a great time with you!

Finally, I would like to thank my parents and family for their support over many years. Lastly, the most important person to this work, the one who was most affected by years of basic lab research, at times in addition to my medical studies, that resulted in nights and weekends in the laboratory, Wiebke, my wonderful wife, mother to our child(ren), and best friend for her enduring support and motivation through all of these years.
Thank you!